Intra and extra-adrenal immune mechanisms regulating adrenal hormonal output

A thesis submitted for the degree of Doctor of Philosophy in Cardiovascular Science

University of Oxford

Michaelmas Term 2023



UNIVERSITY OF
OXFORD

Conan O'Brien

Balliol College

Department of Physiology, Anatomy, and Genetics

"*Do diseases come from without or do their causes arise within the organism*?"

Ilya Mechnikov, in pondering why certain disease-causing agents (e.g. cholera vibrio) were lethal via certain routes and benign when entering via others, yet the tuberculosis bacillus caused a uniform disease whatever the route of entry.

Abstract

The adrenal glands are hormone secreting glands that sit on top of the kidneys. Adrenal glands produce glucocorticoids, mineralocorticoids, and catecholamines, and are therefore critical regulators of the stress response, the immune response, metabolism, and blood pressure. Adrenal hormonal production is regulated by the renin angiotensin aldosterone system and the hypothalamic pituitary adrenal axis. While the non-immune functions of macrophages are gaining wider recognition, the function(s) of macrophages within these systems remain incompletely understood. In this thesis, I use an *in vivo* approach to explore the relationship between macrophages and hormonal regulation in distinct components of the body. In the first part of my thesis, I probe the macrophage compartment of the murine adrenal gland. Despite being identified in the adrenal glands of mice and humans for more than three decades, adrenal macrophages remain incompletely understood. The investigations presented herein reveal two distinct subsets of adrenal macrophages: dendritic-like macrophages distributed throughout the gland in both young and old mice, and "foamy" lipid-laden macrophages accumulating in the adrenal cortex in an age and diet-dependent manner. These foamy-like macrophages play a crucial role in cholesterol accumulation, thereby influencing adrenal hormonal output both at steady state and in the context of obesity. In the second part of this thesis, I demonstrate that the scavenger receptor MARCO suppresses angiotensin-converting enzyme (Ace) expression in the lung and negatively regulates systemic aldosterone levels. These findings point to alveolar macrophages as potential additional players in the renin-angiotensin-aldosterone system and introduce a novel example of interplay between the immune and endocrine systems. Together, this thesis presents a novel perspective on the intricate crosstalk between immune cells and endocrine regulation in different anatomical sites, expanding our understanding of the broader implications of macrophage involvement in hormonal control.

Acknowledgements

What a journey. This thesis is the culmination of over four years of hard work in Oxford, featuring a global pandemic and numerous trials and tribulations, and would not have been possible without the brilliant people I've had the privilege of being surrounded by, in and out of the lab. They have all made possible what at times felt an impossibly daunting task. First and foremost, I would like to thank my supervisor, Ana Domingos. You gave me the freedom to take this work through to completion, and the courage to challenge dogma and think differently. You welcomed me into your lab and your homes in Oxford and Portugal, gave me the space to grow as a scientist and as a person, and provided critical support and opportunities through my studies. Second, I would like to thank my second supervisor, David Greaves. From my interview for the Cardiovascular Science DPhil programme, you made me feel welcome in Oxford. You believed in me and brought me to this city, welcomed me into your lab for my rotational project, and provided crucial scientific training in macrophage biology in my formative first year. I have enjoyed immensely my honorary membership of your lab group and look forward to gate-crashing many more Dunn Drinks and Greaves Lab Socials in the years to come. Though unofficial, I would consider Siamon Gordon my third supervisor. Your passion for macrophage biology is infectious and I consider myself fortunate that our paths crossed during my studies. I also extend my appreciation and thanks to my collaborators – Luis Saraiva, Frederic Geissmann, Celso Gomez-Sanchez, and Tomohiro Ishii, whose efforts in Qatar, the USA, and Japan, made possible many of the experiments presented in this thesis.

I feel so lucky to have started my DPhil in the same lab and at the same time as Emma Haberman. Our almost daily scientific discussions were an absolute pleasure and helped give me new perspectives, new ideas, and the space for my passion for science to grow further. But more than that, your kindness and warmth made the dark days brighter, and gave me the courage to go on when I felt like I couldn't – like during that much needed summer pint after I found out I'd been scooped! I'll always cherish the memories of tearing up the dancefloors at conference, parties, and living rooms, 5am poster presentations, Danny DeVito, all the daily chats over coffee about our DPhils, our lives, and everything else in between. Working with you was an absolute privilege and I know I have a friend for life in you. I would also like to thank my other lab mates in the Domingos group, in particular Yitao Zhu, Giorgio Ratti, Alek Stawiarski, Davi Oliveira, and Charles Sweeney. You all contributed in different ways but together you made the highs even higher and the lows more bearable and I am thankful for

sharing this experience with you. I'm sure you will find success in whatever you do, and I look forward to seeing where you all end up.

I would not have made it to Oxford had I not been fortunate enough to have such inspiring teachers and mentors from school through to university. My biology teachers at Methody – Mr Patrick, Mr Watson, Dr Campton – and my academic mentors Molly Ingersoll and Rob Nibbs. You all taught me the value of curiosity, the beauty of the natural world, and showed me just how exciting academic research could be.

Oxford is a special place, but there is no doubt in my mind that it is the people of Oxford that make it so special. I have found a second family in the friends that I made here. In no particular order, Casey, Maike, Johny, Max, Rowie, Hermione, May, Matt, Agata, Gareth, Ada, Vincent, Laura, Annabel, Ed, and my friend from home, Hayley, who so kindly put me up in her apartment in Valencia when I was homeless in Oxford and writing up. No number of words could ever fully explain how much I appreciate you all. Some of you have stayed in Oxford, some of you will soon, and some of you have scattered around the world. I will always remember fondly the pints, wine and cheese nights, cooking nights, dinner parties, coffees, holidays, casual chats and DMCs. I literally cannot wait for our reunions, wherever they may be, and I am counting the days until we get to make more memories together.

Last but certainly not least, I want to thank my parents and family. You brought me in to this world, brought me up, and believed in me before anyone else did. You supported me to go on this academic journey and without you I would not be where I am or who I am today. Thank you. Thank you all.

Abbreviations

17β-HSD	17β-hydroxysteroid dehydrogenase
ABCA1	ATP-binding cassette subfamily A member 1
ACAT	Acyl coenzyme A:cholesterol acyltransferase
ACE	Angiotensin converting enzyme
ACTH	Adrenocorticotropic hormone
AD	Alzheimer's Disease
AG	Adrenal gland
AGM	Aorto-gonado-mesonephros
AGP	Adrenal gonadal primordium
AM	Alveolar macrophage
AMP	Adenosine monophosphate
Ang	Angiotensin
APA	Aldosterone-producing adenomas
ApoA	Apolipoprotein A
AT1R	Angiotensin II type 1 receptor
ATP	Adenosine triphosphate
ATRM	Adipose tissue resident macrophage
AVP	Arginine vasopressin
BALL	Big autofluorescent lipid-laden macrophage
BMDM	Bone-marrow-derived macrophages
CAH	Congenital adrenal hyperplasia
CALH	Congential adrenal lipoid hyperplasia
CaMK	Calmodulin-dependent protein kinases
cAMP	Cyclic adenosine monophosphate
CCLX	Chemokine ligand X
CCRX	Chemokine receptor X
CD	Cluster of differentiation molecule
CLR	C-type lectin receptors
CREB	Calcium, activating transcription factors
CRH	Corticotropin releasing hormine
CSF1R	Colony stimulating factor receptor
CTD	C terminal domain
CX3CL1	C-X3-C motif chemokine ligand 1
CX3CR1	C-X3-C motif chemokine receptor 1
CXCLX	Chemokine (C-X-C motif) ligand X
CYP	Cytochrome P450 family members
DAMP	Danger-associated molecular patterns
DC	Dendritic cell
DHEA	Dehydroepiandrone
DHEA	Dehydroepiandrosterone
DNA	Deoxyribonucleic acid

DT	Diphtheria toxin
DZ	Definitive zone
EC	Esterified cholesterol
EMP	Erythromyeloid progenitor
ENaC	Apical epithelial sodium channel
ER	Endoplasmic reticulum
FACS	Fluorescence-activated cell sorting
FAdE	Fetal adrenal enhancer
FZ	Fetal zone
GC	Glucocorticoid
GFP	Green fluorescent protein
Gli1	Glioblastoma 1
GLUT1	Glucose transporter 1
GM-CSF	Granulocyte-macrophage colony-stimulating factor
GPCR	G protein coupled receptor
GR	Glucocorticoid receptor
GRE	Glucocorticoid responsive elements
HDL	High density lipoprotein
HFD	High fat diet
HIF	Hypoxia-inducible factor
HMGCR	HMG-CoA reductase
HPA	Hypothalamic-pituitary-adrenal
HSC	Haematopoietic stem cell
HSD	High salt diet
HSD3β	Hydroxysteroid dehydrogenase
HSL	Hormone-sensitive lipase
IBD	Inflammatory Bowel Disease
Ig	Immunoglobulin
IL	Interleukin
ITAM	Immunoreceptor tyrosine-based activation motifs
ITIM	Immunoreceptor tyrosine-based inhibition motifs
JG cell	Juxtaglomerular cell
LDL	Low density lipoprotein
LDLR	Low density lipoprotein receptor
LPS	Lipopolysaccharide
M-CSF	Macrophage colony stimulating factor
MAPK	Mitogen-activated protein kinase
MARCO	Macrophage receptor with collagenous structure
MC2R	Melanocortin receptor 2
MHC	Major histocompatibility complex
MPS	Mononuclear phagocyte system
MR	Mineralocorticoid receptor
MRE	Mineralocorticoid-responsive element

nCEH	Neutral cholesteryl ester hydrolase
ND	Normal diet
NFκB	Nuclear factor kappa B
NK cell	Natural killer cell
NLR	NOD-like receptors
NOD	Nucleotide-binding oligomerization domain
NOS	Nitric oxide synthase
NSD	Normal salt diet
PA	Primary aldosteronism
PAMP	Pathogen-associated molecular patterns
PDGF	Platelet-derived growth factor
PKA	Protein kinase A
Plin2	Perilipin family protein 2
POMC	Pro-opiomelanocortin
PPAR	Peroxisome proliferator-activated receptor
PRR	Pattern recognition receptor
PVN	Paraventricular nucleus
RA	Rheumatoid arthritis
RAAS	Renin-angiotensin-aldosterone system
RCT	Reverse cholesterol transport
RIG-1	Retinoic acid-inducible gene 1
RNA	Ribonucleic acid
RNS	Reactive nitrogen species
ROS	Reactivive oxidative species
RPM	Red pulp macrophage
SAMs	Sympathetic neuron-associated macrophages
SF-1	Steroidogenic factor 1
Shh	Sonic hedgehog
SR	Scavenger receptor
SR-BI	Scavenger receptor B type 1
SRA	Scavenger receptor A1
STAR	Steroidogenic acute regulatory protein
TAM	Tumour-associated macrophage
TGF-β	Transforming growth factor β
TIR	Toll/interleukin 1 receptor
TLRs	Toll like receptor
TNFα	Tumour necrosis factor α
TREM2	Triggering receptor expressed on myeloid cells 2
VEGF	Vascular endothelial growth factor
ZF	Zona fasciculata
ZG	Zona glomerulosa
ZGM	Zona glomerulosa macrophage
ZR	Zona reticularis

Portions of this thesis have been taken or adapted from the following published articles or pre-prints on which I am first author. The portions used were those that I solely authored.

Conan JO O'Brien, Davi Sidarta-Oliveira, Aleksander Stawiarski, Giorgio Ratti, Pierre-Louis Loyher, Mélanie Makhlouf, Eman H AbouMoussa, Emma Haberman, Charles Sweeney, Yusuke Mizuno, Tomohiro Ishii, Tomonobu Hasegawa, Elise P Gomez-Sanchez, Celso E Gomez-Sanchez, Siamon Gordon, David R Greaves, Luis R Saraiva, Frederic Geissmann, Ana I Domingos (2023). Distinct adrenal gland macrophages regulate corticosteroid production. bioRxiv 2023.09.05.556330; https://doi.org/10.1101/2023.09.05.556330.

Conan JO O'Brien, Giorgio Ratti, Emma Haberman, Charles Sweeney, Siamon Gordon, Ana I Domingos (2023). MARCO in alveolar macrophages negatively regulates Ace expression and aldosterone production. Life12:RP91318; https://doi.org/10.7554/eLife.91318.1.

Conan JO O'Brien, Emma Haberman, Ana I Domingos. A Tale of Three Systems: Toward a Neuroimmunoendocrine Model of Obesity (2021). Annu Rev Cell Dev Biol. 2021 Oct 6;37:549-573; https://doi.org/10.1146/annurev-cellbio-120319-114106.

Table of Contents

Abstract ***3***

Acknowledgements ***4***

Abbreviations ***6***

List of figures ***13***

Introduction ***15***

1.1. History of Macrophages 15
1.1.1. The discovery of macrophages as immune cells 15
1.1.2. Evolutionary history of the macrophage 17

1.2. The mononuclear phagocyte system: A spotlight on macrophages 20
1.2.1. Macrophages: Guardians of tissue homeostasis 23
1.2.2. Immune functions of macrophages 24
1.2.3. Homeostatic and physiological functions of macrophages 32
1.2.4. Macrophage dysfunction in disease 34
1.2.5. Macrophage and cholesterol metabolism 37

1.3. The adrenal gland: development, anatomy, physiology, and pathology 39
1.3.1. Adrenal gland development 40
1.3.2. Adrenal gland structure and function 43
1.3.3. Glucocorticoids: regulation and mechanism of action 45
1.3.4. Mineralocorticoids: regulation and mechanism of action 48
1.3.5. Supply of cholesterol for adrenal corticosteroid biosynthesis 53
1.3.6. The adrenal glands as a seat of endocrine disorders 57

1.4. Original hypothesis 60

1.5. Experimental aims 60

Materials and methods ***61***

2.1. Animal experimentation 61
2.1.1 Ethical statement 61
2.1.2. Mouse strains and husbandry 61
2.1.3. Sacrifice and tissue harvest 62

2.2. Fluorescence activated cell sorting (FACS) 63
2.2.1. Tissue collection and preparation for FACS 63
2.2.2. Adrenal digestion 63
2.2.3. Cell counting 63
2.2.4. Staining for surface markers 64
2.2.5. Intracellular staining 64
2.2.6 Data acquisition and analysis 65

2.3 Microscopy 65
2.3.1 Immunofluorescent staining and confocal microscopy 65
2.3.2 Immunohistochemical (IHC) staining and bright field microscopy 67
2.3.3. Image analysis 68

2.4. Irradiation and bone marrow transplantation 68

2.5. Analysis of published single-cell sequencing data 68

2.6. High fat diet (HFD) challenge 69

2.7. High salt diet challenge 70

2.8. Subcutaneous osmotic minipump implantation 70

2.9. Bulk RNA sequencing of adrenal macrophages....70
2.10. Diphtheria toxin receptor-mediated macrophage ablation....71
2.11. Plasma hormone, protein measurements....72
2.12. Cholesterol measurements....72
2.13. Determination of plasma volume....73
2.14. Blood electrolyte readings....73
2.15. RT-qPCR....73
2.16. Temporal deletion of Star....75
2.17. LDL uptake assay....75
2.18. Statistical analysis....75

Characterising the murine adrenal macrophage compartment at steady state....77

3.1 Introduction....77
3.1.1 Tissue macrophage markers....77
3.1.2. Features of the tissue macrophage niche....79
3.1.3. Macrophage ontogeny and experimental methods used to probe macrophage origins....81
3.1.4. The adrenal cortex and medulla: differences in form and function....86
3.1.5. Foam cell origins....87
3.1.6. Adrenal gland macrophages....88
3.1.7. Single cell and bulk RNA sequencing technologies....90
3.2. Rationale and experimental aims....91
3.3. Results....92
3.3.1 Leukocyte populations in the murine adrenal gland....92
3.3.2. Cortico-medullary differences in adrenal myeloid cells....96
3.3.3 The adrenal cortex harbours two spatially distinct macrophage subsets....97
3.3.4 CX3CR1-expressing ZGMs decline with age....100
3.3.5 Big Autofluorescent Lipid-Laden (BALL) adrenal macrophages accumulate with age....101
3.3.6. Aged adrenal autofluorescence is contained inside $CD68^{+}$ macrophages....104
3.3.7 BALL macrophages contain cholesterol and their formation is accelerated in obesity....105
3.3.8 Establishing the ontogeny of adrenal gland macrophages....108
3.3.9 Adrenal gland macrophage-specific transcriptional signatures....113
3.4 Discussion....118
3.4.1. Adrenal macrophages are distinguishable by CX3CR1 expression....118
3.4.2. The adrenal macrophage niche....119
3.4.3. Adrenal specification of Zona Glomerulosa Macrophages....121
3.4.4. Foamy BALL macrophages....122
3.4.5. Ontogeny of adrenal gland macrophages....124
3.4.6. CCR2-independent BMDM accumulation?....126
3.4.7. Limitations....127

Assessing the contribution of adrenal macrophages to adrenal hormonal output....130

4.1. Introduction....130
4.1.1. Physiological factors that stimulate and suppress adrenal corticosteroid production....130
4.1.2 The relationship between adrenal cholesterol stores and hormonal production....134
4.1.3 Evidence for macrophage involvement in steroidogenesis....137
4.2. Rationale and experimental aims....138
4.3 Results....139

4.3.1 ZGMs positively regulate aldosterone production but not other adrenal-derived hormones. 139
4.3.2. Corticosteroid inhibition and stimulation differentially impact BALL macrophage size and cholesterol contents. 140
4.3.4 CX3CR1 regulates BALL formation 142
4.3.5 CX3CR1 regulates intra-adrenal cholesterol stores and corticosteroid output at steady state 144
4.3.6 CX3CR1 regulates corticosterone production in HFD-fed mice 146
4.4. Discussion 147
4.4.1. CX3CR1-expressing ZGMs regulate aldosterone production 148
4.4.2. CX3CR1 as a regulator of intra-macrophage cholesterol accumulation 149
4.4.3. BALL macrophages constitute an intra-adrenal cholesterol store 151
4.4.4. Therapeutic perspective on BALL macrophages in obesity 154
4.4.5. Contributing to the literature on adrenal macrophages 154
4.4.6. Adrenal macrophages and the X zone 156
4.4.7. Limitations 158

Characterising the effects of MARCO on the Renin-Angiotensin-Aldosterone-System (RAAS)..... 160

5.1. Introduction 160
5.1.1. MARCO and SRA: structure and function 160
5.1.2. Alveolar macrophage ontogeny and functions 162
5.1.3. Primary and secondary aldosteronism: causes and consequences 164
5.1.4. ACE: physiological and immune functions 165
5.2. Rationale and experimental aims 166
5.3. Results 167
5.3.1. The effect of the class A scavenger receptors on cholesterol levels and corticosteroid output 167
5.3.2. Marco is expressed in the lung but not the adrenal glands 169
5.3.3. Marco-mediated elevation of aldosterone explained by Ace but not by upregulation of adrenal biosynthetic enzymes, the zona fasciculata, or renin 171
5.3.4. Marco deletion impacts blood pressure and plasma electrolyte levels 176
5.4. Discussion 177
5.4.1. MARCO as a regulator of Ace expression 178
5.4.2. MARCO as a regulator of aldosterone 179
5.4.3. The class A Scavenger receptors as cholesterol regulators? 182
5.4.4. Limitations 183

Thesis summary and final discussion 185

6.1. Key findings 185
6.2. Final discussion 186

Appendix..... 192

Appendix 1. List of publications 192
Appendix 2: Project contributions 193

References 194

List of figures

Figure 1.1. Macrophage lineage and ontogeny

Figure 1.2. Macrophage cholesterol metabolism

Figure 1.3. Adrenal gland structure and function

Figure 1.4. Adrenal corticosteroid biosynthesis

Figure 1.5. Intracellular adrenal corticosteroid biosynthetic pathway

Figure 1.6. The hypothalamic-pituitary-adrenal axis

Figure 1.7. The Renin angiotensin aldosterone system (RAAS)

Figure 1.8. Molecular regulation of corticosteroid production

Table 2.1. List of conjugated flow cytometry antibodies used in this thesis

Table 2.2. List of antibodies used for microscopy in this thesis

Table 2.3. ELISA CVs and limits of detection

Table 2.4. RT-qPCR primers and sequences

Table 3.1. Murine macrophage markers

Figure 3.1. All cell types in the murine adrenal gland

Figure 3.2. Leukocyte populations in the murine adrenal gland

Figure 3.3. Cortico-medullary differences in adrenal myeloid cells

Figure 3.4. The adrenal cortex harbours two spatially distinct macrophage subsets

Figure 3.5. CX3CR1-expressing zona glomerulosa macrophages preferentially localise to aldosterone-producing cells

Figure 3.6. Flow cytometry gating strategy

Figure 3.7. CX3CR1-expressing macrophages decline with age

Figure 3.8. Big autofluorescent CX3CR1 negative macrophages accumulate with age

Figure 3.9. Phenotypically distinct macrophages co-reside in the adult adrenal cortex

Figure 3.10. Aged adrenal autofluorescence is contained in CD68+ cells

Figure 3.11. BALL macrophages contain cholesterol

Figure 3.12. High fat diet feeding accelerates BALL formation

Figure 3.13. Single cell RNA-seq reveals three distinct adrenal macrophage populations

Figure 3.14. Irradiation and bone marrow transplantation

Figure 3.15. CX3CR1-expressing cells seed long-lived adrenal macrophages

Figure 3.16. Bulk RNA-seq data from Zona Glomerulosa Macrophages (ZGMs)

Figure 3.17. Single cell RNA-seq data from adrenal myeloid cells

Figure 3.18. Hypothalamic, pituitary, and adrenal gene expression comparison

Figure 4.1. ZGMs positively regulate aldosterone production
Figure 4.2. Corticosteroid inhibition increases BALL macrophage size and cholesterol contents
Figure 4.3. Effect of AngII stimulation on BALL macrophages
Figure 4.4. CX3CR1 regulates BALL macrophage formation
Figure 4.5. CX3CR1GFP/GFP BMDMs are not defective in their capacity to form foam cells in vitro.
Figure 4.6. CX3CR1 regulates intra-adrenal cholesterol stores
Figure 4.7. CX3CR1 regulates adrenal corticosteroid production
Figure 4.8. RT-qPCR data of corticosteroid biosynthetic gene expression in wild-type and CX3CR1-deficient mice
Figure 4.9. CX3CR1 regulates corticosterone production in HFD-fed mice
Figure 5.1. Alveolar structure and cellular makeup
Table 5.1. Known causes of non-treatment-induced secondary aldosteronism
Figure 5.2. Marco-deficient mice have elevated aldosterone and reduced serum cholesterol
Figure 5.3. Marco is expressed in the lung and not adrenal glands.
Figure 5.4. Marco-mediated elevation of aldosterone is not explained by adrenal biosynthetic enzyme gene expression.
Figure 5.5. Dexamethasone suppression test
Figure 5.6. Marco-deficient mice have enhanced expression of Ace mRNA in the lung
Figure 5.7. Marco-deficient mice have enhanced expression of Ace protein in the lung
Figure 5.8. A model of MARCO-mediated regulation of aldosterone
Figure 5.9. Blood pressure of WT and Marco-/- mice
Figure 5.10. Blood volume and electrolytes in WT and Marco-/- mice

Chapter 1

Introduction

1.1. History of Macrophages

1.1.1. The discovery of macrophages as immune cells

This thesis is principally concerned with macrophages, a term that comes from the Greek words for "big eater". Their name does not bely their function. The "Father of Innate Immunity" Ilya Mechnikov is perhaps best known for his pioneering work on phagocytes – white blood cells that engulf foreign bodies, dead, and dying cells. Mechnikov was not the first to observe phagocytic macrophages performing their synonymous function. However, in a series of experiments in Messina, Italy, in the 1880s Mechnikov was the first to observe, define, and realise, the full functional significance of phagocytosis [1,2]. Prior to this point, observations by Mechnikov and others showed that migrating "mesodermal cells" (the term used to describe macrophages at the time) ingested and removed cells that were rendered superfluous during the process of metamorphosis in echinoderm larvae and drosophila. This process was at the time considered passive, shared by endodermal and mesodermal cells, through which cells ate cellular debris as nutritional material for sustenance [1].

Mechnikov's revelation came from observing that these migrating mesodermal cells also did the same to foreign material and were capable, though not always, of ingesting and digesting this material. In the Messina experiments [1], Mechnikov reported injecting human blood cells and coloured dyes sub-epidermally into transparent organisms fished from the sea – starfish larvae and sea slugs most frequently – upon which he observed that they were immediately engulfed and gradually dissolved by "strangely shaped" migrating mesodermal cells. Goat milk injected into starfish larvae was similarly swarmed by mesodermal cells, milk globules were ingested, broken down, and spread evenly throughout the intracellular space. Similar

experiments revealed that these mesoderm cells couldn't dissolve everything – insertions of glass needles, sea urchin spines, and bone fragments, into deeper layers of Ascidia (sea squirts) were unable to be removed by the migrating cells. Mechnikov also questioned the specificity of these mesoderm cells in ingesting foreign contents. Simultaneous injections containing a drop of goat's milk with a mixture of indigo, carmine, and starch granules (i.e. "digestible and indigestible substances together") into the mucous tissue of Phylliroe (transparent sea slugs) showed that that all these foreign bodies were absorbed without selection. Some mesoderm cells took up some of all four substances at the same time – indicating that they may consume anything. Following the injection of live ovarian eggs of Sphaerechinus granularis (sea urchins) under the skin of sea slugs, it was found that both immature and fully matured eggs were not attacked by mesoderm cells at all. Artificial insemination of the injected eggs into a new host resulted in egg development into normal-looking blastulae. But injection of freshly cooked sea urchin eggs into sea slugs resulted in a rapid mobilisation of the mesoderm cells, which engulfed the yolk cells [1]. Metchnikoff thereby observed specificity in the macrophage phagocytic response, a finding that indicated to him a potentially "not insignificant prophylactic role". These observations were expanded upon by using bacteria as the challenging stimulus. In these experiments, bacteria were also ingested, immobilised, and digested, by the mesoderm cells [1]. Unlike contemporary pathologists who thought of the intracellular localisation of bacteria as a safe haven for growth and dissemination, he observed and understood the destructive capacity of the phagolysosome [2]. He also, by observing selectivity of macrophage particle uptake, caught the first glimpse of pattern recognition as a mechanism mediating phagocytosis.

Paul Baumgarten, a prominent microbiologist and pathologist and an advocate of the new "positivist science" in the 1800s accused Metchnikoff of retrogressive thinking when he sought

to define phagocytic cells on the basis of their function. Baumgarten's scientific philosophy rejected outright Mechnikov's teleological approach, which he considered to focus unduly on the explanation of phenomena through biological function. He instead sought to ground phenomena in a materialistic schema, reducing organic functions to physics and chemistry [3]. Driven by understanding function in the context of function and evolution, rather than adhering to the pervading scientific mindset, Mechnikov advocated for a more holistic approach, acknowledging the significance of biological explanations alongside physico-chemical ones. He argued that while physics and chemistry provide essential foundations, a comprehensive understanding of life's complexities required embracing biological principles and considering the unique and intricate aspects of living organisms, those that might not be fully explained by purely mechanical or chemical laws [3].

Though originally critical of Darwinism, Mechnikov eventually embraced evolution and came to consider the physiology that underpinned organism development and function in an evolutionary context. This drew him to seek to define the mechanism that underpinned the harmonisation of the various elements – or systems – that make up the multicellular organisms. A mindset that ultimately led him to the discovery of the macrophage as we now know it – the big eater with functions in immunity, but also in physiology, metabolism, and homeostasis.

1.1.2. Evolutionary history of the macrophage

Following Mechnikov's example, modern biology understands the macrophage in the context of its long evolutionary history and with relationship to its distant cousins. In this section, I describe the organisms Acanthamoeba, Dictyostelium, and the Amoebocytes, as well as Drosophila plasmatocytes, which as we will see bear striking resemblances to the macrophages which are the subject of our interest.

Acanthamoeba is a free-living heterotrophic protist (single celled organism) that bear many similarities to the macrophages observed by Mechnikoff and the macrophages we observe in all mammals today [4]. These observations have led many to hypothesise that Acanthamoeba are the evolutionary ancestor of eukaryotic macrophages [4–6]. Firstly, acanthamoeba are a similar size to mammalian macrophages, possess dendrites, and are a highly mobile cell type which migrate towards microbes in a directed manner [6]. Acanthamoeba also use chemotaxis for this migration and, like macrophages, use actin and myosin remodelling to reform the cytoskeleton and move towards chemotactic stimuli [7]. Acanthamoeba were shown to be capable of producing directed movement in response to lipopolysaccharides, formyl-methionyl-leucyl-phenylalanine (also known as a macrophage activator), lipoteichoic acid, and cyclic AMP (cAMP) [8]. Acanthamoeba can also phagocytose microbial targets in a manner that is saturable by sugar co-treatment, unlike with silica particles [9,10], indicating that this takes place in a receptor-dependent manner. Upon formation of the phagolysosome, microbial targets are then killed and degraded [11,12], as in macrophages.

Dictyostelium, a close relative of Acanthamoeba, are a model organism commonly used to study facultative multi-cellularity [13]. Like Acanthamoeba, Dictyostelium exist free-living in a haploid amoebae state that also phagocytose microbes for nutritional purposes. Like how Transformers can merge into super-bots and unlike Acanthamoeba, Dictyostelium can gather and aggregate in a cAMP-dependent manner during periods of starvation, forming primitive unitary multicellular organisms termed “slugs”. This model is useful in studies of chemotaxis and phagocytosis, in addition to cell-cell signalling and interactions [13]. The migration and assembly of Dictyostelium is mediated through the secretion of soluble signalling factors [14]. Indeed, studies have demonstrated that Dictyostelium mediate chemotaxis towards microbial

targets similarly to macrophages, via G protein coupled receptor (GPCR)-dependent mechanisms [15,16], though the precise receptors that mediate migration and phagocytosis differ between Dictyostelium and macrophages [17]. Macrophages possess a plethora of receptors which mediate recognition of other cells and pathogen-associated molecular patterns, including toll/interleukin 1 receptor (TIR) domain-containing Toll Like Receptors (TLRs), integrins, scavenger receptors, and C type lectins [17]. Dictyostelium possess certain analogous receptors, including TIR domain-containing proteins which mediate organismal growth [18], lectin-like receptors that mediate binding of sugars [19], and scavenger receptor-like proteins, the functions of which remain to be fully elucidated [17].

One step further along the evolutionary chain in Porifera (sponges), another primitive multicellular organism, we find Amoebocytes – the professional phagocytic cells in Porifera. These cells bear long dendritic extensions, are phagocytic and express genes associated with mammalian innate immunity, including Nuclear factor kappa B subunit (NFκB), which controls cellular inflammatory responses, and high mobility group box 1/2/3 (*Hmgb1/2/3*), which are mediators of nucleic acid–mediated innate immune response and activate key inflammatory pathways. Moreover, amoebocytes express the only *Nfat* ortholog, active in mammalian adaptive and innate immunity, *Gata*, a macrophage-linage defining gene, and *Rab21*, a gene essential for phagolysosome formation [20].

Drosophila melanogaster, a higher order metazoan with clearly defined and specialised tissues and organs, is commonly used immunological research due to the high level of conservation of pathways in innate immunity [4]. Plasmatocytes, the macrophage-equivalent cell in Drosophila, bear many similarities to mammalian macrophages. Early in life they migrate to and self-renew within tissues [21], possess long dendritic processes, mediate phagocytosis and cell death [22], and

also perform higher physiological processes only possible in organisms with tissue diversity. In the context of bacteria-induced brain inflammation, plasmatocytes invade the fly brain, and phagocytose synaptic material and affect locomotor capacities and longevity [23], in a manner similar to how infiltrating mammalian macrophages infiltrate tissues to cause inflammation sometimes with deleterious effects (which will be discussed later in this chapter). Drosophila also have a primitive form of adipocyte termed a fat-body cell. A genetic screen demonstrated that plasmatocytes regulate the storage of lipids within fat-body cells via the platelet-derived growth factor (PDGF)/vascular endothelial growth factor (VEGF)-family ortholog, *Pvf3*. Remarkably, this pathway was shown to be conserved in mammalian macrophages which were shown to regulate lipid storage in adipocytes in adult mice [24]. These examples illustrate that macrophage-like cells are an essential component of eukaryotic life, and that the functional relevance of these cells increases as a function of tissue specification.

Today, macrophages are typically thought of primarily as immune cells, though increasing recognition is being given to the homeostatic and physiological functions of macrophages [25]. Findings of new physiological functions of macrophages are often met with great excitement and/or scepticism – "Oh, wow! I never considered a macrophage capable of doing *that*" is a sentence I often hear from colleagues. However, if you consider macrophages as a primordial cell, potentially deriving from the most ancient of eukaryotes, then their evident multifunctionality becomes a lot less surprising.

1.2. The mononuclear phagocyte system: A spotlight on macrophages

Much of what we have learned about macrophage function has been derived from studies in rodents. It is primarily in this context that I will discuss macrophage function, unless specified otherwise. The mononuclear phagocyte system (MPS) was first defined by Furth and Cohn in

1968 [26]. They described a related family of cells that could be split into two primary groups: circulating monocytes in the peripheral blood and tissue macrophages. They showed that tissue macrophages such those of the peritoneum were relatively long-lived cells, undergoing low rates of turnover at steady state and capable of persisting in tissues for weeks. This contrasted with blood monocytes which had a half-life of < 24 hours. Using *in vivo* radio-labelling of bone marrow they showed that monocytes derived from a bone marrow-derived precursor and that monocytes were capable of giving rise tissue macrophages following irradiation-induced macrophage ablation [26]. Since this original proposal, our understanding of the MPS has developed further, assisted by sophisticated fate mapping approaches. It is now recognised that tissue-resident macrophages are seeded prenatally from fetal yolk sac progenitors and undergo minimal contribution from circulating monocytes at steady state. However, in instances of pathogenic or physiological inflammatory insult, monocyte-derived macrophages accumulate in tissue in response to chemotactic and inflammatory cues [27] (Figure 1.1).

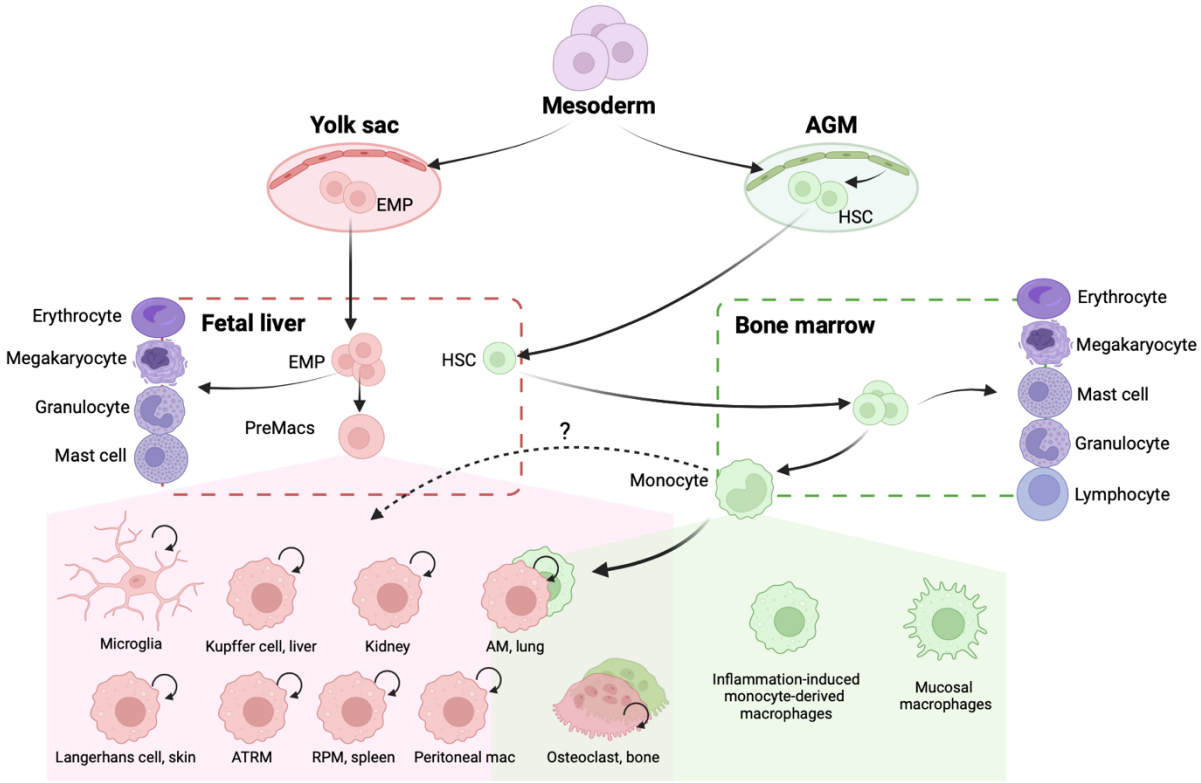


Figure 1.1. Macrophage lineage and ontogeny. Cells of the erythromyeloid progenitor (EMP) lineage are coloured in red and cells of the haematopoietic stem cell (HSC) lineage are coloured in green. Yolk

sac-derived EMPs stem from the yolk sac hemogenic endothelium and localise to the fetal liver where they can seed erythrocytes, certain leukocytes, and the pre-macrophages (PreMacs) that populate tissues prenatally and seed most adult tissue-resident macrophage populations. HSCs stem from the hemogenic endothelium of the aorto-gonado-mesonephros (AGM) and migrate to the fetal liver and embryonic bone marrow, where they self-renew and seed the monocytes that serve as precursors to certain adult macrophage populations, in addition to other haematopoietic cells. Some postulate that the contribution of monocytes to adult tissue resident populations is underestimated and may be greater than currently acknowledged. AM, alveolar macrophage; ATRM, adipose tissue resident macrophage; RPM, red pulp macrophage. Adapted from [28,29].

Colony stimulating factor 1 (*Csf1*; M-CSF) via its receptor CSF1R has since been demonstrated to be the primary differentiation, survival, and proliferation factor that controls the size intra-tissue mononuclear phagocyte pools. Genetic knockout of this gene demonstrates the essential roles that macrophages play in immunity and development; Csf1r-deficient *op/op* mice are osteoporotic, exhibit severe postnatal growth retardation, and have impaired immune responses to pathogenic challenge [30–34]. Though dendritic cells (DCs) are also mononuclear phagocytes, they were not originally included in the MPS [26]. There exists a common DC-macrophage progenitor cell [35], highlighting the close developmental origins of these cells. As such, monocytes and DCs are often difficult to differentiate within tissues by cell surface marker expression. DCs are recognised as professional antigen-presenting cells responsible for the stimulation and activation of naïve T cells [36], but debate exists today on whether DCs and macrophages are truly differentiated on their capacity to present antigens to and activate T cells [37]. The contention is based on 1) macrophages possessing the machinery (MHC molecules) to present antigen and provide co-stimulation; 2) macrophage suppressor cells that suppress T cell activation are difficult to exclude from T cell activation assays; 3) lymph node supcapsular macrophages can activate B cells; 4) macrophages have demonstrable capacity to induce antigen-specific inactivation and peripheral tolerance; and 5) *in vitro* generated macrophages and DCs are both capable of forming immune synapses with T cells, with the nature of antigen determining the precise T cell response [37,38]. Additionally, different nomenclatures for

monocytes, macrophages, and DCs, have been proposed based on their functions and/or ontogenies [28,36,39,40]. This debate is outside the scope of this piece of work.

For the purpose of this thesis, a macrophage is defined as a monocyte or embryonic yolk sac-derived myeloid leukocyte cell, one that is terminally differentiated (i.e. one that does not migrate between tissues), and one that expresses the CSF1R and is dependent upon signalling from this receptor for proliferation and survival.

1.2.1. Macrophages: Guardians of tissue homeostasis

The functions of macrophages can be distilled down to one fundamental process – maintaining tissue homeostasis. At steady state this typically involves phagocytosis and clearance of cellular debris, though awareness is increasing about the plethora of ways in which tissue macrophages maintain intra-tissue and even organismal metabolic homeostasis. Macrophages, whether recruited or tissue-resident, adopt tissue-specific characteristics. They possess the receptors and machinery to detect and respond to cytokines, adipokines, insulin, free fatty acids, hormones, pathogen and danger-associated molecular patterns (PAMPs and DAMPs), and other pathogen-associated mediators. Collectively, these mediators influence macrophage phenotype and function [27,41,42]. Macrophages are principal cells of innate immunity, forming an essential component of the first line of defence against invading pathogens [43]. This is of particular importance in mucosal sites, where tissue resident macrophages are poised to orchestrate inflammatory responses in a context-specific manner. Once a pathogenic or physiological challenge is cleared, macrophages undergo a phenotypic switch whereby they transition to a pro-repair programme which mediates tissue repair and the resolution of inflammation [44]. Macrophages are therefore of critical importance in contexts of health and

disease, and their dysfunction is implicated in autoimmunity, cancer, atherosclerosis, Alzheimer's disease, and numerous other disease contexts characterised and driven by inflammation.

1.2.2. Immune functions of macrophages

Chemotaxis

Similar to their single-celled predecessors, macrophages perform chemotaxis in response to molecular gradients, both soluble and substrate-associated. This mechanism guides their directional migration [45]. Macrophages do this via a mixture of amoeboid and mesenchymal migration, two forms of cellular movement that have different patterns of movement but utilise similar intracellular signalling pathways [45]. In both instances, the binding of a chemoattractant to a G-protein coupled receptor (GPCR; e.g. a chemokine receptor) at the leading edge of the cell induces activation of a PI3K/Akt/p38 cascade. This process induces activation of Rho GTPases, the central mediator of these pathways, which mediate the polymerisation of actin filaments that are used to move the cell in a directional manner. In the mid-region of the cell, acto-myosin-mediated contraction of the cell body moves the rear portion of the cell in the same direction [46]. In amoeboid cells, the Rho GTPases either directly activate myosin II or activate actin polymerisation via SCAR/WASP, and subsequently Arp2/3. In mesenchymal cell migration, Rho GTPases can activate mDia1 and mDia2 which induce adhesion to extracellular matrix (at multiple points – not restricted to the cell leading edge) or alternatively induce actin polymerisation via Arp2/3 that causes the extension of lamellipodia [45,46]. Through these mechanisms macrophages can move towards their targets at ~1.2 micrometres per minute [47]. Via these GPCR-mediated pathways, macrophages are capable of regulating chemotaxis in response to a variety of GPCR ligands, including chemokines, elements of the complement cascade (C3a, C5a), polyunsaturated fatty acid metabolites (leukotrienes and eicosanoids), and

formyl peptide [48,49]. Recently, the adipose tissue-derived protein hormone leptin, the systemic levels of which increase proportionally with fat mass [50,51], was shown to itself be a chemoattractant. Using primary murine bone-marrow-derived macrophages (BMDMs) it was demonstrated that that male BMDMs were intrinsically more migratory than female's, and revealed leptin itself as a chemoattractant for male but not female BMDMs [52].

Target sensing

Unlike lymphocytes of the adaptive immune system, macrophages (and other innate immune cells) do not direct receptor-mediated sensing in an antigen-specific manner [53]. Instead, they rely upon pattern recognition receptors (PRRs) that have evolved to recognise and bind to conserved molecular patterns on invading pathogens, infected cells, and dead, damaged, and dying cells. These conserved molecular patterns include PAMPs DAMPs. The binding of PAMPs and DAMPs by PRRs mediates a macrophage's ability to discriminate "self" from "non-self" and stimulates signal transduction pathways that result in effector function – the release of chemokines, cytokines, growth factors, reactive oxidative species, and the enhancement of phagocytosis – processes that mediate the clearance of pathogens and cellular debris [53–56]. Macrophages possess a veritable smörgåsbord of cell surface and intracellular receptors capable of initiating these responses. These can be subdivided into five main subfamilies of PRRs - Toll-like receptors (TLRs), the nucleotide-binding oligomerization domain (NOD)-like receptors (NLRs), the retinoic acid-inducible gene 1 (RIG-1)-like receptors (RLR; aka RIG-1-like helicases—RLH), the C-type lectin receptors (CLRs), and scavenger receptors [53–57] (SR; which will be discussed in more detail later in this thesis).

TLRs are perhaps the best characterised of the PRRs. The *Toll* gene was identified first in Drosophila in 1985 as a regulator of dorsal-ventral polarity in the Drosophila embryo [58].

Subsequent studies revealed that Toll encoded a transmembrane receptor, the ligands for which control different aspects of dorsal-ventral polarity in Drosophila [59]. In 1991, the signalling domain for Drosophila *Toll* was shown to be homologous to that of human interleukin 1 receptor, a gene with known immune function [60]. In 1996, Lemaitre and colleagues demonstrated that *Toll* plays an essential role in the antifungal response in adult Drosophila by inducing the expression of an antifungal peptide [61]. In 1997, a human homologue of Drosophila *Toll* was discovered – TLR4 – which could induce the expression of the pro-inflammatory cytokines IL-1, IL-6 and IL-8, the costimulatory molecule CD80 and thereby regulate the induction of adaptive immunity via the transcription factor nuclear factor (NF)-κB [62]. Thirteen TLRs have since been described, located on the cell membrane and intracellularly within endosomes, with functions spanning immunity to bacteria, fungi, viruses, and regulation of metabolic homeostasis [53,63,64].

The NLRs NOD1 and NOD2 are found in the cytosol of macrophages, specialised for the detection of pathogens that seek to escape phagosomes or replicate intracellularly. NOD1 and NOD2 recognise components of gram negative and gram positive bacterial cell walls (peptidoglycans) as well as single-stranded RNAs that characterise viral infections [65–67]. NLRs comprise a leucine-rich domain (LRR), a nucleotide-binding domain (NBD), and an effector domain. Binding of PAMP to the LRR induces a change in conformation that exposes the NBD and triggers oligomerisation and activation of the NLR. NLR assembly subsequently triggers activation of mitogen-activated protein kinases (MAPKs) and NF-κB, thereby inducing the expression of inflammatory genes and anti-microbial function [53,68].

RLR family members are intracellular PRRs similarly suited for the detection of intracellular pathogens. This family comprises a DexD/H helicase domain in the middle portion as the core

common element, with ATPase and helicase activities. The C terminal domain (CTD) is responsible for recognition of viral RNA, while the N-terminus caspase activation and recruitment (CARD) is the effector domain [69–71]. In resting state, RLRs are folded in a self-inhibited state, but upon CTD recognition of viral RNA conformational change results in multimerization, downstream signalling events and activation of the type I interferon response [72–74].

CLRs are a family of phagocytic PRRs that recognise carbohydrate on the cell surface of microbes in a calcium-dependent manner [75]. CLRs are upregulated in the context of inflammation and bind carbohydrate through conserved C-type lectin-like domains (CTLDs) [76,77]. The CLRs Dectin-1 and Dectin-2 signal through immunoreceptor tyrosine-based activation motifs (ITAMs) which facilitates the recruitment of SYK kinase and in turn activates the NF-κB-dependent pro-inflammatory response [77].

Another key process mediating macrophage target recognition is opsonisation. Opsonisation is the process by which opsonins – immunoglobulins, collectins, and complement proteins – bind and tag cellular and pathogenic targets to facilitate target phagocytosis [78]. Immunoglobulin G (IgG) antibodies are efficient opsonising agents that are recognised by macrophage-expressed receptors (FcγRs) that bind to the Fc region of IgG [79]. FcγRs containing ITAM intracellular motifs initiate intracellular signalling pathways that recruit kinases and activate phosphorylation cascades, while those containing ITIM (inhibitory) motifs recruit phosphatases that inhibit intracellular signalling [80]. ITAM-induced cascades result in phagocytosis, antibody-dependent cellular cytotoxicity, cytokine, lipid mediator and superoxide production in a context-dependent manner. Other FcRs exist for the different types of immunoglobulin molecules [80]. Complement proteins which circulate in the blood can also

opsonise microbial or cellular targets through antibody-dependent and antibody-independent mechanisms [78].

The complement system is activated through different pathways: the classical pathway (initiated by antibodies binding to target), the alternative pathway (activated by certain pathogen surfaces), and the lectin pathway (activated by the binding of lectins to carbohydrates on pathogen surfaces). Regardless of the activation pathway, the complement system converges at the formation of C3 convertase. This enzyme cleaves the complement protein C3 into two fragments: C3a and C3b. The C3b fragment is crucial for opsonisation. C3b can covalently bind to the surface of pathogens, marking them for recognition by phagocytic cells [78]. Phagocytic cells, particularly macrophages and neutrophils, have receptors on their surfaces (CR1-4 and CRIg) that specifically recognize and bind to C3b-coated pathogens. This interaction enhances the affinity of phagocytes for the opsonized particles [78,81].

Phagocytosis

Once a macrophage has reached an appropriate target for engulfment, they undergo rapid actin polymerization at the site of contact with the target particle. This polymerization drives the extension of pseudopods, membrane protrusions that surround the particle. Actin-binding proteins, such as Arp2/3 complex, facilitate the branching and polymerization of actin filaments, enabling the macrophage to project its membrane around the target [46]. As the pseudopods extend and engulf the particle, the membranes of the pseudopods fuse, enveloping the particle completely. This fusion creates a membrane-bound intracellular compartment termed the “phagosome”, which is the site of intracellular digestion [82,83]. Following the formation of the phagosome, it undergoes a maturation process involving fusion with endosomes and lysosomes, containing numerous factors essential for degradation of the

engulfed material [83,84]. This fusion event allows the phagosome to acquire additional components, including the acidifying proton pump V-ATPase. Acidification is crucial for activating enzymes within the phagolysosome, creating an increasingly acidic environment that is optimal for the activity of hydrolytic enzymes [85]. Subsequently, the maturing phagosome fuses with lysosomes, organelles filled with hydrolytic enzymes such as proteases, lipases, and nucleases, to form a phagolysosome, an organelle with a highly acidic pH and an array of degradative enzymes [11,85–87]. This degradation of the internalized material within the phagolysosome is essential during pathogenesis, for clearing infections, and homeostasis, for eliminating cellular debris [83,84].

Orchestration of the inflammatory response

Macrophages are among the most active secretory cells in the body, synthesising a variety of mediators in a context-specific manner that serve to regulate all aspects of the inflammatory response and the host response to invading pathogens. These mediators include cytokines, chemokines, reactive oxidative species which are integral to a successful anti-microbial response [88].

A functional dichotomy has been proposed for macrophage activation – the M1/M2 paradigm – in which "classically" activated macrophages are considered pro-inflammatory (M1) and "alternatively" activated macrophages are considered anti-inflammatory and pro-repair (M2) [89]. The M1/M2 paradigm is useful to characterise macrophage responses to precise factors *in vitro*. This paradigm becomes less useful *in vivo* and in the context of tissue macrophages, where these hyper-responsive cells are subject to copious amounts of tissue and circulation-derived factors which combine to influence macrophage phenotype and function [90]. Though the M1/M2 paradigm of macrophage polarisation is outdated, it is useful in illustrating the

context-dependent production of mediators by macrophages in a controlled system. M1 macrophages are considered pro-inflammatory and are generated *in vitro* in response to IFN-γ and LPS (or stimuli that induce TNFα). M1 macrophages are considered cytotoxic and anti-proliferative due to production of pro-inflammatory TNFα, IL-1, IL-6, IL-18, type I interferons, and the Th1-steering cytokines IL-12 and IL-23. Additionally, M1 macrophages produce high levels of reactive oxidative species (ROS) and reactive nitrogen species (RNS; e.g. H_2O_2, $ONOO^-$, NO•, and NO_2^-) and express high levels of nitric oxide synthase (NOS), making these cells potent anti-proliferative and cytotoxic effectors [87,91,92]. IL-1β and IL-18 protein production relies upon the assembly of the inflammasome. Upon sensing of activating signals by molecular sensors (NAIP, NLRP3/6/7, AIM2), inflammasome assembly occurs through the assembly of pro-caspase filaments which undergo autoproteolytic activation to form mature caspase 1/8. Caspase1/8-mediated cleavage of pro-IL-1β/18 results in the maturation and secretion of the inflammatory cytokines IL-1β and IL-18 [93,94]. Numerous GPCRs have been identified as regulators of macrophage polarisation. Different protein isoforms/ligands binding the same GPCR can differentially regulate macrophage polarisation. The inhibitory heterotrimeric G-proteins (Gαi) are central intracellular mediators of GPCR-mediated signalling cascades, and $G\alpha i_2$ activity was shown to regulate macrophage polarisation *in vitro* and thereby regulate inflammasome activation and cytokine production [95].

M2 or "alternatively activated" macrophages are induced *in vitro* in response to IL-4, IL-13, IL-10 and TGF-β, and are considered anti-inflammatory and pro-repair, in direct contrast to their M1 counterparts. M2 macrophages secrete low/nil amounts of pro-inflammatory cytokines and RNS/ROS, have high arginase activity, and high amounts of the anti-inflammatory mediators IL-10 and TGF-β. These cells are therefore thought of as immunosuppressive and inhibitors of T cell proliferation [87,91,92]. Indeed, macrophages are

important and have demonstrable roles in the regulation of lymphoid function. F4/80, a murine macrophage-specific protein [39,96], is essential for the induction of antigen-specific immune tolerance. Mice lacking F4/80 are unable to generate antigen-specific regulatory T cells and oral tolerance in response to antigenic challenge and develop a delayed type hypersensitivity response [97]. In the context of filarial infection – characterised by downregulation of the host immune response – $F4/80^+$ cells are recruited to the site of infection that suppress antigen-specific T cell proliferation [98]. In a model of viral infection it was demonstrated that subcapsular sinus lymph node macrophages capture virus particles and present them to migrating B cells in lymph node follicles, thereby inducing antigen-specific B cell activation [38]. *In vitro* studies using murine bone marrow-derived macrophages and macrophage cell lines have demonstrated that cellular metabolic changes underly different types of macrophage inflammatory responses. M1 polarisation via LPS and type I interferon induces a metabolic switch from oxidative phosphorylation to glycolysis, characterised by upregulation of GLUT1, increased glucose uptake and utilisation, HIF-1α and increased generation of ROS [99–101]. In contrast, M2-polarisation via IL-4 does not require glycolytic stimulation, instead relying upon oxidative phosphorylation and fatty acid oxidation, characterised by carbohydrate kinase-like protein and HIF-2α expression, [99,102–104]

In addition to the immunomodulatory effects that macrophages exert via cytokine production, they can also potently regulate the cellular composition of the inflammatory response via the production of chemokines – signalling mediators with a particular ability to attract leukocytes via cognate chemokine receptors. Like their cytokine responses, macrophage chemokine responses are highly context dependent. Macrophages are capable of attracting monocytes (which differentiate into macrophages), neutrophils, basophils, eosinophils, T cells, regulatory

T cells, and B cells, via synthesis and release of the chemokines CCL1, CCL2, CCL5, CCL13, CCL16, CCL17, CCL18, CCL22, CCL24, CXCL8, and CXCL16 [105].

1.2.3. Homeostatic and physiological functions of macrophages

Macrophages are most famous for their immune and inflammatory functions. However, increasingly macrophages are gaining prominence for their "para-immune" functions which maintain and regulate tissue and whole-organism physiology and homeostasis. Gordon and Plüddemann [106] commented that the MPS was comparable to the nervous and endocrine systems in that it is adaptable, regulated, and able to perform trophic functions locally and systemically – "*Macrophages can be thought of as a dispersed homeostatic organ*" [106]. Indeed, macrophages have a diverse and tailored range of homeostatic and physiological functions in virtually every tissue in which they are found.

M-CSF-dependent osteoclasts – the tissue resident macrophages of the bone – are necessary for bone resorption [107]. Pioneering studies demonstrated that osteoclasts are capable of degrading both the inorganic and organic fractions of bone tissue [107]. Osteoclasts first degrade the inorganic fraction of bone matrix by creating a highly acidified microenvironment in the synapse between the osteoclast and bone, via a vacuolar H^+–adenosine triphosphatase expressed from in the cell's bone-facing ruffled membrane [108]. This is followed by degradation of the bone's organic phase mediated by osteoclast-derived cathepsin K which degrades the extracellular matrix [109]. Microglia in the brain have been shown to modulate the wiring of dopaminergic axons in the embryonic forebrain [110]. Postnatally and during periods of active synaptic pruning, microglia were shown to contribute to this process by engulfing and "pruning" presynaptic inputs in a complement-dependent manner [111]. Tissue resident macrophages in the heart's atrioventricular node closely associate with and are electronically

coupled with cardiomyocytes via the gap protein connexin 43. Through this mechanism cardiac macrophages were shown to facilitate electrical conduction in the atrioventricular node [112]. In the context of experimental injury, cardiac macrophages in zebrafish were shown to synthesise and deposit collagen, thereby contributing to tissue repair and scar formation in the damaged heart [113]. In the prenatal lung, macrophages temporally accumulate at branch points during branching morphogenesis and adopt a M2-like, tissue remodelling phenotype indicating a possible role in regulation of lung development [114]. Targeted depletion of muscularis macrophages in the large intestine demonstrates an essential role for the cells in peristalsis – their depletion results in intestinal dysmotility, an effect that has been traced to macrophage signalling to enteric neurons via secreted bone morphogenetic protein 2 [115]. In the liver, Kupffer cells (liver-resident macrophages) via scavenger receptors, and CCR2-dependent recruited liver macrophages via ferroportin, remove dead and damaged erythrocytes and their components from the circulation and recycle iron into hepatocytes [116,117]. In adipose tissues, sympathetic neuron-associated macrophages (SAMs) were shown to supress lipolysis in the context of obesity, an effect mediated by catabolism of lipolytic norepinephrine. SAMs were thereby demonstrated as regulators of whole organism body weight [118]. Similarly, adipose tissue-resident macrophages were recently shown to positively regulate whole organism body weight through a secreted factor, which controls the extent to which adipocytes accumulate lipids – a mechanism that was responsive to antibody-mediated therapeutic intervention. High fed diet-fed mice treated with therapeutic antibody remained lean, in contrast to isotype control antibody-treated mice which gained weight – an effect independent of food intake [24,119].

Collectively these findings demonstrate that macrophages are much more than “just” immune cells. Tissue macrophages perform a variety of tissue-specific, homeostatic, and physiological roles suited to the niche in which they are found. Moreover, these findings demonstrate that

once the mechanisms mediate these effects are fully elucidated, macrophages may be well suited for targeted therapeutic interventions in physiological disorders.

1.2.4. Macrophage dysfunction in disease

As outlined above, macrophages are a highly pleiotropic cell type capable of mediating inflammation, immune tolerance, and normal tissue physiology in a variety of contexts. However, this pleiotropy means that macrophages can be considered a double-edged sword. They possess an outsized capacity to inhibit, but also facilitate disease pathogenesis. Similar to their roles in maintaining tissue physiology, macrophages can also contribute to disease pathophysiology in a numerous contexts.

Microglial phagocytosis of cellular and myelin debris is an important regulator of central nervous system homeostasis [120]. The autophagy protein becilin 1 is essential for this process – its deletion impairs the recycling of the phagocytic receptors TREM2 and CD36 from the cell surface membrane to the phagosome and its levels are reduced in microglia from human Alzheimer's Disease (AD) patients [121]. Indeed, disease associated microglia and inflammatory macrophages expressing TREM2 accumulate in ageing and AD in mice and genome-wide association studies in humans have linked *Trem2* variants with susceptibility to AD [122,123]. In Rheumatoid Arthritis (RA), the chronic inflammatory and autoimmune disease in which synovial tissue becomes inflamed and degraded, macrophages play a central role [124]. In mouse models of the disease, Ly6C^{-} monocytes that differentiate into synovial macrophages are causative in the joint swelling and clinical features that characterise the disease [125]. In humans, proinflammatory macrophages, characterised by high expression of TNFα CCL2, and IL-6, are strongly associated with active disease and their decline is associated with disease remission [126]. TNFα is a main mediator of joint inflammation in RA and its inhibition using therapeutic

antibodies substantially diminishes joint erosion and systemic bone loss as assessed by bone mineral density [127].

In addition to their aforementioned roles in regulation of organism body weight at steady state and in obesity, adipose tissue macrophages are implicated in the metabolic dysfunction that comes with obesity [42]. Upon high fat diet (HFD) feeding, adipose tissue macrophages accumulate in adipose tissue depots and undergo a phenotypic switch from an M2-like phenotype (expressing *Il10, Arg1*) to a pro-inflammatory M1-like state characterised by increased expression inflammatory markers (*Tnfa, Il6, Nos2*) [128,129]. With obesity comes an enhanced risk of developing insulin resistance and type 2 diabetes. TNFα has long had an established tole in insulin resistance, since its levels are increased in obesity, and its neutralisation attenuates insulin insensitivity *in vivo* [130]. Macrophages, as the primary cellular source of TNFα in obesity [129,131] are now firmly implicated in insulin resistance. TNFα reduces glucose uptake of adipocytes in response to insulin [130]. *In vitro* treatment of adipocytes with the TNFα antagonist IL-10 reduces their capacity to attract macrophages via CCL2 and prevents the effects of TNFα on blocking insulin-stimulated glucose uptake [128]. Mice in which the macrophage chemoattractant CCL2 is overexpressed have higher levels of macrophage accumulation in adipose tissue, associated with elevated plasma and adipose TNFα levels and insulin resistance [132].

Though our understanding of COVID-19 pathophysiology remains incomplete, macrophages are believed to play a central role [133]. A study of 600 individuals hospitalized with COVID-19 found that COVID patients had higher levels of blood monocytes than non-COVID afflicted controls, with a depletion of lung-resident alveolar macrophages and an increase in inflammatory monocytes and monocyte-derived macrophages [134]. In a mouse model of

COVID-19, which has a humanised immune system, lung macrophages were shown to be infected by the virus, which caused inflammasome activation, IL-1 and IL-18 production, and pyroptosis, contributing to tissue inflammation. Inflammasome inhibition reversed chronic lung pathology, indicating a causative role for macrophages in disease pathogenesis [135].

The intestine, as a mucosal barrier, is constantly exposed to inflammatory stimuli yet is remarkably effective at suppressing tissue inflammation through a variety of anti-inflammatory pathways that have evolved to ablate TLR signalling [136]. In inflammatory bowel disease (IBD) these pathways are dysregulated. A comparison between quiescent IBD, the healthy intestine, and active IBD found an enrichment of pro-inflammatory monocytes in the colonic mucosa of IBD patients relative to controls. A similar pattern was observed in a mouse model of IBD [137]. A study in humans showed that macrophages were defective in IBD patients – they were less efficient at clearing injected dead E.coli and labelled neutrophils, and exhibited disordered cytokine responses [138]. Tumour-associated macrophages (TAMs) are generally attributed a maladaptive role in oncogenesis and cancer progression [139]. TAMs adopt an M2-like anti-inflammatory phenotype which serves to inhibit what would be a more adaptive M1-like pro-inflammatory response [140]. Additionally, TAMs have been shown to enhance tumour vascularisation via production of VEGF and promote epithelial-mesenchymal transition which precedes tumour invasion and metastasis [140,141]. TAMs are consequently commonly associated with poor prognoses across various cancers [142,143].

Atherosclerosis is a disease which causes a build-up of modified lipids, smooth muscle cells, endothelial cells, and leukocytes in the arterial wall. These accumulations of cells, termed atherosclerotic plaques, causes a narrowing of the arterial lumen and is the primary contributor towards the development of cardiovascular diseases [144]. As plasma LDL cholesterol levels rise

so does their retention in the subendothelial space [145]. Circulating monocytes in the migrate into the intima in response to CCL5 and CXCL4 [146]. Monocyte-derived macrophages scavenge modified LDL to form foamy macrophages – lipid and cholesterol laden cells – that form the fatty streaks that characterise atherosclerosis [147]. Inhibition of monocyte accumulation in the plaque, and thereby inhibition of foam cell formation, substantially slows plaque formation and disease progression [148–150].

1.2.5. Macrophage and cholesterol metabolism

The pathways that have evolved in macrophages to defend the body against infections and mediate tissue homeostasis, such as the phagocytosis of pathogens and cellular debris, also apply to lipid and cholesterol metabolism. Though systemic cholesterol excess is typically considered in the context of atherosclerosis, hypercholesterolaemia has been associated with enhanced risks of numerous pathophysiologies, including chronic kidney disease, non-alcoholic fatty liver disease, non-alcoholic steatohepatitis, diabetes, testosterone deficiency, hypothyroidism, and pituitary disorder [151]. Indeed, high concentrations of free cholesterol are toxic to cells, as evidenced by in vitro studies in which acyl coenzyme A:cholesterol acyltransferase (ACAT) – the enzyme that catalyses the intracellular esterification of cholesterol – is inhibited [152]. Macrophages express ACAT and are capable of esterifying cholesterol, a feature that is believed to underly foam cell formation in atherosclerosis [153,154]. Perhaps an evolutionary consequence of the toxicity of excessive free cholesterol, macrophages are able to uptake cholesterol-laden lipoproteins from the extracellular space via receptor-mediated uptake (CD36, SRA, SR-B1, and lectin-like oxLDL receptor-1; LOX-1), micro and macro-pinocytosis [155,156] and mediate the efficient trafficking of cholesterol from peripheral tissues to the liver in a process known as reverse cholesterol transport (RCT) – a key process in the maintenance of tissue homeostasis [157].

In RCT, ingested lipids are digested in the phagolysosome to form free cholesterol and free fatty acids. Free cholesterol can be re-esterified by the endoplasmic reticulum (ER) for storage intracellularly in lipid droplets or repackaged for efflux via high density lipoprotein (HDL) at the plasma membrane (Figure 1.2). Cholesterol efflux, the movement of cholesterol from cells to HDL and apoA-I takes place via active and passive pathways. In the active pathways, the accumulation of cellular cholesterol triggers the activation of specific transcription factors, including Liver X Receptor α and β (*Lxra, Lxrb*), Retinoid X Receptor (*Rxr*), and members of the Peroxisome Proliferator-Activated Receptor (Ppar) family such as *Ppara* and *Pparg* [157,158].

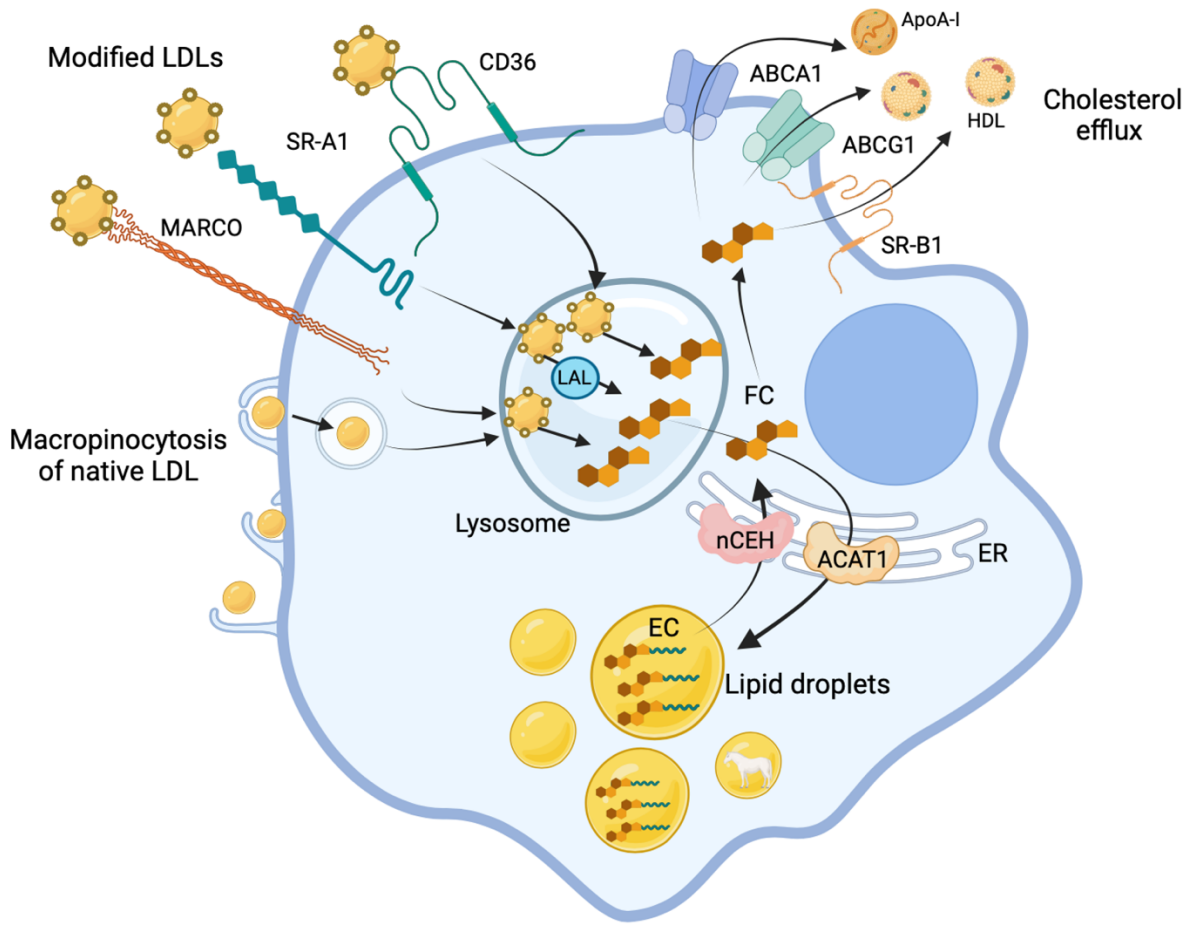


Figure 1.2. Macrophage cholesterol metabolism. Macrophages engulf and take up modified forms of cholesterol via scavenger receptors including MARCO, SR-A1, and CD36, and are capable of taking up native LDL via non-selective micropinocytosis pathways. Internalised LDLs are localised to acidified lysosomes, where lysosomal acid lipase (LAL) hydrolyses cholesterol esters (EC) contained

in LDL to free cholesterol (FC). FC is esterified by ACAT1 in the endoplasmic reticulum (ER) prior to storage in intracellular lipid droplets, and this EC can be further hydrolysed by ER neutral cholesterol ester hydrolase (nCEH) to generate FC that can be exported in cholesterol efflux pathways. The ATP-binding cassette (ABC) transporters ABCA1 and ABCG1, and scavenger receptor SR-BI, mediate the export of free cholesterol to the cholesterol acceptors HDL and apolipoprotein A1 (ApoA-I). Adapted from references [155,159]

These activated transcription factors form heterodimers and enhance the expression of the transporters ATP-binding cassette subfamily A member 1 (ABCA1) and ATP-binding cassette subfamily G member 1 (ABCG1). ABCA1 and ABCG1 mediate the transfer of plasma membrane, endosomal cholesterol, and phospholipids to lipid-poor apolipoprotein A-I and the poorly lipidated lipoproteins to form high density lipoprotein (HDL) [160,161]. Passive pathways of cholesterol efflux can take place via aqueous diffusion or SR-BI-mediated efflux. In aqueous diffusion, cholesterol molecules diffuse from membranes, down a concentration gradient and through a liquid phase towards an acceptor molecule in the cellular membrane where they are adsorbed [162]. In SR-BI-mediated efflux, the scavenger receptor SR-BI mediates the transfer of free cholesterol to phospholipid-containing acceptors e.g. HDL[162]. Once cholesterol has been packaged into HDL particles, HDL travels via the bloodstream to the liver where it is excreted in bile [162]. Macrophages are therefore central regulators of intra-tissue and organismal cholesterol metabolism.

1.3. The adrenal gland: development, anatomy, physiology, and pathology

The adrenal glands (AGs) are multi-layered hormone-secreting glands situated just superior to the kidneys of mammals. The role of each part of the gland is illustrated in Figure 1.3: glucocorticoids (cortisol in humans, corticosterone in rodents) are secreted from the zona fasciculata (ZF); mineralocorticoids (namely, aldosterone) from the zona glomerulosa (ZG); androgens from the zona reticularis (ZR; humans only), and catecholamines (adrenaline, noradrenaline) from the medulla. The AG is therefore a critical regulator of the stress response,

metabolism, cognition, the immune response, and blood pressure [163–167]. The corticosteroids (steroid hormones produced by the cortex) are derived from cholesterol as the common precursor molecule. Adrenal steroidogenesis is tightly regulated to maintain physiological balance in the body. This regulation is the product of interplay between hormones, enzymes, cholesterol, and whole-body axes that cooperate to maintain steroidogenic equilibrium.

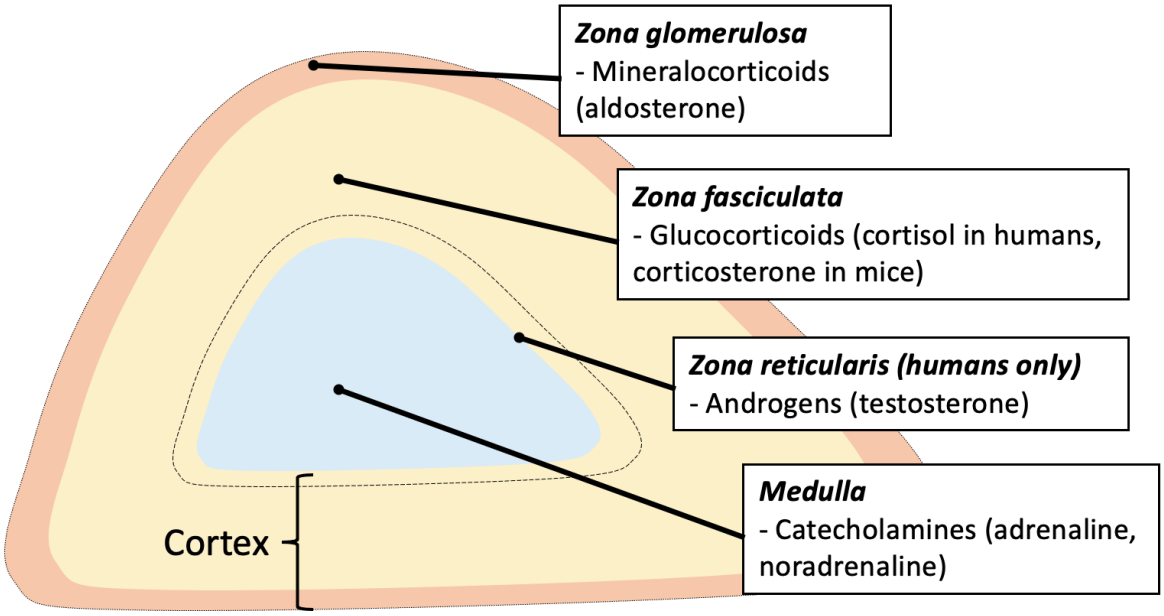


Figure 1.3. Adrenal gland structure and function. The adrenal gland cortical layers secrete hormones in a zone and species-specific manner, while the inner medulla secretes the catecholamines.

1.3.1. Adrenal gland development

The AGs and gonads derive from a common developmental origin – the adrenal gonadal primordium (AGP) which comprises a mix of adrenocortical and somatic gonadal progenitor cells [168]. In the mouse, the AGP first becomes distinct as a thickening of the coelomic epithelium occurring around embryonic day 9.5 (E9.5), which is marked by expression of the nuclear steroidogenic factor 1 (SF-1) [169]. In humans, this occurs 28–30 days post conception (dpc) [170]. By E10.5 the adrenal and gonad developmental pathways separate as AGP cells migrate differentially. Those that migrate dorsolaterally form the gonadal primordial, while

those that migrate dorsomedially and invade the underlying mesenchyme of the intermediate mesoderm to form the adrenal primordial, ventrolateral to the dorsal aorta [168,169,171]. Within the adrenal primordium, two distinct embryologic tissues seed the adrenal medulla and cortex: the medulla derives from neural crest cells, while the cortex develops from the lateral plate mesoderm [168,171]. Neural crest cells that seed the medullary chromaffin cells invade the adrenal primordium at E12.5 [172]. By E14.5 in mice (52 dpc in humans) the adrenal gland primodium separates from the surrounding mesenchyme and becomes encapsulated by a fibrous layer forming the immature adrenal gland [173]. The precise mechanisms that mediate this process remain unclear [174]. In humans, the embryonic adrenocortical zone expands rapidly after this point. The fetal cortex (fetal zone; FZ) proliferates rapidly, comprising ~80% of the AGs prenatally. These cells are large in size and highly steroidogenic, characterised by the expression of CYP17A1 – an enzyme that converts pregnenolone to dehydroepiandrosterone (DHEA) [168]. Eight weeks post gestation marks the development of the SF-1-expressing definitive zone (DZ), which forms between the capsule and the FZ. During the third trimester, cells of the DZ develop into mature, ACTH-responsive, glucocorticoid-synthesising adrenocortical cells, analogous to the zona fasciculata cells of the adult adrenal cortex [168,175].

The murine FZ is characterised by the activity of a fetal adrenal enhancer (FAdE) located in the *Sf1* gene, which regulates expression of SF-1 in the primordial AG [176]. FAdE expression declines after E14.5 as the DZ develops and the regulation of SF-1 expression shifts to another enhancer yet to be defined [176]. Studies using FAdE-Cre mice for lineage tracing suggest that the murine DZ and steroidogenic adult adrenal cortex derive from the FAdE-expressing FZ [177]. In contrast, lineage tracing based on expression of Sonic Hedgehog (*Shh*) and Glioblastoma 1 (*Gli1)*, a downstream activator of the Sonic Hedgehog signalling pathway, revealed that non-steroidogenic Gli1-expressing cells located in the embryonic adrenal capsule are the progenitor

cells for DZ and adult steroidogenic adrenocortical cells [178]. The gap between these seemingly conflicting findings was bridged by a study which demonstrated that Gli1-expressing capsular cells themselves derive from a FAdE enhancer-expressing FZ cells [179]. This finding unifies the two studies, showing that a FAdE enhancer-expressing FZ cells give rise to capsular non-steroidogenic cells, which in turn give rise to steroidogenic DZ and adult steroidogenic adrenocortical cells. In postnatal rodents, the remaining FZ cells, typically termed the X-zone, regresses in a sexually dimorphic fashion. In males, the X zone declines at the onset of puberty, while in females the zone recedes during the first pregnancy [180].

In the adult adrenal gland, linage tracing indicates that adrenocortical zonation results from lineage conversion of differentiated ZG cells to ZF cells [181]. Using Cyp11b2-Cre ; R26RmT/mG-mediated tracing it was shown that *Cyp11b2*-expressing cells migrated centripetally over time in adult mice, in a manner suppressible by dexamethasone treatment and dependent upon ZG cell expression of SF-1 [181]. The SHH and WNT signalling pathways appear to be instrumental in adrenocortical cell maintenance. Similar linage tracing approaches demonstrate that *Shh* and *Gli1*-expressing progenitors in the adrenal capsule seed steroidogenic ZG cells, and inhibition of SHH signalling impairs regrowth of ZF cells following dexamethasone-mediated ZF suppression [182,183]. Progenitor cell-specific deletion of the WNT signalling gene *Rspo3* impairs ZG differentiation and impairs steroidogenic capacity, while genetic ablation of the WNT signalling pathway impairs recovery from dexamethasone-induced adrenal suppression [183,184]. Collectively, these findings demonstrate that in adult mice capsular progenitor cells seed steroidogenic centripetally migrating adrenocortical cells in a WNT and SHH-signalling-dependent manner.

1.3.2. Adrenal gland structure and function

The AGs are multi-layered and are broadly divided into the adrenal cortex and medulla (Figure 1.3). The adrenal cortex derives from the DZ and is further functionally and morphologically subdivided into the zona glomerulosa (ZG), zona fasciculata (ZF), and zona reticularis (ZR). The adrenal cortex is responsible for the production of the corticosteroids – steroids that derive from the cortex – which are all synthesised from cholesterol as the common precursor molecule via a series of enzymatic reactions [168]. The ZG typically forms a continuous subcapsular layer around the outside of the gland and is characterised by expression of CYP11B2 (aldosterone synthase) and is the body's sole producer of the mineralocorticoid aldosterone [168]. Aldosterone-producing ZG cells arrange in distinct multicellular functional "rosettes" that are morphologically distinct from the other cortical zones and work in concert to synthesise aldosterone [185]. However, it has been reported that, due to the effects of high salt diets common in western culture, the ZG in adults is actually comprised of numerous distinct aldosterone producing cell clusters located beneath the capsule [186].

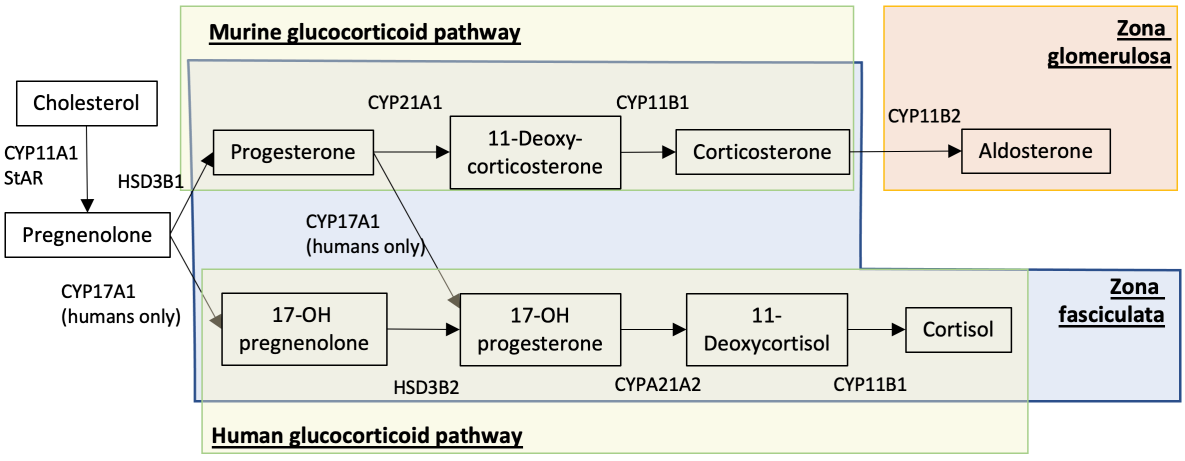


Figure 1.4. Adrenal corticosteroid biosynthesis. The zones and enzymes that mediate the conversion of cholesterol to the glucocorticoids and mineralocorticoids in humans and mice.

The ZF is the primary constituent of the adrenal cortex, comprising cells that are larger and compiled into bundles – fascicles – characterised by expression of CYP11B1. Steroidogenic

ZF cells are the body's primary producer of glucocorticoids [168]. The ZR is the innermost layer of the cortex, present in primates only, and characterised by expression of CYP17A1 which hydroxylates pregnenolone which is subsequently metabolised into cortisol – the primary glucocorticoid in primates (Figure 1.5) [168]. Cells of the ZR also produce the androgen precursor molecules dehydroepiandrosterone (DHEA) and androstenedione from pregnenolone [187]. Pregnenolone is converted to DHEA via the dual action of a complex comprising CYP17A1, its obligate redox partner NADPH-cytochrome P450 oxidoreductase, and cytochrome b5 [187]. DHEA is further converted to DHEA-sulfate via SULT2A1 [168]. These precursor androgens have weak androgenic activity in this form but are taken up by peripheral tissues including the hair follicles, genital skin, and prostate to be converted to androstenedione by 3β-hydroxysteroid dehydrogenase (HSD3β), which can then be converted into the more potent androgen testosterone by 17β-hydroxysteroid dehydrogenase (17β-HSD), or estradiol by aromatase [168,188].

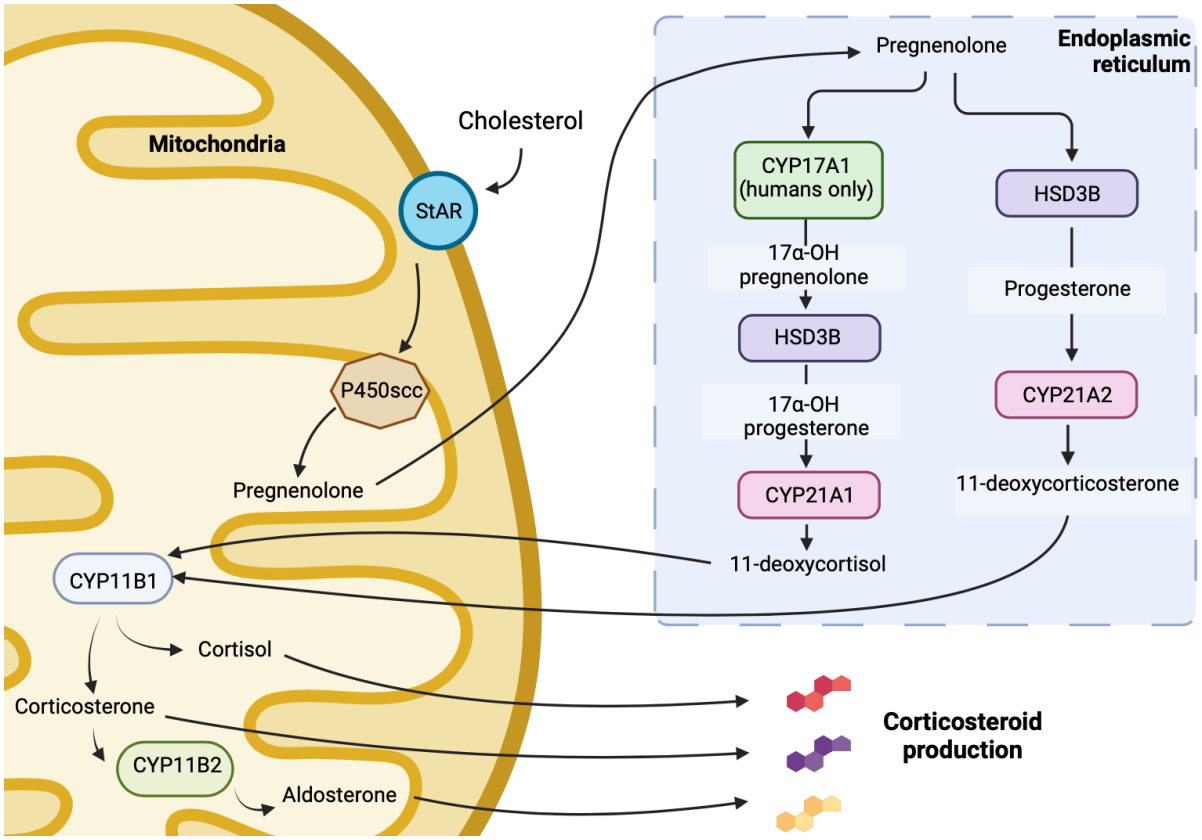


Figure 1.5. Intracellular adrenal corticosteroid biosynthetic pathway. The precursor for cortisol, corticosterone, and aldosterone synthesis is cholesterol, which is derived from circulating lipoproteins. Cholesterol is transported into the mitochondria of adrenal cells, where the initial steps of steroidogenesis take place. The conversion of cholesterol to pregnenolone is catalysed by the enzyme cytochrome P450 side-chain cleavage (P450scc ; CYP11A1) and takes place within the inner mitochondrial membrane. In the human pathway, pregnenolone is then converted to 17α-hydroxyprogesterone through a series of enzymatic reactions, with 17α-hydroxylase (CYP17A1) and 3β-hydroxysteroid dehydrogenase (HSD3β) playing a crucial role. This reaction occurs within the endoplasmic reticulum. In rodents, which lack CYP17A1, pregnenolone is converted into progesterone and 11-deoxycorticosterone via HSD3β and CYP21A2. The next step involves the 21-hydroxylation of 17α-hydroxyprogesterone, catalysed by the enzyme 21-hydroxylase (CYP21A1), resulting in the formation of 11-deoxycortisol. 11-deoxycortisol is imported back into the mitochondria where 11β-hydroxylase (CYP11B1) performs the 11β-hydroxylation of 11-deoxycortisol to from cortisol and corticosterone. For aldosterone synthesis, aldosterone synthase (CYP11B2) mediates the conversion of corticosterone to aldosterone.

1.3.3. Glucocorticoids: regulation and mechanism of action

Glucocorticoids (GCs) are hormonal regulators of numerous essential physiological processes in all mammals, with evident effects on metabolism, water and electrolyte balance, the immune response, growth, cardiovascular function, mood and cognitive functions, reproduction, and development [163,167,189–193]. Once produced by steroidogenic cells, GCs are secreted into the bloodstream where they bind to and are transported by the serum proteins albumin, sex hormone-binding globulin (SHBG), and corticosteroid-binding globulin (CBG). Binding of GCs to transporter proteins maintains the GC in an inactive form [194]. Albumin is the most abundant serum protein and binds all steroid hormones, albeit at a much lower affinity than SHBG and CBG, the latter of which has the highest GC affinity, binding ~90% of GCs [195]. Proteases are responsible for the release (and hence activation) of GCs from carrier proteins, such as neutrophil elastase which targets CBG and causes the release of active GC at sites of inflammation [196,197]. As lipophilic molecules, unbound GCs are free to diffuse through cellular membranes and exert their biological function. Within the cell, the prevalence of two competing enzymes regulates the bioavailability of active GCs. 11β-HSD2 oxidises cortisol into the inert metabolite cortisone, while 11β-HSD1 catalyses cortisone into bioactive cortisol [198]. Mechanistically, active GCs competitively bind to the glucocorticoid receptor (GR)

intracellularly [199–201]. Active GCs and mineralocorticoids are capable of binding to the GR *in vitro* with similar affinities to their structurally related receptor, the mineralocorticoid receptor (MR) [202].

The GR is a member of the nuclear receptor superfamily of ligand-dependent transcription factors, is expressed by nearly every cell in the body, and is essential for survival after birth [203,204]. Upon GC binding, GR undergoes a conformational change that expels bound inhibitory proteins, dimerises (though can function as a monomer), and exposes nuclear-localising moieties that facilitate its rapid trafficking into the nucleus. In the nucleus, the GR binds glucocorticoid responsive elements (GREs) of DNA to initiate or suppress transcription [205,206]. It is by this mechanism that GCs exert their effects.

The production of GCs from the adrenals is regulated by the hypothalamic-pituitary-adrenal (HPA) axis (Figure 1.6). The HPA axis is seated in the paraventricular nucleus (PVN) of the hypothalamus, the pituitary gland, and the adrenal gland, while the circulation acts as the channel that relays signals between these nodes [207]. Circadian rhythm, emotional stress, and physical stress influence the release of corticotropin-releasing hormone (CRH) and arginine vasopressin (AVP) from the PVN which bind their receptors CRH-R1 and V1B in the pituitary gland and stimulate the release adrenocorticotrophic hormone (ACTH) into the circulation [207]. ACTH is generated by cleavage of the precursor polypeptide Pro-opiomelanocortin (POMC) which is synthesised in corticotrophs of the anterior pituitary gland. ACTH travels through the circulation to stimulate the production and secretion of glucocorticoids (and to a lesser extent, aldosterone) from the adrenal cortex [208]. ACTH binds melanocortin receptor 2 (MC2R) expressed by endocrine cells of the adrenal cortex. This induces adenylyl cyclase, and in turn cAMP production, PKA activation, and phosphorylation of specific nuclear factors. The

binding of these nuclear transcription factors stimulates the upregulation of corticosteroid biosynthetic genes including *Star*, *Cyp11a1*, *Cyp17a1*, and *Cyp11b1,* and *Scarb1*, a gene encoding the receptor that mediates the uptake of cholesterol that fuels steroidogenesis [209,210] (Figure 1.8). The rate limiting step of GC and mineralocorticoid biogenesis is the mobilisation of cholesterol and its trafficking across the mitochondrial membrane – a process fundamentally regulated by STAR (steroidogenic acute regulatory protein) (Figure 1.5) [208]. Negative feedback loops induced by GCs serve to limit activation of this axis. Activated GR can bind to negative GREs which suppress the transcription of *POMC*, *CRH*, and *CRH-R1,* and thereby suppress activation of the HPA axis [194,211,212]. The nuclear receptor Nur77 binds the POMC promoter to activate its transcription, but GR can bind Nur77 protein and inhibit its transcription activity, effecting an additional negative feedback loop in the HPA axis [213,214].

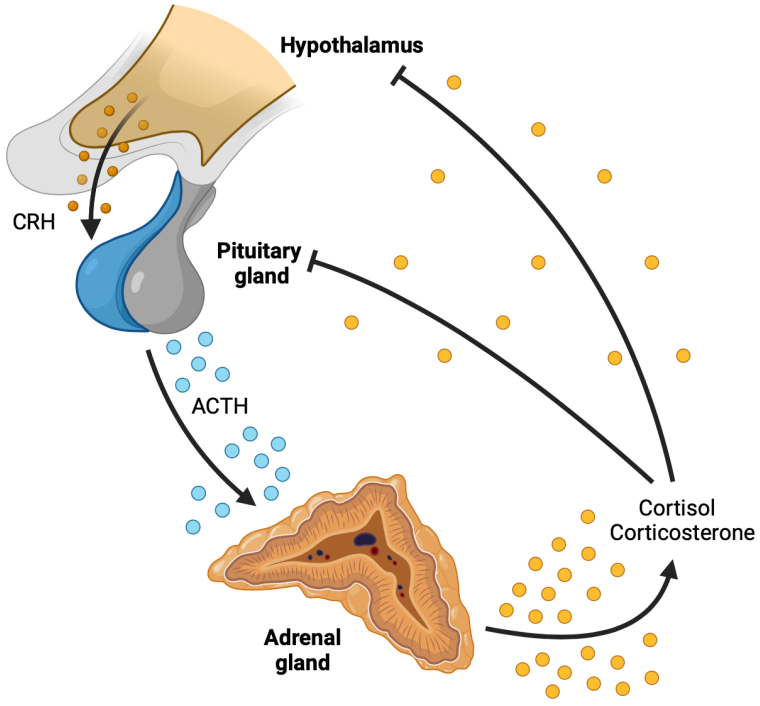


Figure 1.6. The hypothalamic-pituitary-adrenal axis. Various stressors, such as physical, psychological, environmental challenges, can trigger activation of the HPA axis and the stimulation of corticotropin-releasing hormone (CRH) from the hypothalamus. CRH then travels through the bloodstream to the anterior pituitary gland and stimulates the anterior pituitary gland to release adrenocorticotropic hormone (ACTH). ACTH travels via the circulation to the adrenal glands and stimulates the adrenal cortex to produce and release cortisol/corticosterone. Cortisol/corticosterone, once released into the bloodstream, exerts negative

feedback on the hypothalamus and the pituitary gland. Elevated cortisol/corticosterone levels thereby inhibit the release of CRH from the hypothalamus and ACTH from the pituitary, thereby providing a mechanism for self-regulation. Adapted from reference [207].

1.3.4. Mineralocorticoids: regulation and mechanism of action

Aldosterone is the primary mineralocorticoid synthesised by cells of the zona glomerulosa (ZG). The final step of aldosterone synthesis is catalysed by aldosterone synthase (CYP11B2), which mediates the conversion of 11-deoxycorticosterone into aldosterone. Aldosterone is a principal regulator of blood pressure, electrolyte, and fluid homeostasis [215]. Like GC, aldosterone binds serum proteins (mostly albumin) on which the steroid is transported by the circulation to its site of action [195]. Due to aldosterone's lipophilic nature, like GC it also diffuses through the cellular membrane and binds its intracellular receptor – the mineralocorticoid receptor (MR). Like the GR, the MR is a member of the steroid receptor family of ligand activated transcription factors [202]. Upon binding, the MR releases accessory proteins (heat shock proteins, immunophilins), translocates to the nucleus, binds mineralocorticoid-responsive elements (MREs), and thereby activates or represses transcription of target genes [216]. The MR is expressed most prominently in the vasculature and on epithelial cells in the kidney where it exerts its cardiovascular effects, but also in the adipose tissue, heart, endothelial cells, vascular smooth muscle cells, and the brain where it exerts effects on memory, neuronal differentiation, metabolism, inflammation, endothelial dysfunction, and ageing [202,215]. The MR shares significant structural and functional kinship with the GR and has similar affinity for aldosterone and GCs *in vitro* [217]. Despite promiscuity in ligand binding and similar affinities of MR for multiple ligands, mineralocorticoids exert differential biological effects from GCs *in vivo* due to MR exhibiting different "preferences" for ligands in different tissues. The MR has a higher preference for aldosterone in the kidney and colonic mucosa, but higher preference for GC in the brain [202,218,219]. Mechanistically, this preference is thought to be mediated by differing cellular expression of 11β-HSD1 and 11β-HSD2. In epithelial cells, endothelial cells,

and smooth muscle cells, 11β-HSD2 converts GC to its inactive metabolites and thereby promotes activation of MR by aldosterone [220–222]. In non-epithelial tissues with low or no 11β-HSD2 activity (e.g. brain, heart, adipose tissue) GC activity dominates the MR [215].

Functionally, aldosterone serves to activate sodium reabsorption across epithelia. Aldosterone acts via the MR on the distal tubule of the renal nephron and induces the expression of the apical epithelial sodium channel (ENaC) and the basolateral Na^+-K^+-ATPase [223,224]. This results in the unidirectional transport of sodium from the filtrate into the circulation and the bidirectional transport of potassium, with a net effect of increased potassium excretion into the urine, and sodium retention and water reabsorption into the blood, effects which cause increased blood volume and blood pressure [224]. A study in mice demonstrated that extra-renally, aldosterone-MR signalling in vascular smooth muscle cells also regulates blood pressure in adult mice and even more so in aged mice, via direct action on the myogenic tone of the vasculature [225].

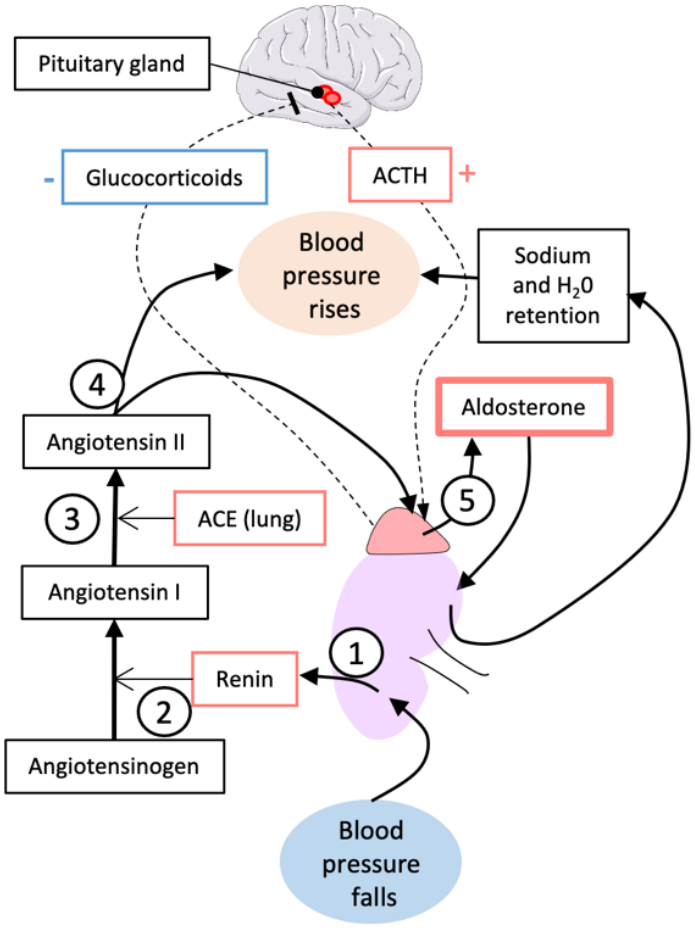


Figure 1.7. The Renin angiotensin aldosterone system (RAAS). Aldosterone is released in response hypotension-induced cascade beginning with kidney-released renin that cleaves plasma angiotensinogen to angiotensin I. Angiotensin converting enzyme 1 (ACE) cleaves angiotensin I to form angiotensin II, which stimulates zona glomerulosa cells of the adrenal cortex to synthesise and release aldosterone. Aldosterone causes sodium and water reabsorption into the blood, which increases blood volume and thereby blood pressure. Pituitary gland derived adrenocorticotropic hormone (ACTH) also stimulates the release of cortical hormones, including aldosterone and glucocorticoids. Glucocorticoid release forms the efferent arm in a negative feedback loop that inhibits ACTH release.

Adrenal production of aldosterone is regulated by the renin-angiotensin-aldosterone system (RAAS; Figure 1.7). In response to falls in blood pressure the kidney secretes renin into the bloodstream. Renin cleaves circulating angiotensinogen to form angiotensin I, which is cleaved by angiotensin converting enzyme (ACE), found primarily in the lung, to the bioactive angiotensin II (AngII). AngII exerts its effects by binding its receptors AT1R and AT2R – both G protein-coupled receptors – which are expressed by ZG cells in the adrenal cortex, vascular smooth muscle cells, endothelial cells, cardiac myocytes, cardiac fibroblasts, and renal

mesangial cells [226]. AngII binding to AT1R induces complex intracellular signalling cascades involving phospholipase C, phospholipase D, phospholipase A2, mitogen-activated protein kinase, trysone kinase, RhoA/Rho, adenylyl cyclase, and ion channels, such as L-type and T-type voltage-sensitive calcium channels. It is primarily though the more highly expressed AT1R that AngII mediates its effects on vascular constriction, aldosterone release, salt and water retention, and blood pressure [226]. The mechanism of this process is shown in Figure 1.8. In ZG cells, AngII induces Ca^{2+} influx into the cytoplasm via voltage-sensitive calcium channels in the endoplasmic reticulum and a rapid increase in intracellular Ca^{2+} levels, followed by decreasing oscillations in calcium levels. Intracellular Ca^{2+} activates the calmodulin-dependent protein kinases (CaMK) which, in turn, inducs the activation of the transcription factor CREB, which transcribes corticosteroid biosynthetic genes [185,227–229]. *In vivo* studies have demonstrated that AngII induces rapid upregulation of *Cyp11b2*, in addition to a delayed upregulation *Star* and *Cyp11a1* – genes encoding the essential aldosterone biosynthetic machinery [230]. K^+ is the other major physiological stimulant of aldosterone production. ZG cells are highly polarised and sensitive to extracellular K^+, which causes membrane depolarisation and an increase in intracellular calcium which stimulates aldosterone via a similar mechanism to AngII [228]. ACTH also stimulates aldosterone production, though to a lesser extent than K^+ and AngII, and via different channels involving cAMP-mediated activation of protein kinase A and subsequent activation of the transcription factor CREB (Figure 1.8)[228,231].

Counter-regulation of the RAAS system exists via angiotensin converting enzyme 2 (ACE2), neprilysin (NEP), and GC release. ACE2, notably expressed in the lung, and NEP cleave AngII to produce angiotensin 1–7 (Ang1-7), and ACE2 cleaves AngI to form angiotensin 1–9 (AngI1-9). Ang1-7 activates the MAS receptor while Ang1-9 activates AT2R, which antagonise classic

activation of the RAAS, causing vasodilation and a reduction in blood pressure [232]. GCs suppress ACTH production from the pituitary gland [194] thereby forming an additional negative feedback loop that suppresses aldosterone production.

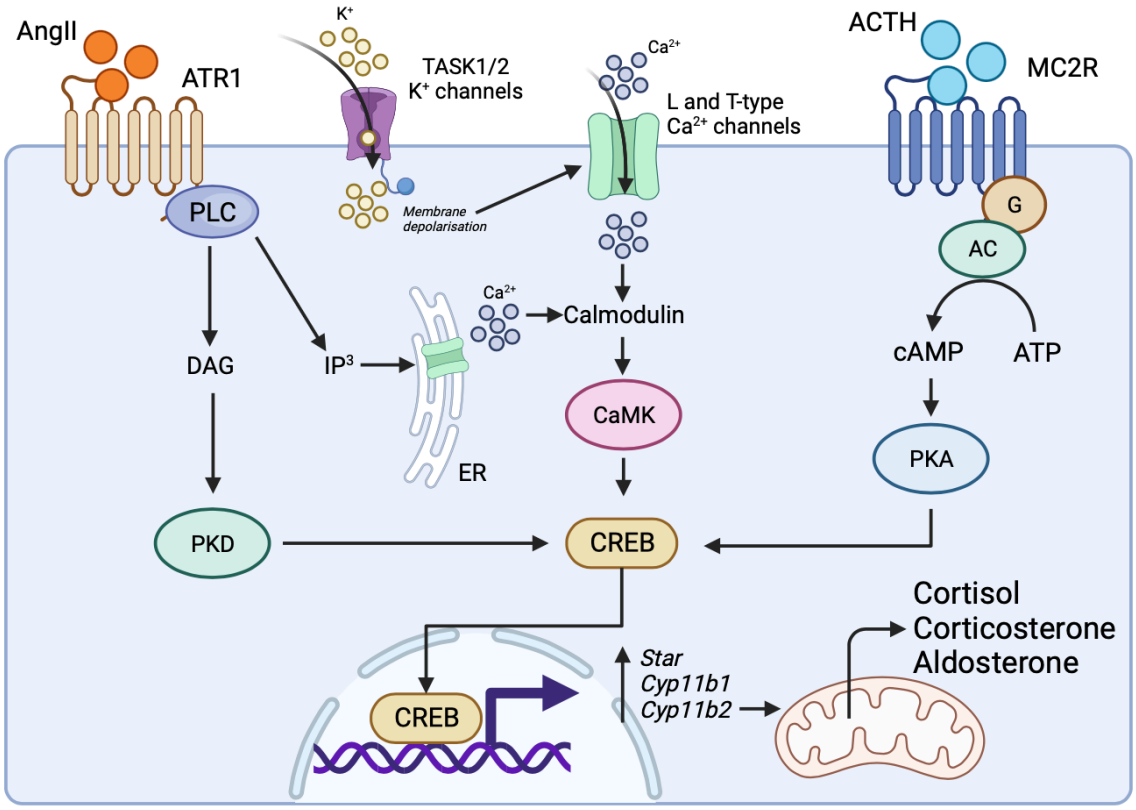


Figure 1.8. Molecular regulation of corticosteroid production. AngII binds the angiotensin 1 receptor (ATR1 to activate phosphoinositide-specific phospholipase C (PLC)-mediated formation of diacylglycerol (DAG) and inositol 1,4,5-trisphosphate (IP_3). IP_3 binds its receptor on the endoplasmic reticulum (ER), triggering the release of intracellular calcium stores and raising cytosolic calcium concentrations. Increases in extracellular potassium (K^+) trigger depolarisation of the glomerulosa cell, activating the voltage-regulated L- and T-type calcium channels, which increases calcium influx. Increased intracellular calcium (Ca^{2+}) concentration activates calcium/calmodulin-dependent protein kinases I/II (CaMK). This pathway, in addition to DAG-mediated activation of protein kinase D (PKD), triggers the phosphorylation and activation of cAMP response element binding protein (CREB), which mediates transcription of corticosteroid biosynthetic genes. In a similar manner, ACTH mediates CREB activation via binding its receptor – melanocortin type 2 receptor (MC2R). This triggers activation of adenylate cyclase (AC), the conversion of adenosine triphosphate (ATP) to cyclic adenosine monophosphate (cAMP), which in turn activates protein kinase A (PKA) and subsequently CREB activation. Adapted from reference [231].

1.3.5. Supply of cholesterol for adrenal corticosteroid biosynthesis

Cholesterol plays an integral role in the normal functioning of the adrenal gland. Adrenocortical steroidogenesis relies upon this low molecular weight, fat-soluble sterol as its necessary substrate molecule. The type of steroid synthesised is dependent upon the steroidogenic cells' complement of peptide hormone receptor (e.g. ATR1, MC2R), its response to peptide hormone stimulation, and its genetically encoded arsenal of steroid biosynthetic machinery. Adrenal steroidogenesis is triggered in response to tropic hormones and signals (ACTH, AngII, K^+) that stimulate the STAR-mediated transport of cholesterol across the mitochondrial membrane where it undergoes P450 side chain cleavage enzyme (P450scc/CYP11A1)-mediated cleavage to form the common steroid precursor, pregnenolone [233,234] (Figure 1.5). There are three principal sources of the cholesterol that fuels corticosteroid steroidogenesis: 1) *De novo* synthesis of cholesterol; 2) Receptor-mediated uptake of plasma lipoprotein-derived cholesterol; and 3) Mobilisation of intracellular cholesterol stored in lipid droplets.

De novo synthesis of the 27-carbon skeleton of cholesterol begins with the condensation of acetate/acetyl-CoA by the rate-limiting enzyme HMG-CoA reductase (HMGCR). Mevalonate is sequentially transformed into 30-carbon squalene by squalene synthase (SQS; FDFT1) by successive condensation reactions. Squalene monooxygenase oxidises squalene to form squalene epoxide and lanosterol synthase catalyses the cyclisation of squalene epoxide, forming lanosterol. From lanosterol, three methyl groups are removed to produce cholesterol that fuels steroidogenesis. The expression of genes related to cholesterol biosynthesis, including the crucial enzyme HMG-CoA reductase, is transcriptionally regulated by the SCAP/SREBP integral membrane protein complex associated with the ER, where most steps of cholesterol biogenesis takes place [235]. Human, bovine, and rat *in vivo* and *in vitro* studies

have demonstrated that HMGCR and other genes in the cholesterol synthesis pathway are rapidly upregulated in response to tropic hormone (ACTH and AngII) stimulation [236–239]. Endogenously synthesised cholesterol initially traffics from the ER to the plasma membrane, after which it can transport back to the ER for esterification prior to storage in lipid droplets [240,241]. The esterification of cholesterol is catalysed by acetyl-CoA acetyltransferase (ACAT1) [241,242]. Lipid droplet-stored esterified cholesterol is mobilised to fuel steroid synthesis following stimulation by tropic hormones [233,243,244]. However, while *de novo* synthesis of cholesterol plays a not-insignificant role in the supply of precursors for steroid synthesis, it is believed that plasma lipoprotein-derived cholesterol esters are preferentially utilised to fuel adrenal steroidogenesis [233].

Receptor-mediated uptake of plasma-lipoprotein cholesterol takes place via two distinct mechanisms which differ depending on the type of plasma lipoprotein and is influenced by the species of animal in which it takes place. Plasma LDL or apolipoprotein B or E (ApoB, ApoE)-containing lipoproteins are acquired via the LDL (B/E) receptor (LDLR)-mediated endocytic pathway. ApoB/E moieties bind the plasma membrane LDLR which localise to membrane regions known as coated pits, characterised by clathrin and other accessory proteins. These coated pits containing bound LDL-LDLR invaginate and pinch off intracellularly forming coated vesicles that fuse with early endosomes, shed the clathrin coats and fuse together forming mature endosomes. These endocytic compartments are acidic and contain hydrolases which mediate the dissociation of LDL from the LDLR and the hydrolysis of LDL cholesterol to form free (unesterified) cholesterol. LDLRs are then rapidly recycled back to the plasma membrane [241]. The released cholesterol is transported to the plasma membrane, to the ER for esterification by ACAT1 and storage in lipid droplets, or mitochondria for steroidogenesis [233,241]. LDL-derived cholesterol, through mechanisms incompletely understood, is believed to

be trafficked intracellularly by Nieman-Pick type C1 and C2 (NPC1 and NPC2), with cholesterol sensing and binding proteins, respectively [233]. Mutations of these proteins in (corpus luteum) steroidogenic cells cause the accumulation of unesterified cholesterol in endosomes and lysosomes, and impaired steroidogenesis [245]. However, the relative contribution of these proteins to adrenal steroidogenesis remains to be fully elucidated. LDLR-mediated cholesterol acquisition appears to be most important in humans and other LDL-dominant species, while rodents tend to rely upon HDL-dependent means of cholesterol procurement [246]. In this pathway, the LDL lipoprotein particle is necessarily degraded, making this endocytic pathway functionally distinct from the "selective" cholesterol pathway that is utilised for HDL [233].

SR-BI-mediated "selective" cholesterol uptake is responsible for the acquisition of HDL-derived cholesterol esters without the necessary uptake and degradation of the lipoprotein particle itself. Scavenger receptor class B type I (SR-BI) is a high affinity receptor for HDL, and binds HDL via an Apolipoprotein A-I (ApoA-I) moiety [247–250] but can also bind Apolipoprotein E, an LDL constituent molecule [251]. Adrenal steroidogenic cells from HDL-dominant rodents heavily rely upon this pathway for tropic hormone-stimulated cholesterol uptake and steroidogenesis. This was demonstrated by studies in which radiolabelled HDL and adrenal steroidogenesis is tracked *in vivo,* which show HDL-derived cholesterol-dependent steroidogenesis that is not coupled with HDL degradation [252,253]. Indeed, SR-BI is broadly expressed by steroidogenic cells in the rodent adrenal cortex, is upregulated upon ACTH and AngII stimulation, is necessary for adrenocortical HDL cholesterol uptake, and for normal basal and hormone-stimulated steroidogenesis [237,247,248,254–256]. *In vivo* studies have noted that SR-BI-expressing cells are characterised by an intricate microvillar system which assists with the trapping of HDL lipoproteins, the internalisation of HDL-derived cholesterol esters via

microvillar channels, and the enhancement of corticosterone production [257]. Interestingly, these functional HDL-capturing and transporting channels are inducible in non-steroidogenic cells *in vitro* upon transfection with an SR-BI-containing construct [258]. Collectively, these data indicate that SR-BI is necessary and sufficient for the formation of these specialised microvillar structures that facilitate both the binding of HDL and selective HDL cholesterol ester uptake. Although SR-BI has high affinity for HDL-associated lipoproteins (ApoA-I) [259], as a scavenger receptor it binds promiscuously to a variety of ligands including LDL, and acetylated and oxidized LDL [260,261], indicating that interpreting SR-BI's specific contribution to HDL-fuelled steroidogenesis is challenging. This would require SR-BI/LDLR double and sequential knockout studies, which to my knowledge have not been carried out.

Mobilisation of cellular lipid droplet cholesterol reserves for steroidogenesis is triggered by tropic hormone stimulation [262]. This stimulation is effected via an elevation in second messenger cAMP, which is followed by the activation of protein kinase A, which mediates the phosphorylation and activation of neutral cholesteryl ester hydrolase (nCEH). This is the enzyme that hydrolyses esterified cholesterol to generate free cholesterol, the necessary substrate in steroidogenesis [233]. Hormone-sensitive lipase (HSL), expressed from the ER, has been identified as the primary nCEH in the murine adrenal gland. HSL-deficient adrenals in comparison to WT adrenals exhibit significantly increased levels of cholesterol ester and a significantly reduced capacity for HDL and ACTH-induced corticosterone production, yet exhibit no intrinsic defect in the capacity to convert cholesterol into steroid [263,264]. Compared with control adrenals, HSL-deficient adrenals also present with a substantial accumulation of lipid droplets both in zona glomerulosa and zona fasciculata, in addition to the presence of "syncytial-lipoid structures" – large lipid-laden cells near the cortico-medullary boundary [265].

1.3.6. The adrenal glands as a seat of endocrine disorders

Adrenal gland disorders are the family of conditions that impede the normal functioning of the gland. These are commonly characterised by the over or under-production of adrenal-derived hormones. Aldosteronism, where the adrenals produce too much aldosterone, is considered "primary" or "secondary" based upon whether it is intra or extra-adrenal in origin, respectively [266,267]. Primary aldosteronism (PA) is the most common cause of secondary hypertension, comprising 5-10% of these hypertensive patients [268–270]. PA is most commonly caused by aldosterone-producing adenomas (APAs), and bilateral adrenal hyperplasia [271]. PA is commonly caused by mutations in genes encoding sodium-potassium channels (e.g. TASK1, KCNJ5, ATP1A1 and ATP2B3) which cause an increased intracellular Na^+ or Ca^{2+} concentration and stimulation of aldosterone biosynthesis [272–275]. Activation of the WNT/β-catenin pathway, a key pathway that drives the proliferation of adrenocortical cells during embryonic development and adulthood [276], is found in a majority of APA cases [277,278]. This pathway is also involved in adrenal tumour pathogenesis. ZNRF3, an E3 ubiquitin ligase that promotes endocytic turnover of WNT receptors and thereby negatively regulates the pathway, is frequently mutated in adrenocortical carcinoma [279,280]. A recent study demonstrated that loss of *Znrf3* in adrenocortical cells in mice induces cellular senescence as well as resulting in tissue remodelling and the permission of metastatic adrenal cancer in old (12 months plus) mice. Moreover, this effect was sexually dimorphic and influenced by the senescence-recruited myeloid cells. Female mice exhibited poorer myeloid cell infiltration and enhanced malignancy compared with male mice, an effect driven by androgens – patterns that mirror the human condition [281,282]. Pheochromocytoma is a type of adrenal cancer that originates from chromaffin cells in the adrenal medulla and result in an excess of catecholamines [283]. These tumours are rare and believed to be causative in between 0.1 and 0.6% of hypertensive individuals [284].

Cushing syndrome is a sustained elevation in plasma cortisol levels, commonly caused by exogenous glucocorticoid administration or, less commonly, endogenous elevations in glucocorticoid production [285]. Cushing syndrome is characterised by hyperglycaemia, immunosuppression, osteoporosis, and mood disorders including depression [286]. The most common endogenous form of Cushing syndrome is Cushing disease, which is a result of ACTH-producing pituitary adenomas that cause chronic stimulation of cortisol production via the HPA axis [287]. Intra-adrenal sources of Cushing syndrome centre on cortisol-producing adenomas – mutations in the endocrine cells of the ZF. These are commonly driven by somatic mutation in the genes encoding the catalytic subunit of protein kinase A (PKA), resulting in chronic PKA activation and sustained elevations in cortisol production [288,289]. Addison's disease (primary adrenal insufficiency) is a condition characterised by destruction of the adrenal cortex, resulting in glucocorticoid, mineralocorticoid, and adrenal androgen deficiencies [290]. These broad deficiencies commonly result in numerous clinical presentations including fatigue, weight loss, abdominal pain, melanoderma, hypotension, salt craving, hyponatremia, and hyperkalemia [290]. Addison's disease is thought of as an autoimmune condition, the classification of which is driven by histological observations showing that afflicted adrenals exhibit fibrosis with a mononuclear cell infiltrate, plasma cells, and, less frequently, germinal centres [291]. Additionally, levels of autoantibodies against CYP21A2 (21-hydroxylase) were shown to be predictive in the development of clinical Addison's disease [292]. However, the precise biological mechanisms that mediate the immunopathology of Addison's disease remain incompletely understood. Congenital adrenal hyperplasia (CAH) describes an inherited group of conditions characterised by an impairment in adrenal steroid synthesis, primarily aldosterone and glucocorticoids. More than 95% of CAH cases are caused by mutations in *CYP21A2.* Classic CAH results in increased androgen production due to a lack of negative feedback on the HPA axis and a shift in hormone synthesises towards the unaffected

androgen pathways [293]. Classic CAH results in numerous long term consequences, including increased mortality, hypertension, increased cardiovascular risk, insulin resistance and diabetes, and osteoporosis [294]. Glucocorticoid and mineralocorticoid replacement are critical for long term disease management, though long term supra-physiological concentrations of doses of synthetic steroids may be a contributing factor towards many of the long term consequences of CAH [294].

Congential adrenal lipoid hyperplasia (CALH) is another condition which presents with deficiencies in all adrenal (and gonadal) steroid hormones. Affected individuals have grossly enlarged adrenals, engorged with cholesterol and cholesterol esters [295,296]. The genetic basis for the disease has been traced to loss of function mutations in the genes encoding STAR and P450scc/CYP11A1, though the former is more common. These mutations result in a build-up of cholesterol, inconvertible to pregnenolone, in endocrine cells that cannot feed down the corticosteroid biosynthetic pathway [297,298]. The currently accepted model for the pathogenesis of CALH is the two-hit hypothesis – an initial loss of steroidogenesis caused by the loss of function mutation in *STAR* followed by the second hit which is protein independent and caused by cellular damage due to accumulated cholesterol esters [296]. CALH is fatal shortly after birth if replacement hormone treatment is not initiated [299].

Immune checkpoint inhibitor-induced adrenalitis is a rare but well documented adverse event associated with monoclonal antibody anti-cancer immunotherapies. Antibodies that target and inhibit the immune checkpoints PD-1, PD-L1, and CTLA-4 have been demonstrated to precede the development of adrenal insufficiency – adrenal dysfunction characterised by reduced production of adrenal-derived hormones – in an estimated 4-9% of treated patients [300,301]. The mechanism that underlies this pathology remains unclear, and any contributing role of tissue

resident or recruited immune cells (including macrophages) to this pathology remains speculative at this point.

1.4. Original hypothesis

At the beginning of my studies, I observed a gap in the literature. Macrophages in other major bodily tissues were slowly but surely gaining recognition for their tissue-specific, para-immune, homeostatic, and physiological roles. While macrophages had been identified in the adrenals glands of mice and humans for more than 30 years, their function(s) within the tissue remained, at best, incompletely understood. I hypothesised that adrenal gland macrophages possess tissue-specific functions beyond their classical immune roles. Additionally, inspired by the non-random spatial localisation within the gland I hypothesised that they have a role in supporting adrenal aldosterone production.

1.5. Experimental aims

The experimental aims for this thesis were as follows:

- To thoroughly characterise the macrophage compartment of the murine adrenal gland in health and obesity by immunofluorescent imaging and flow cytometry.
- To investigate the contribution of adrenal macrophages to aldosterone production and other adrenal-derived hormones.

Chapter 2

Materials and methods

2.1. Animal experimentation

2.1.1 Ethical statement

All experiments on mice were conducted according to institutional, national, and European animal regulations. Specifically, animal protocols were approved by the animal welfare and ethics review board of the Department of Physiology, Anatomy, and Genetics at the University of Oxford, and all animal usage complied with the University of Oxford Local Ethical Guidelines and the Animals (Scientific Procedures) Act 1986 of the United Kingdom. The keeping and use of these animals was covered by the UK Home Office Project License (PPL) of Prof. Ana I. Domingos (P80EDA9F7). I hold personal license (PIL) I59631289 and have been authorised to perform Schedule 1 procedures, intraperitoneal (IP) and intravenous injections (IV), IV blood sampling, perfusion, mouse restraint, anaesthesia by isoflurane, and subcutaneous osmotic minipump implantation.

2.1.2. Mouse strains and husbandry

Mice (*Mus musculus*) were the sole laboratory species used in this work. Mice were chosen as the animal model in which to investigate the interactions between immune function and endocrine output. This is due to several factors. A wealth of literature exists in which mice are used to probe immune and endocrine function and mice largely phenocopy humans in the mediators of immune and endocrine function. Additionally, many of the methodological models used throughout this thesis were originally developed in mice, and so mice were used here to remain as true to the literature as possible.

C57BL/6J, CX3CR1-GFP, B6SJL CD45.1, Cx3cr1-Cre, iDTR, Marco$^{-/-}$, and hCD68GFP/GFP mice were bred on site at the University of Oxford. Occasionally, C57Bl/6J mice were purchased from Charles River Laboratories, UK. When necessary, mouse genotype was established using Transnetyx or PCR. All mice were housed in the local Biomedical Services Building, Pathology Support Building, or departmental holding room prior to experimental use. Animals were housed in groups of approximately 2-6 in individually ventilated cages (IVCs) at 20-24°C air temperature, 55% humidity, and a 12-12 day/night lighting cycle. Unless otherwise stated, all cages were supplied with standard mouse chow diet and water *ad libitum* in addition to woodchip, Sizzle Nest, and environmental enrichment.

2.1.3. Sacrifice and tissue harvest

Unless otherwise stated, at the time of sacrifice mice were anaesthetised with (10ul/g) 200mg/ml pentobarbitone sodium (Animalcare) solution, and cardiac perfused with 15-20mL of either 4% paraformaldehyde (PFA; Thermo Fisher Scientific, 043368.9M; used when adrenals were to be used for image analysis) or phosphate buffered saline (PBS; Sigma Aldrich; used when adrenals were processed for all other analyses, unless otherwise stated). All tissues were collected between 0930 and 1130 to control for circadian rhythm. Prior to perfusion blood samples were taken from the right atria into EDTA-coated tubes. Blood samples were centrifuged at 1000g for 15 minutes to separate the plasma. Plasma samples were frozen at -80^{o}C until use in subsequent assays. Adrenal glands in all instances were dissected and any peri-adrenal adipose tissue was removed using a stereomicroscope. Tissues to be used for microscopy and image analysis were fixed additionally overnight in 200uL 4% PFA at 4^{o}C. After overnight fixation, PFA was removed from the samples and tissues were stored until use at 4^{o}C in PBS containing 0.1% NaN_3. Adrenals that were used in other experiments were frozen post-dissection at -80^{o}C until further analyses.

2.2. Fluorescence activated cell sorting (FACS)

2.2.1. Tissue collection and preparation for FACS

Adrenals were harvested from PBS-perfused mice into FACS buffer (2% FCS, 0.1% Sodium Azide in 1X PBS) and kept on ice at all points unless otherwise stated. The cortex and medulla of dissected adrenal glands were separated manually using fine tweezers and scissors under a stereomicroscope, while submerged in FACS buffer.

2.2.2. Adrenal digestion

Cortices were minced using scissors and digested in 500uL of 2.5 mg/mL type I collagenase (Sigma, C2674) diluted in sterile HBSS without Mg^{2+} and Ca^{2+} (Life Tech, 14170138), and with 12.5 units DNAse I (New England Biolabs, M0303L), for 1hr in a shaking 37ºC incubator. Every 20 minutes, solutions were gently passed through a 1mL syringe several times, attached to a 21G, 23G, or 25G needle to aid digestion. Digestions were quenched with the addition of 4.5mL FACS buffer, filtered using an in-house-made 70 µm cell strainer. Suspensions were washed by centrifugation at 4ºC for 5 min at 400g and resuspended in 1mL FACS buffer.

2.2.3. Cell counting

For cell counting, 100uL (10%) of the digested single cell suspension was removed and kept in FACS tubes separately on ice. To these tubes, 20µL CountBright™ Absolute Counting Beads (Life Technologies, C36950) and 200µL FACS buffer. These tubes were kept on ice until acquisition. Cell counts were calculated according to manufacturer's instruction. Briefly, by comparing the ratio of bead events to cell events in a given sample, the absolute numbers of cells in each sample were calculated.

2.2.4. Staining for surface markers

Cells were live/dead stained using Fixable Aqua Live/Dead (Life Technologies, L34966) for 40 minutes, and non-specific antibody staining was blocked using Fc block (BD) for 15 minutes on ice. Subsequently, cells were stained with fluorophore conjugated antibodies for 40 minutes on ice. Antibodies used are listed in Table 2.1.

Marker	**Fluorophore**	**Isotype**	**Clone**	**Location**
CD45	AF700	Rat IgG2b	30-F11	Surface
CD45	BUV395	Rat IgG2b	30-F11	Surface
CD45.1	BV605	Mouse (A.SW) IgG2a, κ	A20	Surface
CD45.2	BUV395	Mouse SJL IgG2a, κ	104	Surface
F4/80	AF647	Rat IgG2a	BM8	Surface
F4/80	PE-Cy5	Rat IgG2a	BM8	Surface
MHCII	PE-Cy7	Rat IgG2b, κ	M5/114.15.12	Surface
CX3CR1	PE	Mouse IgG2a, κ	SA011F11	Surface
CD11b	BV605	Rat IgG2b, κ	M1/70	Surface
Gr-1 (Ly6G)	PerCP/Cy5.5	Rat IgG2b, κ	RB6-8C5	Surface
CD68	APC-Cy7	Rat IgG2a	FA-11	Intracellular
Ki-67	AF488	Mouse IgG1, κ	B56	Intracellular

Table 2.1. List of conjugated flow cytometry antibodies used in this thesis.

2.2.5. Intracellular staining

Cells were permeabilised for intracellular staining using Foxp3 / Transcription Factor Staining Buffer Set (eBioscience) according to manufacturer's instructions. Briefly, following the final

wash of the surface staining protocol, cells were fixed in Fixation/Permeabilization buffer for 30 mins at 4°C. Cells were then washed and resuspended in permeabilization buffer. Intracellular antibodies were then added and incubated overnight at 4°C. Antibodies used are listed in Table 2.1. Cells were washed once more in permeabilization buffer, resuspended, and filtered prior to running on the FACS machine.

2.2.6 Data acquisition and analysis

Single stains for compensation were done using UltraComp eBeads™ Compensation Beads (Invitrogen). Samples were run on a BD Fortessa X20 flow cytometer and BD Diva Software was used during acquisition. Flow cytometry data was analysed using FlowJo (Tree Star Inc) and Graphpad Prism 9 software.

2.3 Microscopy

2.3.1 Immunofluorescent staining and confocal microscopy

All adrenals used for immunofluorescent and confocal microscopy were from animals perfused and overnight fixed with 4% paraformaldehyde, as described earlier. Fixed adrenals were transferred to 30% sucrose and incubated overnight at 4°C for cryopreservation. Samples were embedded in OCT matrix and snap-frozen with liquid nitrogen. 15um sections were cut from embedded tissues using a Leica cryostat and mounted onto charged microscope slides. Cryosectioned tissue slices either stained fresh or, if frozen previously, were thawed in PBS for 10 min at room temperature, tissue sections were circled using a super PAP pen (Life Technologies), blocked and permeabilised for 1 hour at room temperature in perm/block solution (3% bovine serum albumin, 2% goat serum, 1% Triton X-100, 0.01% NaN_3 in PBS). Primary stains were done overnight at 4°C and secondary stains were done for 1hr at room temperature. For staining against ACE in the lung, the secondary stain was done with goat anti-

rabbit Alexa Fluor 488 Tyramide Super Boost kit (Invitrogen, B40922), according to manufacturer's instruction. DAPI was used to stain nuclei at room temperature for 5 minutes. Three five-minute washes in PBS took place between all stains. Antibodies used are listed in Table 2.2. All slides prepared for immunofluorescence were imaged using a Zeiss 880 confocal microscope.

Target	**Antibody type**	**Conjugation**	**Host**	**Clone**
Cyp11b2 (rAS 2084)	Primary	N/A	Rabbit	Polyclonal
F4/80	Primary	N/A	Rat	CI:A3-1
CD68	Primary	AF647	Rat	FA-11
Marco	Primary	N/A	Rat	ED31
MHCII	Primary	N/A	Rat	M5/114.15.2
GFP	Primary	N/A	Chicken	Polyclonal (ab13970)
ACE	Primary	N/A	Rabbit	JM59-32
Anti-chicken IgY (H+L)	Secondary	AF488	Goat	Polyclonal
Anti-chicken IgG (H+L)	Secondary	AF647	Goat	Polyclonal
Anti-rat IgG (H+L)	Secondary	Alkaline phosphatase	Goat	Polyclonal
Anti-rat IgG (H+L)	Secondary	AF488	Goat	Polyclonal
Anti-rat IgG (H+L)	Secondary	AF647	Goat	Polyclonal
Anti-rat IgG (H+L)	Secondary	AF546	Goat	Polyclonal

Anti-rabbit IgG (H+L)	Secondary	AF594	Goat	Polyclonal

Table 2.2. List of antibodies used for microscopy in this thesis.

2.3.2 Immunohistochemical (IHC) staining and bright field microscopy

Adrenal glands were first dehydrated in 70% (60 mins), 90% (45 mins) and absolute ethanol (45 mins), cleared with xylene (3x 60 mins), and infiltrated with Cellwax Plus paraffin wax (CellPath) at 60ºC (2x 30 mins, 1x overnight). Samples were then embedded in cassettes in molten paraffin wax and left to cool. 10um sections were cut using a microtome, water mounted to charged slides, and melted onto slides for 1 hour. For antigen retrieval, first boil antigen retrieval solution (Stock: EDTA 10 mM SDS 0.5% pH 9.0, dilute 1:10 with Milli-Q water) with 900 Watt, afterwards place slides on a solution of EDTA 1mM, pH 9.0, SDS 0.05%, then heat up the solution again until it is boiling then sub-boil the buffer for 30 minutes at 150 Watts in a microwave. Slides were immediately washed and incubated in tap water for 5 minutes each time, with regular gentle agitation. Slides were rinsed in distilled water prior to staining. Sections were blocked for 1 hour at room temperature with the blocking buffer as described above, and stained with rat anti-mouse CD68 antibody (clone FA-11, BioLegend) overnight at 4ºC. Slides were washed in PBS and incubated with goat anti-rat alkaline phosphatase (Invitrogen, A18868) for 1 hour at room temperature. Fast Red staining was done using Liquid Fast-Red Substrate Kit (Abcam, ab64254) according to manufacturer's instructions. Sections were counterstained with Mayer's hematoxylin solution diluted 1:5 in water for 1 minute and washed in PBS. Fluoromount G mounting medium was used to mount coverslips to slides which were then sealed with clear nail varnish. IHC prepared slides were imaged using the EVOS M7000 imaging system.

2.3.3. Image analysis

All image analysis was done using FIJI software on MacOS. Quantitation of the $CD68^+$ cell area and autofluorescent (raw integrated densities; RID) of immunofluorescent stains was done using FIJI image analysis software. 3-6 adrenal cryosections of stained tissue were analysed per mouse. After testing numerous cell segmentation plugins, $CD68^+$ cells were segmented using the Otsu thresholding plugin and autofluorescent RIDs were taken from these segmented cells. Otsu was selected as it resulted in preferential and accurate segmentation of $CD68^{++}$ macrophages. Otsu did not recognise smaller areas of $CD68^+$ staining and so did not segment the dendritic zona glomerulosa macrophages, and so this method allowed for accurate, robust, unbiased, and reproducible cell size measurements. Median fluorescence intensity (MFI) for ACE was measured via the integrated density of the stain, which was normalised to the area of DAPI staining. Cell size and autofluorescence values from all slices were plotted as mean +/- s.e.m.

2.4. Irradiation and bone marrow transplantation

10-week-old male B6SJL $CD45.1^+$ mice were irradiated with a total dose of 11Gy, which was administered as 2 doses of 5.5Gy, separated by ~20 hours. These mice were injected intravenously with $9x10^6$ bone marrow cells from male hCD68-GFP mice. Mice were culled by CO_2 11 weeks later and adrenals were harvested as previously described.

2.5. Analysis of published single-cell sequencing data

Single-cell RNA-seq data from Dolfi *et al.* [302] were obtained from Gene Expression Omnibus (accession GSE203095). Analysis was performed by Dr Davi Oliveira-Sidarta under my direction. FASTQ sequencing libraries were used to generate digital gene expression matrices with 10x Genomics Cell Ranger 3.1.0, and the *scanpy* (PMID 29409532) python toolkit was

used to orchestrate the analysis. For each sample (4 males, 4 females), cells were then filtering according to current quality control standards [303], and cells with at least 300 and less than 2,000 detected genes, less than 4,000 total mRNA counts and less than 5% of mitochondrial reads were kept for downstream analyses. Data for each cell were then library-size normalized and multiplied by a 10,000 scaling factor before log-normalization. Highly-variable genes were selected based on their dispersion and mean expression, and 3,166 genes were kept for embedding and clustering. Myeloid cells were detected by the expression of *Cd68, Cx3cr1, Ccr2 or Lyz2* and by the automatic cell-type assignment algorithm CellTypist[304]. After filtering myeloid clusters and subclustering, we identified an artefactual cluster that was visibly separate from the three others in the embedding and which was marked by the expression of *Pf4*, a platelet marker. After removal of this cluster, 6,377 high-quality myeloid cells were retained, comprising three separate clusters with specific marker genes. Embedding to a two-dimensional space was performed using Diffusion Maps (Ref Diffusion Maps). Gene expression was shown either on top of the embedding or as dotplots of standardized gene expression. For RNA velocity, we used Velocyto to quantify spliced and unspliced reads, and CellRank with standard parameters for the remaining analyses, the only particularity being the use of the Diffusion Components (DCs) as a latent orthogonal basis instead of Principal Component Analysis (PCA).

2.6. High fat diet (HFD) challenge

At eight weeks old, mice of the indicated genotypes were given *ad libitum* access to a high fat diet (60% fat, D12492: Research Diets) for a period of 12 weeks. Mice on the control arm of the experiments were given ad libitum access to a normal chow diet (3.7% fat, D2916: Teklad). After 12 weeks, tissues were harvested as described earlier for subsequent analyses.

2.7. High salt diet challenge

For the high salt diet challenge experiment, 21 week old CX3CR1$^{GFP/+}$ mice were a fed diet containing 0.1% NaCl (diet D11112201; Research Diets) or a diet containing 2.5% NaCl (diet D22033001 with added NaCl; Research Diets) for six days. Tissues were harvested as described earlier for subsequent analyses.

2.8. Subcutaneous osmotic minipump implantation

Osmotic minipump implantation was carried out as previously described [305]. In short, Alzet osmotic mini-pumps (model 1002) containing vehicle or Ile5–Ang II (1000 ng/kg per minute, 14 days subcutaneous, Sigma Aldrich) were implanted into 25-week-old CX3CR1$^{GFP/+}$ mice under isoflurane anaesthetisation. 14 days later mice were euthanised and adrenals and blood samples were harvested as described earlier.

2.9. Bulk RNA sequencing of adrenal macrophages

I performed RNA was extraction from FACS sorted adrenal cell populations using the RNeasy Plus Micro Kit (Qiagen). Bulk RNA sequencing and analysis was outsourced to Mélanie Makhlouf, Eman H. AbouMoussa and Luis Saraiva at Sidra Medicine, Qatar. Reverse transcription, cDNA pre-amplification and sequencing library preparation were performed as previously described in [PMID: 35320714]. Briefly, reverse transcription and cDNA pre-amplification were performed using the SMART-Seq v4 Ultra Low Input RNA Kit for Sequencing (Clontech/Takara). cDNA was harvested and quantified with the Bioanalyzer DNA High-Sensitivity kit (Agilent Technologies). Libraries were prepared using the Nextera XT DNA Sample Preparation Kit and the Nextera Index Kit (Illumina) as per manufacturer instructions. Multiplexed libraries were pooled and paired-end 150-bp sequencing was performed on the Illumina HiSeq 4000 platform at Sidra Medicine. A standard RNA-Seq

pipeline was launched using bcbio nextgen toolkit (**https://doi.org/10.5281/zenodo.5781867**). Briefly, sample Fastq files were mapped to the mouse reference genome GRCm38.p6 (GCA_000001635.8) using STAR (version 2.6.1d). Reads were retained only if uniquely mapped to the genome. FeatureCounts (v2.0.0) was used to obtain the number of reads that mapped to each gene. Sample Transcriptome data quality was assessed by evaluating homogeneity and similarity between samples. We used variance stabilizing transformation (vst) and regularized log transformation(rlog) functions (DESeq2 package (v1.26.0) [306]) to transform the raw count data, (dist) function to calculate sample-to -sample distances. We plotted heatmaps of distance matrix along with PCA of 1000 most highly variable genes to identify putative outlier samples. These samples if present were excluded from the following differential expression analyses. We also used DESeq2 (v1.26.0) to normalize the raw count matrix according to sequencing depth and RNA composition (median of ratios method).

2.10. Diphtheria toxin receptor-mediated macrophage ablation

Homozygous CX3CR1-Cre mice (Jackson Laboratories) were crossed with homozygous Gt(ROSA)26Sortm1(Dtr)ThBu (iDTR; R26iDTR) mice to generate heterozygous mice which express the diphtheria toxin receptor (DTR) from CX3CR1-expressing cells. At 10 weeks of age, 750ng Corynebacterium diphtheriaediptheria toxin (Calbiochem) or vehicle control was injected intraperitoneally in 200µL PBS. 24 hours later mice, were euthanised by pentobarbitone sodium solution as previously described, and blood samples were taken from the heart and processed as described earlier. Adrenals were harvested and processed for flow cytometry as previously described.

2.11. Plasma hormone, protein measurements

Plasma aldosterone and corticosterone concentrations were measured from mouse plasma samples using the reverse competition ELISA kits (Enzo Life Sciences). All blood and plasma samples were collected from mice between 0930 and 1130. Plasma norepinephrine was measured by ELISA (ImmuSmol). Plasma renin was measured using the Mouse Renin 1 (REN1) ELISA Kit (Invitrogen), plasma ACTH was measured using Mouse/Rat ACTH SimpleStep ELISA® Kit (Abcam), and plasma Angiotensin II was measured by reverse competition ELISA (Enzo Life Sciences). All ELISAs were carried out according to the manufacturer's instructions. Colorimetric and fluorimetric readouts from these assays were attained using a FLUOstar Omega plate reader (BMG Labtech).

ELISA kit	**Intra-assay coefficient of variation (CV) (%)**	**Limits of detection**
Aldosterone	10.8 - 16.3	3.9 – 250 pg/mL
Corticosterone	6.6 - 8.0	32 – 20,000 pg/mL
Norepinephrine	8.4-15.6	0.2 – 32 ng/mL
Renin	< 10	12.1 – 12,500 pg/mL
ACTH	4.2	7.81 – 500 pg/mL
Angiotensin II	4.7 – 7.3	3.9 – 10,000 pg/mL

Table 2.3. ELISA CVs and limits of detection.

2.12. Cholesterol measurements

Plasma cholesterol was measured using the Cholesterol Quantitation Kit (Sigma Aldrich, MAK043) according to manufacturer's instructions. To prepare adrenal glands for cholesterol quantitation, whole adrenals were homogenised into 200ul chloroform:isopropanol:IGEPAL CA-630 (7:11:0.1) in a Precellys homogenisation tube (MK28-R). Tissues were homgenised using the PreCellys 24 tissue homogeniser. Homogenates were mixed thoroughly with 40ul sterile H_2O, centrifuged at 13,000g for 10 minutes, and the upper aqueous phase was manually removed. The organic phase was transferred to a clean tube and vacuum dried at room temperature using a SpeedVac machine. Dried lipid pellets were dissolved with Cholesterol Assay Buffer and vortexed to ensure complete homogenisation. The homogenised solution was

used in the Cholesterol Quantitation Kit (Sigma Aldrich) according to manufacturer's instructions.

2.13. Determination of plasma volume

Blood plasma volume was determined as previously described[307]. Briefly, under general anesthesia with isoflurane (2 mL/min), 100µL PBS solution containing 2mg/mL FITC-dextran 500000 conjugate (46947-100MG-F, Sigma-Aldrich) was injected into the tail vein. 40 minutes later, mice were euthanised with pentobarbitone as described earlier and blood was withdrawn from the right atria. Plasma was separated by centrifugation of the blood at 1000 g for 15 min in the dark. Fluorescence levels were measured using a FLUOstar Omega plate reader (BMG Labtech; Ex/Em 485/520). The concentration of FITC-dextran in plasma was calculated based on a standard curve generated by serial dilution of the 2mg/mL FITC-d solution that was injected.

2.14. Blood electrolyte readings

Blood electrolyte readings were carried out by Pinmoore Animal Laboratory Services Limited. Blood plasma samples, frozen initially at -80°C, were shipped to Pinmoore on dry ice. Sodium and potassium electrolyte readings were taken using an I-Smart 30 Vet electrolyte analyser (Woodley Equipment).

2.15. RT-qPCR

Adrenals were homogenised using the Precellys Hard Tissue Grinding Kit (MK28-R; Bertin Technologies). Total RNA from homogenised adrenals or lungs was isolated using RNeasy Plus Micro Kit (Qiagen, cat# 74034). RNA concentration was quantified using a Nanodrop

ND-1000 machine. cDNA was reverse transcribed using SuperScript II (Invitrogen) and random primers (Invitrogen). Quantitative PCR was performed using SYBR Green (Applied Biosystems) in C1000 TouchTM Thermal Cycler (BioRad). B-actin was used as the housekeeping gene to normalize samples. The following formula was used to calculate the relative expression levels: RQ = 2^−ΔCt × 100 = 2−(Ct gene of interest – Ct β actin) × 100. The following mouse-specific primers were used:

Primer	**Sequence**
Star forward	5'-CAGGGCCAAGAAAACCTACA-3'
Star Reverse	5'-ACGAGCATTTTGAAGCACCT-3'
Cyp11a1 forward	5'- AGGACTTTCCCTGCGCT -3'
Cyp11a1 reverse	5'-GCATCTCGGTAATGTTGG-3'
Hsd3b1 forward	5'-GCGGCTGCTGCACAGGAATAAAG-3'
Hsd3b1 reverse	5'-TCACCAGGCAGCTCCATCCA-3'
Cyp11b1 forward	5'-GGAAGAGAAGAGAGGGCAATGTGT-3'
Cyp11b1 reverse	5'-GGAAGAGAAGAGAGGGCAATGTGT-3'
Cyp11b2 forward	5'-CAGGGCCAAGAAAACCTACA-3'
Cyp11b2 reverse	5'-ACGAGCATTTTGAAGCACCT-3'
Ace forward	5'-GCTTCCTCTTTCTGCTGCTCTG-3'
Ace reverse	5'-TGCCCTCTATGGTAATGTTGGT-3'
Marco forward	5'-ACAGAGCCGATTTTGACCAAG-3'
Marco reverse	5'-CAGCAGTGCAGTACCTGCC-3'
B-actin forward	5'-TCATGAAGTGTACGTGGACATCC-3'
B-actin reverse	5'-CCTAGAAGCATTTGCGGTGGACGATG-3'

Table 2.4. RT-qPCR primers and sequences.

2.16. Temporal deletion of Star

Cre-ER^{TM} ; Star$^{flox/flox}$mice were generated by our collaborators Yusuke Mizuno, Tomohiro Ishii, and Tomonobu Hasegawa in Japan as described in previously [308]. To induce knockout of Star in these mice, 8-week-old male Cre-ER^{TM} ; Star$^{flox/flox}$mice were injected with 75 mg/kg body weight tamoxifen (Sigma Aldrich) three times every other day, then aged for 8 weeks prior to sacrifice.

2.17. LDL uptake assay

Bone marrow derived macrophages were generated as described previously [86,309]. Briefly, bone marrow was obtained from tibae and femurs of 8–10-week-old male C57Bl/6 mice or CX3CR1$^{GFP/GFP}$ mice. Whole bone marrow isolates were cultured for 6 days in DMEM, 10% Fetal Bovine Serum (FBS), 10% L929 fibroblast-conditioned media as a source of M-CSF, 1% Penicillin/Streptomycin (P/S) in non-tissue culture treated 10cm petri dishes and incubated at 37°C, 5% CO_2. On day 5, 3 mL media was replaced with 5 mL fresh media. On day 6, cells were gently detached from dishes using a cell scraper, counted, and plated for experiments in DMEM containing 2% FBS in 96 well plates at a density of 100,000 cells per well. Cells were allowed to settle overnight before subsequent experimentation. On day 7, BMDM cultures were treated with 250ug/uL BODIPY™ FL complex Low Density Lipoprotein (Invitrogen) for 24 hours. Cells were then fixed with 4% PFA for 15 minutes, washed with PBS, and fluorescence intensity was measured using the FLUOstar Omega plate reader (BMG Labtech; Ex/Em 515/520).

2.18. Statistical analysis

All experiments, where possible, were designed to have equal groups of biological replicates (n) per experimental group. Data in all instances was presented as mean +/- standard error mean

(s.e.m.). Technical replicates were used in plate-based assays, the average of which was used to represent each individual n. Statistical analysis was done using Graphpad Prism 10.0 for MacOS, GraphPad Software, Boston, Massachusetts USA, www.graphpad.com. For comparison of two experimental groups, an unpaired student's t test was used. For comparison of more than two groups, a one-way ANOVA with Tukey's post-hoc test for multiple comparisons. Significance in all cases was denoted as follows. *$P < 0.05$, **$P < 0.01$, ***$P < 0.001$, ****$P < 0.0001$.

Chapter 3

Characterising the murine adrenal macrophage compartment at steady state

3.1 Introduction

3.1.1 Tissue macrophage markers

Numerous markers exist to label macrophages within tissues (Table 3.1). Perhaps the most commonly used is CD68/macrosialin. CD68 is a heavily glycosylated glycoprotein and is a member of the lysosome-associated membrane protein family [310,311]. Expression of CD68 is therefore mainly restricted to the intracellular endosomal/lysosomal compartment [312]. CD68 is considered a pan-macrophage marker and a faithful marker of mononuclear phagocytes [311,313]. A transgenic mouse reporter line in which GFP is expressed under the control of the human CD68 promoter exhibits high GFP expression in both monocyte- and embryo-derived tissue resident macrophages in adult animals [314]. The functional significance of CD68 *in vivo* remains incompletely understood but endogenous ligands for the protein include oxidised LDL, phosphatidylserine, and apoptotic cells [315–317]. C-X3-C Motif Chemokine Receptor 1 (CX3CR1) is a membrane-bound seven transmembrane GPCR. As a chemokine receptor it is thought to be mainly involved in mediating chemotaxis through binding to its sole ligand, CX3CL1 [318]. The receptor can be found to varying extents on monocytes. Murine monocytes are typically defined on the basis of their expression of CX3CR1 and Ly6C – CX3CR1^{low} Ly6C^{high} classical monocytes and CX3CR1^{high} Ly6C^{low} non-classical monocytes, which are analogous to human CD14^{+} CD16^{-} and CD14^{low} CD16^{+} monocytes [319]. CX3CR1 is also used as a marker for tissue macrophages, and can be found on subsets of T cells, NK cells, gamma-delta T cells, and certain dendritic cell subsets [319–323]. A CX3CR1-GFP reporter mouse line was

first used in the context of studying microglia [320], but has since been used for studying macrophages in various tissue contexts [118,324,325].

F4/80 is a membrane-bound mouse macrophage-specific antigen [96]. Its expression is restricted to myeloid cells and is found on subsets of tissue macrophages, monocytes and dendritic cells [39,326]. Though it is not expressed on certain macrophage subsets such as splenic marginal zone macrophages [326] it is expressed on adrenal macrophages among many others [326,327]. Functionally, it is highly related to GPCRs involved in adhesion and cell signalling and has a demonstrated role in the induction of T cell tolerance [328]. C-C chemokine receptor type 2 (CCR2) is a chemokine receptor that binds CCL2. It is expressed most prominently on monocytes and monocyte-derived macrophages, some resident macrophages, and subsets of T cells [329]. Other markers include Colony stimulating factor 1 receptor (CSF1R; CD115) which binds interleukin 34 (IL-34) and macrophage colony stimulating factor (M-CSF), both known macrophage trophic factors [330]. Indeed, CSF1R expression is essential for the development, survival, recruitment and proliferation of tissue macrophages [331,332]. CSF1R expression is restricted to myeloid cells, in particular monocytes and macrophages, and certain dendritic cell subsets [333–335]. CD64 is an Fc receptor with expression observed on monocytes, macrophages, and dendritic cells [336].

The overlap in expression of the typically used macrophage markers between macrophages and other immune cell types, in particular dendritic cells, makes distinguishing these cell types based on immune-histological assessment exceedingly difficult. Indeed, dendritic cells and macrophages share a common progenitor cell type [35] and their developmental trajectories are closely aligned [35]. Consequently, distinguishing based on protein expression can be challenging

but single cell technologies are proving a valuable asset in mononuclear phagocyte immune cell classification.

Marker	Function	Expression	References
CD68	Lysosome-associated membrane protein	Pan-macrophage, monocytes, splenic DC, neutrophil	[311,314]
CX3CR1	Chemokine receptor	Macrophages, monocytes, DCs, certain lymphoid cells	[319–323]
F4/80	Regulates T cell tolerance	Macrophages, dendritic cells	[96,328]
CCR2	Chemokine receptor	Macrophages, monocytes, T cells	[329]
CSF1R	M-CSF / IL-34 receptor	Macrophages, monocytes, DCs	[333–335]
MHCII	Antigen presentation	Macrophages, monocytes, DCs, B cells	[337–339]
CD64	Fc receptor	Macrophage, neutrophil, DC	[340,341]
CD11b	Integrin / leukocyte adhesion protein	Macrophages, myeloid cells	[313]

Table 3.1. Murine macrophage markers.

3.1.2. Features of the tissue macrophage niche

Macrophages are most commonly recognised for their classic immune and inflammatory functions. However, these multifaceted cells are gaining increasing prominence for their para-immune, homeostatic, and physiological functions. While macrophages perform their immune and para-immune activities within a tissue, an increasing body of evidence now indicates that the tissues in which macrophages reside provide factors that support macrophage survival and function – termed the macrophage niche [330]. The four fundamentals of the macrophage niche are:

1) To provide a physical scaffold to which macrophages can adhere and utilise to move around within the tissue.
2) To provide trophic factors that nourish the residing macrophages, promoting their survival, replenishment, self-maintenance, and intra-tissue function.
3) The niche imprints a tissue-specific identity onto residing macrophages via induction of transcription factors.
4) Resident macrophages provide a benefit for the niche tissue.

The most important macrophage trophic factor appears to be M-CSF. Most macrophages depend on the local provision of either soluble or membrane-bound M-CSF isoforms. This is evidenced in studies showing that Op/Op mice, which lack the gene encoding M-CSF (*Csf1*), lack tissue macrophages [30,31,342]. However, restoration of cell surface M-CSF normalises macrophage populations in the perinatal liver, bladder, subinguinal salivary gland, kidney cortex, dermis, and synovial membrane, but not adult liver, adrenal gland, kidney medulla, spleen, peritoneal cavity, or intestine. Additionally, this manipulation restores growth rates and partial improvements to the osteoporotic phenotype [331]. Op/Op mice in which only the soluble M-CSF form has been restored exhibit improved growth rates and improved bone densities, in comparison to Op/Op mice, and retain tissue macrophages (albeit with reduced dendrites) in the skin, kidney, bladder, tendon, and marginal zone splenic macrophages [343]. Antibody-mediated inhibition of the M-CSF (and IL-34) receptor CSF1R induce reductions in tissue macrophage populations in the bone marrow, liver, skin, and kidney [344]. IL-34 is also an important survival factor for certain, but not all, macrophage populations. Its deficiency specifically ablates Langerhans cells and brain microglia [345,346].

Notch signalling has also been implicated in maintenance of the macrophage niche in certain tissues. NicheNet modelling [347] which predicts ligand–target links between interacting cells based on gene expression and published literature-established links, implicates the notch ligands DLL1 and DLL4 as upstream signals that induce monocyte to Kupffer cell differentiation. DLL1/4 inhibition by antibodies significantly inhibited expression of Kupffer cell-specific genes in monocytes [348]. Similarly mammary stem cell-derived DLL1 was shown to stimulate production of WNT ligands in mammary gland macrophages, which are known important survival factors for stem cells [349]. *In vitro*, it was shown that DLL4 induces expression of Kupffer cell lineage factors in bone marrow-derived macrophages and isolated bone marrow progenitor cells [350]. Thus, Notch signalling appears to an important candidate pathway that supports macrophages differentiation within their niche.

Models currently exist that seek to explain macrophage patterning within a tissue. The local M-CSF threshold model, posits that macrophage death leads to an excess of M-CSF, causing macrophages to proliferate locally to fill the void [330]. Repulsion through contact inhibition suggests that each macrophage occupies its own territory and macrophage loss triggers nearby macrophages to replenish empty territory [28,351]. The nurturing scaffold model proposes that membrane bound M-CSF forms a scaffold that dictates macrophage positioning within a tissue [330].

3.1.3. Macrophage ontogeny and experimental methods used to probe macrophage origins

For decades, “The Mononuclear Phagocyte System” (MPS) model [352] was used to explain the relationship between fully differentiated tissue macrophages and monocytes. In this model, it was posited that “*Monocytes in the circulation constitute a mobile pool of relatively immature cells on their way from the place of origin to the tissues*", where the cells differentiate fully into

tissue macrophages. This was supported by evidence from *in vitro* studies showing that bone marrow cells or monocytes had the capacity to differentiate into macrophages [40]. However, these studies did not consider the extent to which this differentiation actually took place *in vivo*. In recent decades, advances in experimental techniques have informed a paradigm shift, in which tissue macrophages are broadly distinguished on the basis of their ontogeny – tissue resident macrophages are seeded from the fetal liver or yolk sac prenatally, while bone marrow-derived macrophages are recruited to tissues in response to chemotactic or inflammatory cues in a CCR2-dependent manner [40].

Studies in the 2000s first revealed that the monocyte → macrophage paradigm was becoming an outdated concept. It was shown that in lethally irradiated mice that had received bone marrow transplants, Langerhans cells (dermal tissue-resident macrophages) of host origin persisted for at least 18 months. Additionally, the same study showed that no mixing of Langerhans cells occurred in parabiotic mice that share a blood supply [353], collectively indicating that these tissue-resident macrophages self-maintain locally and do not receive a significant contribution from circulating monocytes. Lineage tracing of microglia, in which yolk sac progenitors are labelled at specific embryonic timepoints, showed that they derive exclusively from yolk sac progenitors [354]. However, the extent to which monocytes contribute to tissue macrophage pools varies depending on tissue. Parabiosis and lineage tracing approaches tell us that the heart and intestines receive contribution from monocyte precursors to self-maintain at steady state [355–357]. Using parabiosis it was shown that microglia, lung macrophages, red pulp splenic macrophages, and peritoneal macrophages, receive no contribution from the bloodstream or bone marrow [358,359]. However, lineage tracing based on expression of *Ms4a3*, expressed specifically by granulocyte-monocyte progenitors in the bone marrow, indicates that monocytes contribute to adult tissue resident macrophage pools in the

lung, spleen, peritoneum, kidney, colon and small intestine, but not the brain, liver, or skin [360]. This finding may indicate that parabiosis experiments underestimate the contribution of monocytes to tissue resident macrophage populations, an effect that could be mediated by stress-induced immunosuppression.

The observation that macrophages at steady state in all tissues undergo non-total reconstitution from monocytes tells us that the pre-natal, embryonic seeding of tissue macrophages constitutes an integral initial developmental step. Our current understanding of embryonic haematopoiesis tells us that tissue macrophages develop from three distinct progenitors which arise at distinct temporal and spatial points ("waves") in the developing embryo. In the first wave, at E7.25, primitive haematopoietic progenitors emerge in blood islands of the extraembryonic yolk sac [361]. These primitive yolk sac progenitors give rise to megakaryocytes and microglia [362–364]. In the second "transient-definitive" wave at E8.25-E8.5, erythromyeloid progenitors appear from the hemogenic endothelium. With an increased lineage potential these cells can produce erythrocytes, megakaryocytes, macrophages, granulocytes, and mast cells [360,365–368]. EMPs enter the fetal bloodstream and begin to populate the fetal liver and produce lineage-committed precursors. Between E12.5 and E16.5, EMP-derived fetal monocytes seed developing tissues and differentiate into macrophages [365,366,369,370]. The third and final wave comprises primarily haematopoietic stem cells (HSCs) which first emerge at E10.5 from the aortic endothelium [371]. These HSCs initially migrate to the fetal liver [372] before terminating their migration in the bone marrow [373], where they become the primary cell type responsible for reconstituting haematopoietic lineages postnatally. Postnatal recruitment of HSC-derived monocytes, which differentiate into macrophages within tissues, depends on CCR2 for monocyte egress from the bone marrow [374,375]. However, CCR2-independent monocyte-derived macrophage accumulation has been documented. In the context of urinary tract infection, it was shown that

CCR2 was dispensable for the recruitment of Gr-1-high (CX3CR1^{low}) monocytes, but not Gr-1-low (CX3CR1^{high}) monocytes, to the bladder [376]. During acute *O. tsutsugamushi* infection, CCR2 is necessary for the early infiltration of macrophages into the lung parenchyma, but not for accumulation of macrophages in bronchus-associated lymphoid tissue [377]. In experimental autoimmune uveitis, adoptively transferred CCR2-deficient monocytes were no different in their capacity to enter the retina compared to monocytes from wild-type mice [378]. Therefore, recruitment of monocyte-derived macrophages to tissues is possible in certain contexts.

The studies outlined above have relied primarily upon three methods to delineate macrophage ontogeny. Bone marrow chimeras are commonly used in immunological research. This method relies upon the grafting of congenic or otherwise labelled bone marrow progenitors into lethally irradiated hosts [41]. This method has been used to discriminate bone marrow-derived from resident macrophages [379], since resident macrophages should proliferate at low levels and thus be radio-resistant, in contrast to bone marrow-derived macrophages which should be the opposite. However, the method is limited by the fact that certain tissue resident macrophage populations like microglia and Kupffer cells, are radio-resistant, while others like alveolar macrophages are radio-sensitive and will be depleted by irradiation. Additionally, the method cannot be considered homeostatic – the process is genotoxic and donor cells are frequently given in large excess which could impact cell-cell contact and competition for trophic factors, which could thereby skew results and interpretations [41]. Considering its limitations, an appropriate use of the method would be to test the robustness of the tissue macrophage niche – a reconstitution of the tissue macrophage compartment post-irradiation that resembles the non-irradiated mice in cell distribution and function would indicate a strong tissue niche that can reform post-injury.

Parabiosis is the surgical fusion of two animals and their bloodstreams. The method allows the discrimination of blood-derived cell types via the tracking of genetic tags. The method has been used successfully to assess the contribution of monocyte-derived macrophages to tissue macrophage pools [24,380]. However, inflammation resulting from the surgical procedure, post-operative animal death [381,382], the inability to use male animals, and ethical considerations, mean the method is now not allowed in many jurisdictions [41].

Fate mapping, or linage tracing, is an approach used to trace the origins of macrophages via the genetic introduction of a traceable label, commonly a fluorescent molecule, to monocytes or other macrophage progenitor cells. Such approaches are typically driven by a cell-specific expression of Cre-recombinase, where Cre is expressed under the control of a cell-specific gene. Animals with cell-specific Cre expression are crossed with animals with a fluorescent reporter (e.g. TdTomato) that is flanked by a loxP-STOP-loxP sequence. In animals expressing both constructs, Cre recombinase will excise the DNA between the loxP sites (the STOP codon) which happens in a cell type-specific manner, dictated by the promoter driving Cre-expression [383]. In this example, recombination will permanently and selectively label cells expressing Cre via excision of the STOP codon and subsequent expression of TdTomato fluorophore. This genetically encoded tag will be present in all cells in which recombination has occurred as well as their progeny. This recombination can be constitutive – it will occur in all instances where the promoter-driven Cre is expressed. Further specificity can be achieved using the Cre-ERT2 complex [384]. In this model, Cre is fused to a mutated human oestrogen receptor ligand-binding domain which is induced by the oestrogen analogue tamoxifen and thereby allows temporal control of Cre-expression. This approach is now recognised as the gold standard for macrophage lineage tracing [41] and via cell-specific gene expression facilitates tracking of cells of fetal and adult origin.

3.1.4. The adrenal cortex and medulla: differences in form and function

The adrenal gland is divided into the outer adrenal cortex and the inner adrenal medulla. The cortex is subdivided into the Zona Glomerulosa (ZG), which secretes aldosterone, the Zona Fasciculata (ZF) which secretes glucocorticoids (cortisol in humans, corticosterone in rodents), and the Zona Reticularis (ZR), in humans only, which synthesises androgen precursors (Figure 1.3). The adult adrenal cortex comprises 80-90% the size of the adrenal gland [385]. The most important function of the adrenal cortex is adrenal steroidogenesis which occurs in all zones of the cortex. All adrenal corticosteroids – steroid hormones synthesised in the adrenal cortex – derive from cholesterol as the common precursor molecule. As described earlier, cholesterol is metabolised into the steroid hormones through a series of enzymatic reactions (Figure 1.4, 1.5). Consequently, the cortex is characterised by a very high lipid content and prominently exhibits lipid droplets containing neutral fats, phospholipids, and especially high levels of cholesterol, mostly in esterified form [386,387]. The adrenal cortex is also highly autofluorescent which is generally attributed to this lipid content and to lipofuscin [388]. A 2018 study generated a mouse with the tamoxifen-inducible knockout of *Star*, the rate limiting enzyme in corticosteroid synthesis [308]. They reported an intense accumulation of adrenocortical lipids, as measured by Oil Red O staining (which stains neutral lipids), in the adrenal cortex eight weeks post *Star* deletion[308]. This was driven by the build-up of cholesterol that could not be metabolised into the steroid hormones. Cholesterol ester accumulation in adrenocortical cells is essential for normal steroid production [389].

In contrast, the adrenal medulla has been described as a modified sympathetic ganglion [385]. The medulla's primary function is the synthesis and release of catecholamines – adrenaline and noradrenaline (otherwise known as epinephrine and norepinephrine) which are secreted from

chromaffin cells – the functional cells of the medulla [390]. The medulla comprises 10-20% of the total size of the adrenal gland [385]. The enzyme tyrosine hydroxylase (TH) is a defining feature of the medulla, and catalyses the rate-limiting step in catecholamine biosynthesis - the conversion of tyrosine to l-dihydroxyphenylalanine [385]. The catecholamines are stored within chromaffin cells in intracellular vesicles and are released in response to splanchnic nerve activity or chemicals that reach the adrenal medulla via the circulation [390,391].

3.1.5. Foam cell origins

Foam cells, named after their "foamy" appearance, are macrophages that have become overloaded with lipids. Much of what we know about foam cells has been learned through human and rodent studies on atherosclerosis – a disease in which lipid accumulation within arteries causes arterial lumen narrowing and increased risk for adverse cardiovascular events. Foam cells are a defining feature of the fatty streaks that characterise atherosclerotic plaques [144]. The observation that CCR2-deficient mice are resistant to hypercholesterolemia-induced atherosclerosis first indicated a role for monocyte-derived macrophages in foam cell formation [148]. Since then, CCR2, CCR5, and CX3CR1 have been shown to differentially regulate monocyte / macrophage accumulation within the atherosclerotic plaque [392]. Inhibition of these receptors or their ligands reduces plaque formation by ~90% [150], strongly indicating that foam cells in this context form primarily from monocytes, though smooth muscle cell-derived foam cells have been reported [393].

Foamy atherosclerotic macrophages contain LDL cholesterol [159,394]. Many lines of evidence suggest that modification of cholesterol is necessary for foam cell formation. Indeed, modifications such as oxidation stimulates monocyte-endothelial cell interactions [395] and oxidised LDL has been found in human atherosclerotic plaques [396]. However, foam cell

formation has also been observed in human and murine macrophages with the addition of non-modified native LDL, at concentrations associated with hypercholesterolemia [159,397]. Macrophage uptake of whole native LDL is mediated via fluid phase endocytosis [159]. Additionally, cholesterol ester and free cholesterol can be taken up from lipoproteins independently of apolipoprotein in a process known as selective lipid uptake [397]. Indeed, the majority of macrophage LDL-derived cholesterol is acquired by selective uptake of cholesterol ester [397]. Taken collectively, the evidence would indicate that foam cells can be generated from uptake of both modified and non-modified forms of LDL cholesterol. Scavenger receptors also contribute to cholesterol uptake and foam cell formation. The scavenger receptor MARCO mediates the uptake of oxidised LDL in bone marrow-derived macrophages (unpublished observation). CD36, a receptor for oxidised LDL [398], positively regulates atherosclerosis and its targeted inhibition significantly reduces atherosclerotic lesion area. Scavenger receptors class A-I/II also are involved in the uptake of modified LDL and their knockout inhibits the formation of atherosclerotic plaques [399]. Macrophage foam cell formation is therefore a complex process mediated via multiple different forms of cholesterol and mechanisms of cholesterol uptake. Foam cells formed via cell-autonomous cholesterol synthesis have not been reported.

3.1.6. Adrenal gland macrophages

Macrophages were first identified in the adrenal medulla and cortex of both mice and humans in 1984 and 1994, respectively [39,400]. They describe macrophages that fall into one of two general categories: those located adjacent to vascular sinuses and those located throughout the parenchyma. The parenchymal macrophages extend dendrites though, and come into direct contact with parenchymal cells [39,400], indicating potential paracrine interactions. However, to date, few studies have directly characterised and probed the ontogeny and function of the

macrophage compartment of the murine adrenal gland. One recent study [302] used fate mapping and lineage tracing to attempt to trace the origins of adrenal macrophages.

Dolfi et al. [302] showed that 48 hours post tamoxifen administration to CCR2-CreERT2;R26TdTomato mice ~5% of macrophages are TdTomato+ in female mice, indicating a robust monocyte contribution to the macrophage pool. This was dependent on CCR2 as demonstrated by double knockin-knockout CCR2-CreERT2;R26TdTomato;$CCR2^{-/-}$ mice. However, in male mice only ~1% of macrophages were TdTomato+ and this was independent of CCR2, indicating that adrenal gland macrophages in male mice do not undergo significant replenishment from monocytes. Longer term pulse chase experiments showed that monocyte contribution to the macrophage pool increased with time in female mice, but data was not shown for male mice. Fate mapping using Ms4a3cre ; R26TdTomato mice, in which monocyte-derived cells are labelled with TdTomato [360], suggested that at 16 weeks of age ~40% male macrophages were monocyte-derived, compared to ~50% of female macrophages. They also showed that levels of macrophages were similar in wild-type and CCR2-deficient mice in both male and female mice. This data indicates either that monocyte-derived macrophages contribute to the adrenal macrophage pool in a CCR2-independent manner, or that adrenal macrophages can compensate for reduced monocyte input via increased proliferation. Ki-67 expression was increased in $CCR2^{-/-}$ female, but not male, adrenal macrophages, suggesting that increased proliferation may be the compensatory mechanism. By tamoxifen pulsing pregnant female CX3CR1-CreERT2 ; R26TdTomato mice at E14.5 the authors showed that ~15% of adrenal macrophages were $TdTomato^{+}$ in 8 week old progeny, indicating embryonic origin of adult adrenal macrophages.

3.1.7. Single cell and bulk RNA sequencing technologies

RNA sequencing (RNA seq) is a technique by which next generation sequencing is applied to detect and quantify the presence of RNA within a particular biological sample. The method gives a snapshot of all transcribable genetic material within the cells or tissue analysed, collectively termed the transcriptome. Sequencing generally involves a conserved workflow: RNA extraction from biological samples, mRNA enrichment, followed by cDNA synthesis and preparation of an adaptor-ligated sequencing library, sequencing, and data analysis [401].

RNA sequencing has proven a powerful tool in biomedical research and has been used to deliver new insights into RNA splicing [402], non-coding RNA regulation of gene expression [403], enhancer RNAs [404], cancer classification, biomarker and companion diagnostic development [405]. Bulk RNA sequencing (Bulk-seq) comprised the first iteration of this technology. Bulk-seq relies upon sequencing of all of the RNA in a tissue or cell population and averaging the gene expression in that population to establish gene expression [406]. This method of sequencing is useful for its cost effectiveness and simplicity [405] and remains in broad usage, but lacks resolution at the cellular level. While FACS can be used to improve resolution by isolating cell types based on protein expression, transcriptional variances can still occur within cell populations that can cloud results in traditional bulk RNA-seq experiments.

Cells' transcriptional signature can be influenced by somatic alterations, transcriptional regulations, and epigenetic regulations [405]. Single cell RNA sequencing (ScRNA-seq) technologies, in which cDNA synthesis, library preparation, and sequencing, occur at a cellular resolution, has been the next iteration in sequencing technologies [405]. This method has been used to dissect intra-tumour cellular heterogeneity and inform therapeutic strategy [405], in

addition to applications in numerous other tissues including the adrenal gland [302,407]. Changes in gene and protein expression and RNA contamination between cell types is possible during enzymatic and mechanical digestion procedures and can lead to false reads during data analysis. Refinements to ScRNA-seq methods have been proposed to counteract this possibility, including single nucleus RNA sequencing [408] and RiboTag sequencing in which ribosomes are immunoprecipitated for sequencing, resulting in a more accurate measurement of the transcriptome [409]. Additionally, traditional ScRNA-seq gives a temporal snapshot of cellular gene expression, which limits the scope of the method for studying continuous processes, such as cell differentiation, tissue development or regeneration. But by examining the balance between unspliced and spliced mRNAs, which is predictive of cellular state progression, it is possible to predict position of cells along a differentiation trajectory and the future differentiation state of a cell. This method is known as RNA velocity and can be applied to ScRNAseq datasets [410].

The latest iteration of RNA sequencing technologies is spatial transcriptomics. This method relies upon sequencing within intact tissues and combines the global transcriptional capacity of bulk RNA-seq with the single cellular resolution of *in situ* hybridisation [405]. Moreover, the method can be combined with ScRNA-seq to facilitate simultaneous *in situ* cell-type identification and spatial mapping [411], thereby offering one of the most powerful methods to date to probe cell and tissue biology.

3.2. Rationale and experimental aims

The adrenal gland is known to harbour a variety of immune cells. Though this is to be expected to an extent, the adrenal gland is not a mucosal surface and so the extent to which these cells are necessary for immune surveillance remains unclear. Non-immune functions have been

ascribed to macrophages in a variety of other tissue contexts. The immune cell compartment, and specifically the myeloid fraction of the murine adrenal gland remains incompletely understood at both the phenotypic and functional level. I hypothesised that phenotypic heterogeneity exists among adrenal gland macrophages and that adrenal macrophages have tissue-specific characteristics.

The aims of this chapter were:

1) To characterise the murine adrenal macrophage compartment spatially and temporally.
2) To establish the ontogeny of adrenal gland macrophages.
3) To identify adrenal gland macrophage-specific gene expression patterns.

3.3. Results

3.3.1 Leukocyte populations in the murine adrenal gland.

To first understand the total cellular composition of the murine adrenal gland, I utilised a published single cell RNA seq dataset [407] of whole male mouse adrenal glands at 10 weeks old. Using select gene markers, I established four primary cell types in the murine adrenal glands. Cells expressing *Nr5a1* (steroidogenic factor 1; SF-1) were categorised as cortical cells, and represented the largest cluster among all the adrenal cells (Figure 3.1A). Cells of the adrenal medulla were defined based on the expression of *Th* and were among the smallest of detectable cell populations (Figure 3.1A). *Ptprc* (CD45) expressing cells were defined as the immune cells of the adrenal gland, while *Pecam1*-experessing (CD31) cells were defined as the endothelial cell fraction (Figure 3.1A). Next, I sought to evaluate the adrenal gland cells in relation to the factors known to regulate the intra-tissue macrophage niche [330]. Interestingly, the endothelial cell fraction was the primary population expressing *Csf1* which encodes M-CSF, the macrophage survival factor (Figure 3.1B). *Csf2* was not expressed significantly in

any cell cluster. The cytokine *Il34* (IL-34; CSF1R ligand) was expressed by Zona fasciculata cluster 4 (ZF4), while the capsular cluster, Zona Glomerulosa clusters 1-3 (ZG1-3), and to a lesser extent ZF1-3, expressed *Cx3cl1* (Figure 3.1B). Neither *Il4* nor *Il13* were expressed significantly by any cell type (Figure 3.1B). The Notch ligand *Dll1* was expressed at low levels by endothelial cluster 1, whereas *Dll4* was expressed in the capsule and by endothelial clusters 1 and 2 (Figure 3.1B). The endothelial 2 cluster appears to express modest levels of *Il34* (Figure 3.1B).

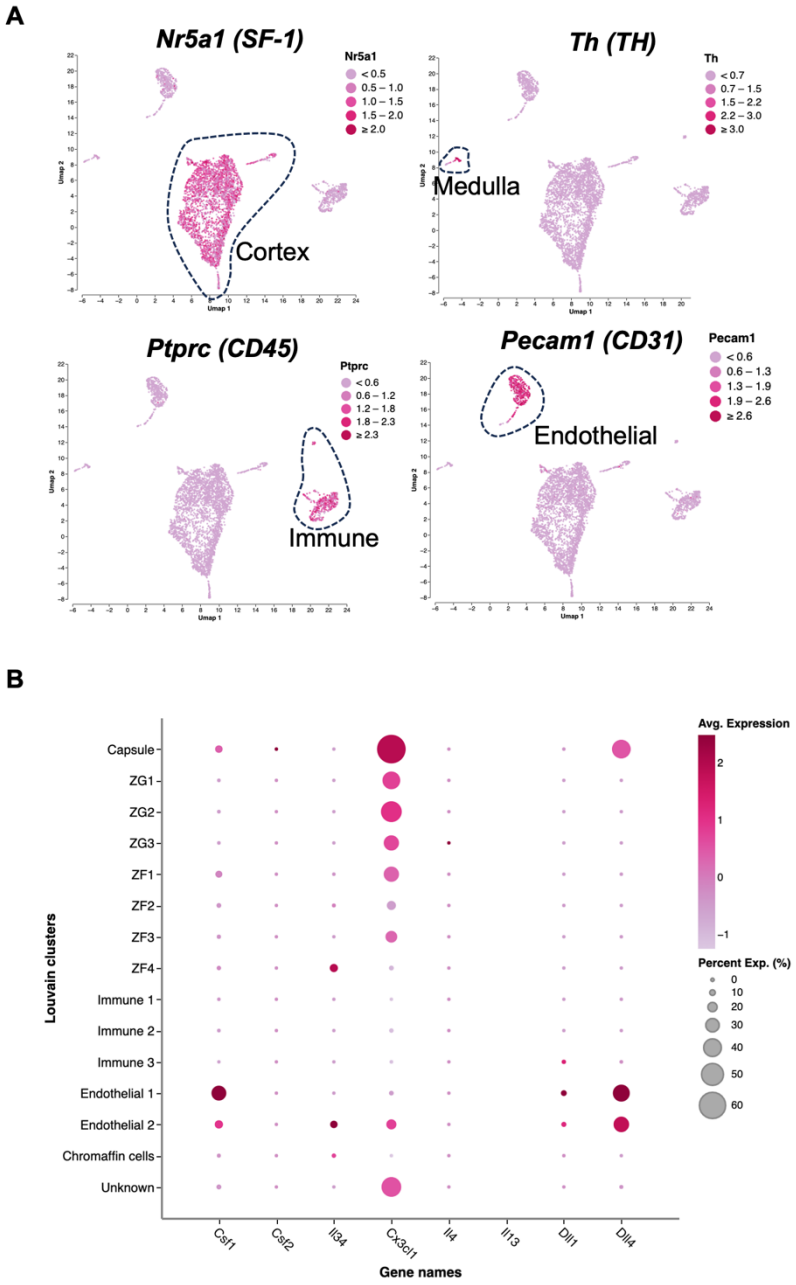


Figure 3.1. All cell types in the murine adrenal gland. (A) Single cell RNA seq data clustering of the adrenal gland cell subsets with the gene expression of marker genes for the cortex (Nr5a1; SF-1), medulla chromaffin cells (Th; TH), immune cells (Ptprc; CD45)), and endothelial cells (Pecam1; CD31). (B) A dot plot showing gene expression of each of the indicated macrophage trophic factors.

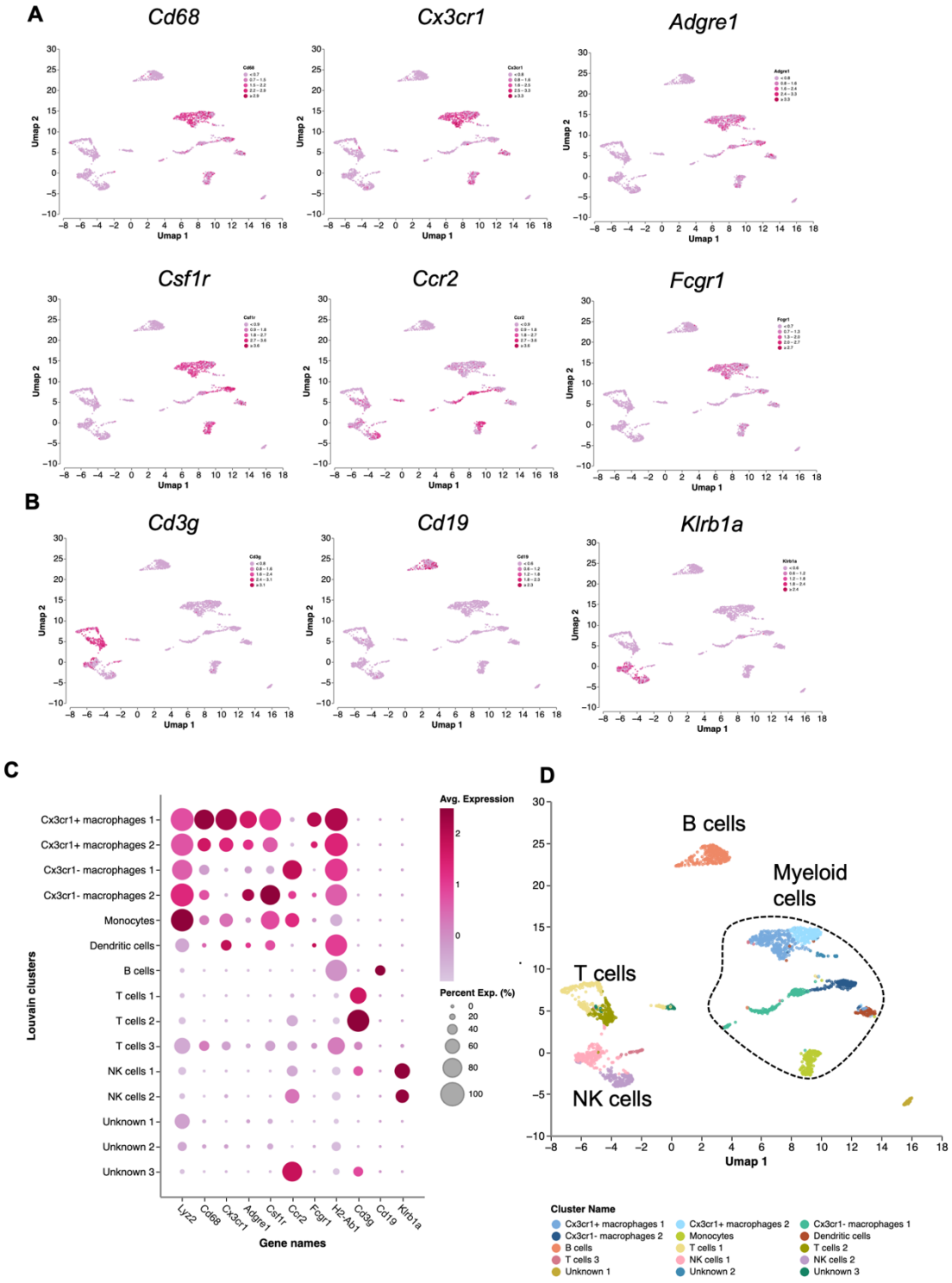


Figure 3.2. Leukocyte populations in the murine adrenal gland. Single cell RNA-seq data (PMID 35705045) showing gene expression of the the indicated myeloid (A) and lymphoid (B) cell-associated genes in murine adrenal gland leukocytes. (C) Leukocyte clusters in the adrenal gland according to the gene expression data in A and B.

Next, I sought to establish the total immune cell makeup of the murine adrenal gland. To this end, I used published single cell RNA-seq dataset of $CD45^+$ leukocytes from male 7-week-old mice [302]. This dataset was used as opposed to the dataset from figure 3.1 because of the larger cell number. The whole adrenal dataset contains 800 immune cells [407], as opposed to 2340 in the $CD45^+$ cell-only dataset [302]. I generated heat maps showing gene expression of the myeloid genes *Cd68, Cx3cr1, Adgre1* (F4/80), *Csf1r, Ccr2, Fcgr1* (CD64) (Figure 3.2A), and the lymphoid genes *Cd3g* (CD3), *Cd19*, and *Klrb1a* (Figure 3.2B, C). From these heatmaps I was able to identify 15 distinct and discrete myeloid and lymphoid cellular clusters. The myeloid cluster could broadly be defined by *H2-Ab1* (MHCII) and *Lyz2* expression. Within the myeloid cluster, macrophages were defined as cells expressing *Cd68, Adgre1 (*F4/80*)*, and *Csf1r*, and could be differentiated on the basis of *Cx3cr1* expression. Monocytes were defined as myeloid cells with low *Adgre1* expression, and high *Csf1r* and *Ccr2* expression. Dendritic cells were defined as myeloid cells with low macrophage marker expression and high *H2-Ab1 (*MHCII*)* expression. Collectively, myeloid cells comprised over half of the total immune cells in the adrenal glands (Figure 3.2C, D). Lymphoid cells were also apparent in the adrenals, and could be differentiated into *Cd3g* (CD3) expressing T cells, *Klrb1a*-highly expressing NK cells, and H2-Ab1 (MHCII) and *Cd19*-expressing B cells (Figure 3.2C, D). Three additional immune cell clusters could not be identified as a known immune cell type and were termed Unknown clusters 1, 2 and 3 (Figure 3.3C, D).

3.3.2. Cortico-medullary differences in adrenal myeloid cells.

To assess the myeloid fraction of the adrenals at the cellular and protein level, a flow cytometry panel was designed to detect myeloid cells in the murine adrenal gland. Leukocytes ($CD45^+$), myeloid cells ($CD45^+$ $CD68^+$), macrophages ($CD45^+$ $CD68^+$ $F4/80^+$), neutrophil-like cells ($CD45^+$ $CD68^+$ $Ly6G^+$ $CD11b^+$ $F4/80^-$) and other myeloid ($CD45^+$ $CD68^+$ $CD11b^-$ $F4/80^-$) cells were measured in the murine adrenal cortex and medulla of 20-week-old male mice (Figure 3.3A). Leukocytes constitute a similar proportion of total cells in the cortex and medulla and exist at similar frequencies in both adrenal zones (Figure 3.3B). Myeloid cells constitute a significantly higher fraction of leukocytes in the cortex relative to the medulla (Figure 3.3C). Macrophages comprise a majority of the myeloid fraction in both the adrenal cortex and medulla, though this is significantly higher (87%) in the cortex relative to the medulla (60%) (Figure 3.2D). $Ly6G^+$ $CD11b^+$ cells comprise ~30% myeloid cells in the medulla, relative to <10% in the cortex (Figure 3.3E). Other myeloid cells negative for F4/80 and Ly6G comprise 5-6% of myeloid cells in both the cortex and the medulla (Figure. 3.3F). Collectively, these data indicate that the adrenal cortex and medulla constitute separate and distinct immune cell niches within the adrenal gland.

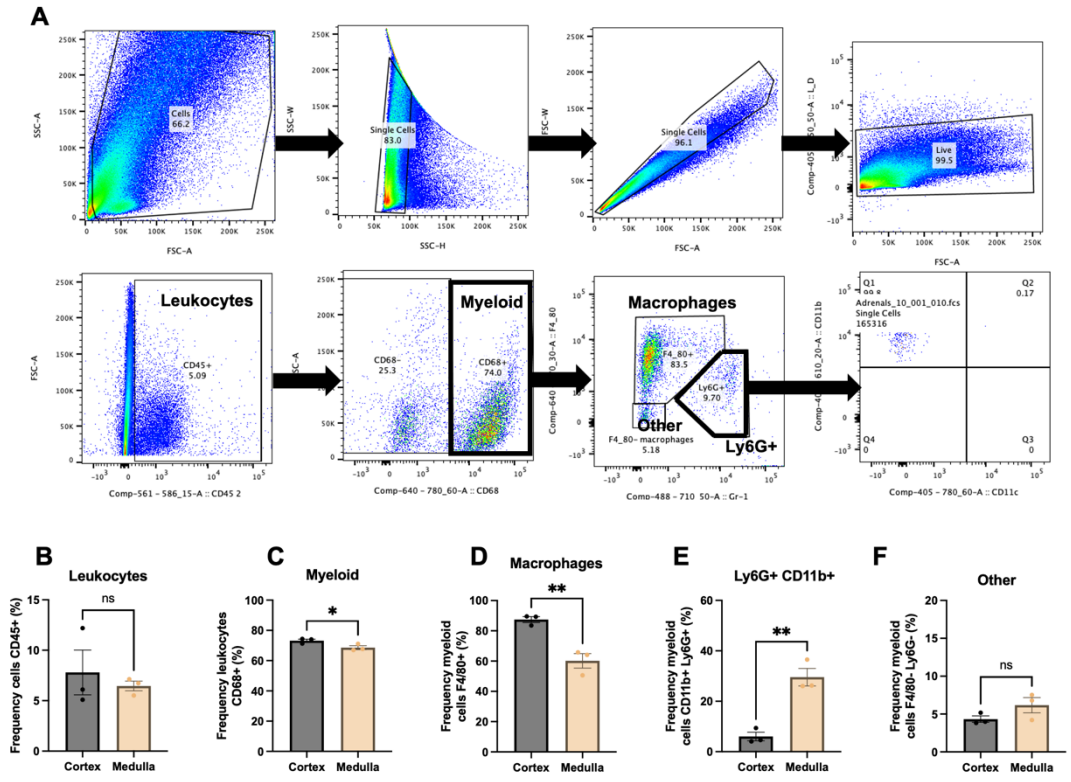


Figure 3.3. Cortico-medullary differences in adrenal myeloid cells. (A) Gating strategy for the data depicted in B-F. Flow cytometry data depicting the frequency of total cells that are CD45+ (B) and frequency of leukocytes that are CD68+ (C). Data showing the frequency of myeloid (CD68+) cells that are F4/80+ (D), Ly6G+ (E), and F4/80- Ly6G-.

3.3.3 The adrenal cortex harbours two spatially distinct macrophage subsets.

This study subsequently focused on the macrophage component of the murine adrenal gland, as these were the largest proportion of leukocytes in the cortex and medulla. Since cellular location can frequently be linked with cellular function, I sought to characterise the spatial distribution of macrophages within the adrenal gland using immunofluorescent imaging. Immunofluorescent imaging was carried out on the CX3CR1-GFP murine adrenal gland, with macrophages marked with via transgenic GFP, and immunostaining against the pan-macrophage marker CD68. I observed CX3CR1-expressing macrophages in the cortex and medulla of the adrenal gland (Figure 3.4). However, CX3CR1-expressing cells existed at the highest densities in the outermost ZG region of the cortex and in the medulla (Figure 3.4). CX3CR1-expressing cells were most sparsely distributed in the zona fasciculata, particularly

in the peri-medullary region (Figure 3.4). CD68 labelling marked macrophages throughout the adrenal gland, including the CX3CR1-expressing macrophages in the cortex and the medulla. However, this staining revealed a population of $CD68^{++}$ macrophages in the ZF region of the adrenal cortex that was non-overlapping with CX3CR1-expressing cells (Figure 3.4).

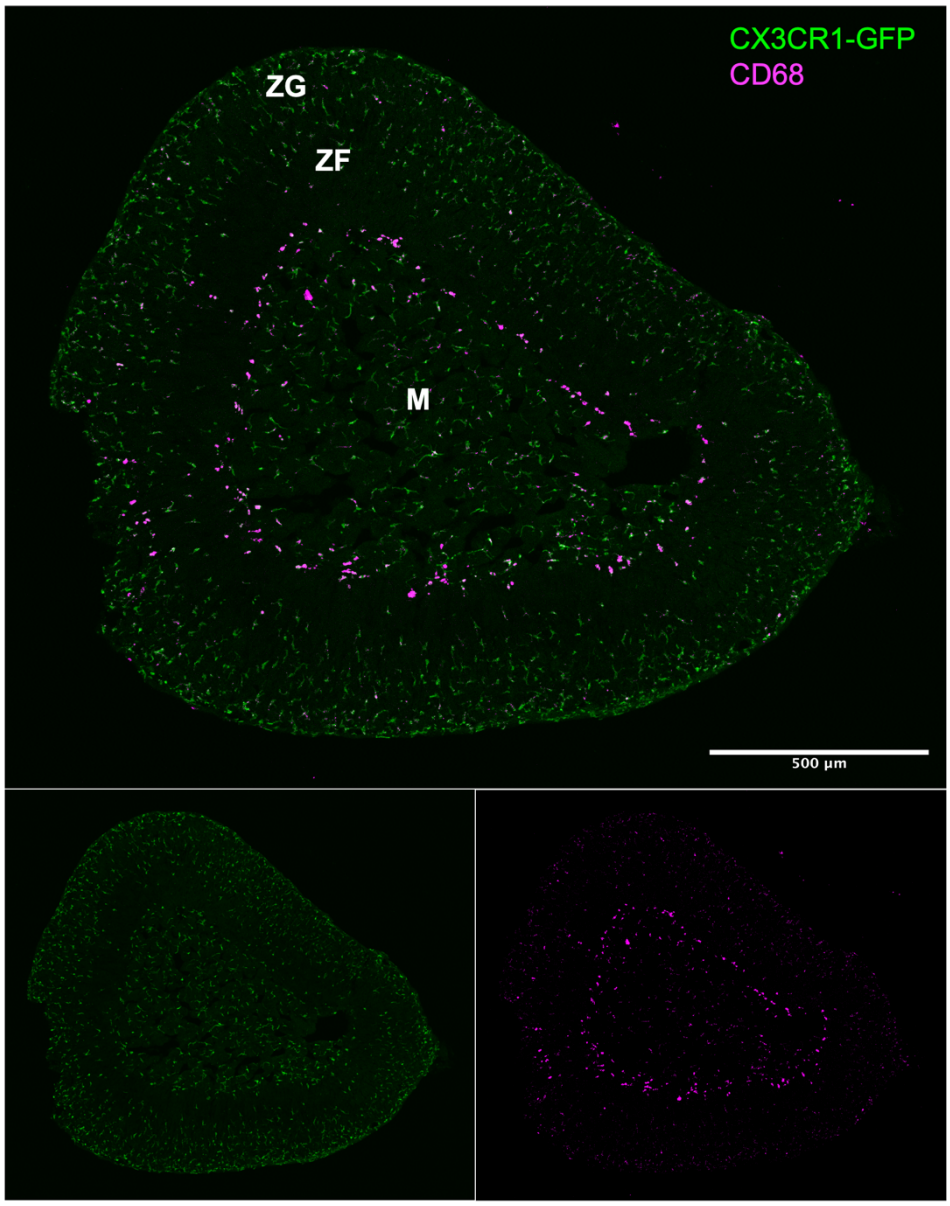


Figure 3.4. The adrenal cortex harbours two spatially distinct macrophage subsets. A representative confocal image showing a cross section of a mouse adrenal gland isolated from a 12 week old $CX3CR1^{GFP}$ mouse and stained using an anti-GFP (green) and an anti-CD68 (magenta) antibody. ZG = zona glomerulosa ; ZF = zona fasciculata ; M = medulla.

Next, I wanted to establish whether the CX3CR1-expressing cells I observed at high densities in the zona glomerulosa come into contact with the aldosterone-producing cells in this zone. Using an anti-CYP11B2 (aldosterone synthase) antibody (kindly provided by Celso Gomez-Sanchez) I first performed an antibody titration to establish the working concentration of this antibody. Testing multiple concentrations, I found that the antibody produced the characteristic staining in the zona glomerulosa at a concentration of 1/200 (Figure 3.5A). I next used the antibody at this concentration on male adrenals from CX3CR1-GFP mice. The dendritic CX3CR1-expressing macrophages that preferentially localise to the zona glomerulosa were observed in direct contact with aldosterone-producing cells in this zone, wrapping around and enveloping the endocrine cells (Figure 3.5B), indicating possible paracrine interaction between these two cell types. From this point onwards, these macrophages are referred to as Zona Glomerulosa Macrophages (ZGMs).

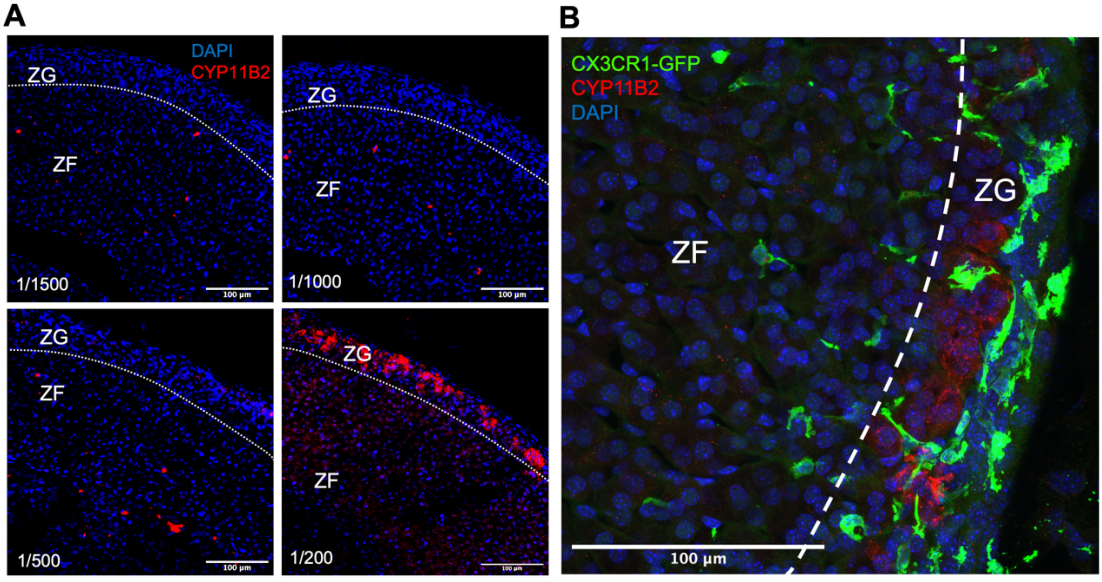


Figure 3.5. CX3CR1-expressing zona glomerulosa macrophages preferentially localise to aldosterone-producing cells. (A) Titrating the anti-CYP11B2 (aldosterone synthase) antibody at the indicated concentrations. (B) A representative confocal image focusing on the adrenal zona glomerulosa of a CX3CR1^{GFP} mouse and stained with an anti-GFP (green) antibody, an anti-CYP11B2 (red) antibody, and DAPI (blue). Scale bars in (A) and (B) are 100µm. ZG = zona glomerulosa ; ZF = zona fasciculata.

3.3.4 CX3CR1-expressing ZGMs decline with age.

To assess the adrenal macrophage compartment in a more quantitative manner, I used flow cytometry to discriminate between the CX3CR1-positive ZGMs and CX3CR1-negative cortical macrophages and assess their proportions longitudinally. Using the gating strategy outlined in Figure 3.6A and 3.6B, I found that while CX3CR1-was expressed by virtually all macrophages at 10-weeks-old, CX3CR1 expression declined with age, a fall particularly prominent at the 20-week timepoint, relative to earlier timepoints (Figure 3.7A). Numbers of ZGMs remained similar at 10 and 15-weeks, then significantly fell at 20-weeks-old from comprising >95% of adrenal macrophages, to ~70% (Figure 3.7B). CCR2-deficient mice, which have defective monocyte egress from the bone marrow [375], had similar numbers of ZGMs as wild-type mice at the 20-week timepoint (Figure 3.7C).

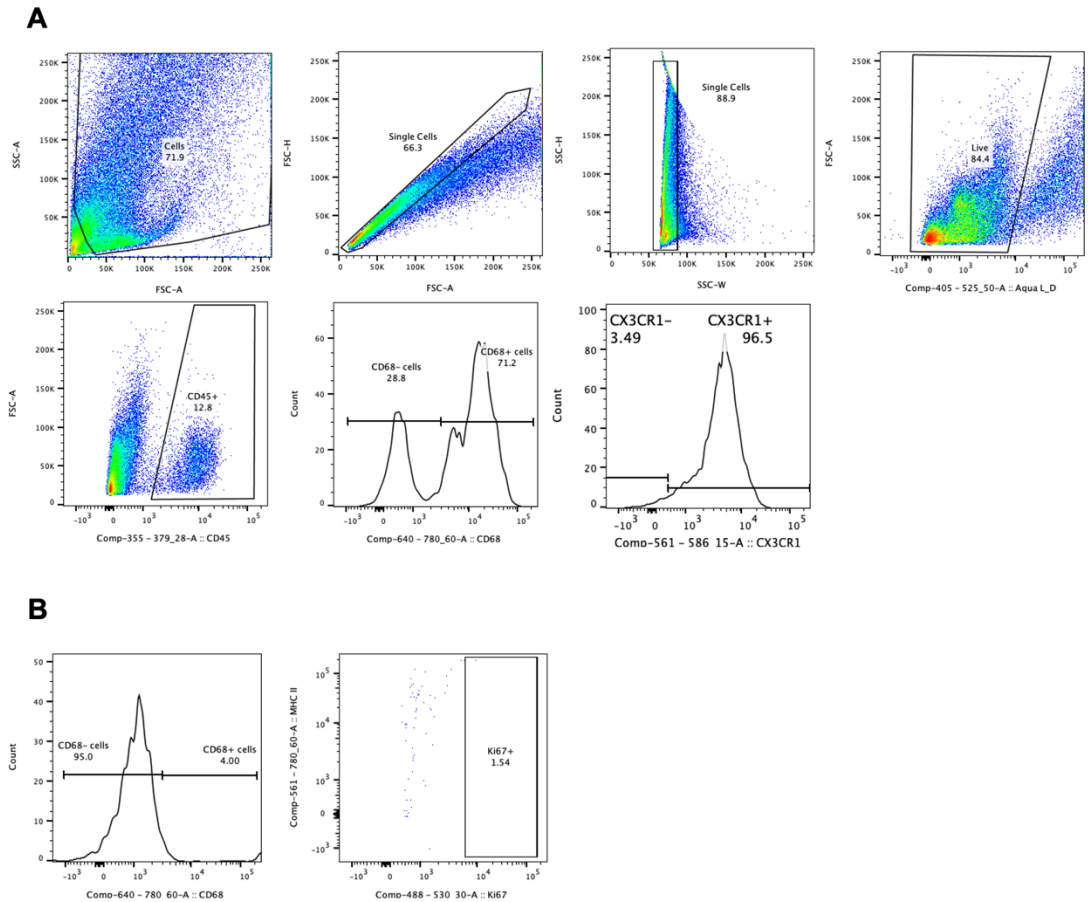


Figure 3.6. Flow cytometry gating strategy. (A) Flow cytometry gating strategy used for the longitudinal macrophage experiments depicted in Figure 3.7. (B) Intracellular stain isotype (negative) controls used to define CD68 and Ki-67 expressing cells.

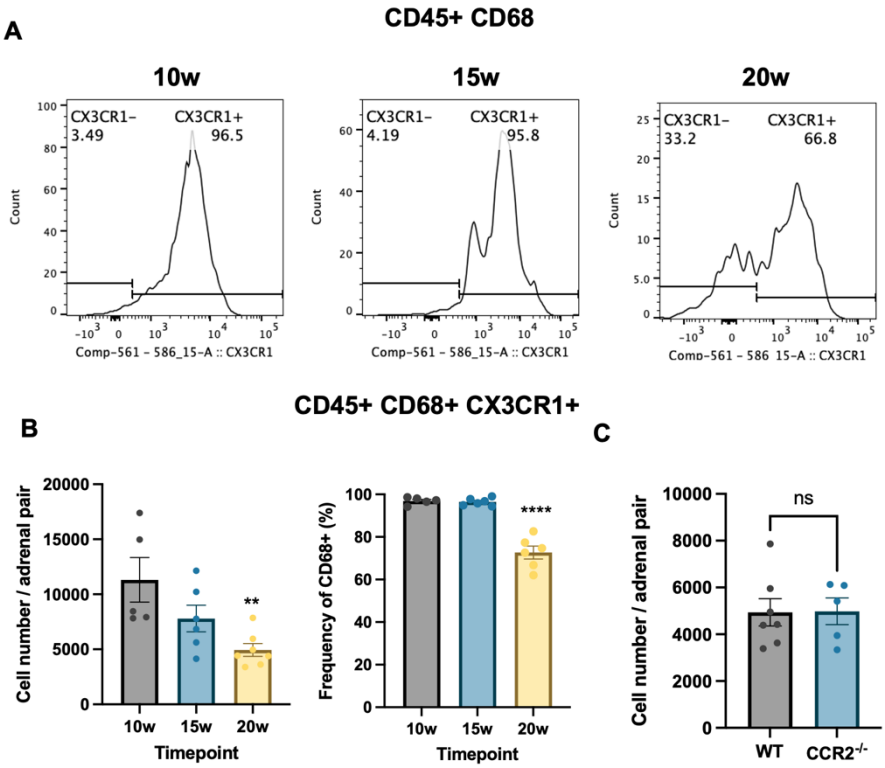


Figure 3.7. CX3CR1-expressing macrophages decline with age. (A) Histograms depicting the level of macrophage (CD68+) CX3CR1 expression at 10, 15, and 20, weeks of age in the adrenal cortex. (B) (E) Flow cytometry data showing the absolute number of CD68+ CX3CR1+ cells (left) and frequency of CX3CR1- cells among CD45+ CD68+ cells (right) in the adrenal cortex at the indicated timepoints. Each data point depicts the data from one mouse. (C) The absolute number of CD45+ CD68+ CX3CR1+ cells in wild-type (WT) and CCR2$^{-/-}$ mice at 20 weeks of age.

3.3.5 Big Autofluorescent Lipid-Laden (BALL) adrenal macrophages accumulate with age.

The next objective was to characterise the CX3CR1-negative fraction of adrenal macrophages. I observed an age-dependent accumulation of CD68^{++} macrophages in the ZF, with cells becoming more populous and bigger in size with age (Figure 3.8A). Flow cytometry revealed that CX3CR1-negative macrophages were significantly increased in number and proportion in the adrenal cortexes of 20-week-old mice relative to earlier timepoints (Figure 3.8B). In contrast to ZGMs, CD68^{++} cortical macrophages have a "foamy" morphology, similar to the

cholesterol-loaded foam cell macrophages that characterise atherosclerotic plaques [144,412]. These macrophages have a highly autofluorescent cellular content, which is located in intracellular vacuoles (Figure 3.8C).

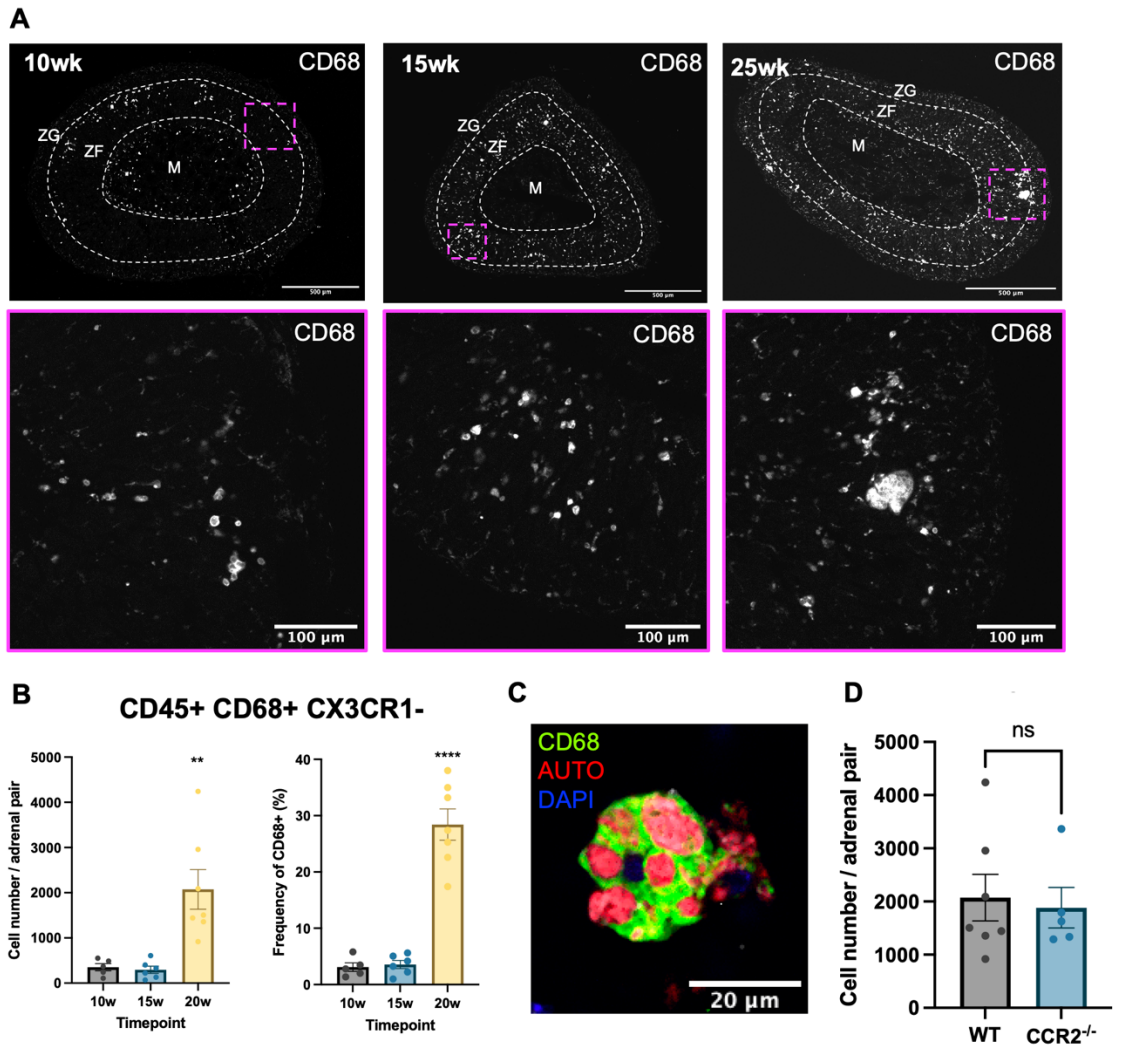


Figure 3.8. Big autofluorescent CX3CR1 negative macrophages accumulate with age. (A) Representative confocal images showing cross sections of wild-type mouse adrenal glands at the indicated timepoints stained against CD68 (white). White dotted lines indicate demarcation of the different zones of the adrenal gland. Dashed magenta boxes in the above images for each timepoint indicate the areas that are enhanced in the magenta boxes below. Scale bars in the top images are 500µm and the bars in the below images are 100µm. (B) Flow cytometry data showing the absolute number of CD68+ CX3CR1- cells (left) and frequency of CX3CR1- cells among CD45+ CD68+ cells (right) in the adrenal cortex at the indicated timepoints. Each data point depicts the data from one mouse. (C) A close-up confocal image of a cortical CD68+ (green) macrophage showing the autofluorescent (red) contents in intracellular vacuoles. DAPI is shown in blue – scale bar 20µm. (D) The absolute number of CD45+ CD68+ CX3CR1- cells in wild-type (WT) and $CCR2^{-/-}$ mice at 20 weeks of age.

Consequently, these macrophages were termed Big Autofluorescent Lipid-Laden (BALL) macrophages, and this term is used to describe these cells in the remainder of this thesis. Similar to ZGMs, CX3CR1-negative BALL macrophages exist at similar numbers in the adrenals of wild-type and CCR2-deficient animals (Figure 3.8D). These two phenotypically and morphologically distinct macrophage populations co-reside in the adrenal cortex (Figure 3.9A). Additionally, they differ on the basis of Ki-67 expression, with CX3CR1^{+} ZGMs being Ki-67^{low} and CX3CR1^{-} BALL macrophages being Ki-67^{high} at two out of the three timepoints tested (Figure 3.9B).

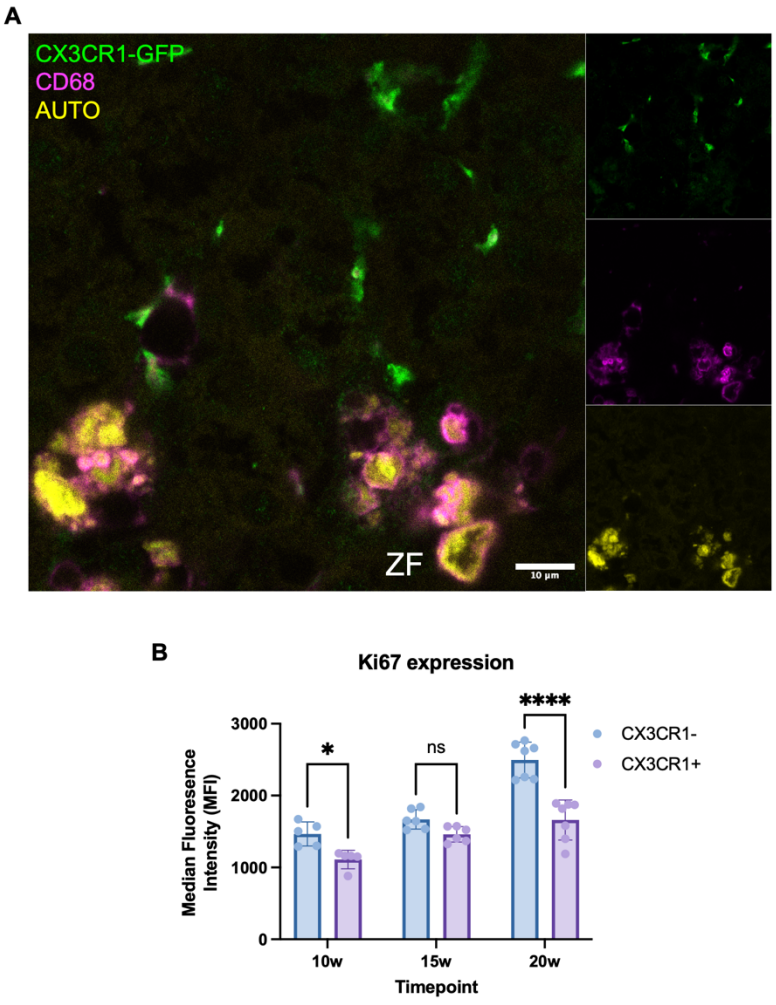


Figure 3.9. Phenotypically distinct macrophages co-reside in the adult adrenal cortex. (A) A representative confocal image of the adrenal cortex of a 22 week old male CX3CR1$^{GFP/+}$ reporter mouse stained with anti-GFP (green), anti-CD68 (magenta) and autofluorescence shown in yellow - scale bar 10µm. (B) Flow cytometric data showing the median fluorescence intensity of Ki-67 expression in the indicated macrophage (CD45+ CD68+) subpopulations at the indicated timepoints.

3.3.6. Aged adrenal autofluorescence is contained inside CD68^{+} macrophages

The adrenal gland is widely known to be autofluorescent, which is attributed to its high lipid content [388]. To ensure that the autofluorescent macrophages were not an artefact of fluorescent imaging, I next characterised the autofluorescent signature of the aged (20-week-old) adrenal gland, finding wide spectral autofluorescent signals which decline approaching the far-red end of the light spectrum (Figure 3.10A). By staining with a directly conjugated anti-CD68 antibody with a fluorophore that emits outside the adrenal autofluorescent signal, the adrenocortical BALL macrophages were confirmed to not be an artefact and were established as the source of the autofluorescent signal inherent to the aged adrenal gland (Figure 3.10B). CD68 staining in the adrenal cortex was additionally verified using classical immunohistochemistry with Fast Red staining (Figure 3.10C).

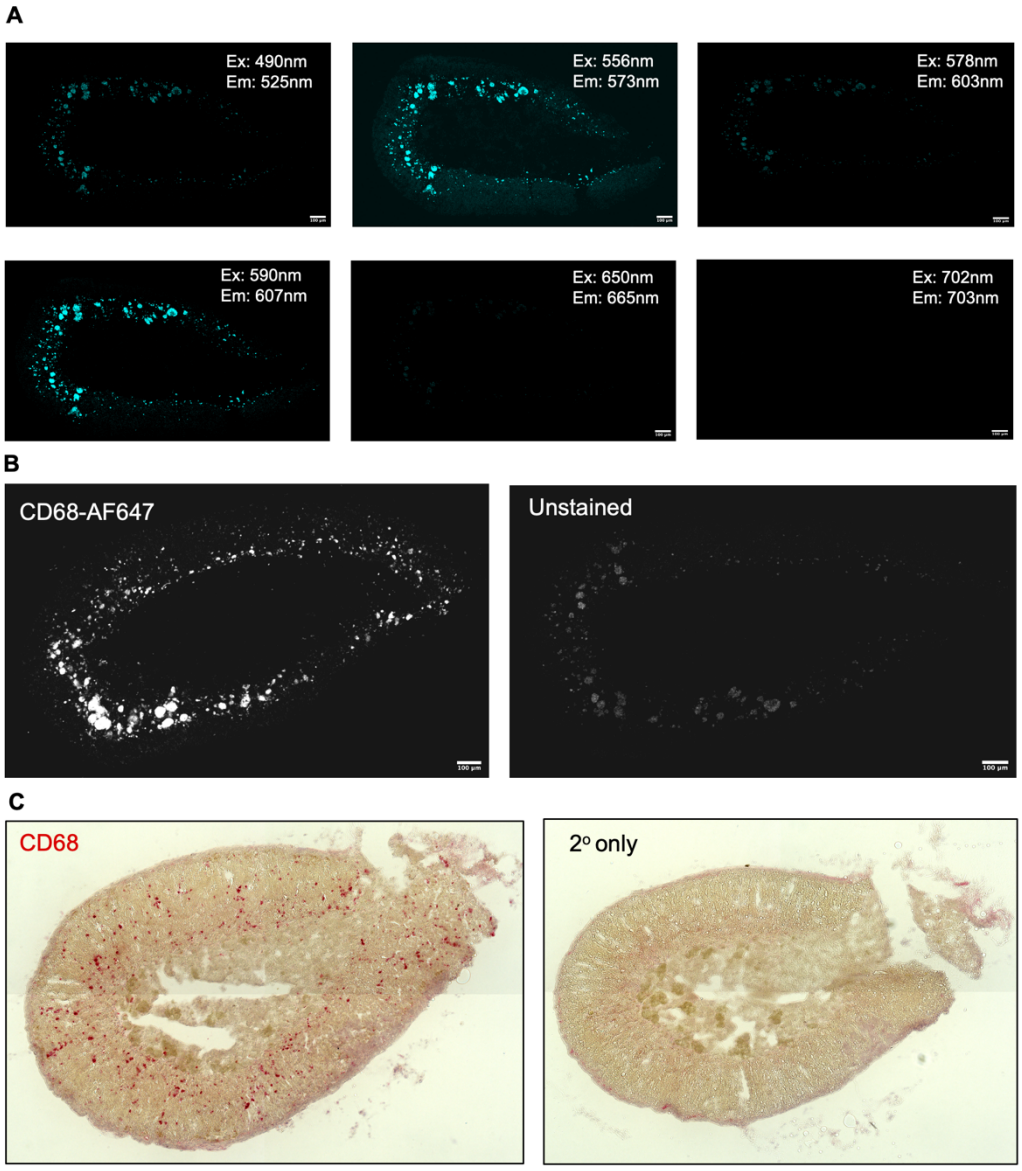


Figure 3.10. Aged adrenal autofluorescence is contained in CD68+ cells. (A) Confocal images showing the autofluorescent signals at the indicated excitation/emissions from unstained 22-week-old male adrenal glands. (B) Confocal images showing a cross section of a 22-week-old male wild-type murine adrenal gland stained with anti-CD68-AF647 (white) (left) and an unstained slice (right) taken from the same mouse adrenal gland. (C) An optical micrograph of a 22-week-old male mouse adrenal gland stained with H&E and ant-CD68 Fast Red staining (left) and a secondary antibody-only control (right). Scale bars are 100µm.

3.3.7 BALL macrophages contain cholesterol and their formation is accelerated in obesity

The next objective was to establish the nature of the autofluorescent contents of BALL macrophages. I hypothesised that the lipid contained in BALL macrophages is cholesterol, given its metabolic and physiological relevance in the adrenal gland as the necessary precursor

molecule to the adrenal steroid hormones corticosterone and aldosterone. A previous study [308] generated mice (Cre-ER^{TM};Star$^{flox/flox}$mice) which were used to generate temporal ablation of steroidogenic acute regulatory protein (*Star*) gene in adult mice upon tamoxifen administration (Figure 3.11A). Using Oil Red O staining, they observed extensive lipid accumulation in large vacuolated cells in the adrenals of these mice [308], driven by accumulating cholesterol that can not be metabolised into the steroid hormones. These adrenal glands were stained against the pan macrophage marker CD68, and it was found that the accumulating lipid / cholesterol in these adrenals is contained entirely inside macrophages (Figure 3.11B). This macrophage-bound cholesterol was highly autofluorescent (Figure 3.11C), in agreement with the previous findings (Figure 3.10A).

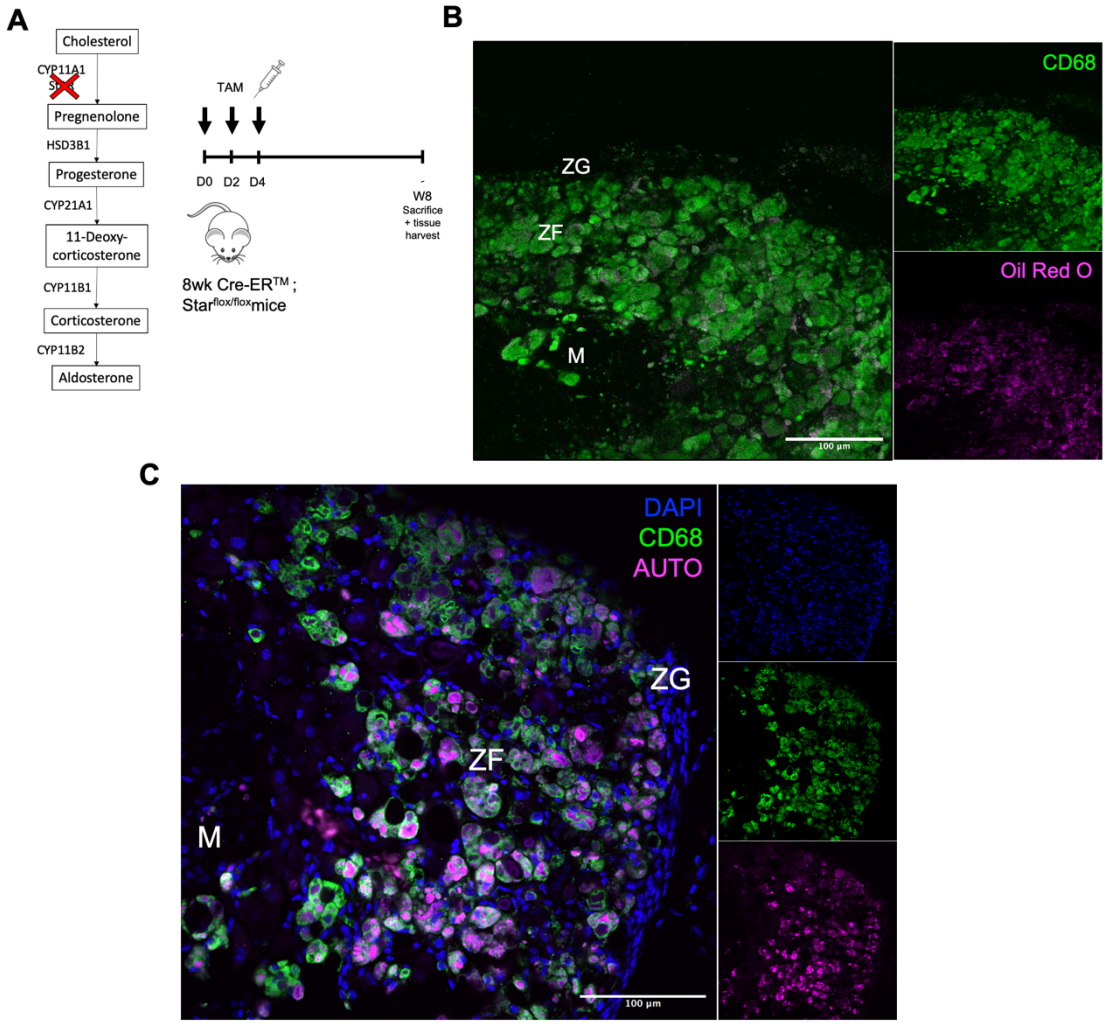


Figure 3.11. BALL macrophages contain cholesterol. (A) Schematic depicting the experimental protocol used to generate the tissue that was analyzed in panel B. Eight week old CAGGCre-ER^{TM} ; Star$^{flox/flox}$ mice were pulsed with tamoxifen on days 0, 2, and 4 to induce temporal deletion of Star, the rate-limiting enzyme in the adrenal corticosteroid biosynthetic pathway. Eight weeks later adrenal glands were harvested for subsequent microscopic analyses. (B) A representative confocal image showing an adrenal gland from a CAGGCre-ER^{TM} ; Star$^{flox/flox}$ mouse stained with anti-CD68 (green) and Oil Red O (magenta). (A) A representative confocal image showing an adrenal gland from a CAGGCre-ER^{TM} ; Star$^{flox/flox}$ mouse stained with anti-CD68 (green) and DAPI (blue), with autofluorescence (magenta). ZG = zona glomerulosa ; ZF = zona fasciculata ; M = medulla ; AUTO = autofluorescence.

The adrenals used in Figure 3.11 were from a knockout mouse exhibiting a severe phenotype. Next, I wanted to determine the effect of a physiologically relevant challenge – one that increases plasma cholesterol – on BALL macrophages. To induce hypercholesterolaemia, CX3CR1$^{GFP/GFP}$ mice were fed a high fat diet (HFD) for 12 weeks Figure (3.12A). HFD-fed mice had elevated total plasma cholesterol levels and plasma cholesterol esters, relative to normal diet-fed mice (Figure (3.12B, C). HFD-fed mice also had accelerated BALL macrophage formation, with more extensive cortical CD68 staining and macrophage-derived autofluorescence relative to normal diet (ND)-fed mice (Figure 3.12D). Image analysis revealed that the BALL macrophages were significantly more autofluorescent and lipid-laden in HFD-fed mice relative to ND-fed mice (Figure 3.12E, F). Collectively, the data indicate that BALL macrophages contain cholesterol and that their formation is accelerated in obesity where plasma cholesterol levels rise.

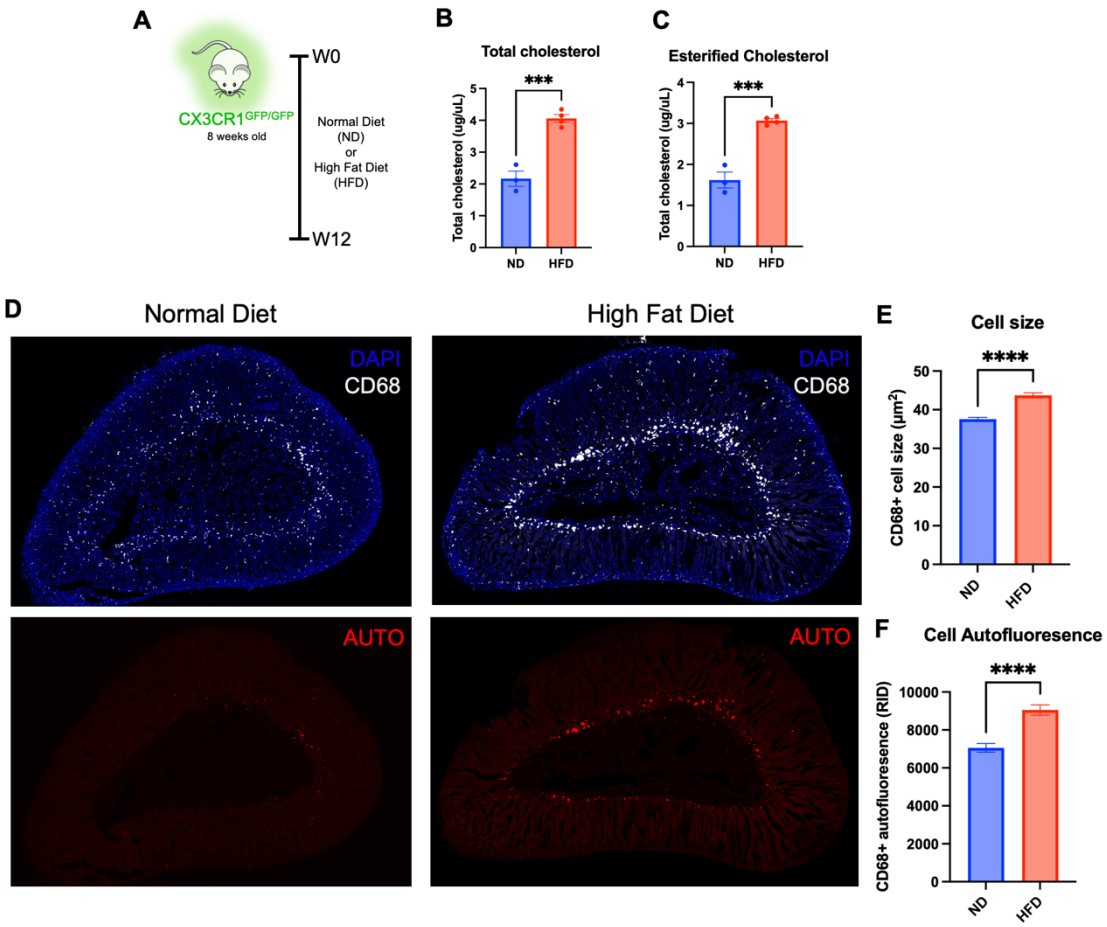


Figure 3.12. High fat diet feeding accelerates BALL formation. (A) A schematic representation of the experimental procedure used to generate data in B-F. Eight-week-old male CX3CR1$^{GFP/GFP}$ mice were fed a normal (ND) or high fat diet (HFD) for 12 weeks before tissue harvest. Total plasma cholesterol (B) and cholesterol esters (C) in mice fed a normal or high fat diet. (D) Representative confocal images of adrenal cross sections from 22-week-old male CX3CR1$^{GFP/GFP}$ mice that were fed a normal diet (ND) or high fat diet (HFD) for 12 weeks, with DAPI (blue), anti-CD68 staining (white) and autofluorescence (red). Bar charts quantifying the mean CD68+ cell size (E) and autofluorescence (F) in ND and HFD-fed mice.

3.3.8 Establishing the ontogeny of adrenal gland macrophages

The next objective was to establish the ontogeny of the priorly identified macrophage populations. First, using a single cell RNA seq dataset comprising CD45^{+} leukocytes in the adrenal gland [302] the genes *Lyz2*, *Ccr2*, *Cd68* and *Cx3cr1* were used as myeloid markers and an unsupervised cell-type annotation tool [304] was used to filter 6,377 myeloid cells for downstream analyses. Further sub-clustering of these myeloid cells identified three distinct populations of myeloid cells in the adrenal gland (Figure 3.13A). All three populations

expressed *Cd68,* while populations one and two express *Cx3cr1* (Figure 3.13A). Using RNA velocity, trajectory analysis was performed on this myeloid cell fraction, which suggests that populations two and three derive from population one, a monocyte-like Cx3cr1^{+} population (Figure 3.13B).

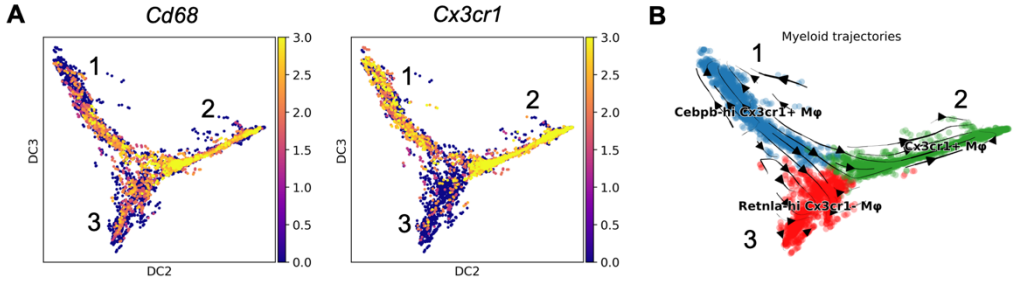


Figure 3.13. Single cell RNA-seq reveals three distinct adrenal macrophage populations. (A) Heat maps showing the expression of Cd68 and Cx3cr1 genes in adrenal myeloid cells. (B) Single cell RNA seq plot showing RNA trajectories of the myeloid compartment of the adrenal gland.

Next, I wanted to establish experimentally whether the CX3CR1^{+} ZGMs and BALL macrophages are bone marrow-derived, and whether they had the capacity to regenerate following irradiation-induced injury. To this end, I decided to carry out an irradiation and bone marrow transplantation experiment. First, I had to determine whether the hCD68-GFP mouse line [314] carries the CD45.1 or CD45.2 allelic variant. Using flow cytometry and the gating strategy outlined in Figure 3.13A, I determined that immune cells (splenocytes) from these animals, including CD68-GFP-expressing macrophages, expressed the CD45.2 variant (Figure 3.14A).

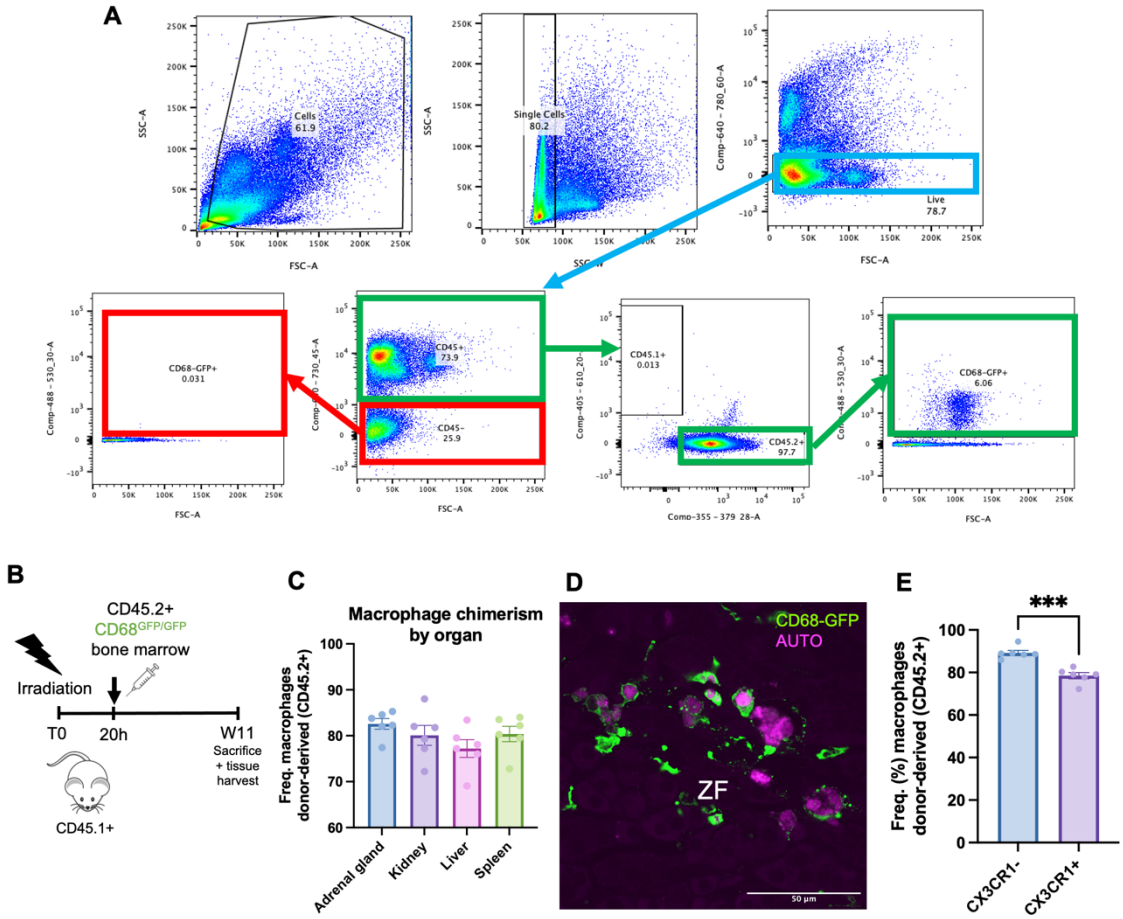


Figure 3.14. Irradiation and bone marrow transplantation. (A) Gating strategy used to identify whether (splenic) immune cells from CD68-GFP mice express the CD45.1 or CD45.2 allele variant. (B) A schematic depicting the experimental procedure followed for panels D-F. Wild-type mice were irradiated then rescued by injection with CD68-GFP bone marrow and culled 11 weeks later. (C) Bar chart showing CD45+ F4/80+ macrophage chimerism by organ. (D) Representative confocal image showing CD68-GFP+ (green) autofluorescent (magenta) macrophages in the adrenal cortex of mice that underwent bone marrow transplantation. (E) Bar chart with frequencies of CD45.2+ (donor-derived) cells in CX3CR1+ and CX3CR1- adrenal macrophages.

Next, I wanted to determine experimentally whether the CX3CR1^{+} ZGMs and BALL macrophages can be replaced after irradiation-induced injury and can redistribute to the same spatial location within the adrenal. Secondly, I wanted an indication of whether these cells are bone marrow-derived. I performed an irradiation and bone marrow transplantation experiment in which 9 week old wild-type CD45.1-expressing mice were irradiated to induce bone marrow depletion, then injected with bone marrow from CD45.2-expressing CD68^{GFP} reporter mice. 11 weeks later, when the mice were 20 weeks old, I analysed the adrenal macrophage compartment by immunofluorescent imaging and flow cytometry (Figure 3.14B). Examining

the (F4/80$^+$ MHCII$^+$) macrophage compartment in the adrenal gland, kidney, liver, and spleen, similar levels of chimerism (CD45.2 positivity) were observed across all tissues (Figure 3.14C). By imaging, it was observed that BALL macrophages were largely GFP$^+$ (Figure 3.14D), indicating that they derived from the transplanted bone marrow. CX3CR1-positive and negative adrenal macrophages differed in their frequency chimerism, with CX3CR1-negative macrophages (BALLs) deriving from the bone marrow at a significantly higher rate than CX3CR1$^+$ ZGMs (Figure 3.14E).

To test the hypothesis that the CX3CR1-negative BALL macrophages develop from a CX3CR1-positive precursor, as predicted by RNA velocity trajectory analysis (Figure 3.13B), a linage tracing experiment was performed. First Cx3cr1-CreERT; Rosa26mTmG mice were generated by crossing Cx3cr1-CreERT mice with Rosa26mTmG mice. This cross generated Cx3cr1-CreERT; Rosa26mTmG mice which, upon tamoxifen administration, undergo recombination in the Cx3cr1-expressing cells and a switch in the membrane-tagged fluorescent molecules from *TdTomato* to *Gfp* expression (Figure 3.15A). Five to six month old Cx3cr1-CreERT; Rosa26mTmG mice were pulsed with tamoxifen to induce recombination in CX3CR1-expressing cells. Two months later, adrenals were harvested (Figure 3.15B). In this way, it was possible to measure the longevity of adrenal gland macrophages, as only the cells expressing GFP two months post-tamoxifen would be cells present at the time of administration, or their progeny. Additionally, via a retained GFP tag this approach could be used to establish if CX3CR1-negative BALL macrophages derived from a CX3CR1-expressing precursor.

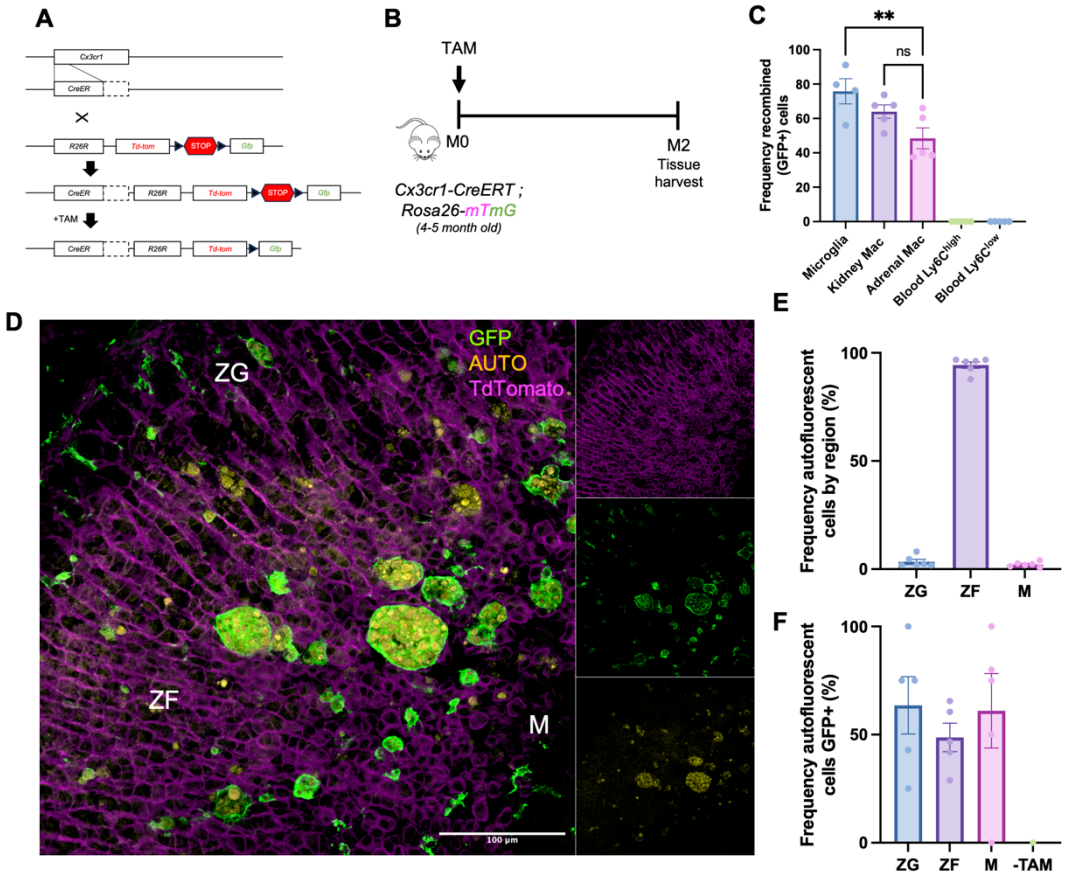


Figure 3.15. CX3CR1-expressing cells seed long-lived adrenal macrophages. (A) Schematic representation of the mouse cross used to generate the Cx3cr1-CreERT ; Rosa26mTmG mice. (B) The experimental timeline used to generate the data in H-K. (C) Frequency of CD45+ F4/80+ CD64+ tissue macrophages or blood monocytes that are recombined (GFP+) 2 months following tamoxifen administration. (D) Representative confocal image showing mouse adrenals from the experiment depicted in panel (B) with GFP (green) autofluorescence (yellow) and TdTomato (magenta). (E) Frequency of autofluorescent cells divided by region in the adrenal gland. (F) Frequency of autofluorescent cells that have recombined (GFP+) in each adrenal region two months following tamoxifen administration. TAM = tamoxifen administration; ZG = zona glomerulosa ; ZF = zona fasciculata ; M = medulla ; AUTO = autofluorescence.

Approximately 50% of total adrenal gland macrophages expressed GFP, similar to kidney macrophages, and at a slightly lower rate than microglia (Figure 3.15C), indicating that adrenal macrophages as a whole are a long-lived macrophage population. GFP was observed from macrophages in the ZG, as well as autofluorescent BALL cells in the zona fasciculata (Figure 3.15D). To quantitatively assess whether BALL macrophages come from CX3CR1-expressing precursors, I measured the frequency of autofluorescent cells in each adrenal region. In agreement with the prior data, the vast majority of autofluorescent cells situated in the zona

fasciculata (Figure 3.15E). Recombination among autofluorescent cells occurred at ~50% in all adrenal regions (Figure 3.15F). Taken collectively, the data indicate that both ZGMs and BALL adrenal gland macrophages undergo repopulation from the bone marrow, albeit at slightly different rates. Adrenal gland macrophages are a long lived-cell type, similar to macrophages from other tissues. Additionally, the data indicate that BALL macrophages derive from a CX3CR1-expressing precursor cell.

3.3.9 Adrenal gland macrophage-specific transcriptional signatures

Having established the morphological, spatial, and ontogenetic characteristics of adrenal gland macrophages, I next assessed the transcriptional signature of these cells. To examine the gene expression patterns of CX3CR1-expressing ZGMs, FACS was used to sort the CD45- (endocrine fraction) and $CD45^+$ $MHCII^+$ $F4/80^+$ $CX3CR1^+$ ZGMs (Figure 3.16A). These cells were lysed, RNA was extracted and underwent bulk RNA sequencing. As expected, abundant expression of the macrophage marker genes *H2-Ab1, Lyz2, Csf1r, Cd68,* and *Adgre1* was detected in the sorted ZGMs, in contrast to the endocrine fraction (Figure. 3.16B). ZGM gene expression was then interrogated in line with the M1/M2/metabolic activation paradigm [90]. ZGMs were found to exhibit a mixed phenotype, characterised by expression of the M1 marker *Il1b,* the M2 markers *Mrc1* (CD206*)* and *Tgfb1,* and the metabolic activation markers *Cd36* and *Plin2* (Figure 3.16C). As expected, high expression of the corticosteroid biosynthetic enzyme genes was detected in the $CD45^-$ endocrine fraction, but surprisingly we detected substantial levels of these transcripts, most notably *Cyp11a1*, *Star*, and *Hsd3b1*, in ZGMs as well (Figure 3.16D).

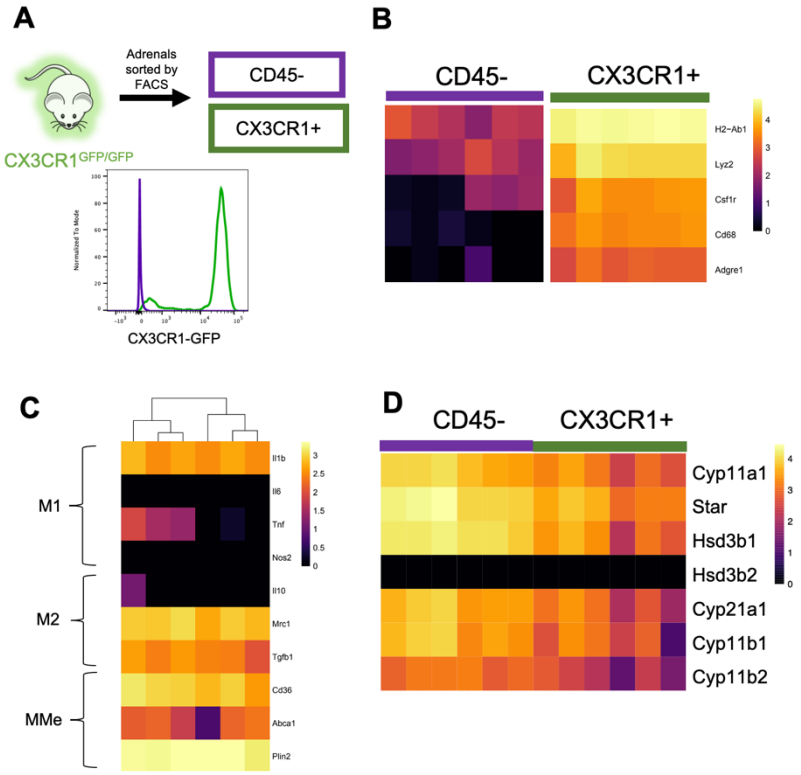


Figure 3.16. Bulk RNA-seq data from Zona Glomerulosa Macrophages (ZGMs). (A) A schematic (above) depicting the experimental outline for the data shown in figures B-D. CD45- (purple; endocrine) and CX3CR1+ (green) cells were sorted from the adrenal glands of CX3CR1$^{GFP/GFP}$ mice for bulk RNA sequencing. The histogram below shows the CX3CR-GFP expression in the sorted cell populations. (B) Heatmaps showing expression of the indicated macrophage marker genes (B), polarization marker genes (C) and corticosteroid biosynthetic genes (D) in the CD45- and CX3CR1+ cell populations. Each box in the horizontal axis represents data from one mouse.

Next, I wanted to use the single cell RNA-seq data of filtered myeloid cells (Figure 3.13A) to validate this finding. All three populations of myeloid cells expressed macrophage markers to varying extents (Figure 3.16B, 3.17A). In agreement with the bulk RNA-seq data, gene expression analysis showed that the *Cx3cr1*$^{+}$ macrophages (population two) expressed relatively high levels of the corticosteroid biosynthetic genes, except for *Cyp11b2* (Figure 3.17C, D).

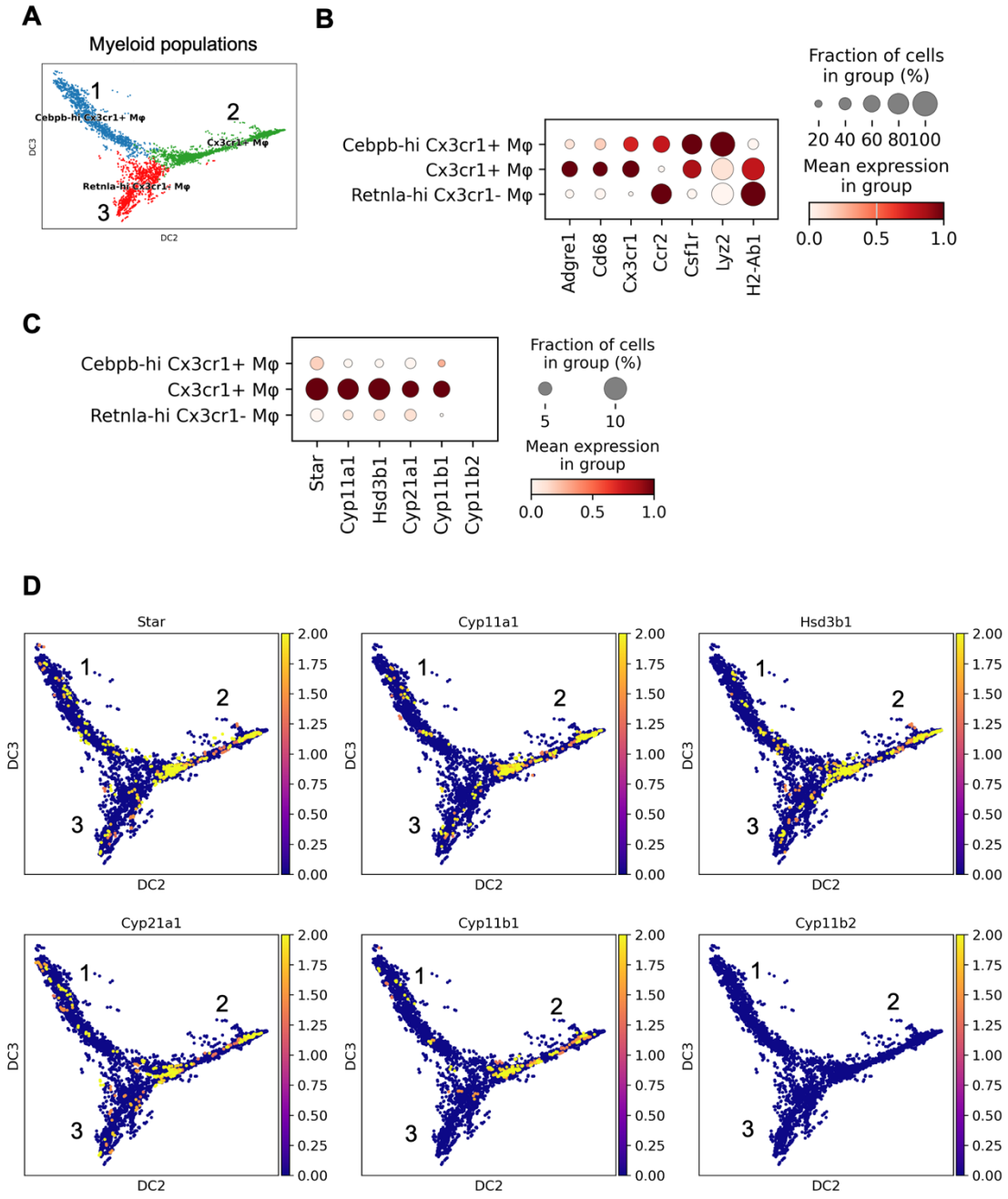


Figure 3.17. Single cell RNA-seq data from adrenal myeloid cells. (A) Single cell RNA seq data clustering of the adrenal myeloid compartment. (B) ScRNA-seq dotplot showing the normalised gene expression of macrophage marker genes in adrenal myeloid cells. (C) Single cell RNA seq dot plots showing the expression of adrenal corticosteroid biosynthetic genes in the indicated myeloid populations. (D) Gene expression data showing the expression of corticosteroid biosynthetic enzymes in adrenal myeloid cells.

By taking advantage of another single cell RNA-seq dataset [407] which includes single cell preparations from the adrenal gland, pituitary gland, and the paraventricular nucleus of the hypothalamus (the three sites of the hypothalamic-pituitary-adrenal axis) I sought to establish

whether these gene expression patterns were unique to immune cells / macrophages of the adrenal gland. Other datasets exist for these tissues, plus datasets from many more tissues, but the decision was made to validate these findings within a single set of datasets to ensure consistency across tissue collection, sequencing, and dataset preparation. Total immune cells were defined as *Ptprc* (CD45) expressing cells, as is done in flow cytometry. Myeloid cells constituted the largest immune cell presence in all three tissues, with limited presence of lymphoid-associated genes. Macrophages, defined as cells *expressing Cx3cr1, Cd68, Adgrel,* and *Csf1r,* were found across all three tissues (Figure 3.18A). Adrenal immune cells were the only tissue immune cell type to express the corticosteroid synthesis genes *Cyp11a1, Star, Hsd3b1, Cyp21a1,* and *Cyp11b1*, with no expression observed in pituitary or PVN immune cells (Figure 3.18B).

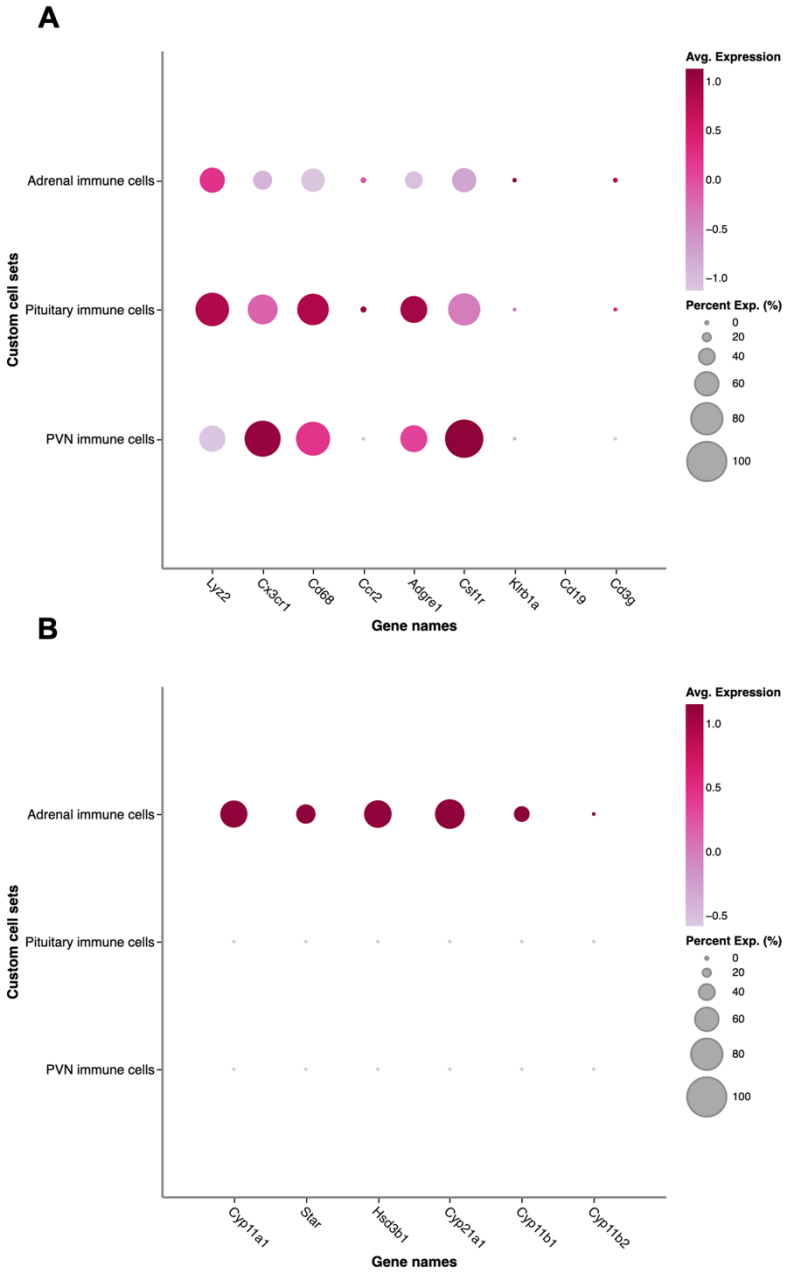


Figure 3.18. Hypothalamic, pituitary, and adrenal gene expression comparison. Comparing adrenal and pituitary immune cells (Ptprc-expressing) in their expression of immune (A) and corticosteroid biosynthetic (B) genes.

3.4 Discussion

The main findings of this chapter are:

1) Adrenal gland macrophages heterogeneous and two different populations (BALLs and ZGMs) can be distinguished based on their autofluorescent signature, CX3CR1 expression, and replicative capacity.
2) Both subsets of adrenal gland macrophages derive from CX3CR1-expressing precursors.
3) ZGMs have an adrenal-specific phenotype and express corticosteroid biosynthetic machinery.
4) BALL macrophages contain cholesterol and their formation is accelerated in obesity.

The inspiring hypothesis for this study was that phenotypic and heterogeneity exists among adrenal gland macrophages, and that adrenal macrophages have tissue-specific characteristics. The experiments and data described in this chapter suggest would support that hypothesis. The adrenal gland's myeloid cell compartment is the largest population of immune cells in the gland. Moreover, macrophages are the dominant immune cell type in the adrenal cortex, to a greater extent than in the medulla (Figure 3.3). Within the macrophage compartment in the adrenal cortex, we observe heterogeneity in form – CX3CR1-expressing macrophages are dendritic, co-localise to aldosterone producing cells in the zona glomerulosa, and express corticosteroid biosynthetic enzymes. CX3CR1-negative BALL macrophages accumulate in the zona fasciculata in an age and diet dependent manner and contain cholesterol – the necessary precursor to adrenal corticosteroids.

3.4.1. Adrenal macrophages are distinguishable by CX3CR1 expression

CX3CR1 has been used to differentiate discrete macrophage populations in other tissues. In the skin, CX3CR1-high macrophages (identified using the CX3CR1-GFP mouse model also

used in this study) mark cells derived from long-lived tissue-resident macrophages which exhibit an alternatively-activated (M2-like) phenotype [413]. Moreover, using a bone-marrow transplantation study they reveal that CX3CR1^{high} macrophages recruited to a wound are derived from long-lived skin-resident macrophages, whereas CX3CR1^{low} macrophages come from the bone marrow and exhibit a mixed classical/alternative activation state [413]. Additionally, in the blood CX3CR1^{high} (Ly6C^{low}) monocytes are known as patrolling monocytes – intravital microscopy reveals they "crawl" along the vascular endothelium in search of infections or tissue damage [414,415]. This is in contrast to CX3CR1^{low} (Ly6C^{high}) monocytes that are inflammatory and actively recruited to inflamed tissues [416]. In the skin and blood therefore, precedence exists for functionally distinct myeloid/macrophage populations differing on the basis of CX3CR1 expression and in terms of their gene expression. These studies did not directly assess the morphological differences between the CX3CR1^{high} and CX3CR1$^{low/negative}$ cell types.

3.4.2. The adrenal macrophage niche

The data described in this chapter show or imply that the four elements of a macrophage niche [330] exist in the murine adrenal gland: **(i)** The endocrine cells of the adrenal gland, found in the medulla and the cortical zonas fasciculata glomerulosa, act as a *cellular scaffold*, to which the tissue macrophages can adhere to. This is particularly apparent with ZGMs, which can be observed extending dendritic projections in between and around the endocrine cells within the zona glomerulosa; **(ii)** *Macrophage survival/trophic factors* are expressed by the endocrine and endothelial cell compartments of the gland. Notably, *Csf1,* the essential macrophage survival factor, is produced by endothelial cells and likely serves a critical role in maintaining the niche. *Cx3cl1*, which encodes the ligand for CX3CR1, expressed by ZGMs, is expressed most highly by cells in the capsule, followed by cells of the ZG, and then by cells in the ZF. This observation

complements the finding that CX3CR1^{+} ZGMs preferentially localise to the subcapsular area and ZG over other regions of the adrenal. CX3CR1-CX3CL1 chemokine attractions could underly this spatial localisation of macrophages within the adrenal cortex. CX3CR1-CX3CL1 has not previously been linked to the macrophage niche but the evidence suggests that chemokine receptor-chemokine ligand signalling could therefore represent another additional component of the macrophage niche that serves to determine macrophage positioning within a tissue. Substantial expression of the notch receptor ligands were observed in endothelial cells and capsule cells, which could represent further functionally relevant features of the adrenal macrophage niche; **(iii)** Our data indicate that some features of the adrenal gland, which remain to be defined, are responsible for *imprinting adrenal macrophages with adrenal-specific functions*, such as the expression of corticosteroid biosynthetic enzymes, which are not found in macrophages in other tissues. The transcription factor(s) responsible for this process remain to be determined; **(iv)** The data presented here indicate that, like atherosclerotic foamy macrophages, adrenal BALL macrophages accumulate cholesterol with age and high fat diet feeding. Cholesterol is the necessary precursor molecule for the steroid hormones corticosterone and aldosterone. This data may suggest of a role for BALL macrophages in the production of steroid hormones. However, at this stage the extent to which adrenal macrophages *interact with their niche in a beneficial manner* remains to be elucidated. This fourth and final element of the macrophage niche will be explored further in Chapter four of this thesis.

Demonstrating the necessity and functional relevance of these niche elements, particularly the identified trophic factors and unidentified transcription factors, is challenging. However, with the increasing prevalence of state-of-the-art techniques such as single cell RNAseq, lineage tracing, and spatial transcriptomics, such experiments become more tangible. Moreover, the

advent of more and more sophisticated means of inducing targeted and inducible genetic manipulations in experimental models, understanding the cellular crosstalk within tissues, including the adrenal glands, becomes a real possibility. One could envisage using an endothelial or endocrine-specific Cre mouse to selectively ablate *Csf1* or *Cx3cl1* to determine whether these factors are indeed essential for establishment of the adrenal macrophage niche. Assuming functional relevance, approaches such as these could provide the proof of principle for therapeutics that manipulate a tissue macrophage niche, to get around the problem of the broad selectivity of typical macrophage markers that are used to target macrophages *in vivo*.

3.4.3. Adrenal specification of Zona Glomerulosa Macrophages

Murine adrenal gland macrophages were first described in 1984 by Hume et al [327]. The findings presented in this chapter suggest that the abundant F4/80-expressing population of the ZG described in that initial study are the same as the CX3CR1-expressing ZGMs described in this thesis. We observed that the ZF has a lower density of CX3CR1-expressing cells than the ZG, in agreement with the initial study [327]. The study presented here goes beyond the initial characterising study in several ways. Herein, evidence is provided describing features of the macrophage niche[330] and the ontogeny of the adrenal gland macrophages, in addition to showing evidence of an additional adrenal macrophage subset – the BALL macrophage – present at 20 weeks plus, which was not apparent in the 1984 study due to the age of mice used (10-14 weeks) [39].

In a recent study that examined adrenal macrophages in CX3CR1-GFP reporter mice [302], flow cytometric data indicated that most macrophages, at an unspecified timepoint (presumably 7-10 weeks) were CX3CR1^{+}. The results in this chapter would confirm this finding, but additionally show that CX3CR1 expression decreases in adrenal macrophages with time.

Moreover, the data presented in this chapter show that ZGMs, unlike other tissue macrophages, express the corticosteroid biosynthetic genes, indicating that they could contribute to adrenal corticosteroid output. One could test the steroidogenic capacity of ZGMs *ex vivo* following cell sorting. Sorted ZGM cells could either be lysed and assayed for intracellular steroid contents, or sorted ZGMs could be stimulated *ex vivo / in vitro* with steroid-stimulating factors (angiotensin II, ACTH), and corticosteroid production could be measured. Alternatively, bone marrow-derived macrophages could be treated with homogenates from lysed adrenal glands. By measuring the expression of steroidogenic genes and proteins, and the possible production of steroid hormones, it may be possible to determine whether intra-adrenal factors can induce macrophage steroidogenic capacity.

In other tissue contexts, tissue-specific macrophage gene expression profiles have been observed. Sympathetic neuron-associated macrophages express *Slc6a2* and monoamine oxidase a, a norepinephrine transporter and degradation enzyme, respectively [118]. Splenic macrophages express the transcription factor SPI-C, which is induced in response to heme [417]. Liver monocytes express *SLC40A1*, an iron transporter [116] while muscularis macrophages express bone morphogenetic protein 2 [115]. Each of these examples of tissue macrophage-specific expression profiles have demonstrable functional relevance (which will be detailed in Chapter Four of this thesis). The functional relevance of this finding in ZGMs remains to be determined and will be explored experimentally in the following chapter.

3.4.4. Foamy BALL macrophages

Though CX3CR1-expressing cells have been observed in murine atherosclerotic plaques [418], it is unclear whether these cells are monocytes, non-foamy macrophages, or foamy macrophages. A literature review conducted as part of this thesis has been unable to establish whether

CX3CR1 expression has been reported on foamy macrophages in humans or mice. The CX3CR1-negative "foamy" BALL macrophages that accumulate cholesterol in a time and age-dependent manner are novel in the adrenal gland, but have been described in other tissue contexts. In multiple sclerosis, foamy macrophages arise through the internalisation of myelin debris, which occurs via scavenger receptors, Fc receptors, complement receptors, and other receptor-based mechanisms [419]. Additionally, macrophages are known mediate the formation of fatty streaks in the arterial walls in the context of atherosclerosis. These macrophages take up oxLDL via scavenger receptors class A-I/II and CD36 to form lipid-loaded foam cells [147]. These foam cells contain cholesterol [394] and are critical in the initiation, development, and instability, of atherosclerotic plaques [420]. Like BALL macrophages, these foam cells are also proliferative, as measured by Ki-67 staining [421]. Atherosclerotic foamy macrophages, like the BALL macrophages, are known to be autofluorescent, a feature that has been used to detect the cells *in situ* in the context of disease [422]. This autofluorescence is likely a feature of the esterification cholesterol goes under to facilitate intracellular storage. Esterification of cholesterol is necessary for its intracellular storage, as high concentrations of unesterified cholesterol are cytotoxic [423]. *In vitro*, the degree of cholesterol esterification has been shown to increase autofluorescence in macrophages in the context of LDL uptake [424]. In the context of atherosclerosis, macrophage uptake of cholesterol is part of process that responds to excessive intracellular lipid accumulation, termed reverse cholesterol transport. In this process, macrophages unload excess cholesterol via ABCA1 and ABCG1 to apoA1 and HDLs, respectively [425–428]. Whether macrophages in the adrenal gland are involved in the uptake of cholesterol and its reverse transport is currently unclear. The data presented in this chapter does indicate that adrenal macrophages express the cholesterol transporter *Cd36* (Figure 3.16C), *Abca1* (albeit at low levels), and *Plin2*, a gene that regulates the formation of lipid droplets [429,430]. The precise mechanisms that regulate cholesterol accumulation in BALL macrophages

remain unclear, as is the source of this cholesterol. We report that high fat diet feeding increases BALL size and cholesterol contents. This could be consistent with BALL macrophages scavenging cholesterol from the circulation via receptor-mediated mechanisms. Alternatively, adrenal macrophages could synthesise their own cholesterol as they express key enzymes involved in cholesterol synthesis, albeit at low levels. BALL macrophages could also recycle cholesterol from centripetally migrating, phagocytosed endocrine cells [181], in a similar manner to the transient liver macrophages that recycle iron from senescent erythrocytes [431]. Ultimately, further experimentation will be needed to establish the precise source of cholesterol that accumulates in BALL macrophages.

3.4.5. Ontogeny of adrenal gland macrophages

My initial observation of BALL macrophages accumulating in the adrenal cortex with age suggested to me that these macrophages are bone marrow-derived and are recruited to the tissue in response to age-associated chemotactic cues. I was therefore surprised to observe that CX3CR1-negative macrophages (BALLs), as well as ZGMs, existed at similar numbers in wild-type mice and CCR2-deficient mice, in which monocyte egress from the bone marrow is inhibited [432]. It was previously thought that bone marrow transplantation and irradiation experiments could reveal the tissue resident macrophage (TRM) population and bone marrow-derived macrophage (BMDM) populations. This was based off the differing replicative capacities of the two populations. TRMs are Ki-67^{low} and proliferate at low levels, and so it was thought they would be radio-resistant, in contrast to BMDMs which are Ki-67^{high}. However, it is now known that only microglia are radio-resistant while other TRMs are susceptible and are ablated upon irradiation [359,363]. The results in Figure 3.14 show that adrenal macrophages exhibit ~80% chimerism following irradiation and bone marrow transplantation, like macrophages in the kidney, liver and spleen. We did observe that within the adrenal

macrophage compartment, ZGMs and BALL macrophages exhibit slightly different levels of chimerism, which mirrors their differing levels of Ki-67 expression (Figure 3.9).

In a recent study that probed the ontogeny of adrenal macrophages [302] the authors show that in tamoxifen-pulsed CCR2-CreERT2 ; R26TdTomato ; CX3CR1-GFP mice, most CX3CR1-expressing macrophages were TdTomato positive, and posited that $CCR2^{+}$ monocytes "preferentially give rise to $CX3CR1^{+}$ macrophages upon their entry into the adrenal gland. Our data show that *Ccr2* is expressed by two of the three populations of adrenal macrophages, and not just monocytes, indicating that Dolfi and colleagues could be over-estimating the contribution of monocytes to the adrenal macrophage pool. Using tamoxifen pulsed CX3CR1-CreERT2/GFP ; R26TdTomato mice, the authors showed that most macrophages 48hrs and 7 days post-pulse were GFP-TdTomato double positive, and therefore concluded that $CX3CR1^{+}$ cells are not precursors of $CX3CR1^{-}$ macrophages in adults. My data with tamoxifen pulsed CX3CR1-CreERT2 ; mTmG mice shows that BALL macrophages (and ZGMs) are GFP^{+} two months post pulse, indicating that they do derive from $CX3CR1^{+}$ macrophages. The authors in the Dolfi study do not indicate the sex or age of the mice used in these lineage tracing experiments, which may explain the discrepancies in the two sets of data. The findings in this Chapter corroborate other aspects of the Dolfi study. I show that CX3CR1-expressing ZGMs are $Ki\text{-}6^{low}$ and the pulse-chase study shows that CX3CR1-expressing ZGMs are long lived and $Ki\text{-}67^{low}$, consistent the phenotype of embryonically-derived macrophages [40], which were demonstrated in the study by Dolfi et al [302].

The results presented this chapter tell us that adrenal macrophages are similar to tissue macrophages in other organs. In the CX3CR1 pulse-chase linage tracing experiment (Figure 3.15) it was observed that tissue macrophages as a whole are a relatively long lived population,

with a substantial fraction (~50%) of these cells (or their progeny) situating in the adrenal gland for at least two months, levels similar to kidney macrophages and slightly lower than microglia. Using a *Ms4a3*-Cre based fate mapping approach which specifically labels monocyte-derived cells, it was previously that kidney macrophages undergo slow repopulation from circulating monocytes [360], which is consistent with long-lived cells. In the same study, microglia were shown to undergo no repopulation from circulating monocytes [360]. Microglia in mice are known to have a lifespan of at least 15 months, with some lasting the entire lifespan [433]. Adrenal macrophages therefore most closely resemble another population of tissue-resident macrophages living outside the blood-brain barrier – the kidney macrophage. This experiment also showed that the CX3CR1^{-} BALL macrophages derive from a CX3CR1^{+} precursor, since they express GFP two months following tamoxifen induction. This would suggest that CX3CR1 is downregulated as cholesterol is accumulated within these cells. This could reflect the different spatial localization of BALLs sand ZGMs. BALL macrophages may lack the chemotactic cue that keeps ZGMs close to the zona glomerulosa and capsule, the cells which express *Cx3cl1* to the greatest extent (Figure 3.1).

The data collectively informs a model in which both ZGMs and BALL macrophages are self-sustaining, long-lived macrophage populations, which undergo limited or no replenishment from CCR2-dependent monocytes. Moreover, the populations are robust, evidenced by their capacity to replenish to the same spatial zone and adopt the same phenotypic characteristics following irradiation-induced apoptosis.

3.4.6. CCR2-independent BMDM accumulation?

The possibility exists that BALL macrophages and/or ZGMs could derive from the bone marrow in a CCR2-independent fashion. The CX3CR1 lineage tracing of BALL macrophages

could reflect a CX3CR1-expressing monocyte origin rather than a macrophage origin. Indeed, CCR2-deficient mice have increased monocyte retention in the bone marrow and monocytopenia, but not total ablation of blood monocytes [375]. This indicates that some monocyte egress from the bone marrow is still possible without CCR2. The chemokine-chemokine receptor system is notoriously promiscuous and CCR2 binds multiple ligands [434,435]. Many studies examining macrophage recruitment typically are done in the context of acute infection or inflammatory challenge, in young mice between six and ten weeks old [436–438]. This study demonstrated the presence of ZGMs at 8-10 weeks and BALL macrophages at 20 weeks plus. The data showing neither ZGMs nor BALL macrophages are CCR2-dependent was from 20-week-old male mouse adrenals. It is conceivable that this later time would be sufficient for other chemokines/chemokine receptors to compensate for the lack of CCR2. A telling experiment would be to perform a fate mapping experiment using the previously mentioned Ms4a3-Cre mouse line [360], in which *Ms4a3* is selectively expressed granulocyte-monocyte progenitors and therefore selectively labels monocyte-derived cells. Parabiosis experiments, in which two mice with different genetic tags are surgically attached with circulatory systems connected, have also been used to identify TRMs from monocyte-derived macrophages [24] and could be usefully employed here to definitely determine adrenal macrophage origin.

3.4.7. Limitations

The experimental approach taken in this chapter is not without its limitations, though the best approach was taken where possible. Firstly, cholesterol was not measured directly within BALL macrophages. I used the *Star*-ablation-mediated enhancement of cholesterol, high fat diet induced hypercholesterolemia, and Oil Red O staining to show that the autofluorescent contents of BALL macrophages, like foamy atherosclerotic macrophages, is cholesterol. Other methods presented in chapter 4 provide additional evidence for the cholesterol contents of

BALL macrophages. However, the most sensitive method would be to directly assay for cholesterol using liquid chromatography mass spectrometry in sorted BALL macrophages. It may be that other lipids also constitute a fraction of the lipids found in BALL macrophages. Second, in this study single cell RNA seq and bulk RNA seq were used to detect the expression of corticosteroid biosynthetic enzyme mRNA within ZGMs. These are widely used and robust techniques through which cellular gene expression can be measured. However, one of macrophage's prime functions is to ingest dead cells and remove cellular debris and foreign material. Some have raised the question of whether false positive readouts are more likely with macrophages when performing transcriptomic analysis, due to mechanical and enzymatic digestion protocols inherently leading to risk of artefacts through inter-cell mRNA contamination [439]. An alternative would be to use the RiboTag technique [409] in which ribosome molecules are immunoprecipitated from sorted cell populations and sequenced, therefore giving transcriptomic analysis of the "translatome". However, with this technique single cellular resolution would be lost and so it was decided to use bulk and single cell RNA seq in tandem. The fact that that corticosteroid biosynthetic enzyme expression is observed in only one of the macrophage populations identified by single cell RNA seq (Figure 3.17), and not all three, would suggest that the readout is a specialized feature of a particular macrophage subset and not an artefact common to all macrophages. To provide further validation of this finding I wanted to stain the adrenals for biosynthetic enzyme proteins to test for macrophage-specific expression. However, antibodies against these mitochondrial proteins are not knockout validated. Additionally, the only antibody that would reliably work in our tissue samples was one against CYP11B2 – but this was not one of the enzymes our single cell seq data suggested was expressed by ZGMs. Another method of detection would be to perform spatial transcriptomics, so that the expression of corticosteroid biosynthetic genes could be tested for in adrenal macrophages *in situ*. Lastly, this study is somewhat limited in its capacity to be

compared to other published studies, including the other major published study on adrenal gland macrophages [302], due to the age of mice used. Most pre-clinical and basic science studies use mice that are between six and ten weeks old. In this study, I have revealed a cell type (BALL macrophages) that only becomes apparent at the 20-week timepoint. Consequently, there is limited scope to compare and contrast the findings (in this chapter and in chapter four of this thesis) with other studies. This observation highlights a broader problem in biomedical research in which research is done in organisms at a life stage that does not accurately reflect much of the human population.

Chapter 4

Assessing the contribution of adrenal macrophages to adrenal hormonal output

4.1. Introduction

4.1.1. Physiological factors that stimulate and suppress adrenal corticosteroid production

Numerous factors have been shown to both stimulate and suppress adrenal corticosteroid production *in vitro* and *in vivo*. Much of our mechanistic understanding of the modulatory effects of these factors has been ascertained through *in vitro* and animal-based studies. The effects can be summarised as follows. The immediate regulator of aldosterone is angiotensin II (AngII). AngII binds the Ang II type 1 receptor (AT1R) on cells of the zona glomerulosa (ZG) and promotes the upregulation of corticosteroid biosynthetic genes and thereby stimulates aldosterone production[230]. Potassium is another notable positive regulator of aldosterone production that works by stimulating calcium influx and membrane depolarisation in ZG cells [440,441]. The immediate regulator of cortisol and corticosterone is ACTH. ACTH, produced by the pituitary gland, binds to the M2CR receptor present on the surface of adrenocortical cells and upregulates corticosteroid biosynthetic genes [209], the HDL-binding receptor SCARB1 [442], and LDLR [443]. It also is a positive regulator of aldosterone, though to a much lesser extent than for glucocorticoids [444].

Diet and diet-associated factors also have demonstrable effects on corticosteroid production. Dietary sodium is a negative regulator of aldosterone production via suppressive effects on the RAAS system, specifically a suppression of renin. Conversely, reducing sodium intake activates the RAAS system and enhances renin activity in humans and mice [445,446]. Renin is produced by juxtaglomerular (JG) cells in the kidney. JG cell production of renin is regulated

by the juxtaglomerular apparatus, comprising JG cells, the macula densa, and extraglomerular mesangial cells. The macula densa is a group of cells in the wall of the distal tubule that monitors the sodium chloride content of the filtrate [447]. Macula densa cells in the distal nephron sense luminal NaCl via the sodium-potassium-chloride NKCC2 [448]. Low sodium concentrations in macula densa cells triggers the activation of several intracellular signalling molecules including p38, AMP-activated protein kinase (AMPK), (ERK1/2) mitogen-activated protein (MAP) kinases, cyclooxygenase-2 (COX-2) and microsomal prostaglandin E synthase, and the release of prostaglandin E_2 (PGE_2). PGE_2 acts upon its cognate receptors EP2 and EP4 in JG cells which stimulates renin release [449–451].

Obesity is frequently linked to dysregulation in corticosteroid production. In humans, experimental weight gain is associated with increases in plasma cortisol levels [452]. It has also been shown that in spontaneously obese individuals a restriction of energy intake causes a spike in cortisol levels [453]. High fat diet-feeding is associated with enhanced basal corticosterone levels in mice and fluctuations in the circadian rhythm of corticosterone levels [454]. Aldosterone levels are also increased in high fat diet-fed mice relative to lean mice [455] and heightened levels of plasma aldosterone have been described in obese subjects relative to lean controls in clinical studies 13,14. In a study of the effects of high fat diet on the murine adrenal gland it was shown that obese adrenals exhibit cortical hyperplasia, increased expression of corticosteroid biosynthetic genes – *Star, Cyp11a1, Hsd3b1, Cyp21a1, Cyp11b1* – and increased corticosteroid production [459]. The precise molecular(s) mediator controlling corticosteroid alterations observed in obesity is unclear, but the adipokine leptin has been touted as a potential link between obesity-associated elevations in aldosterone and hypertension [460]. Indeed, chronic leptin infusion increases plasma aldosterone levels in mice and *in vitro* leptin treatment

increases aldosterone production from human adrenocortical cells [461]. While mice fed a high fed diet will get obese, develop hypertension, and exhibit elevated plasma leptin levels, mice with non-functional mutations in leptin or the leptin receptor are resistant to obesity-induced hypertension. High fat diet-fed mice treated with an anti-leptin antibody are similarly resistant to obesity-induced hypertension, as are humans lacking function leptin and leptin receptor [462]. The effect in mice is traced to leptin signalling in the dorsomedial hypothalamus which stimulates autonomic outflow and thereby regulates peripheral blood pressure [462].

Cholesterol is fundamentally necessary for the synthesis of adrenal corticosteroids as the common precursor molecule. Though Steroidogenic Acute Regulatory protein (StAR) is considered the rate limiting enzyme for adrenal corticosteroid biosynthesis [463], cholesterol appears to also be a rate limiting factor. In cultured human and bovine adrenocortical cells, LDL (and HDL to a lesser extent) supplementation boost ACTH-induced cortisol production and in a dose-dependent manner [464]. Similarly, pre-incubation of bovine ZG cells with HDL (and LDL to a lesser extent) enhances basal and AngII-induced aldosterone production [465]. Fluorescent tagging of HDL-derived esterified cholesterol shows that this cholesterol is taken up by bovine and human ZG cells and this process accompanies the increase in aldosterone production that comes with cholesterol supplementation [466]. In a human AngII-responsive adrenocortical cell line, LDL stimulates aldosterone release, as does oxidised LDL. However the increasing extent to which LDL is oxidised reduces the potency of LDL in stimulating aldosterone release [467]. Likewise, *in vivo* modifications (oxidation and glycoxidation) to of LDL (from diabetic patients) attenuate its potency at stimulating aldosterone and cortisol production from cultured human adrenocortical cells [468]. Taken collectively, the data indicate that HDL, LDL, and modified forms thereof, are all capable of regulating the production of

adrenal corticosteroids in a dose-dependent and rate limiting manner, though increasing modifications appear negatively correlated with corticosteroid-stimulating capacity.

Various *in vitro* and *in vivo* studies have demonstrated the potential for monocytes/macrophages to influence hormone production from adrenal cells. The cytokines TNFα, IL-1β, and IL-6 are all expressed from macrophages in the human adrenal gland, as evidenced in studies using immunohistochemistry and *in situ* hybridisation [469–471], indicating potential paracrine interactions between endocrine and immune cells in the adrenals. Stimulation of cultured human adrenal cells with isolated human monocytes, but not T cells, elicits cortisol production *in vitro* [472], indicating a possible stimulatory effect of monocytes upon adrenal endocrine cells. Human primary adrenal cultures stimulated with IL-6 exhibit enhanced aldosterone and cortisol production in a dose-dependent manner [471]. In cultured rat adrenocortical cells, IL-6 was shown to induce increases in corticosterone production over a 24hr stimulation, but not after 12 or 3 hours [473]. Infusion of IL-1β into rats causes an increase in plasma corticosterone in an IL-1R-dependent manner [474,475]. However, IL-1β suppresses AngII-induced aldosterone production in primary rat ZG cells [476]. The literature on the effects of TNFα on adrenal corticosteroid production is similarly murky. Like IL-1β, TNFα has an inhibitory effect on corticosterone production on cultured rat adrenocortical cells and on AngII-induced aldosterone production in primary rat ZG cells [476,477]. In human cells cultured *in vitro*, TNFα increases cortisol production from adult adrenal cells but suppresses cortisol from fetal adrenal cells [478,479]. Co-culture of a mouse zona fasciculata (ZF) cell line with a human monocyte/macrophage cell line shows that these myeloid cells suppress *Star, Il6,* and *Sf1* mRNA expression in the endocrine cell fraction, indicating a possible suppressive role of monocytes/macrophages on adrenal corticosteroid production [480]. Conflicting findings, the lack of *in vivo* studies, and the variation in *in vitro* experimental protocols used, limit our

understanding of immune-endocrine interactions in the adrenal gland. Collectively, the literature presents an incomplete picture of how or if macrophage-derived cytokines impact corticosteroid production from adrenal glands *in vivo*.

4.1.2 The relationship between adrenal cholesterol stores and hormonal production

Cholesterol is the common precursor molecule to all the steroid hormones and therefore serves a fundamental physiological role in the adrenal gland. Currently, adrenal corticosteroid biosynthesis is believed to rely upon three cholesterol sources – intra-endocrine cell *de novo* synthesis of cholesterol, endocrine cell cholesterol stored in lipid droplets, and plasma lipoprotein-derived cholesterol [233,234]. Early studies by Andersen and Dietschy in which rats were infused with HDL or LDL, showed that the rodent adrenals preferentially utilise HDL over LDL cholesterol to fuel steroidogenesis. They also showed via 4-APP-mediated suppression of plasma cholesterol levels that plasma lipoprotein-derived cholesterol was the major substrate for adrenal sterol and corticosteroid synthesis. Moreover, it was shown that adrenal esterified cholesterol content had a positive correlation with plasma cholesterol content and corticosterone production [481,482]. They use this evidence to suggest that most corticosteroid production uses plasma lipoprotein-derived cholesterol, but tools available and the prevailing paradigm at the time meant that they could not account for a potential contribution of tissue macrophages to the observed phenotype.

Liver X receptor α (LXRα), expressed on endocrine cells across the adrenal cortex, is a nuclear hormone receptor that regulates genes that control cholesterol efflux, storage, and corticosteroid synthesis [483]. At steady state, LXRα promotes expression of efflux genes, such as the transporters *Abca1*, *Abcg1*, and *ApoE*. When LXR α is knocked out in mice, these efflux pathways are inhibited and the steroid hormone synthesis genes *Star*, *Cyp11a1*, and *Hsd3b1*,

are upregulated. This results in heavier adrenal weights, enhanced intra-adrenal esterified cholesterol stores, and increased corticosterone, but not aldosterone, production [483]. LXRα is thereby a negative regulator of adrenal cholesterol contents and corticosterone production, but not aldosterone. This indicates that the adrenal ZG and ZF may acquire their cholesterol for steroidogenesis via different sources. Notably, this study did not document the timepoints at which their blood samples were collected. Given circadian fluctuations in corticosteroid production, which are different for corticosterone and aldosterone, this is an important factor to control for.

Steroid hormones, unlike catecholamines from the adrenal medulla, are not able to be stored intracellularly for rapid release and therefore require immediate availability of their precursors to facilitate their timely synthesis [484]. Cholesterol ester-rich lipid droplets in the adrenal cortex are believed to be efficient intracellular organelles that sequester and release cholesterol via esterification and lipolysis, respectively [485]. Key regulators of this process are Perilipin (Plin) family proteins, a related family of lipid droplet scaffolding proteins, which recruit lipases and thereby mediate lipolysis [486]. A 2021 study demonstrated a role for Plin2 in mediating intra-adrenal cholesterol balance in mice [484]. Plin2 deletion resulted in enlarged adrenals and increased intra-adrenal total cholesterol and esterified cholesterol stores. They did not detect an impact of these increased cholesterol stores on corticosterone responses and did not measure aldosterone responses in their study. The authors focused their attention on the effect of *Plin2*-deletion on lipid droplet size within the endocrine cells of the adrenal cortex, but also documented an accumulation of highly autofluorescent lipid-droplet-containing “ceroid-like structures” in the adrenal cortex of Plin2-deficient mice, a phenotype which was enhanced in female mice relative to males. These structures highly resemble the cholesterol-containing BALL macrophages described earlier in this thesis. The authors sought to characterise the lipid

species that make up these "ceroid-like structures". In doing so they removed neutral lipids, including cholesterol, from their preparations before carrying out mass spectrometry. They found modest differences in polar lipid species between Plin2-sufficient and deficient adrenals made up primarily by small differences in phosphatidylglycerol. Interestingly, the authors did report increased levels of *Adgre1* (F4/80) mRNA in adrenals of Plin2-deficient mice relative to wild type, indicating a higher abundance of macrophages, in addition to the enhanced intracellular cholesterol stores, consistent with the findings presented in this thesis showing that macrophages are cholesterol-storing cells within the adrenal glands. This study could therefore be interpreted as a BALL macrophage gain of function study. Other consequences of Plin2 deletion were enhanced expression of lysosomal acid lipase (*Lipa*), and the cholesterol efflux genes *Abcg1* and *ApoE* [484]. Plin2 is therefore another negative regulator of intra-adrenal cholesterol stores.

Molecular players that act as positive regulators of intra-adrenal cholesterol stores are primarily believed to be the lipoprotein receptors, low density lipoprotein receptor (LDLR) and SCARB1 (HDL receptor). Mice are an HDL-dominant species with little circulating LDL, in contrast to humans which are LDL-dominant [246]. Adrenals from mice that lack SCARB1 are heavier than wild-type adrenals but exhibit an almost entire depletion of lipids in the adrenal cortex, coupled with reduced (but not abolished) intra-adrenal cholesterol stores, and a diminished corticosterone response to fasting, relative to wild type mice [256]. This is attributed to a reduced capacity to uptake serum cholesterol [255]. Aldosterone was not measured in these studies.

While the LDL receptor is not necessary for acute steroidogenesis in mice [487], evidence supports a role for the LDL receptor in adrenal steroidogenesis in other species including humans. In Watanabe heritable hyperlipidemic rabbits, which lack LDLR, have have

substantially smaller intra-adrenal cholesterol stores and ACTH-stimulated corticosterone responses that are significantly reduced compared to normal rabbits [488]. In human fetal adrenal gland explants, cortisol production in response to ACTH is enhanced by the addition of LDL, but not HDL [489]. To mimic human physiology, studies into adrenal steroidogenesis are often done in LDLR-knockout mice which have a similar lipoprotein profile to that observed in normolipidemic humans [490]. Genetic deletion of ApoA1, a core component of HDL, in LDLR-knockout mice results in HDL-deficiency and a substantial reduction in adrenal cholesterol stores and adrenal cortex lipids. Interestingly, this has no impact on basal corticosterone levels nor the adrenal glucocorticoid response to stress [491]. This indicates that HDL is redundant for adrenal steroidogenesis in mice with a human-like lipoprotein profile, but also that LDLR and HDL-independent mechanisms may exist to support adrenal steroidogenesis.

4.1.3 Evidence for macrophage involvement in steroidogenesis

Macrophage involvement in steroidogenesis has been posited in tissues other than the adrenal gland. It was shown that human alveolar macrophages, isolated via bronchopulmonary lavage and centrifugation, can convert dehydroepiandrosterone, a human steroid precursor, into downstream steroids. The presence of the requisite enzymes was inferred by metabolite production [492,493]. Human THP-1 cells-derived macrophages upregulate *Cyp19a1* mRNA, a key gene that regulates conversion of androgens to oestrogens, in response to dexamethasone [494] – a synthetic glucocorticoid. This may indicate that corticosteroids induce a steroidogenic phenotype in tissue macrophages.

In the testes, it was shown that testicular macrophage-conditioned medium stimulated testosterone production from Leydig cells [495]. Later, it was shown that Leydig-cell associated macrophages contain 25-hydroxycholesterol (25-HC) as demonstrated by organic extraction

and high-performance liquid chromatography. 25-HC was shown to stimulate testosterone production within 3 hours by injection into rat testes [496,497]. Recently, 25-HC was identified as an alternative substrate for testosterone biosynthesis [498]. Endocrine gland macrophages therefore have pretence in regulating hormonal output. Additionally, mice lacking macrophage colony stimulating factor (*Csf1*) are resistant to angiotensin II-induced elevation of blood pressure [305], as are mice that have undergone macrophage depletion via clodronate liposomes [499]. These findings point towards macrophage involvement in the RAAS system. While macrophages are known to be regulated by glucocorticoids, a role for macrophages in regulating glucocorticoid output has yet to be demonstrated.

4.2. Rationale and experimental aims

Chapter three of this thesis has demonstrated that Zona Glomerulosa Macrophages (ZGMs) are constitutively present in the mouse adrenal cortex and these cells express corticosteroid biosynthetic genes. Big Autofluorescent Lipid-Laden (BALL) macrophages accumulate in the ZF and ZG in an age and diet dependent manner. These BALL macrophages contain cholesterol, the necessary precursor molecule to the adrenal corticosteroids – aldosterone and corticosterone. The functional significance of these observations remains to be determined. The aims of this chapter were:

1) To establish whether ZGMs contribute to adrenal hormonal output.
2) To establish the effect of adrenal hormonal output on BALL macrophage size and cholesterol contents.
3) To determine whether BALL macrophages contribute to adrenal corticosteroid output via the provision of cholesterol.

4.3 Results

4.3.1 ZGMs positively regulate aldosterone production but not other adrenal-derived hormones.

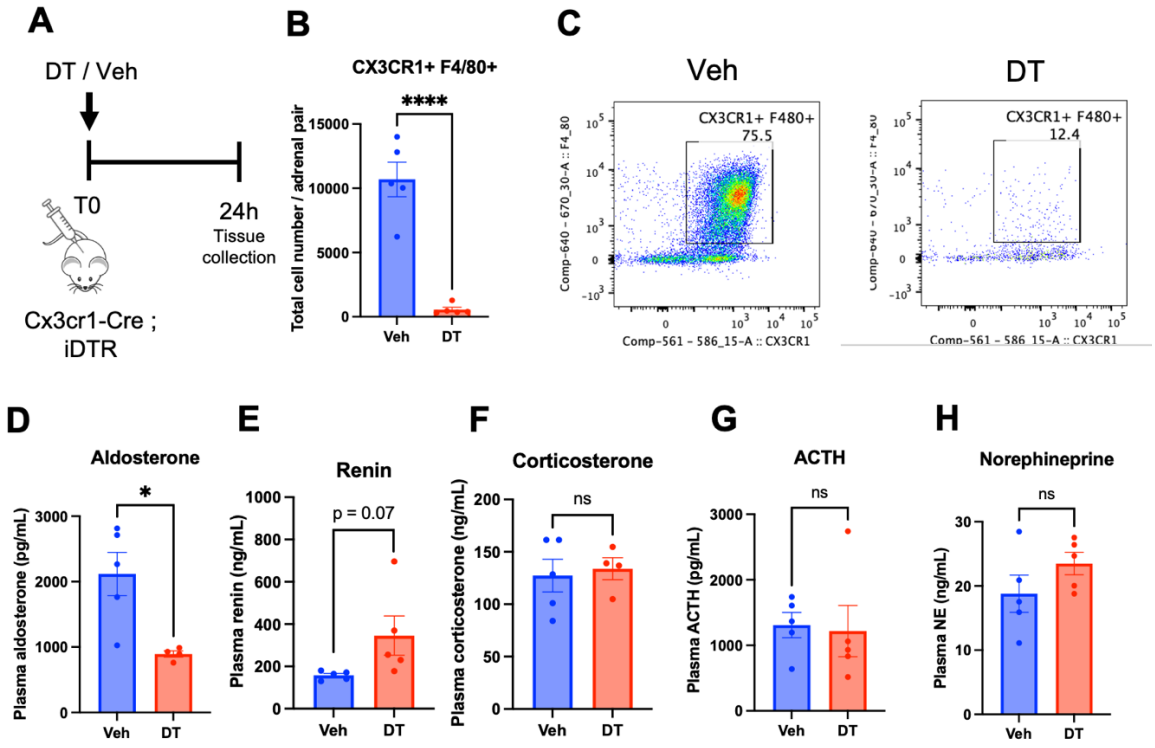


Figure 4.1. ZGMs positively regulate aldosterone production. (A) A schematic showing the experimental procedure followed for the data shown in B-H. Cx3cr1-Cre ; iDTR mice were injected with diphtheria toxin (DT) or vehicle (Veh) control and tissues were collected from mice 24 hours later. (B) Flow cytometry data quantifying the total number of CX3CR1+ F4/80+ cells in Vehicle or DT-treated mice. (C) Representative flow cytometry plots showing the presence of F4/80+ CX3CR1+ cells in vehicle (left) or DT-treated (right) adrenals. Bar charts showing the levels of aldosterone (D), renin (E), corticosterone (F), ACTH (G), and norepinephrine (H) in the plasma of vehicle or DT-treated mice. Each data point denotes data from one mouse. Data in B-H were analysed by two-tailed unpaired Student's *t*-test and are shown as average ± s.e.m. $*P < 0.05$, $**P < 0.01$.

Since the data to this point suggest that ZGMs express the machinery to contribute to the synthesis of adrenal corticosteroids, I next assessed the contribution of ZGMs to adrenal hormonal output. Cx3cr1-Cre mice were crossed with Cre-inducible diphtheria toxin receptor mice to generate Cx3cr1-Cre ; iDTR mice. To induce depletion of adrenal CX3CR1-expressing macrophages, at 10 weeks old mice were injected with 750ng diphtheria toxin (DT) or vehicle control and then sacrificed 24 hours later (Figure 4.1A). I validated depletion of ZGMs by flow

cytometry, observing a significant and almost complete ablation of ZGMs in DT-treated mice relative to controls, in absolute numbers and as a frequency of total leukocytes (Figure 4.1B, C). In the plasma, a significant reduction was observed in aldosterone concentration (Figure 4.1D), with the expected compensatory relative increase in renin in DT-treated mice relative to vehicle (Figure 4.1E). Corticosterone, ACTH, and norepinephrine levels were unaffected by ZGM depletion (Figure 4.1F-H). Taken collectively, these findings are consistent with a model in which ZGMs contribute to adrenal aldosterone output via the synthesis of steroid precursors to the endocrine cells of the ZG.

4.3.2. Corticosteroid inhibition and stimulation differentially impact BALL macrophage size and cholesterol contents.

Given that BALL macrophages contain cholesterol, the necessary precursor molecule for the steroid hormones, it was hypothesised that if BALL macrophages were contributing cholesterol to support adrenal corticosteroid output, then BALL size and cholesterol contents would change with corticosteroid production. To test this, mice underwent manipulations that stimulated or suppressed adrenal hormonal production. First, to suppress aldosterone production, CX3CR1$^{GFP/+}$ mice were fed a high salt diet (HSD) for six days (Figure 4.2A). HSD-fed mice had significantly reduced levels of plasma aldosterone (Figure 4.2B) and marginally (though not significantly) reduced plasma corticosterone relative to normal salt diet-fed mice (Figure 4.2C). While CX3CR1-expressing macrophages appeared relatively similar between NSD and HSD-fed mice (Figure 4.2D), HSD-fed mice had significantly larger and more autofluorescent BALL macrophages than those in NSD-fed mice (Figure 4.2D-F).

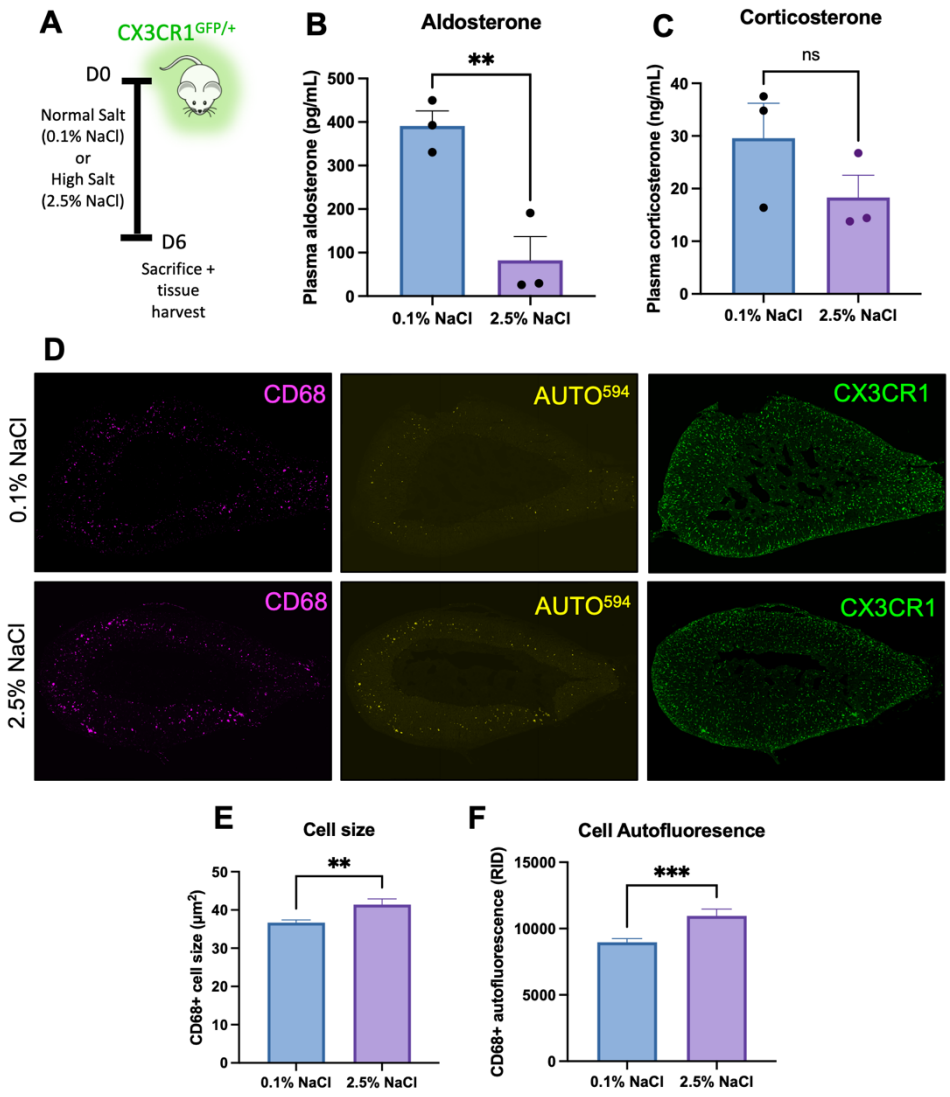


Figure 4.2. Corticosteroid inhibition increases BALL macrophage size and cholesterol contents. (A) Schematic depicting the experimental protocol used to generate the tissue that was analyzed in panel B-F. CX3CR1$^{GFP/+}$ mice were fed either a normal (0.1% NaCl) or high salt (2.5% NaCl) diet for six days before tissue harvest for subsequent analyses. Bar charts showing plasma aldosterone (B) and corticosterone (C) levels in the indicated treatment groups. (D) Representative confocal images of adrenal glands from the indicated experimental groups with anti-CD68 staining (magenta), autofluorescence (yellow), and anti-GFP staining (green). Bar charts showing the average cell size (E) and average cell autofluorescence (F) in the indicated treatment groups. . Each data point denotes data from one mouse. Data were analysed by two-tailed unpaired Student's *t*-test and are shown as average ± s.e.m. *$P < 0.05$, **$P < 0.01$

To stimulate aldosterone production, CX3CR1$^{GFP/+}$ mice were implanted subcutaneously with an osmotic minipump containing Ile^5–Angiotensin II (AngII; 1000 ng/kg per minute), or a minipump containing vehicle control (Figure 4.3A) [305]. AngII-treated mice had significantly elevated plasma aldosterone concentrations relative to controls, while corticosterone levels

remained unchanged (Figure. 4.3B, C). BALL macrophages in AngII-treated mice had trends towards reductions in BALL cell size and autofluorescence, though these changes were not statistically significant (Figure 4.3D, E). Taken collectively, these findings indicate that BALL macrophages respond differently to corticosteroid stimulation and inhibition, with changes apparent in BALL macrophage size and cholesterol contents.

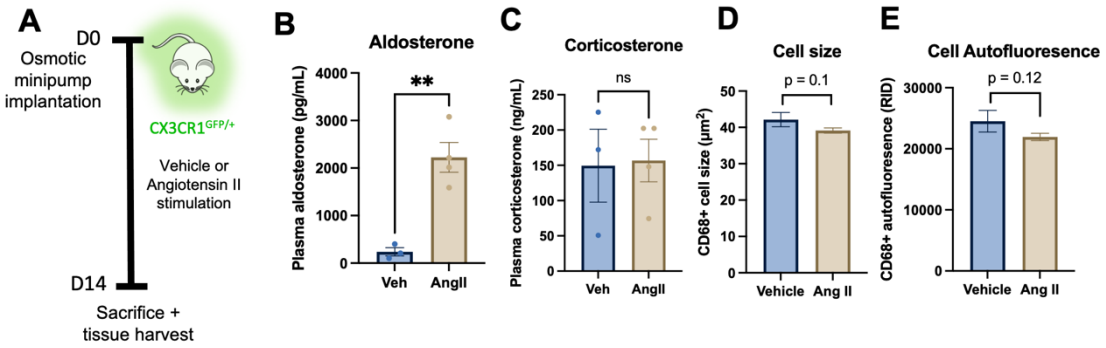


Figure 4.3. Effect of AngII stimulation on BALL macrophages. (A) On day 0 mice were implanted subcutaneously with an osmotic minipump containing either vehicle or Ile^5–Angiotensin II (AngII; 1000 ng/kg per minute) for 14 days, prior to sacrifice and tissue harvest. Bar charts showing plasma aldosterone (B) and corticosterone (C) levels in the indicated treatment groups. Bar charts showing the mean cell size (D) and mean cell autofluorescence (E) in the indicated treatment groups. Data in C-F and H-K were analysed by two-tailed unpaired Student's *t*-test and are shown as average ± s.e.m. *P < 0.05, **P < 0.01, ***P < 0.001, ****P < 0.0001.

4.3.4 CX3CR1 regulates BALL formation

In light of the observation that BALL macrophages can dynamically respond to adrenal corticosteroid output, I next tested the hypothesis that BALL macrophages support adrenal hormonal output via the provision of cholesterol. While the CX3CR1-GFP mouse line is commonly used as a macrophage reporter, as a knock-in-knock-out mouse line [320] mice homozygous for the transgene are functional knockouts for the *Cx3cr1* gene. It was observed that CX3CR1$^{GFP/GFP}$ mice had almost an entire ablation of BALL macrophages in the adrenal cortex relative to wild type mice (Figure 4.4A). When BALL macrophages were present, they were significantly smaller in size and in autofluorescent cholesterol contents when compared

to BALLs in wild-type mice (Figure 4.4B, C), indicating that CX3CR1 regulates BALL macrophage formation.

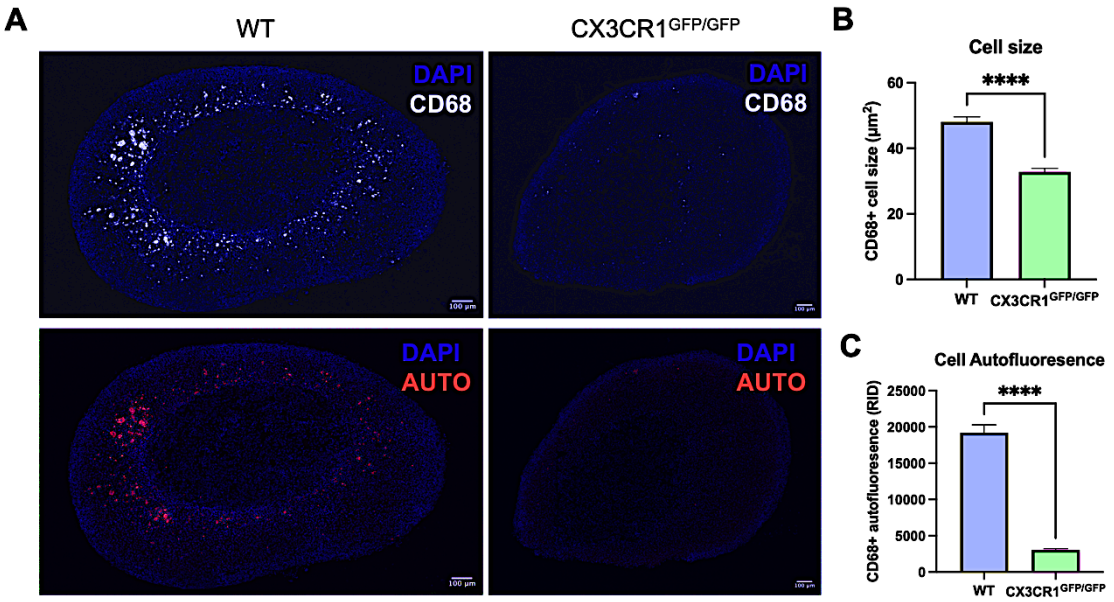


Figure 4.4. CX3CR1 regulates BALL macrophage formation. Representative confocal images of adrenal cross sections from 22-week-old male wild type and CX3CR1$^{GFP/GFP}$ mice that were fed a normal with DAPI (blue), anti-CD68 staining (white) and autofluorescence (red). Bar charts quantifying the mean CD68+ cell size (B) and autofluorescence (C) in the indicated genotypes. Pairwise comparisons were analysed by two-tailed unpaired Student's *t*-test and are shown as average ± s.e.m. *$P < 0.05$, **$P < 0.01$, ***$P < 0.001$, ****$P < 0.0001$.

To test whether CX3CR1-deficient macrophages were inherently defective in their ability to uptake cholesterol, WT or CX3CR1$^{GFP/GFP}$ bone marrow-derived macrophages (BMDMs) were generated and treated with fluorescent BODIPY-FL Low Density Lipoprotein (Figure 4.5A) and their ability to take up cholesterol was assessed. Both sets of BMDMs were observed to take up fluorescent cholesterol within the 24hr treatment period (Figure 4.5B, C). No significant difference was found between the two genotypes in their ability to form take up cholesterol and form foamy-like cells *in vitro* (Figure 4.5D).

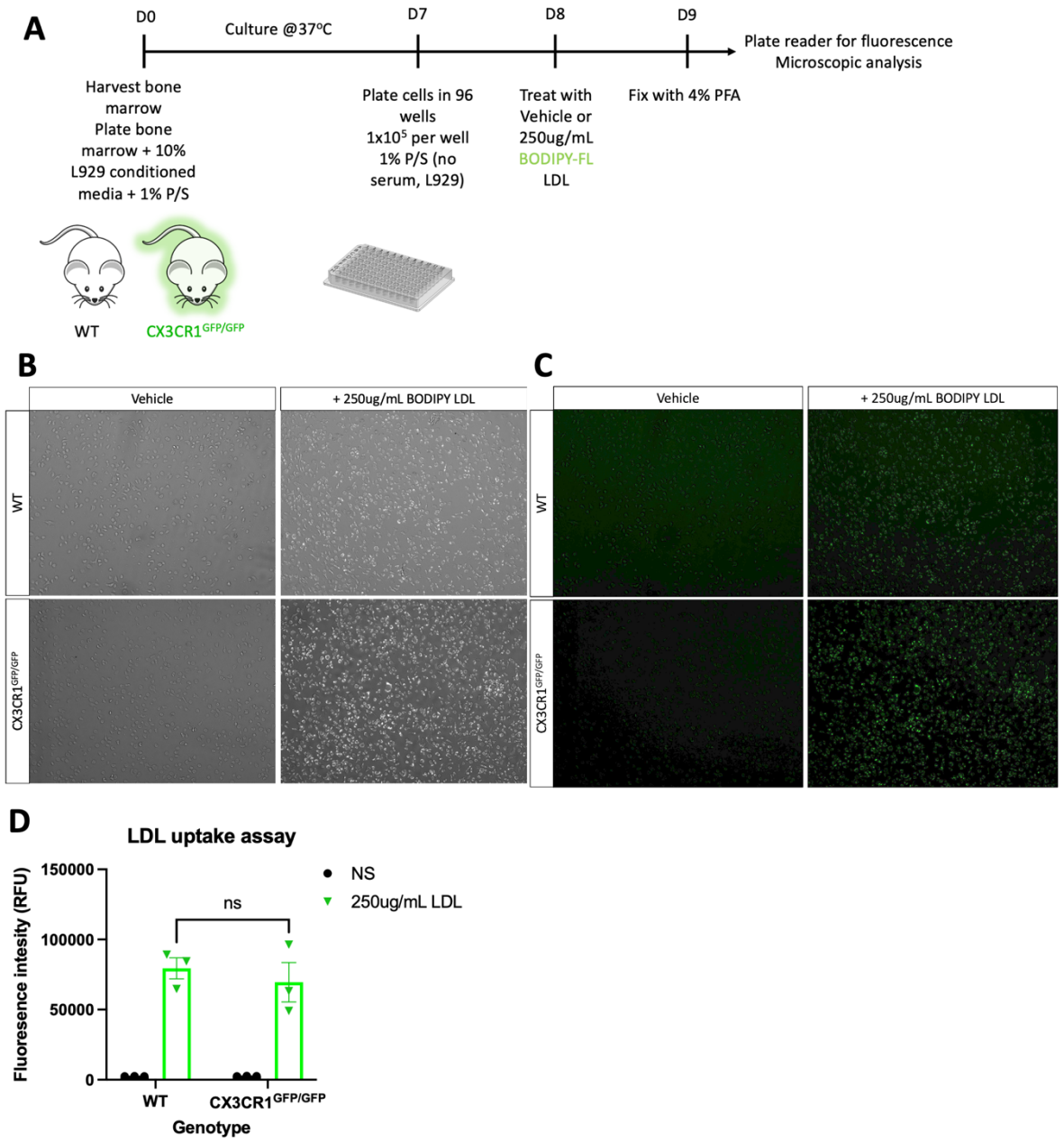


Figure 4.5. CX3CR1$^{GFP/GFP}$ BMDMs are not defective in their capacity to form foam cells *in vitro*. (A) A schematic representation of the experimental protocol used to generate bone marrow derived macrophages (BMDMs) and foam cells. Representative images showing bright field (B) and fluorescence (C) from BMDMs in the indicated groups. (D) Bar graph showing the relative fluorescence intensities from non-stimulated (NS) or fluorescent LDL-treated BMDMs from the indicated genotypes.

4.3.5 CX3CR1 regulates intra-adrenal cholesterol stores and corticosteroid output at steady state

Since BALL macrophages were shown to contain cholesterol and since CX3CR1-deficient adrenals lack BALL macrophages, I next measured the intra-adrenal cholesterol stores between

wild-type and CX3CR1$^{GFP/GFP}$ mice. While adrenal weights did not differ between wild type and knockout mice (Figure. 4.6A), CX3CR1$^{GFP/GFP}$ mice had intra-adrenal cholesterol stores approximately half the levels of wild-type controls (Figure 4.6B), consistent with the ablation of cholesterol-containing BALL macrophages. Systemic plasma cholesterol titres were similar between the genotypes (Figure. 4.6C).

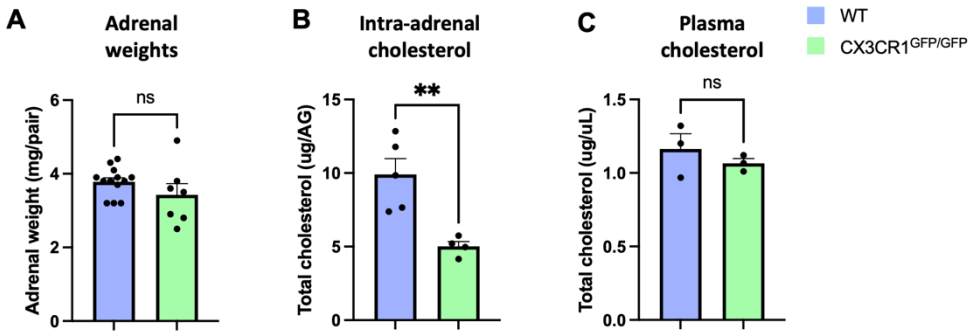


Figure 4.6. CX3CR1 regulates intra-adrenal cholesterol stores. Bar charts showing the adrenal weights (A), intra-adrenal total cholesterol levels (B) and (C) plasma cholesterol levels in the indicated genotypes. Pairwise comparisons were analysed by two-tailed unpaired Student's *t*-test and are shown as average ± s.e.m. *$P < 0.05$, **$P < 0.01$, ***$P < 0.001$, ****$P < 0.0001$.

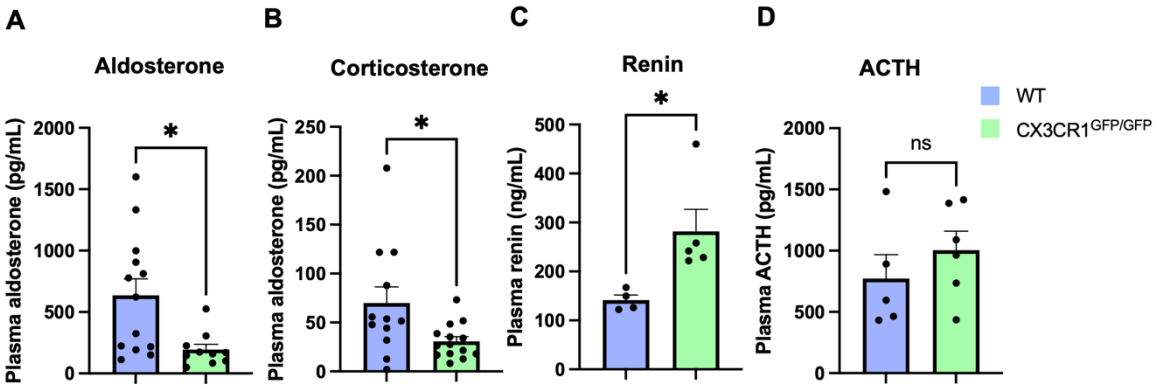


Figure 4.7. CX3CR1 regulates adrenal corticosteroid production. Bar charts showing plasma aldosterone (A), corticosterone (B), renin (C), and ACTH (D) levels in the indicated genotypes. Pairwise comparisons were analysed by two-tailed unpaired Student's *t*-test and are shown as average ± s.e.m. *$P < 0.05$, **$P < 0.01$, ***$P < 0.001$, ****$P < 0.0001$.

Consistent with reduced intra-adrenal cholesterol stores, CX3CR1$^{GFP/GFP}$ mice had significantly reduced plasma aldosterone and corticosterone concentrations relative to wild-

type mice at steady state (Figure. 4.7A, B). As expected, a compensatory increase in plasma renin was observed in knockout animals relative to wild-type (Fig. 6J) mice, with ACTH levels similar between the two genotypes (Fig. 4.7D). As adrenal corticosteroid production is also regulated by biosynthetic enzyme gene expression, I also measured the expression of these genes by RT-qPCR. Adrenal corticosteroid biosynthetic enzyme expression was mostly unchanged between wild type and CX3CR1$^{GFP/GFP}$ mice, except for *Hsd3b1* which was significantly elevated in knockout mice relative to controls (Fig. 6D). Taken collectively, the data indicate that the reduced aldosterone and corticosterone production from CX3CR1-deficient adrenals is caused by reduced intra-adrenal cholesterol stores in these mice.

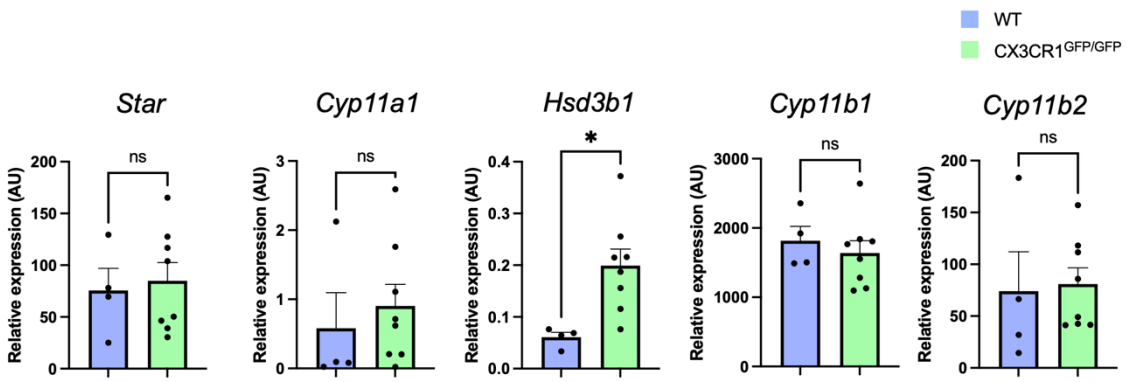


Figure 4.8. RT-qPCR data of corticosteroid biosynthetic gene expression in wild-type and CX3CR1-deficient mice. Pairwise comparisons were analysed by two-tailed unpaired Student's *t*-test and are shown as average ± s.e.m. *$P < 0.05$, **$P < 0.01$, ***$P < 0.001$, ****$P < 0.0001$.

4.3.6 CX3CR1 regulates corticosterone production in HFD-fed mice

Finally, CX3CR1$^{GFP/+}$ and CX3CR1$^{GFP/GFP}$ mice were put on high fat diet for 12 weeks to test whether BALL macrophages regulate corticosteroid responses in the context of obesity. High fat diet-fed CX3CR1$^{GFP/GFP}$ mice had marginally higher total body weights compared to CX3CR1$^{GFP/+}$ mice (Figure 4.9A). Like in steady state, adrenal weights did not differ between high fat diet-fed CX3CR1-sufficient and CX3CR1-deficient animals (Figure 4.9B), but BALL cell size and autofluorescent cholesterol contents were significantly reduced in knockouts

relative to control mice (Figure 4.9C, D). Plasma aldosterone concentrations did not differ between the two genotypes, but corticosterone concentrations were significantly reduced in CX3CR1 knockout mice relative to controls (Figure 4.9D, E). Together, these results indicate that CX3CR1 regulates the formation of BALL macrophages and the establishment of additional intra-adrenal cholesterol stores. Moreover, these stores appear necessary for supporting adrenal corticosteroid output at steady state and in obesity.

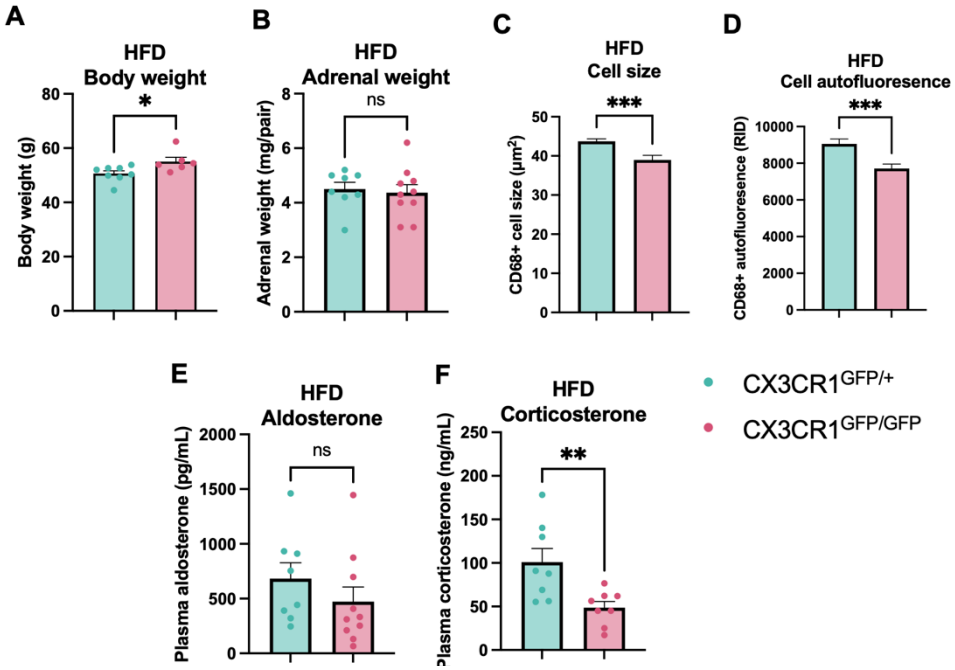


Figure 4.9. CX3CR1 regulates corticosterone production in HFD-fed mice. Bar charts showing the body weights (A), adrenal weights (B), mean CD68+ cell size (C) and autofluoresence (D), plasma aldosterone concentrations (E) and plasma corticosterone concentrations (F) in high fat diet-fed mice of the indicated genotypes. All pairwise comparisons were analysed by two-tailed unpaired Student's *t*-test and are shown as average ± s.e.m. *$P < 0.05$, **$P < 0.01$, ***$P < 0.001$, ****$P < 0.0001$.

4.4. Discussion

The main findings of this chapter are:

1) ZGMs regulate the production of aldosterone, but not the production of other adrenal gland-derived hormones.

2) BALL macrophage size and autofluorescent cholesterol contents changes depending on corticosteroid output.
3) BALL macrophages form in a CX3CR1-dependent manner, constitute an intra-adrenal cholesterol store, and regulate corticosteroid output in steady state and in obesity.

4.4.1. CX3CR1-expressing ZGMs regulate aldosterone production

The data presented in this chapter show that ZGMs positively regulate aldosterone production, but not the production of corticosterone or epinephrine at steady state. This corroborates the data presented in Chapter Three which showed that ZGMs express notable levels of the corticosteroid biosynthetic enzymes. However, according to our data ZGMs themselves do not express the last enzyme in the aldosterone biosynthetic pathway, aldosterone synthase (*Cyp11b2*). This data is therefore consistent with a model in which ZGMs provide the precursors to aldosterone and in this way support aldosterone production. CYP11B1 catalyses the synthesis of corticosterone, which in turn can be converted to aldosterone by CYP11B2. In this way, aldosterone production via CYP11B1 is a legitimate biosynthetic route, as evidenced by *Cyp11b1* deletion in mice significantly suppressing aldosterone production [500]. CX3CR1 and biosynthetic enzyme-expressing macrophages preferentially localise to the ZG, which may explain why the depletion of CX3CR1-expressing macrophages did not impact corticosterone levels in this study. To further test whether ZGMs have steroidogenic capacity, one could perform a macrophage-specific knockout of *Star* or *Cyp11a1* to establish the extent to which adrenal aldosterone production relies upon macrophage steroidogenesis.

Macrophages have previously been linked with playing a role in the renin-angiotensin-aldosterone-system (RAAS). Op/Op mice lack the colony stimulating factor 1 gene (*Csf1*), a key survival factor for tissue macrophages, are resistant to Angiotensin II-induced elevations in blood pressure, in contrast to wild type mice [305]. This is consistent with my findings that

ZGMs situate adjacent to the aldosterone producing cells of the ZG and that they express corticosteroid biosynthetic genes. ZGMs may therefore represent a new therapeutic target for treating hyperaldosteronism or hypertension caused by elevated aldosterone.

4.4.2. CX3CR1 as a regulator of intra-macrophage cholesterol accumulation

While a link between circulating cholesterol levels and adrenal corticosteroid output may seem intuitive, linking the two is not straightforward. According to my data, BALL macrophages comprise a sizeable intra-adrenal cholesterol store that is distinct from endocrine cell cholesterol stores and the circulating pool of cholesterol found in plasma. I show that this store changes in size with differing corticosteroid output demands. Further, the data indicate that the reductions in corticosteroid output observable in BALL macrophage-deficient adrenals are attributable to diminished intra-adrenal cholesterol stores, rather than fluctuations in renin, ACTH, or corticosteroid biosynthetic enzymes – the major known regulators of corticosteroid output. CX3CR1 was previously shown to promote atherogenesis and the formation and survival of lipid/cholesterol-laden foam cells in atherosclerotic plaques [501,502]. Here, I present evidence of another context in which CX3CR1 inhibition could be beneficial – via suppression of intra-adrenal cholesterol stores and corticosteroid output. Intriguingly, attempts to therapeutically inhibit the CX3CR1-CX3CL1 axis in atherosclerotic mice via pharmacological inhibition with F1, an amino terminus–modified CX3CR1 ligand with CX3CR1 antagonist activity, significantly reduces atherosclerotic Oil Red O staining, lesion development and total macrophage accumulation, but not macrophage density. Additionally F1 treatment reduces monocyte adhesion and CX3CR1-dependent monocyte survival [503]. Collectively, the data would indicate that, in addition to providing benefit in the context of atherosclerosis, CX3CR1 inhibition could prove useful in modulating adrenal hormonal output via a similar mechanism – namely, reducing macrophage cholesterol accumulation. In the clinical setting, increased

levels of CX3CL1 have been observed in in patients with severe carotid artery stenosis relative to those with moderate disease, and the number of CX3CL1-expressing cells positively correlates with the number of CX3CR1-expressing cells in carotid plaques [504]. Genetic polymorphisms in CX3CR1 have long implicated the receptor as a risk factor in coronary artery disease. The CX3CR1 I249 polymorphism results in reduced ligand receptor affinity and a reduced risk of acute coronary events [505,506], indicating that the CX3CR1-CX3CL1 axis plays a role in human foam macrophage accumulation and may be amenable to therapeutic intervention. CX3CL1 has previously been linked to endocrine function – it has been associated with type 2 diabetes in humans [507] – but CX3CR1-CX3CL1 has not been linked with human adrenal endocrine disorders. Indeed, the axis has not been discussed in the context of the adrenal gland, nor has foam macrophage formation been described in the adrenal gland. This latter point may reflect that much of the human tissue analysis is based on immunohistochemical staining of parrafin-embedded sections that have undergone delipidation and may therefore remove lipids that are a defining feature of BALL macrophages. However, CX3CR1 expression is detected in the adrenal gland according to the Human Protein Atlas [508], indicating that similar mechanisms mediating adrenal BALL macrophage formation may be present in human adrenal glands. Future investigations should probe the *in vivo* significance of the CX3CR1-CX3CL1 axis in human adrenal function.

While I have shown that CX3CR1 regulates adrenal BALL macrophage formation, the cellular pathways that mediate this function remain incompletely understood. In the context of murine atherosclerosis, CX3CR1 signalling was shown to promote monocyte cell survival, a finding complemented by *in vitro* study of human monocytes. This study also showed that CX3CR1 deletion suppressed foam cell formation and lesion development [501]. CX3CR1 also promotes macrophage survival in tumour metastasis [509]. Similarly, CX3CR1 may promote BALL

macrophage survival, and their depletion in CX3CR1-deficient animals would therefore indicate another context in which CX3CL1 acts as a survival factor for foamy macrophages. CX3CR1-CX3CL1 signalling could also act as a differentiation signal that mediates BALL macrophage formation, but my demonstration that BMDMs form foam cells in response to LDL *in vitro* at the same rate as wild-type mice suggests that this is not the case.

4.4.3. BALL macrophages constitute an intra-adrenal cholesterol store

The concept of intra-adrenal cholesterol stores being directly linked to corticosteroid output is not a new one. Liver X receptor α, which immunostaining indicates is expressed across endocrine cells in the adrenal cortex, is a negative regulator of adrenal cholesterol stores and corticosterone synthesis [483]. A recent paper reported that Plin2, a gene that promotes formation of lipid droplets, negatively regulates intra-adrenal cholesterol and cholesterol ester stores [484]. While this study focused on analysing the size of lipid droplets within the endocrine cells of the adrenal cortex, it also found that that Plin2-knockout adrenals had, an increased abundance of highly autofluorescent "ceroid like structures" in the inner region of the adrenal cortex containing lipid droplets, coupled with increased intra-adrenal cholesterol relative to wild-type animals. The present study indicates that these autofluorescent lipid-containing cell bodies are in fact cholesterol-containing BALL macrophages, a finding consistent with what is known about cholesterol containing-macrophages in other settings. Indeed, the degree of cholesterol esterification is known to increase autofluorescence in macrophages in the context of LDL uptake [424]. Additionally, cholesterol-containing foamy macrophages in the context of atherosclerosis [394] are known to be autofluorescent, a feature that has been used to detect the cells in situ in the context of disease [422]. Importantly, the Plin2 study [484] did not identify which cells are the source of Plin2 intra-adrenally. The transcriptomic data in chapter three indicate that Plin2 is expressed by adrenal macrophages, and therefore indicates that the autofluorescent

cell phenotype observed in Plin2 knockout mouse adrenals was the primary phenotype, and not secondary to endocrine cells, as was presented in the study. These findings indicate that adrenal macrophage Plin2 is an additional molecular player in the regulation of BALL macrophage formation. This would appear to be a separate and distinct phenotype from that previously observed in relation to Liver X receptors. The above studies [483,484] have measured only corticosterone output as the consequence of perturbations in intra-adrenal cholesterol balance, but the results in this chapter demonstrate that aldosterone production is also impacted by intra-adrenal cholesterol stores.

Considering these findings collectively, it would suggest that BALL macrophages constitute a sizeable and functionally significant intra-adrenal cholesterol store that is distinct from, and additional to, the endocrine cell compartment's own cholesterol stores. I have shown that this store contributes to corticosterone and aldosterone output under steady state, and corticosterone output in obesity, but the other contexts in which the store contributes to hormonal output remains to be explored. Certain questions remain unanswered in relation to this cholesterol store. First, it is unclear the extent to which different forms of cholesterol contribute to this adrenal store. Mice are considered an HDL-dominant species since most cholesterol is transported in HDL forms. This is in contrast to humans, which are an LDL-dominant species [510]. Therefore, it is likely that mouse BALL macrophages contain HDL cholesterol, though this remains to be experimentally determined. Additionally, whether the cholesterol is esterified, and the nature of any such esterification, is currently unclear. While esterifications such as oxidation are believed to enhance macrophage ability to take up LDL [511,512], macrophages are capable of taking up native LDL to form foam cells at concentrations similar to concentrations associated with hypercholesterolemia [159,397]. Ultimately, lipidomic analysis of BALL macrophages, or a comparison of wild-type and CX3CR1-deficient adrenal lipids will be

necessary to fully elucidate the lipid makeup of the BALL macrophage cholesterol pool. This caveat reflects a broader gap in adrenal knowledge, in that it is unclear whether differently esterified forms of cholesterol-loaded lipoproteins differ in their capacity to fuel steroidogenesis and whether this differs between species. Additionally, in my model the mechanism of cholesterol transport between BALL macrophages and endocrine cells remains unclear. Macrophages participate in cholesterol efflux via packaging of cholesterol into lipoprotein molecules, the receptors for which are expressed on endocrine cells of the adrenal gland [255,487,490]. Inter-cellular cholesterol transfer may occur via this mechanism. Alternatively, BALL macrophages are located throughout the adrenal cortex and directly adjacent to endocrine cells, indicating that a juxtacrine mechanism of cholesterol transfer may be taking place. Live super-resolution microscopic analysis and selective inhibition of efflux pathways will be needed to delineate these mechanisms in their entirety. Lastly, macrophage-bound cholesterol-containing lipid droplets were first observed in chapter three of this thesis and their functional significance has been demonstrated in this chapter. The lipid droplet could however constitute more than a storage organelle. Lipid droplets isolated from the adrenals of young (8-10 week old) rats were shown to express PLIN2 and numerous other proteins involved in the intracellular processing and utlisation of cholesterol for corticosteroid biosynthesis [513], indicating that lipid droplets may be an active site in cholesterol metabolism and corticosteroid biosynthesis. It is unclear the extent to which macrophage lipid droplets were represented in this study, but the abundance of PLIN2, a gene I showed to be expressed by macrophages in the adrenals of mice, suggests macrophage lipid droplets are included. Further proteomic analysis and/or spatial transcriptomic analysis of adrenals are therefore justified to fully elucidate the function of BALL macrophage lipid droplets in adrenal steroidogenesis.

4.4.4. Therapeutic perspective on BALL macrophages in obesity

Distinct macrophage subtypes, mostly CCR2-dependent monocyte-derived macrophages, have been previously linked with obesity-associated adipose tissue inflammation, insulin resistance, and hepatic steatosis [24,514–516]. In the present study, our data suggest that CX3CR1-dependent BALL macrophages are responsible for the increase in corticosterone that comes with obesity [517,518]. The data suggest therefore that BALL macrophages could represent a therapeutic target that could decouple obesity from the immune and metabolic dysfunction that is frequently synonymous with the condition. I have shown that these cells derive from a CX3CR1-expressing precursor, but whether this precursor is a yolk-sac erythro-myeloid progenitor, fetal liver progenitor, or haematopoietic stem cell-derived monocyte is currently unclear. Answering this question may be critical to inform attempts to target these cells for therapeutic benefit.

Obese mouse adrenals have previously been characterised. It was shown that adrenals from mice fed a high fat diet were significantly heavier, had cortical hyperplasia, and produced more corticosterone and aldosterone *ex vivo* than adrenals from mice fed a normal diet [459]. However, this study did not control for the size of the adrenal gland. In this study, I report that adrenals from high fat-diet-fed CX3CR1$^{GFP/+}$ and CX3CR1$^{GFP/GFP}$ mice weigh the same yet differ in their corticosterone output as measured in the plasma. This would therefore indicate that it is the adrenal cholesterol content, but not overall size, that determines corticosterone output in the context of obesity.

4.4.5. Contributing to the literature on adrenal macrophages

A recent study also sought to characterise the adrenal macrophage compartment in depth [302]. This study focused primarily on the sex-specific diversity of the macrophage compartment, but also established a link between macrophages and adrenal lipid metabolism. In contrast to the

present study, Dolfi and colleagues [302] reported that global macrophage depletion reduced intra-adrenal, but not circulating, levels of aldosterone, and reported no effect on corticosterone. Notably, different experimental protocols were used in these studies, which can help explain the discrepancies in findings. The Dolfi study used a pan-macrophage targeting approach – anti-CD115 antibodies – to deplete adrenal macrophages in 8-week-old female mice and measured corticosteroid responses under cold challenge. I used a CX3CR1-targeting inducible diphtheria toxin receptor model to deplete ZGMs specifically in 10-week-old male mice, and measured corticosteroid responses at steady state under no challenge. This 8-10-week timepoint would also not be appropriate to assess the contribution of BALL macrophages to adrenal hormonal output as the timepoint is before significant accumulation of these cells (20 weeks +). Our study is therefore compatible with the Dolfi study and provides further mechanistic insight into how adrenal macrophages regulate corticosteroid output – via biosynthetic enzyme expression (ZGMs) and storage of the necessary corticosteroid precursor, cholesterol (BALLs).

Another study showed that in the context of experimental arthritis in rats, MHCII-expressing cells inhibit corticosterone production in an IL-1, IL-18, and inflammasome-dependent manner. The authors showed that these cells accumulate in rat adrenals in the context of arthritis. Co-culture of adrenal $MHCII^+$ cells or recombinant IL-1β with adrenal $MHCII^-$ (endocrine and other non-macrophage) cells caused reduced corticosterone production from cultures [519]. These results could indicate an inhibitory effect of $MHCII^+$ cells on corticosterone production from the adrenal. However, the study has a number of caveats. The identity of the $MHCII^+$ cells is unclear – they could be macrophages, dendritic cells, or B cells. Some of their experiments relied upon co-culture of *ex vivo*-generated bone marrow-derived dendritic cells with adrenal endocrine cells, the rationale for which was not fully explained. Additionally, their

experiments were primarily done using primary cell cultures from rat adrenals. The tissue digestion protocols may have influenced/enhanced MHCII^{+} cell IL-1β production. The lack of *in vivo* validation and of a phenotype in steady state context limits the ability to ascertain an effect of MHCII-expressing cells on corticosterone output.

The data presented in this chapter has demonstrated, using the inducible diphtheria toxin receptor (iDTR) depletion model, that CX3CR1-expressing ZGMs regulate adrenal aldosterone production, but not the production of other adrenal-derived hormones. BALL macrophages, as evidenced using CX3CR1-deficient mice (CX3CR1$^{GFP/GFP}$), regulate intra-adrenal cholesterol levels as well as corticosterone and aldosterone production. The notable difference between these observations, other than the models used to generate them, are that the mice used were of different ages at the time of hormone measurement. In the iDTR model, mice were 10 weeks old at the time of cell depletion and hormone measurement. This timepoint is earlier than when BALL macrophages accumulate, which is in mice 20 weeks of age or older. In the CX3CR1$^{GFP/GFP}$ model, hormone measurements were taken from mice at 20 weeks of age, after BALL macrophages accumulate in WT mice. In data not shown CX3CR1$^{GFP/GFP}$ mice have normal hormone measurements at 10 weeks of age. Thus, the data indicate that different adrenal macrophage populations differentially regulate hormone production in an age and hormone-dependent manner.

4.4.6. Adrenal macrophages and the X zone

The relationship between the adrenal X zone and adrenal macrophages is unclear. This understanding is further limited by the unknown function of the X zone [520]. Probing the function of the adrenal X zone and any potential relationship with adrenal macrophages is

outside the scope of this project, but the observations and perspectives I describe here may help inform future lines of investigation.

Removal of androgen signalling results in X zone development, as measured by 20-α-hydroxysteroid dehydrogenase (20 alpha-HSD) – an X zone marker [521] - thereby indicating that its development is suppressed by androgens and/or androgens induce regression of the X zone. In male Parkes strain mice, testosterone increases from birth to 15 weeks of age, then declines with age [522]. Another study shows that the X zone declines with puberty in male mice [523]. Age associated decline in testosterone has been previously observed in SAMP8/TaJf mice between 4 and 12 months old [524]. Data could not be found for age-associated changes in C57Bl/6 mice (used in this thesis) and so direct comparisons are not possible but similar changes are to be expected. Pregnancy ablates the X zone in female mice, and castration results in an enlarged "reticular" zone (X zone) in male mice [525,526]. A recent study used MHCII staining to demonstrate an increase in macrophages in 7 week old castrated male mice when compared with sham-operated animals, which was localised to peri-medullary region of the adrenal cortex [302] where BALL macrophages first appear. The female adrenal X zone declines with pregnancy [520]. Lineage tracing experiments have traced X zone cells to the fetal adrenal cells using a GFP molecule for the tracing signal [177]. To my knowledge, no one has ever co-stained for X zone and macrophage markers. Collectively, these data suggest that the X zone negatively correlates with androgen levels and pregnancy.

Informed by the above evidence and my own observations I propose a model in which the X zone is partially or entirely constituted by adrenal BALL macrophages. In this model, the relative lack of testosterone in female mice is why the X zone regresses at a later stage. Rather than an early regression in male mice, the zone is simply repressed by testosterone. The age-

associated increase in BALL macrophages in male mice (demonstrated in chapter three) reflects the age-associated decline in testosterone and is similar to X zone reappearance post-castration. I posit that lineage tracing of X zone cells to a fetal origin is a false positive caused by the autofluorescent signal that is a defining feature of the BALL macrophage. I hypothesise that the formation of BALL macrophages is evident in sexually mature female mice earlier than age-matched males, and that the cholesterol contents of BALL macrophages serves to support the elevations in corticosterone and aldosterone that are necessary for healthy pregnancy in mice [527–529]. This would explain why the X zone regresses in female mice post-pregnancy.

4.4.7. Limitations

The main limitation of this study would be the lack of tissue-specific tools that enable specific manipulation of the adrenal macrophage compartment, but not those in other tissues. This reflects a general lack of tissue-specific Cre models in the macrophage field. As a result, it is possible that the plasma hormone phenotypes that I observe in Cx3cr1-Cre ; iDTR and CX3CR1-deficient mice could arise as a consequence of off-target effects of our manipulations. I posit that this is unlikely for two reasons: 1) corticosterone and aldosterone are mainly and solely (respectively) produced by the adrenal gland, and so effects on hormonal release are unlikely to come from other tissues; 2) corticosteroid biosynthetic enzyme expression, renin, and ACTH were all measured and could not explain the phenotypes observed, indicating they have not contributed to the phenotypes observed. Another limitation of this study is that all experiments were done using male mice. The adrenal gland is known to have sexually dimorphic structure and function, and so it is currently unclear the extent to which my findings can be translated to female mice. Lastly, I have not measured intra-adrenal cytokine responses

in CX3CR1-deficient and sufficient animals, which could contribute to the corticosteroid phenotypes observed in this chapter.

Chapter 5

Characterising the effects of MARCO on the Renin-Angiotensin-Aldosterone-System (RAAS)

5.1. Introduction

5.1.1. MARCO and SRA: structure and function

Macrophage receptor with collagenous structure (MARCO; *Marco*) and Macrophage scavenger receptor class A-1 (SRA; *Msr1*) are both class A scavenger receptors, linked by their scavenger receptor cysteine-rich (SRCR) domains and collagenous domains on the extracellular portions of the receptor [530]. However, the SRCRs of MARCO and SRA differ in the distribution of cysteine residues [531]. SRA is widely expressed on myeloid cells, including macrophages in most lymphoid and non-lymphoid organs, as measured by tissue immunostaining, in addition to mast cells and certain subpopulations of DCs [532–534]. At steady state, MARCO is constitutively expressed by certain macrophage populations including those in the spleen marginal zone, lymph node medullas, the peritoneum, the liver, and lung [531,535]. MARCO expression can also be upregulated on macrophages that do not usually express it upon bacterial challenge [536].

Studies in which class A scavenger receptor ligand binding has been investigated have found that MARCO binds bacteria via its SRCR domain, while SRA was shown to bind acetylated LDL via its collagenous domain [531,537]. This has been interpreted as indicative of different binding domains of the two receptors [530], though direct comparisons of receptors and common ligands or common ligand classes (e.g. bacterial vs lipoproteins) have not been done. Given the broad specificity of the class A scavenger receptors it is possible that different ligand classes bind similar regions on each receptor. Unlike the class B scavenger receptor SR-BI, which

binds HDL and thereby regulates adrenal cholesterol uptake and corticosteroid output [247,250,255,538], the class A scavenger receptors are united in their capacity to bind modified forms of LDL. Indeed, MARCO and SRA bind an unusually broad range of endogenous and exogenous ligands. SRA binds gram positive bacteria, lipopolysaccharide (LPS), lipoteichoic acid, CpG DNA, E. Coli, S. aureus, Neisseria meningitidis, and modified forms of LDL (acetylated and oxidised), via both their apolipoprotein and lipid moieties [537,539–548]. MARCO binds LPS, Escherichia Coli, Staphylococcus aureus, Neisseria meningitidis, exosomes, β5 integrins of tumour cells, and modified forms of LDL [531,549–552]. Through these binding properties, these receptors contribute to classical macrophage functions, such as phagocytosis, regulation of immunity, and maintaining internal homeostasis [553–555]. Both SRA and MARCO have regulatory roles in TLR4-mediated inflammatory responses. TLR4 stimulation with LPS induces an upregulation of both SRA and MARCO in splenic macrophages, and the expression of these receptors contributes toward LPS-induced mortality in mice. Indeed, MARCO/SRA-deficient mice exhibit increased production of anti-inflammatory IL-10 and anti-LPS antibodies, both protective factors in the LPS challenge model [555]. MARCO-expressing TAM macrophages are linked to poor prognostic outcome in breast cancer patients [556]. Antibody-mediated inhibition of MARCO on TAMs shifts macrophages from an M2-like immunosuppressive phenotype to the M1-like proinflammatory phenotype and enhances tumour cell clearance in multiple murine cancer models [557]. In addition to its demonstrable immune functions, SRA has been implicated as a mediator of insulin resistance in the context of obesity. Compared to obese WT mice, obese $Msr1^{-/-}$ mice exhibit increased blood glucose levels and reduced insulin-stimulated glucose uptake in the adipose tissue [558]. Similarly, SRA expression in human adipose tissues strongly negatively correlates with sensitivity to insulin, independently of obesity status and overall macrophage load [559].

5.1.2. Alveolar macrophage ontogeny and functions

Alveolar Macrophages (AMs) are the tissue-resident macrophage population of the lung. Fate mapping studies in mice demonstrate that they derive from the fetal yolk sac and fetal liver in a GM-CSF-dependent manner [560–562]. Fate mapping of AMs in a humanised mouse model indicates that hematopoietic stem and progenitor cells, via monocyte intermediates, seed all lung macrophages, including AMs and interstitial macrophages [563]. This is the dominant macrophage population in the lung, comprising 60-70% of lung macrophages, the other 20-30% being interstitial macrophages [564]. Parabiosis experiments and bone marrow progenitor lineage tracing further demonstrate that AMs receive minimal contribution from monocytes during adulthood, and self-maintain locally through chronic low level proliferation [565]. AMs reside in the lumen of the alveolus and are directly exposed to the air while also in close proximity to alveolar epithelial cells, as well as the alveolar capillary endothelium [566].

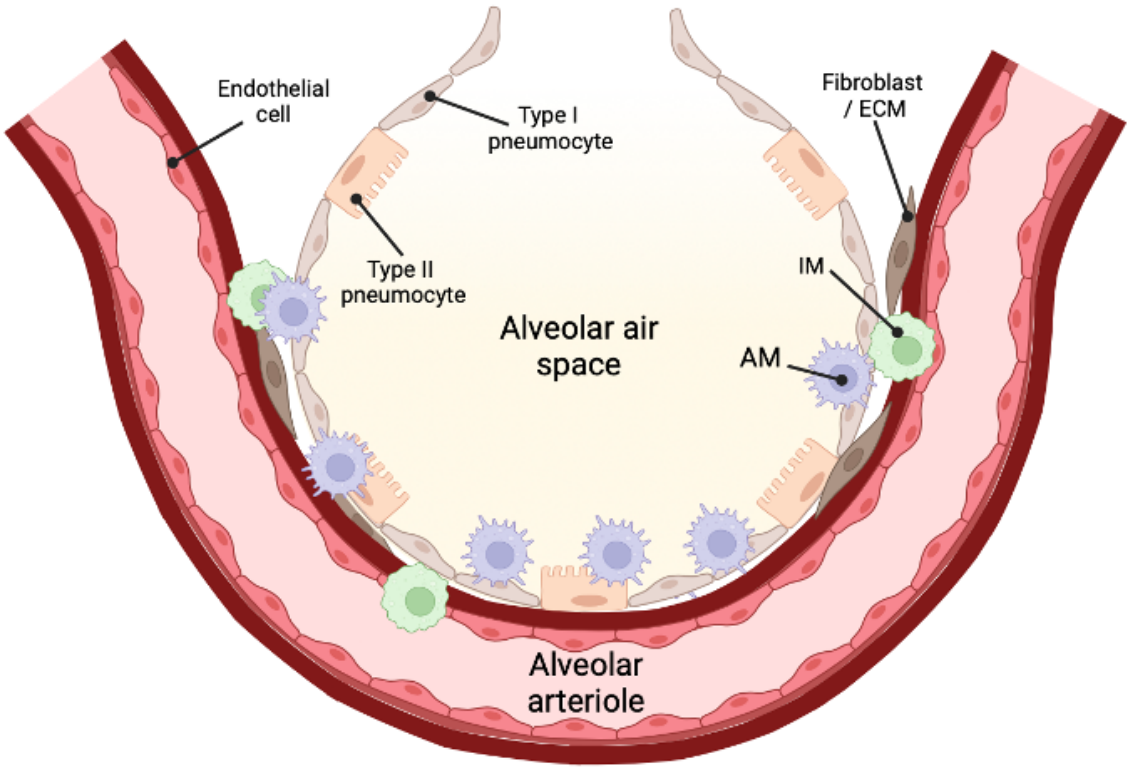


Figure 5.1. Alveolar structure and cellular makeup. Type I and Type 2 pneumocytes, specialized lung epithelial cells, form a single celled layer juxtaposed to the alveolar arteriole, between which gas exchange takes place. These cell types are separated by a layer of extracellular matrix (ECM) comprising mostly fibroblasts. Alveolar macrophages (AMs) are the dominant macrophage phenotype in the alveoli, located primarily adjacent to the epithelial cells of the alveolar airspace. Interstitial macrophages (IMs) are found in the interstitial space between the alveoli and blood vessels. Figure was adapted from [567] using Biorender.com.

AMs are dependent upon GM-CSF from alveolar epithelial type 2 cells for their development pre and postnatally [568]. Functional studies in which AMs are ablated, for example via GM-CSF-deficiency, demonstrate that AMs are phagocytic and pathogen-killing cells and regulators of the inflammatory response [569]. At steady state, AMs produce low levels of cytokines and suppress innate and adaptive immunity [566]. However, AMs are highly plastic cells and regulate their phenotype and that of the lung microenvironment in a context-dependent manner. Upon LPS inflammatory challenge, AMs induce alveolar cytokine release as well as neutrophil and monocyte recruitment [570]. In the context of viral infection, AMs produce IFNα which is essential for effective viral clearance [571]. Additionally, AMs play a critical role in the resolution of inflammation following bacterial challenge [572]. In addition to their immune functions, AMs also are involved in catabolising surfactant proteins produced by alveolar epithelial cells [569]. GM-CSF and GM-CSF receptor-deficient mice lack functional AMs [569], and develop pulmonary abnormalities characterised by the progressive accumulation of surfactant lipids and proteins, and peribronchovascular lymphoid infiltrates (mainly B cells), in the alveolar space [573–576]. This phenotype has been traced to the function of AMs – GM-CSF-deficient AMs cannot effectively bind, uptake, and catabolise surfactant proteins and lipids [569]. This condition is collectively termed pulmonary alveolar proteinosis and occurs in AM-deficient humans and mice [577].

5.1.3. Primary and secondary aldosteronism: causes and consequences

Aldosteronism is a condition caused by excessive adrenal gland production of the mineralocorticoid aldosterone. Consequences of aldosteronism include elevated blood pressure, resultant organ damage, electrolyte imbalance, endothelial dysfunction, left ventricular hypertrophy, coronary heart disease, and heart failure [266,578,579]. The condition can be divided into primary and secondary aldosteronism, based on the site of origin of the aldosterone-producing effect. Primary aldosteronism (PA) is the most common form, characterised by hyperactivity of one or both adrenal glands and normal/low renin activity. PA is typically caused by a unilateral aldosterone producing adenoma (Conn's syndrome) or bilateral primary adrenocortical hyperplasia [580]. Mechanistically, PA is caused by somatic mutations in aldosterone-producing adenomas and germline mutations. The mutated genes are commonly those encoding transport ATPases and ion channels. Such mutations cause a rise in intracellular calcium ion concentrations which cause membrane depolarisation that triggers aldosterone production [271].

Secondary aldosteronism (SA) is much less frequently diagnosed and researched than PA. During the writing of this thesis a PubMed search for “Primary aldosteronism” returned 4814 results in the period from 1954-2023. In contrast, a search for “Secondary aldosteronism” returned 170 results from 1960-2023. SA is caused by activation of the RAAS and subsequent zona glomerulosa (ZG) stimulation that arises extra-adrenally. In theory, this can be caused by a single factor or multiple stimuli. The vast majority of instances of SA are caused by factor(s) of the RAAS (e.g. elevations in renin, AngII) [267]. Much of the literature on PA and SA has centred upon clinical studies of patients presenting with aldosteronism. RAAS-associated causes of SA can be split into those that present with hypertension and those that do not. Hypertension-associated SA include cases of renovascular hypertension, malignant

hypertension, and renin-producing tumours. Non-hypertension-associates SA includes pregnancy, chronic renal failure, and in individuals with Bartter's syndrome (**Table 5.1**).

Secondary aldosteronism type	**Hypertensive?**	**Renin (high, normal or low)**	**Potassium (high or low)**
Renovascular hypertension	Y	Normal/low	Low
Malignant hypertension	Y	High	Low
Renin-producing tumours	Y	High	Low
Pregnancy	N	High	Low
Chronic renal failure / anepehric	N	Normal/low	High
Bartter's syndrome	N	High	Low

Table 5.1. Known causes of non-treatment-induced secondary aldosteronism. Adapted from [267,579].

While potassium stimulates aldosterone production initially, it also reduces plasma renin activity, and the stimulated aldosterone production impacts renal electrolyte transport to increase sodium reabsorption and potassium excretion, thereby reducing aldosterone production in the long term [579,581]. Low potassium levels are therefore typically associated with high aldosterone levels, and *vice versa*. However, high potassium levels have been shown to be causative to increased aldosterone clinically in cases of chronic renal failure and in an anephric man [582–584], indicating that when lacking appropriate kidney function, aldosterone secretion is primarily regulated by potassium levels.

5.1.4. ACE: physiological and immune functions

Angiotensin converting enzyme (ACE) is a zinc metalloprotease that serves two important physiological functions; 1) ACE converts the inactive Angiotensin I into the biologically active AngII, which is a vasoconstrictor and potent stimulant of aldosterone production from the

adrenal gland; 2) ACE degrades active bradykinin, a vasodilator and stimulator of vascular permeability [585,586]. ACE therefore is an important regulator of blood pressure. ACE is expressed on vascular endothelial cells throughout the body [587] but is highly expressed by pulmonary microvascular endothelial cells on the luminal surface [588,589] and thereby cleaves bloodborne Angiotensin I to AngII – a core element of the RAAS. The lung is therefore considered the primary site of ACE expression in the RAAS [590].

ACE is also recognised as an inflammatory mediator via the generation of AngII, which has been shown to act as a proinflammatory mediator via several mechanisms [591]. In endothelial cells, AngII stimulates intracellular oxidative stress, activation of the proinflammatory transcription factor Nuclear Factor-κB, and the upregulation of the monocyte-attracting protein VCAM-1 [592]. Similarly, AngII induces of Nuclear Factor-κB activation in monocytes and smooth muscle cells [593,594], indicating its broad capacity to regulate inflammation. Further, AngII stimulates NADH-/NADPH-oxidase activity in endothelial and smooth muscle cells, thereby enhancing the production of reactive oxidative species [595,596]. Indeed, in pre-clinical animal models ACE inhibitor treatment has been shown to attenuate both LPS and ventilator-induced lung injury via the suppression of Nuclear Factor-κB and pro-inflammatory cytokines [597,598]. Moreover, a clinical meta-analysis evaluating the effect of ACE inhibitor treatment on the inflammatory markers C-reactive protein, IL-6, and TNFα found that ACE inhibitors reduced the levels of all three inflammatory molecules [599], demonstrating that ACE's in vivo relevance as an inflammatory mediator.

5.2. Rationale and experimental aims

Scavenger receptors are expressed on macrophages in a variety of tissue contexts and are capable of binding a plethora of ligands, including modified forms of LDL cholesterol.

Scavenger receptors have demonstrable physiological activities in addition to their immunomodulatory roles. Moreover, the data presented in this thesis and evidence from studies in the preceding decades have demonstrated that macrophages carry out a range of homeostatic and physiological functions in virtually every tissue in which they are found. While the class B scavenger receptor SCARB1 has a demonstrable role in regulating adrenal steroidogenesis, whether the class A scavenger receptors carry out similar functions remains unclear.

The aims of this chapter were:

1) To assess the effect of class A scavenger receptors on adrenal corticosteroid production.
2) To characterise the effect(s) of MARCO on the RAAS system and blood pressure.

5.3. Results

5.3.1. The effect of the class A scavenger receptors on cholesterol levels and corticosteroid output

Given that the adrenal-derived mouse (and human) corticosteroids, most notably corticosterone and aldosterone, derive from cholesterol as the common precursor (Figure 5.2A) I hypothesised that cholesterol binding class A scavenger receptors could modulate adrenal corticosteroid output by regulating the availability of cholesterol that could feed into the steroid hormone biosynthetic pathway. To test this hypothesis, I measured the concentrations of aldosterone and corticosterone in the plasma of wild-type (WT), Marco$^{-/-}$, and of SRA$^{-/-}$ mice. I found that Marco$^{-/-}$ mice had significantly elevated levels of plasma aldosterone relative to wild-type and SRA$^{-/-}$ mice, in which aldosterone concentrations were similar (Figure 5.2B). In contrast, plasma corticosterone levels were not significantly altered in mice lacking MARCO, but SRA-deficient mice had significantly reduced corticosterone levels relative to WT mice (Figure. 5.2C). Female Marco-deficient mice had similar levels of plasma aldosterone and

corticosterone compared to WT mice (Figure 5.2D, E). For the remainder of this chapter, I focused on the elevated aldosterone phenotype in male Marco-deficient mice due to mouse availability. Male Marco-deficient adrenals were significantly lighter in weight than age-matched WT adrenals (Figure 5.2F)

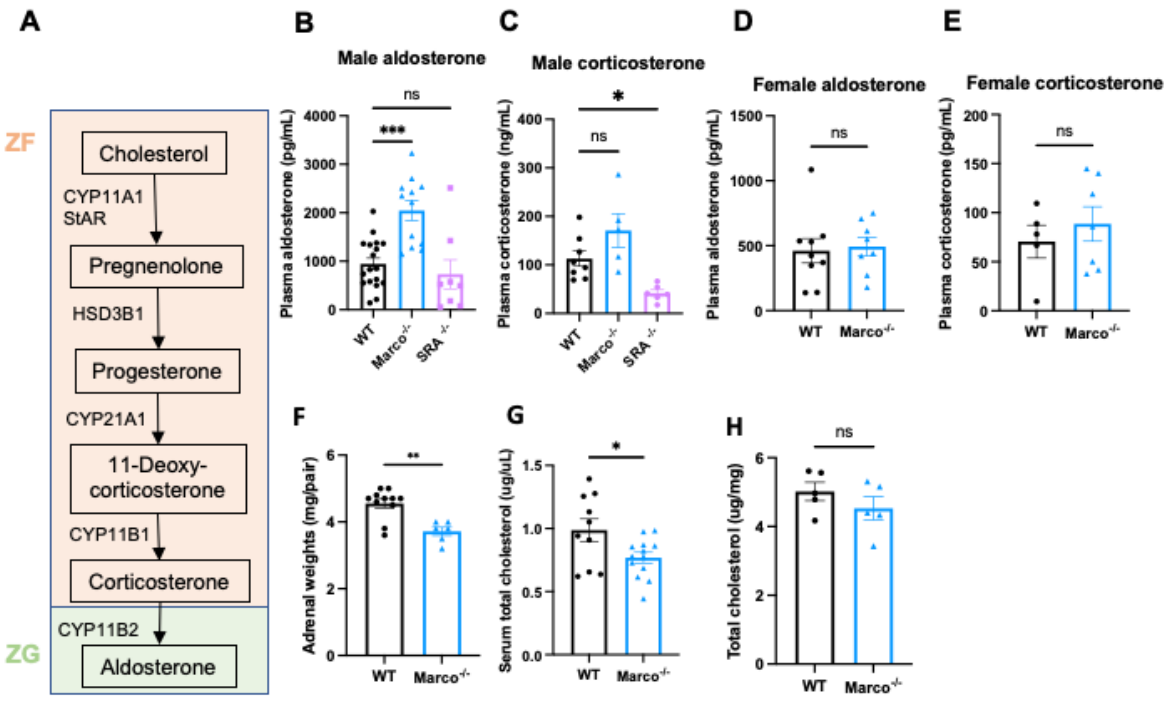


Figure 5.2. Marco-deficient mice have elevated aldosterone and reduced serum cholesterol. (A) Schematic depicting the murine adrenal corticosteroid biosynthetic pathway. Plasma aldosterone (B) and corticosterone (C) concentrations from wild type (WT), Marco-deficient, and SRA-deficient male mice. Plasma aldosterone (D) and corticosterone (E) concentrations in wild-type and Marco-deficient female (D, E) mice. (F) Weights of both adrenal glands from WT or Marco-deficient male mice. Serum total cholesterol levels (G) and relative intra-adrenal cholesterol levels, normalised to adrenal weight, in WT and Marco-deficient male mice (H). Data in B-H were analysed by two-tailed unpaired Student's *t*-test and are shown as average ± s.e.m. $*P < 0.05$, $**P < 0.01$, $***P < 0.001$, $**** P < 0.0001$.

To establish whether cholesterol levels could explain the elevated plasma aldosterone I observed in Marco-deficient male mice, I measured the levels of total serum cholesterol and intra-adrenal cholesterol. I hypothesised that plasma or intra-adrenal cholesterol levels would be higher in Marco-deficient mice relative to WT mice. Contrary to my hypothesis, I found

that Marco$^{-/-}$ mice had reduced serum cholesterol relative to wild-type controls (Figure 5.2G), while the levels of intra-adrenal cholesterol, normalised to gland weight, were similar between both mouse strains (Figure 5.2H). Taken collectively, these findings suggest that, while Marco-deficient mice have elevated plasma aldosterone concentrations, this is not dependent on systemic or local cholesterol availability.

5.3.2. Marco is expressed in the lung but not the adrenal glands

I next hypothesised that adrenal gland-derived MARCO could play a role in modulating aldosterone output. Analysis of publicly available Single cell sequencing data from murine adrenal glands shows that adrenals do contain a substantial population of macrophages expressing *Ptprc* (CD45), *Adgre1* (F4/80), and *Cd68* (CD68). However, I did not detect Marco expression in this cluster of cells, nor any other cluster identified in these analyses (Figure 5.3A). This finding was corroborated by immunostaining of male murine adrenal glands, which showed CD68^{+} macrophages in the adrenal ZF and ZG that did not stain positively for MARCO (Figure. 5.3B). Given that the lung is the other main site in the RAAS axis, I postulated that *Marco*-expressing cells in the lung could be involved in mediating the aldosterone phenotype observed in Figure 5.2. Indeed, single cell RNA seq analysis of the murine lung shows that *Ptprc* (CD45), *Adgre1* (F4/80), and *Cd68* (CD68) expressing cells (Alveolar Macrophages) also express *Marco,* but it was not observed in other cell types within the lung *(*Figure 5.3C). Immunostaining in the lung found CD68 and MARCO co-staining, further corroborating the single cell RNAseq findings (Figure 5.3D). To further validate the single cell sequencing and immunofluoresence data, I carried out qPCR for *Marco* in the lungs and adrenal glands from WT and Marco$^{-/-}$ mice. Marco was relatively highly expressed in the WT lung, but was not observed in WT adrenal glands, nor Marco-deficient adrenals or lungs (Figure 5.3E).

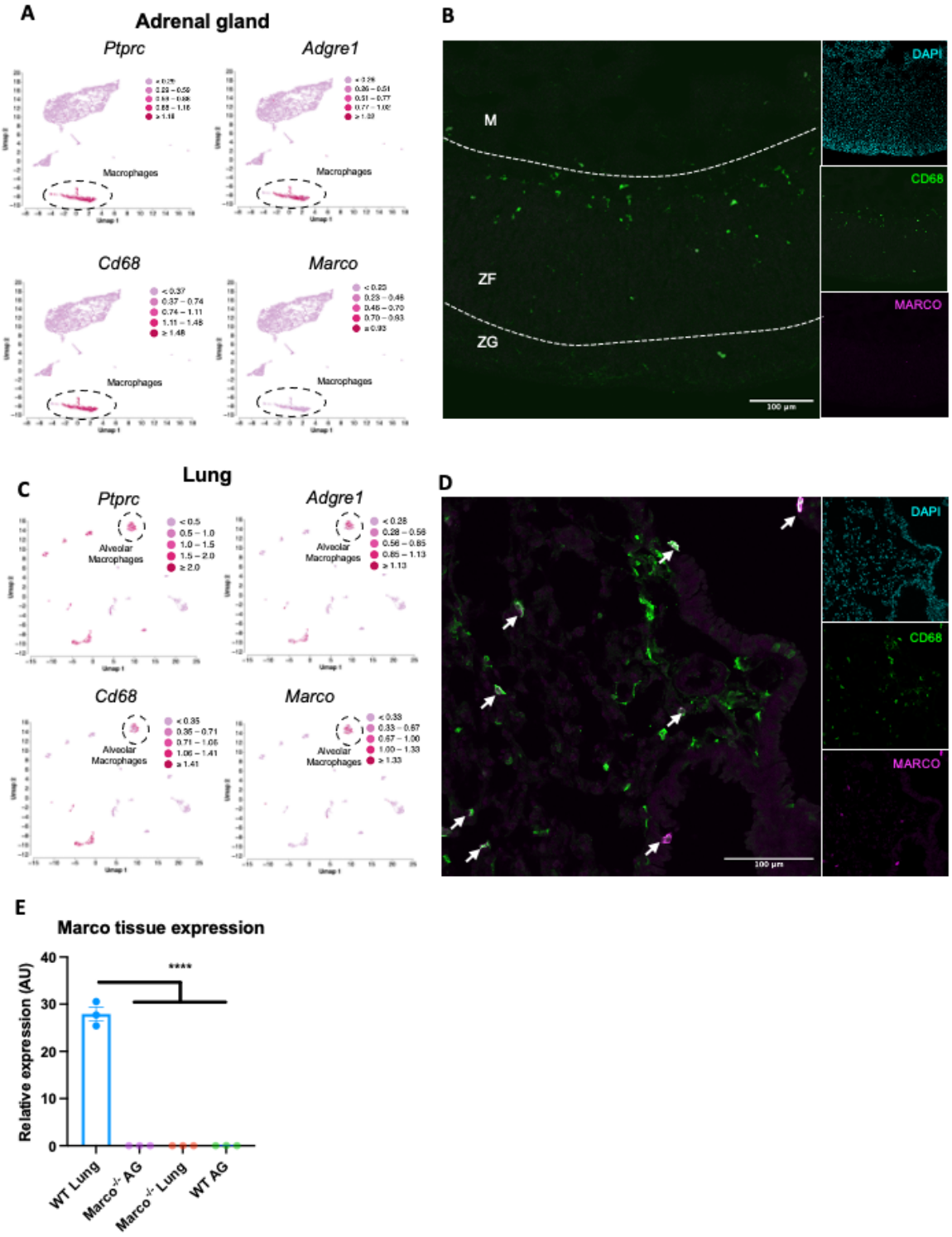


Figure 5.3. Marco is expressed in the lung and not adrenal glands. (A) Single cell RNA seq data plots from PMID 33571131 representing mRNA expression of Ptprc (CD45), Adgre1 (F4/80), Cd68, and Marco, in male murine adrenal glands. (B) Representative image showing a central cryosection of the male murine adrenal gland from a C57bl/6 mouse stained against CD68 (green) Marco (magenta), and DAPI (cyan). (C) Single cell RNA seq data plots from PMID 30283141 representing mRNA expression of Ptprc (CD45), Adgre1 (F4/80), Cd68, and Marco, in the male murine lung. (D) Representative image showing a cryosection of the male murine lung from a hCD68-GFP reporter mouse stained against GFP (green) Marco (magenta), and DAPI (cyan). (E) qPCR data showing the

relative gene expression data for *Marco* in the indicated tissues. M = medulla, ZF = zona fasciculata, ZG = zona glomerulosa.

5.3.3. Marco-mediated elevation of aldosterone explained by Ace but not by upregulation of adrenal biosynthetic enzymes, the zona fasciculata, or renin

Aldosterone is a potent blood pressure-regulating hormone, the dysregulation of which can cause hypertension and increased cardiovascular risk [224]. It therefore follows that its production is tightly regulated. Aldosterone biosynthesis is fundamentally regulated intra-adrenally by cytochrome P450 family members in the corticosteroid biosynthetic pathway (Figure 5.2A). I therefore tested whether altered expression of enzymes in this pathway could explain the hyperaldosteronism observed in Marco-deficient mice. Marco$^{-/-}$ mice showed similar expression of aldosterone biosynthetic enzymes (*Star, Cyp11a1. Hsd3b1, Cyp11b1, Cyp11b2)* as wild type mice (Figure 5.4A-E), indicating that changes in biosynthetic enzyme expression are not responsible for the aldosterone phenotype.

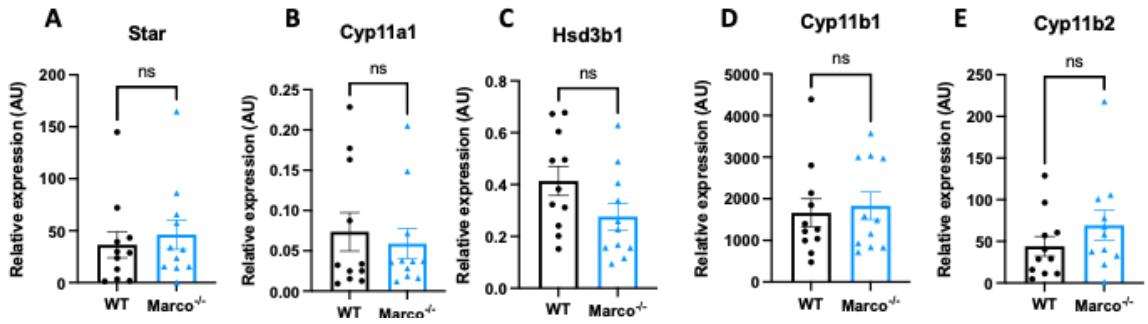


Figure 5.4. Marco-mediated elevation of aldosterone is not explained by adrenal biosynthetic enzyme gene expression. qPCR data reporting the expression of (A) Star, (B) Cyp11a1, (C) Hsd3b1, (D) Cyp11b1, and (E) Cyp11b2. Data in A-E were analysed by two-tailed unpaired Student's *t*-test and are shown as average ± s.e.m. **P* < 0.05, ***P* < 0.01, ****P* < 0.001, **** *P* < 0.0001.

CYP11B1 catalyses the conversion of 11-deoxycorticosterone to corticosterone. Corticosterone can be catalysed to aldosterone by CYP11B2 (Figure 5.2A). In this sense, synthesis via CYP11B1 is a bona fide route for the generation of aldosterone, as evidenced by the fact that *Cyp11b1* deletion in mice results in a significant reduction in aldosterone

production [500]. This route is one that is suppressible via the suppressive action of dexamethasone on ACTH and *Cyp11b1* expression (Figure 5.5A). Moreover, ACTH is a known stimulator of aldosterone [444,600]. Dexamethasone-mediated suppression of the zona fasciculata (Figure 5.5B) [183] was used to test whether the elevated aldosterone phenotype was zona fasciculata-dependent. Marco-deficient mice fed dexamethasone-supplemented drinking water had plasma aldosterone concentrations comparable to vehicle-treated mice (Figure. 5.5B), indicating that zona fasciculata activity does not contribute to elevated aldosterone levels in Marco$^{-/-}$ mice.

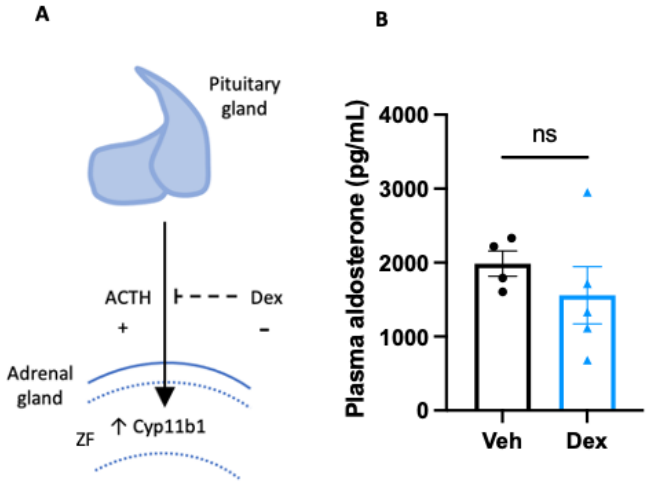


Figure 5.5. Dexamethasone suppression test. (A) A schematic illustrating that pituitary-derived adrenocorticotropic hormone (ACTH) stimulates the upregulation of Cyp11b1 from the zona fasciculata (ZF) and the dexamethasone-mediated suppression of this effect. (B) A bar graph showing the plasma aldosterone concentrations of Marco-deficient mice treated with vehicle or dexamethasone-supplemented drinking water for 14 days. Data in B were analysed by two-tailed unpaired Student's *t*-test and are shown as average ± s.e.m. **P* < 0.05, ***P* < 0.01, ****P* < 0.001, **** *P* < 0.0001.

Taken collectively, these findings indicate that elevated aldosterone observed in Marco-deficient mice arises extra-adrenally and can therefore be considered a form of secondary hyperaldosteronism. Kidney-derived renin is the major regulatory hormone in the enzymatic cascade that generates angiotensin II, a potent stimulator of adrenal aldosterone production [601]. I therefore compared plasma renin activity between WT and Marco$^{-/-}$ mice, finding no significant differences between the two strains (Figure 5.6A).

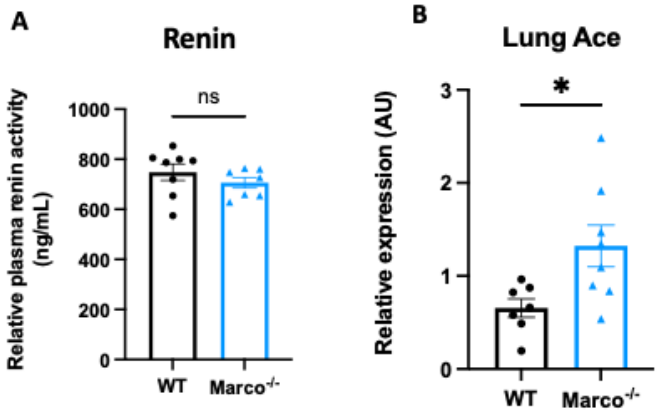


Figure 5.6. Marco-deficient mice have enhanced expression of *Ace* in the lung. (A) Plasma renin activity in wild-type and Marco-deficient male mice. (B) qPCR data reporting the expression of angiotensin converting enzyme (*Ace*) in the lungs of wild type (WT) and Marco-deficient male mice. Data in A-B were analysed by two-tailed unpaired Student's *t*-test and are shown as average ± s.e.m. *$P < 0.05$, **$P < 0.01$, ***$P < 0.001$, **** $P < 0.0001$.

I next investigated whether lung-derived angiotensin converting enzyme (*Ace*) could explain the elevated aldosterone levels observed in Marco$^{-/-}$ mice, since ACE in the lung catalyses the conversion of Angiotensin I to the aldosterone-stimulating peptide Angiotensin II [590]. I carried out a qPCR test for *Ace* in the lungs of WT and Marco$^{-/-}$ mice, finding that Marco-deficient animals had elevated levels of lung *Ace* relative to WT controls (Figure 5.6B). Immunofluorescent staining of WT and Marco$^{-/-}$ lungs revealed a substantially higher level of ACE protein in Marco-deficient mice, while myeloid cells, as detected by CD68 staining, remained unchanged (Figure 5.7A, B). While very low levels of ACE expression could be detected in CD68^{+} cells (data not shown), the vast majority of ACE was outside of monocytes and macrophages (Figure 5.7A). I used image analysis software (FIJI) to quantify these changes, finding that ACE median fluorescence intensity (MFI) was significantly increased in Marco-deficient lungs (Figure 5.7B), while CD68^{+} myeloid cells were present in wild type and knock-out animals at similar levels (Figure 5.7C). I then turned back to analysis of single cell RNA-seq data to identify the cells in the lung that could be mediating this effect.

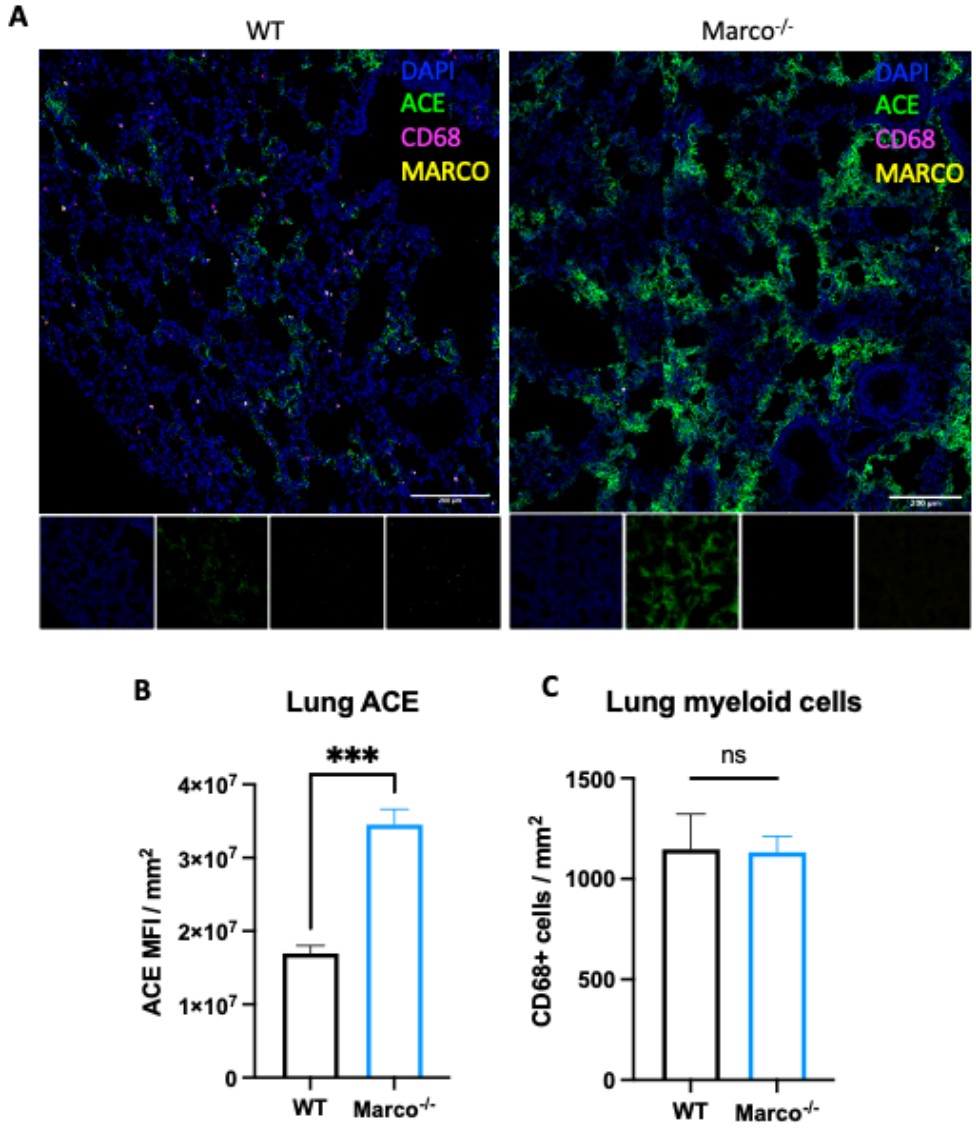


Figure 5.7. Marco-deficient mice have enhanced expression of Ace protein in the lung (A) Representative images showing a cryosection of wild-type and Marco-deficient male murine lungs stained against ACE (green) CD68 (magenta), MARCO (yellow) and DAPI (blue). Quantitation of DAPI-normalised ACE median fluorescence intensity (MFI) (B) and CD68+ myeloid cell presence (C) in the lungs of wild type and Marco-deficient male mice. Data in B-C were analysed by two-tailed unpaired Student's *t*-test and are shown as average ± s.e.m. *$P < 0.05$, **$P < 0.01$, ***$P < 0.001$, **** $P < 0.0001$.

In the lung, unsupervised cluster analysis revealed a total of 12 cell clusters with distinct gene expression signatures (Figure 5.8A, B). I determined the identity of each cell cluster based on the expression of established cell type-specific marker genes, aided by the marker genes identified and outlined in Figure 5.8B. I next used dot plots to visualize expression of *Marco* and *Ace* across the different cell clusters. I observed notable *Marco* expression only in (AMs)

amongst all the different cell clusters (Figure 5.8C). *Ace* was shown to be primarily expressed by lung endothelial clusters 1 and 2 (Figure 5.8C), in agreement with what is known about lung *Ace* expression. Taken collectively, these data align with a model in which MARCO^{+} Alveolar Macrophages, in response to an as-of-yet unidentified factor, inhibit *Ace* expression at the gene and protein level, and thereby negatively regulate the cleavage of Angiotensin I to form Angiotensin II, and aldosterone production (Figure 5.8D).

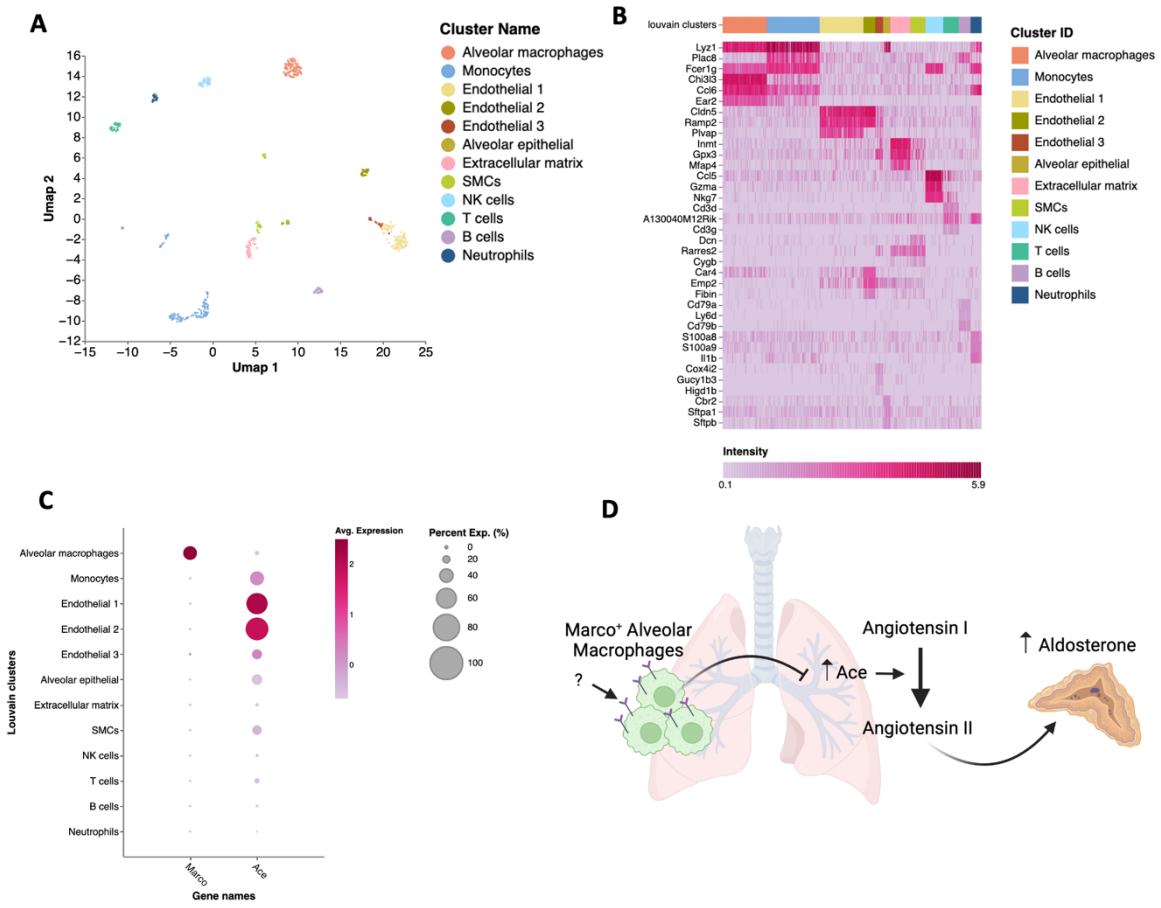


Figure 5.8. A model of MARCO-mediated regulation of aldosterone. (A) Single cell RNA seq UMAP plot depicting the cell types present in the male murine lung. (B) Marker heatmap showing the top three gene markers for each cell cluster in (A). (C) A dot plot showing the gene expression levels of Marco and Ace in the different cell clusters of the male murine lung. (D) A schematic, generated using BioRender, showing the working model by which Marco+ alveolar macrophages regulate aldosterone output from the adrenal gland.

5.3.4. Marco deletion impacts blood pressure and plasma electrolyte levels

Lastly, I sought to measure the downstream consequences of the elevated aldosterone observed in male Marco-deficient mice relative to WT mice. Mouse systolic blood pressures were similar between wild type and Marco-deficient animals (Figure 5.9A), but diastolic blood pressure was significantly reduced in Marco-deficient animals relative to wild type mice (Figure 5.9B). Marco-deficient mice had a trend towards reduced mean blood pressure compared to wild-type mice, but this was not statistically significant (Figure 5.9C).

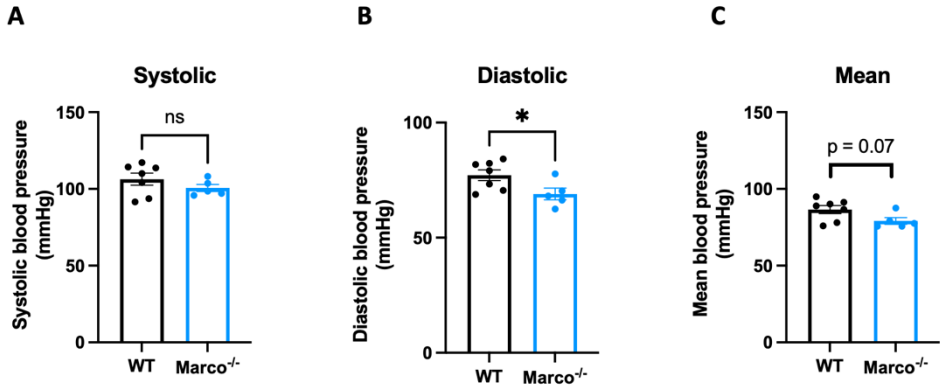


Figure 5.9. Blood pressure of WT and Marco$^{-/-}$ mice. Bar graphs showing the (A) systolic, (B) diastolic, and (C) mean blood pressure in wild-type and Marco-deficient mice as measured by the tail cuff occlusion method. Data in A-C were analysed by two-tailed unpaired Student's *t*-test and are shown as average ± s.e.m. *$P < 0.05$, **$P < 0.01$, ***$P < 0.001$, **** $P < 0.0001$.

To measure blood plasma volume, mice were injected intravenously with FITC-dextran, which was then left to circulate in the bloodstream. Later, blood was collected and plasma isolated. Blood volume was extrapolated from the extent to which the FITC signal diluted in the blood. The absolute interpolated blood volumes were similar between wild type and Marco-deficient mice (Figure 5.10A). Blood volumes normalised to individual mouse body weights were also similar between the strains (Figure 5.10B). Plasma sodium and potassium ion concentrations were both significantly elevated in Marco-deficient mice relative to wild type animals (Figure 5.10C, D).

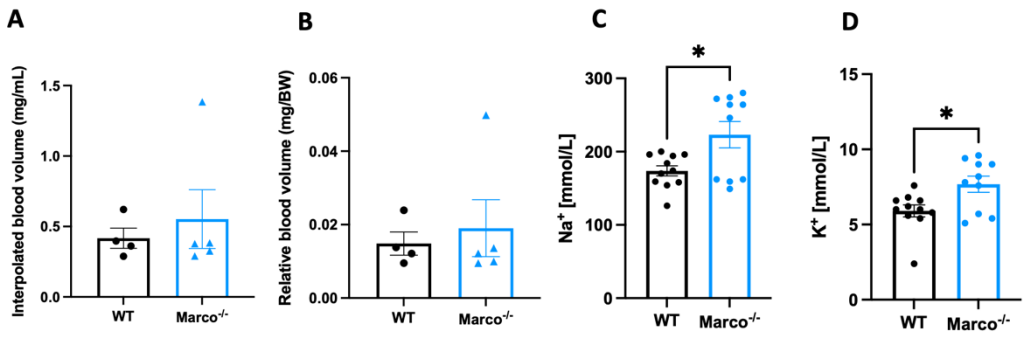


Figure 5.10. Blood volume and electrolytes in WT and Marco$^{-/-}$ mice. Bar charts showing (A) the interpolated absolute blood volume, (B) weight-normalised blood volume, and plasma (C) sodium and (D) potassium electrolyte concentrations in wild type and marco-deficient male mice. Data in A-D were analysed by two-tailed unpaired Student's *t*-test and are shown as average ± s.e.m. *$P < 0.05$, **$P < 0.01$, ***$P < 0.001$, **** $P < 0.0001$.

In conclusion, I hereby demonstrate that Marco is a negative regulator of aldosterone production, potentially via suppression of angiotensin converting enzyme expression in the lung. I propose a model in which extra-adrenal MARCO-expressing alveolar macrophages, through tissue crosstalk with lung endothelial cells, actively inhibit Ace expression and thereby inhibit the production of aldosterone from the adrenal glands.

5.4. Discussion

The main findings of this chapter are:

1) MARCO negatively regulates adrenal aldosterone production while SRA positively regulates corticosterone production.
2) Marco regulation of aldosterone is independent of cholesterol.
3) Marco is not expressed in the adrenal gland and instead appears to regulate aldosterone production via modulation of Ace gene and protein expression in the lung.

Numerous studies over preceding decades have shown that macrophages are much more than simply immune and inflammatory cells. Macrophages have been shown to mediate a wide variety of physiological functions and support homeostasis in virtually every tissue they are

found [24,111,112,115,118,431]. My original hypothesis centred on the regulation of corticosteroid output via modulation of cholesterol availability. While I ended up disproving this hypothesis, at least in the context of aldosterone, I hereby provide evidence of another putative para-immune function of tissue macrophages.

5.4.1. MARCO as a regulator of Ace expression

Contrary to the original hypothesis, it was observed that Marco-deficient mice exhibited elevated plasma aldosterone levels without corresponding changes in systemic or intra-adrenal cholesterol levels. This finding suggests that the increased aldosterone concentration in Marco-deficient mice is not dependent on alterations in cholesterol availability within the adrenal gland. Indeed, while Marco was not detected in adrenal glands, single-cell RNA sequencing and immunostaining confirmed its presence in the lung, specifically in alveolar macrophages. This finding led me to hypothesise that the lung may play a crucial role in mediating the observed hyperaldosteronism in Marco-deficient mice. In support of this hypothesis, Ace mRNA and protein expression was elevated in Marco-deficient lungs relative to wild-type lungs. This would therefore suggest that Marco-expressing alveolar macrophages are suppressing Ace expression in steady state conditions. With high Ace protein and mRNA, and high aldosterone, it would follow that AngII is also elevated in Marco-deficient mice. However, this remains to be experimentally tested.

ACE and Angiotensin II are pleiotropic molecules. In addition to their physiological roles, they are also exhibit immunomodulatory functions. *In vitro*, lipopolysaccharide (LPS) treatment of the HUVECs endothelial cell line or human primary endothelial cells causes a reduction in ACE activity, mRNA and protein levels. Similarly, ACE expression in human lung tissue is reduced in sepsis patients relative to control tissues [602,603]. Supernatant from LPS or TNFα-

treated endothelial cells shows a high proportion of ACE^+ endothelial microparticles (EMPs). ACE^+ EMPs are also increased in plasma of mice undergoing experimental lung injury and in human septic patients [603], indicating shedding of lung endothelial ACE in the context of inflammation. As described earlier, Ace and AngII have been shown to enhance inflammation in a variety of contexts. It may therefore be that Marco-expressing AMs exert an immune-modulatory function within the murine lung via controlling tissue Ace expression. Alveolar macrophages, which use MARCO to bind and uptake bacteria [604], could serve to enhance lung immunity in a pathogen and ACE-dependent manner. Pharmacologic ACE inhibition was previously shown to dampen pro-inflammatory immune cell inflammation in radiation-induced pneumonitis [605]. Future experiments could therefore explore whether Marco regulates lung tissue Ace expression in the context of inflammation and/or pathogenic challenge. Endothelial cells, through secreted Rspondin3 (a Wnt signalling modulator) mediate the formation of protective anti-inflammatory interstitial macrophages in the lungs of endotoxemic mice [606], demonstrating the presence of crosstalk pathways between these cell types in the lung. A reverse relationship could exist whereby AMs also regulate the ACE-expressing phenotype of lung endothelial cells.

5.4.2. MARCO as a regulator of aldosterone

Whether MARCO evolved to regulate aldosterone production as a primary adaptation, or a secondary effect of an immune-centred adaptation is unclear, though the latter may be more likely. However, the consequences of the effect on aldosterone could be equally significant. It is known that immunosuppressants such as cyclosporine can increase blood pressure [607] yet the mechanism remains incompletely understood. This observation is consistent with this study's data showing Marco-mediated negative regulation of the blood pressure-controlling hormone aldosterone. Additionally, the fact that higher ACE/ACE2 ratios have been linked to

hypertension and worse outcomes in Covid-19 [608] could implicate MARCO in the susceptibility to severe disease via effects on blood pressure.

Secondary aldosteronism (SA) is distinguished from primary aldosteronism through renin – SA is characterised by high aldosterone and high or non-suppressed renin levels [609]. By this definition, Marco-deficient mice exhibit SA, due to their high aldosterone and normal renin levels. SA is also defined as elevated aldosterone that originates outside of the adrenal gland – in this case from ACE in the lung. This finding raises the intriguing possibility that aldosteronism could be triggered or aggravated by MARCO-binding ligands. According to the measurements presented in this chapter, Marco-deficient mouse blood pressure is not elevated relative to that of WT mice. These mice exhibit increased plasma sodium, as would be expected, but also increased potassium, which is unexpected. Hyperkalemia is generally associated with low aldosterone levels, as aldosterone triggers sodium absorption and potassium excretion by the kidneys [441]. The reason for the hypokalaemia in Marco-deficient mice is therefore unclear. Marco-deficient mice present with a phenotype similar to that of chronic renal failure, characterised by normal renin activity and high potassium levels. Assessment of the glomerular filtration rate of Marco$^{-/-}$ mice relative to wild-type mice should therefore be used to assess whether overall kidney function is similar in these strains. Potassium homeostasis is regulated by catecholamines and insulin [610] and investigations into the levels of these regulators are also therefore warranted in Marco-deficient mice. Despite high aldosterone levels in Marco-deficient mice, concomitant increases in blood pressure and blood volume were not detected. These mice are constitutive knockouts for the *Marco* gene, and blood pressure is controlled via a variety of competing mechanisms, and so these seemingly conflicting observations may be due to compensatory mechanisms that "correct" blood pressure during development. The lack of increased blood volume resulting from elevated

aldosterone could be due to inadequate experimental assessment of blood volume, or a sample size that lacks sufficient power to detect differences between experimental groups. Alternatively, the elevation in aldosterone in Marco-deficient mice may be of a size insufficient to induce blood volume or pressure changes. While acute increases of plasma aldosterone have varying effects on endothelial function in humans and animal models, chronic (i.e. genetic) elevations of plasma aldosterone are virtually universally associated with endothelial dysfunction [611]. This is frequently characterised by reduced endothelial NOS activity from, and acetylcholine action on, endothelial cells [611]. It would therefore be logical to test whether vascular dysfunction is present in the endothelia of Marco-deficient mice relative to wild type mice.

The findings of elevated aldosterone, slightly diminished blood pressure, and elevated potassium and sodium in Marco-deficient mice may alternatively be consistent with the human condition of Pseudohypoaldosteronism (PHA). PHA refers to a group of rare genetic disorders characterised by non-responsiveness to aldosterone. Type 1 PHA is thought to be due to mutations to the gene encoding MR or the epithelial sodium channel (ENaC) subunits. Type 2 PHA is caused by mutations in the genes encoding proteins involved in aldosterone signalling pathways, such as the serum and glucocorticoid-regulated kinase 1 (SGK1) gene or the WNK1 and WNK4 genes [612]. Future investigations could therefore involve testing the sensitivity of the MR in Marco-deficient mice, or sequencing of the Marco-deficient mouse genome to determine whether any of these mutations co-occur with Marco deficiency. Such analyses may help determine whether Marco-deficiency could be genetic contributor to PHA.

5.4.3. The class A Scavenger receptors as cholesterol regulators?

The HDL-binding scavenger receptor SR-B1 is known for its role in the provision role of cholesterol as a substrate molecule for fuelling steroidogenesis in the adrenal gland [247,250]. Though I have shown that Marco is not expressed in the murine adrenal gland, the data presented in Figure 5.2 shows that Marco-deficient mice have reduced plasma cholesterol levels relative to WT mice, indicating that Marco regulates systemic cholesterol levels at steady state. The site of origin of this phenotype is unclear, but Marco expression is a defining feature of macrophages resident in the liver (Kuppfer cells), the body's main site of liver metabolism [613]. Future investigations could therefore probe whether liver Kuppfer cells are involved in regulating systemic cholesterol levels via MARCO. A previous study showed that clodronate liposome-mediated depletion of macrophages in mice with a human-like lipoprotein metabolism results in a reduction of plasma VLDL and an increase in HDL, but no overall decrease in total cholesterol titres [614], lending credence to the hypothesis that Kuppfer cells could play a role in regulating liver cholesterol metabolism. Moreover, Kuppfer cells are known to be central players in cholesterol homeostasis, mediating the transfer LDL-derived cholesterol to hepatocytes, supposedly via LDLR-mediated LDL uptake [615], though this has not been experimentally demonstrated. The nature of the cholesterol that is reduced (i.e. LDL or HDL) in Marco-deficient mice remains to be determined, but defining this may aid our understanding of how Marco is involved in regulating plasma cholesterol titres, and whether targeting MARCO could be used to manipulate cholesterol levels for therapeutic benefit.

Lastly, I also demonstrated that SRA-deficient mice have reduced levels of plasma corticosterone relative to WT mice. The precise mechanism mediating this effect was not explored in this chapter and remains unclear. However, this observation may provide a mechanistic basis for BALL macrophage cholesterol uptake. Future investigations could test

whether *in vivo* targeting of SRA has any effect on intra-adrenal cholesterol stores, and whether the strategy could be used to reduce corticosterone levels temporally *in vivo*. If successful, such an approach could inform novel therapeutic strategies for treating conditions characterised by excessive glucocorticoid levels such as Cushing's syndrome.

5.4.4. Limitations

The results listed in this chapter provide novel insights into how systemic aldosterone levels are regulated. However, important questions remain to be answered, such as the precise mechanism by which MARCO-expressing AMs suppress Ace expression, and the ligand(s) responsible for stimulating this effect via the MARCO receptor. *In vitro* studies in which AMs are co-cultured, either together or in transwell format, with lung endothelial cells, could be used to identify whether soluble mediators or cell-cell contact is required for ACE inhibition. Additionally, does ACE inhibition reduce plasma aldosterone titres in Marco-deficient mice? Would Marco receptor manipulation modulate plasma aldosterone levels? Further experiments in which Marco-deficient mice are treated with ACE-inhibitors or Marco receptor-agonists/antagonists could provide further mechanistic evidence for the aldosterone phenotype observed in this chapter. While I detected increased aldosterone in Marco-deficient mice, an elevation in blood pressure was not detected. Rather, diastolic blood pressure was increased in Marco-deficient mice relative to wild-type mice as measured indirectly via the tail cuff method. While mice were habituated to restraint prior to experimental readings, there exists the potential for restraint-induced distress to confound results [616,617]. The gold standard for blood pressure measurements in rodent models is the implantation of telemetry-based blood pressure probes into the aortic arch, allow real-time direct measurements of blood pressure that are not susceptible to stress-induced effects. Similar to adrenal gland macrophages, it is not yet possible to selectively experimentally manipulate lung macrophage gene expression, and this

study has relied upon constitutively Marco-deficient mice. While Marco is expressed on subsets of tissue macrophages at steady state, and only on AMs as cells in the RAAS, at this stage I cannot exclude the possibility of off-target effects of the Marco deletion. Lastly, this study did not probe the mechanism underlying why Marco-deficient male mice have elevated aldosterone relative to WT mice, yet Marco-deficient females do not. Further studies could probe whether sex hormones differentially impact scavenger receptor expression differences sex hormones underly these sex differences.

Chapter 6

Thesis summary and final discussion

At the beginning of my graduate studies, I identified a gap in the literature – macrophages had been identified in the in the adrenal glands of humans and mice for over 30 years, yet their functions had been incompletely defined. Presumably, the notion that macrophages simply act as immune sentinels, orchestrators, and cellular hoovers had directly or indirectly hampered research into their non-immune roles. In the preceding decades macrophages in other tissues slowly gained recognition for their para-immune functions, yet adrenal gland macrophages flew largely beneath the radar. The intra-adrenal functions of macrophages served as the inspiration for most experiments carried out and presented in this thesis, but also lead me to the lung to reveal another seemingly macrophage-mediated phenotype which feeds back to the adrenals to regulate hormonal output.

6.1. Key findings

The experimental aims for this thesis were as follows:

- To thoroughly characterise the macrophage compartment of the murine adrenal gland in health and obesity by immunofluorescent imaging and flow cytometry.
- To investigate the contribution of adrenal macrophages to aldosterone production and other adrenal-derived hormones.

With regard to these aims I made the following key findings:

- Adrenal gland macrophages heterogeneous and two different populations (BALLs and ZGMs) can be distinguished based on their autofluorescent signature, CX3CR1 expression, and replicative capacity.

- Both subsets of adrenal gland macrophages derive from CX3CR1-expressing precursors.
- ZGMs have an adrenal-specific phenotype and express corticosteroid biosynthetic machinery.
- BALL macrophages contain cholesterol and their formation is accelerated in obesity.
- ZGMs regulate the production of aldosterone, but not the production of other adrenal gland-derived hormones.
- BALL macrophage size and autofluorescent cholesterol contents changes depending on corticosteroid output.
- BALL macrophages form in a CX3CR1-dependent manner, regulate intra-adrenal cholesterol stores, and corticosteroid output in steady state and in obesity.
- MARCO negatively regulates adrenal aldosterone production while SRA positively regulates corticosterone production.
- MARCO regulation of aldosterone is independent of cholesterol.
- MARCO is not expressed in the adrenal gland and instead appears to regulate aldosterone production via modulation of Ace gene and protein expression in the lung.

6.2. Final discussion

Tissue macrophages are not a homogenous population of cells. It is generally acknowledged that macrophages can be broadly distinguished and categorised on the basis of their ontogeny – embryonic and bone marrow-derived – and by their function. Adrenal gland macrophages appear to be similarly heterogeneous. My findings, and those of others [302] have demonstrated that the murine adrenal gland hosts both embryonic and bone marrow-derived macrophage subsets. I have shown that the adrenal macrophage compartment changes in an age and diet-dependent manner and that two main adrenal macrophage subsets – BALLs and ZGMs – can

be distinguished by their morphology, replicative capacity, and CX3CR1 expression. Additionally, I show that they differentially regulate corticosteroid production at steady state and in the context of obesity. Moreover, macrophage MARCO is revealed as a regulator of lung Ace expression and adrenal aldosterone production. I therefore believe that the argument can and should be made that macrophages in these contexts are endocrine cells – not those that actively secrete hormones, but cells with demonstrable endocrine functions. This should not detract from their immune functions. I therefore suggest that adrenal macrophages should be the subject of future pre-clinical investigations into the pathogenesis of adrenal disorders including Addison's and Cushing's disease.

Though here I did not specifically investigate them in inflammatory and immune-related contexts, it is likely that adrenal macrophages, and clear that alveolar macrophages, are capable of effecting and orchestrating immune responses to invading pathogens. Given their demonstrated roles in regulating adrenal hormonal output, they may also thereby regulate the immune response throughout the organism. This possibility should be explored further. However, the perception of macrophages as immune cells can potentially hamper our ability to fully explore their non-immune functions. Researchers may refrain from or not think to explore the functions of these cells outside of immunity. Funding and resources are often allocated based on perceived priorities, and historically, the emphasis has been on understanding immune functions. This may result in fewer resources being devoted to investigating the non-immune functions of macrophages and indeed other "immune" cells. Conceptual barriers within the scientific community may slow the adoption of alternative perspectives on macrophage functions, or those of other immune cells. This can limit the integration of non-immune macrophage functions into broader biological and medical frameworks. By actively challenging the traditional view of macrophages as solely immune

cells, researchers can uncover novel insights into their multifaceted roles in maintaining tissue homeostasis.

In this vein, macrophage associated proteins and receptors should be considered not solely as immune receptors, but as putative endocrine or metabolic mediators. The data presented in this thesis indicate that the chemokine receptor CX3CR1 and the class A scavenger receptors MARCO and SRA have roles in regulating systemic corticosteroid and cholesterol levels. The contribution of these and other macrophage-associated receptors to other physiological processes remains unclear but could represent an untapped mine of therapeutically relevant clinical targets. Indeed, the results presented in this thesis – in particular the positive regulators of cholesterol and corticosteroids – could inform future studies that test the potential of pharmacologically targeting macrophages or their factors for therapeutic benefit. For example, endogenous corticosteroids and glucocorticoids in particular are known to play integral roles in the stress response, fear, and anxiety responses, as evidenced by studies demonstrating that adrenalectomized rodents lose their fear responses in a corticosterone-dependent manner [164]. Attempts to pharmacologically recreate this effect, via HPA axis inhibition with dexamethasone have demonstrated some success at reducing fear responses in rodents *in vivo* [618]. However, synthetic glucocorticoids are not specific drugs. Side effects are common, as are off target effects due to broad receptor expression in target and non-target tissues [163,619]. Indeed, while synthetic glucocorticoids are effective anti-inflammatory agents, their side effects are numerous and often themselves require additional therapeutic management [620]. Pre-clinical rodent and clinical human data has demonstrated that 11β-HSD1, which forms active cortisol from inactive cortisone, is causal in the development of adverse clinical features as a result of glucocorticoid excess [621,622]. Combining synthetic steroid treatment with 11β-HSD1 inhibition with the drug AZD4017 has demonstrated that this strategy has potential for limiting adverse

glucocorticoid effects [623]. Mineralocorticoid receptor antagonism via spironolactone and eplerenone has demonstrated efficacy in treating hypertension via reducing aldosterone levels [624]. However, these approaches are limited by side effects including hyperkalemia and acute deterioration of renal function [625]. Similarly, while ACE inhibitors are effective at reducing blood pressure long term, aldosterone levels are often not suppressed effectively and sometimes even increase with long term treatment (aldosterone breakthrough), raising important questions on the supposed organ-protective effects of the drugs [626]. Statins, commonly and effectively used to reduce LDL cholesterol levels, present an increased risk for diabetes mellitus and hepatic transaminase elevations [627]. Collectively, the data indicate that currently prescribed drugs (synthetic corticosteroids and statins) used to treat numerous endocrine and physiological conditions have variable off-target effects that hinder long term adoption.

Future studies should therefore investigate the therapeutic potential of 1) targeting BALL macrophages and intra-adrenal cholesterol levels for the prevention of corticosteroid-mediated pathologies; and 2) targeted inhibition of scavenger receptors to reduce plasma cholesterol titres to protective levels. The tissue-specific functions of macrophages could mean that such approaches would circumvent the off-target effects characteristic of drugs such as dexamethasone, while retaining their therapeutic benefit.

As explained in the introduction of this thesis, it is generally acknowledged that cholesterol that fuels steroidogenesis comes mostly from plasma lipoprotein-derived cholesterol esters[233]. However, the *in vitro* and *in vivo* systems used to demonstrate this effect have unintentionally excluded macrophages as a potential contributing factor. I have demonstrated that BALL macrophages mirror plasma lipoproteins in the context of obesity – with HFD feeding BALL macrophages get bigger and more cholesterol-laden, in contrast to ND-fed mice. In data not

shown I have observed that Marco-deficient animals, which have significantly reduced plasma cholesterol titres, have substantially smaller BALL macrophages than those observed in wild-type animals. Similarly, studies in rats have demonstrated that chronic exposure to energy drinks, which is associated with increased ACTH and cortisol production in humans, causes a decrease in lipid droplets and a reduction in the presence of vacuolated cells in adrenal cortex [628] – effects that may be localised to BALL macrophages. It is therefore possible that many of the studies which have attributed changes in steroidogenesis to plasma lipoproteins or adrenal endocrine cell lipid droplets, have actually been describing effects mediated by BALL macrophages. These data suggest that future studies are warranted that assess the effects of energy drinks on BALL macrophages, and those that assess side-by-side the contribution of plasma and macrophage-derived cholesterol in fuelling adrenal steroidogenesis.

Foam cells are known to play an essential role in the initiation and propagation of atherosclerosis [148,501,502,629–631]. Atherosclerotic development is commonly assessed by histological quantification of lesion size based on Oil Red O staining. The data presented in chapters 3 and 4 of this thesis demonstrates that, in the adrenal gland, 1) Oil Red O staining is not specific to macrophage lipids; and 2) macrophage-specific Oil Red O staining mirrors the autofluorescent signature of macrophages. If the same were true with foam cells in atherosclerotic lesions, then the foam cell autofluorescent signature could be used as an alternative, cheaper, and simpler way to quantify macrophage-specific lipid burden.

Terms such as neuroimmunity, immunometabolism, and neuroendocrinology are becoming more commonplace as we discover more about how our bodily systems, which all evolved side-by-side, intertwine to regulate whole organism homeostasis. While the influence of steroid hormones on immune system function has long been recognised, the reverse – the impact of

immune cells on steroid hormones – is just now becoming apparent. To this end we should embrace “immunoendocrinology” as a new and emerging field. I hope that this thesis can play some role in demonstrating that macrophages are more than “just” immune cells and that immunoendocrinology is a field worth pursuing further.

Appendix

Appendix 1. List of publications

Conan JO O'Brien, Davi Sidarta-Oliveira, Aleksander Stawiarski, Giorgio Ratti, Pierre-Louis Loyher, Mélanie Makhlouf, Eman H AbouMoussa, Emma Haberman, Charles Sweeney, Yusuke Mizuno, Tomohiro Ishii, Tomonobu Hasegawa, Elise P Gomez-Sanchez, Celso E Gomez-Sanchez, Siamon Gordon, David R Greaves, Luis R Saraiva, Frederic Geissmann, Ana I Domingos (2023). Distinct adrenal gland macrophages regulate corticosteroid production. bioRxiv 2023.09.05.556330; https://doi.org/10.1101/2023.09.05.556330.

Conan JO O'Brien, Giorgio Ratti, Emma Haberman, Charles Sweeney, Siamon Gordon, Ana I Domingos (2023). MARCO in alveolar macrophages negatively regulates Ace expression and aldosterone production. Life12:RP91318; https://doi.org/10.7554/eLife.91318.1.

Conan JO O'Brien, Emma Haberman, Ana I Domingos. A Tale of Three Systems: Toward a Neuroimmunoendocrine Model of Obesity (2021). Annu Rev Cell Dev Biol. 2021 Oct 6;37:549-573; https://doi.org/10.1146/annurev-cellbio-120319-114106.

Conan JO O'Brien, Ana I Domingos. An anti-obesity immunotherapy? Science. 2021 Jul 2;373(6550):24-25. https://doi.org/10.1126/science.abj5072.

Conan JO O'Brien, Ana I Domingos. Old and "hangry" monocytes turn from friend to foe under assault. Immunity. 2023 Apr 11;56(4):747-749. https://doi.org/10.1016/j.immuni.2023.03.013.

Haberman ER, Sarker G, Arús BA, Ziegler KA, Meunier S, Martínez-Sánchez N, Freibergerová E, Yilmaz-Özcan S, Fernández-González I, Zentai C, **O'Brien CJO,** Grainger DE, Sidarta-Oliveira D, Chakarov S, Raimondi A, Iannacone M, Engelhardt S, López M, Ginhoux F, Domingos AI. Immunomodulatory leptin receptor+ sympathetic perineurial barrier cells protect against obesity by facilitating brown adipose tissue thermogenesis. Immunity. 2023 Dec 5:S1074-7613(23)00488-0. doi: 10.1016/j.immuni.2023.11.006.

Appendix 2: Project contributions

This thesis was written by Conan O'Brien. All experiments were designed by Conan O'Brien and Prof Ana Domingos and performed by Conan O'Brien. Data was analysed and presented by Conan O'Brien, with help from Prof Domingos. ZGM lineage tracing experiments were done by Conan O'Brien with Pierre-Louis Loyher and Frederic Geissmann. Bulk RNA sequencing and single cell RNA sequencing experiments and analysis were performed by Conan O'Brien with Davi Oliveira-Sidarta, Mélanie Makhlouf, Eman H. AbouMoussa and Luis Saraiva.

References

1. Metchnikoff, E. (1883). Untersuchungen über die intracelluläre Verdauung bei wirbellosen Thieren (A. Hölder).
2. Gordon, S. (2016). Leading Edge BenchMarks Phagocytosis: The Legacy of Metchnikoff. Cell *166*, 1065–1068. 10.1016/j.cell.2016.08.017.
3. Tauber, A.I. (2003). Metchnikoff and the phagocytosis theory. Nat Rev Mol Cell Biol *4*, 897–901. 10.1038/NRM1244.
4. Bajgar, A., and Krejčová, G. (2023). On the origin of the functional versatility of macrophages. Front Physiol *14*. 10.3389/FPHYS.2023.1128984.
5. Rayamajhee, B., Willcox, M.D.P., Henriquez, F.L., Petsoglou, C., Subedi, D., and Carnt, N. (2022). Acanthamoeba, an environmental phagocyte enhancing survival and transmission of human pathogens. Trends Parasitol *38*, 975–990. 10.1016/J.PT.2022.08.007.
6. Siddiqui, R., Khan, N.A., and Khan, A. (2012). Acanthamoeba is an evolutionary ancestor of macrophages: A myth or reality? 10.1016/j.exppara.2011.11.005.
7. Leoni Swart, A., Harrison, C.F., Eichinger, L., Steinert, M., and Hilbi, H. (2018). Acanthamoeba and Dictyostelium as Cellular Models for Legionella Infection. Front Cell Infect Microbiol *8*. 10.3389/FCIMB.2018.00061.
8. Schuster, F.L., and Levandowsky, M. (1996). Chemosensory responses of Acanthamoeba castellanii: visual analysis of random movement and responses to chemical signals. J Eukaryot Microbiol *43*, 150–158. 10.1111/J.1550-7408.1996.TB04496.X.
9. Alsam, S., Sissons, J., Dudley, R., and Khan, N.A. (2005). Mechanisms associated with Acanthamoeba castellanii (T4) phagocytosis. Parasitol Res *96*, 402–409. 10.1007/S00436-005-1401-Z.

10. Allen, P.G., and Dawidowicz, E.A. (1990). Phagocytosis in Acanthamoeba: I. A mannose receptor is responsible for the binding and phagocytosis of yeast. J Cell Physiol *145*, 508–513. 10.1002/JCP.1041450317.

11. Oates, P.J., and Touster, O. (1980). In vitro fusion of Acanthamoeba phagolysosomes. III. Evidence that cyclic nucleotides and vacuole subpopulations respectively control the rate and the extent of vacuole fusion in Acanthamoeba homogenates. J Cell Biol *85*, 804. 10.1083/JCB.85.3.804.

12. Albuquerque, P., Nicola, A.M., Magnabosco, D.A.G., da Silveira Derengowski, L., Crisóstomo, L.S., Xavier, L.C.G., de Oliveira Frazão, S., Guilhelmelli, F., De Oliveira, M.A., do Nascimento Dias, J., et al. (2019). A hidden battle in the dirt: Soil amoebae interactions with Paracoccidioides spp. PLoS Negl Trop Dis *13*, e0007742. 10.1371/JOURNAL.PNTD.0007742.

13. Bozzaro, S. (2013). The model organism Dictyostelium discoideum. Methods Mol Biol *983*, 17–37. 10.1007/978-1-62703-302-2_2.

14. Golé, L., Rivière, C., Hayakawa, Y., and Rieu, J.P. (2011). A quorum-sensing factor in vegetative Dictyostelium discoideum cells revealed by quantitative migration analysis. PLoS One *6*. 10.1371/JOURNAL.PONE.0026901.

15. Takeda, K., Shao, D., Adler, M., Charest, P.G., Loomis, W.F., Levine, H., Groisman, A., Rappel, W.J., and Firtel, R.A. (2012). Incoherent feedforward control governs adaptation of activated ras in a eukaryotic chemotaxis pathway. Sci Signal *5*. 10.1126/SCISIGNAL.2002413.

16. Wang, C.J., Bergmann, A., Lin, B., Kim, K., and Levchenko, A. (2012). Diverse sensitivity thresholds in dynamic signaling responses by social amoebae. Sci Signal *5*. 10.1126/SCISIGNAL.2002449.

17. Dunn, J.D., Bosmani, C., Barisch, C., Raykov, L., Lefrançois, L.H., Cardenal-Muñoz, E., López-Jiménez, A.T., and Soldati, T. (2018). Eat prey, live: Dictyostelium discoideum as a model for cell-autonomous defenses. Front Immunol *8*, 1. 10.3389/FIMMU.2017.01906/FULL.

18. Chen, G., Zhuchenko, O., and Kuspa, A. (2007). Immune-like Phagocyte Activity in the Social Amoeba. Science *317*, 678. 10.1126/SCIENCE.1143991.

19. Vogel, G., Thilo, L., Schwarz, H., and Steinhart, R. (1980). Mechanism of phagocytosis in dictyostelium discoideum: phagocytosis is mediated by different recognition sites as disclosed by mutants with altered phagocytotic properties. J Cell Biol *86*, 456. 10.1083/JCB.86.2.456.

20. Musser, J.M., Schippers, K.J., Nickel, M., Mizzon, G., Kohn, A.B., Pape, C., Ronchi, P., Papadopoulos, N., Tarashansky, A.J., Hammel, J.U., et al. (2021). Profiling cellular diversity in sponges informs animal cell type and nervous system evolution. Science (1979) *374*, 717–723. 10.1126/SCIENCE.ABJ2949/SUPPL_FILE/SCIENCE.ABJ2949_DATA_S1_TO_S3.ZIP.

21. Makhijani, K., and Brückner, K. (2012). Of blood cells and the nervous system: Hematopoiesis in the Drosophila larva. Fly (Austin) *6*, 254. 10.4161/FLY.22267.

22. Tepass, U., Fessler, L.I., Aziz, A., and Hartenstein, V. (1994). Embryonic origin of hemocytes and their relationship to cell death in Drosophila. Development *120*, 1829–1837. 10.1242/DEV.120.7.1829.

23. Winkler, B., Funke, D., Benmimoun, B., Spéder, P., Rey, S., Logan, M.A., and Klämbt, C. (2021). Brain inflammation triggers macrophage invasion across the blood-brain barrier in Drosophila during pupal stages. Sci Adv *7*, 50–77. 10.1126/SCIADV.ABH0050/SUPPL_FILE/SCIADV.ABH0050_SM.PDF.

24. Cox, N., Crozet, L., Holtman, I.R., Loyher, P.-L., Lazarov, T., White, J.B., Mass, E., Stanley, E.R., Elemento, O., Glass, C.K., et al. (2021). Diet-regulated production of PDGFcc by macrophages controls energy storage. Science (1979) *373*, eabe9383. 10.1126/science.abe9383.

25. Mosser, D.M., Hamidzadeh, K., and Goncalves, R. (2020). Macrophages and the maintenance of homeostasis. Cellular & Molecular Immunology 2020 18:3 *18*, 579–587. 10.1038/s41423-020-00541-3.

26. van Furth, R., and Cohn, Z.A. (1968). THE ORIGIN AND KINETICS OF MONONUCLEAR PHAGOCYTES. J Exp Med *128*, 415. 10.1084/JEM.128.3.415.

27. Shi, C., and Pamer, E.G. (2011). Monocyte recruitment during infection and inflammation. Nature Reviews Immunology 2011 11:11 *11*, 762–774. 10.1038/nri3070.

28. Hume, D.A., Irvine, K.M., and Pridans, C. (2019). The Mononuclear Phagocyte System: The Relationship between Monocytes and Macrophages. Trends Immunol *40*, 98–112. 10.1016/J.IT.2018.11.007.

29. Lazarov, T., Juarez-Carreño, S., Cox, N., and Geissmann, F. (2023). Physiology and diseases of tissue-resident macrophages. Nature 2023 618:7966 *618*, 698–707. 10.1038/s41586-023-06002-x.

30. Wiktor-Jedrzejczak, W., Bartocci, A., Ferrante, A.W., Ahmed-Ansari, A., Sell, K.W., Pollard, J.W., and Stanley, E.R. (1990). Total absence of colony-stimulating factor 1 in the macrophage-deficient osteopetrotic (op/op) mouse. Proc Natl Acad Sci U S A *87*, 4828–4832. 10.1073/PNAS.87.12.4828.

31. Węgiel, J., Wiśniewski, H.M., Dziewiątkowski, J., Tarnawski, M., Kozielski, R., Trenkner, E., and Wiktor-Jędrzejczak, W. (1998). Reduced number and altered

morphology of microglial cells in colony stimulating factor-1-deficient osteopetrotic op/op mice. Brain Res *804*, 135–139. 10.1016/S0006-8993(98)00618-0.

32. Total Absence of Colony-Stimulating Factor 1 in the Macrophage-Deficient Osteopetrotic (op/op) Mouse on JSTOR https://www.jstor.org/stable/2354416.

33. Wiktor-Jedrzejczak, W., … M.R.-E., and 1992, undefined CSF-1 deficiency in the op/op mouse has differential effects on macrophage populations and differentiation stages. europepmc.orgW Wiktor-Jedrzejczak, MZ Ratajczak, A Ptasznik, KW Sell, A Ahmed-Ansari, W OstertagExperimental hematology, 1992•europepmc.org.

34. Wiktor-Jedrzejczak, W., Dzwigala, B., Szperl, M., Maruszynski, M., Urbanowska, E., and Szwech, P. (1996). Colony-stimulating factor 1-dependent resident macrophages play a regulatory role in fighting Escherichia coli fecal peritonitis. Infect Immun *64*, 1577–1581. 10.1128/IAI.64.5.1577-1581.1996.

35. Fogg, D.K., Sibon, C., Miled, C., Jung, S., Aucouturier, P., Littman, D.R., Cumano, A., and Geissmann, F. (2006). A clonogenic bone marrow progenitor specific for macrophages and dendritic cells. Science *311*, 83–87. 10.1126/SCIENCE.1117729.

36. Guilliams, M., Ginhoux, F., Jakubzick, C., Naik, S.H., Onai, N., Schraml, B.U., Segura, E., Tussiwand, R., and Yona, S. (2014). Dendritic cells, monocytes and macrophages: a unified nomenclature based on ontogeny. Nat Rev Immunol *14*, 571. 10.1038/NRI3712.

37. Hume, D.A. (2008). Macrophages as APC and the Dendritic Cell Myth. The Journal of Immunology *181*, 5829–5835. 10.4049/JIMMUNOL.181.9.5829.

38. Junt, T., Moseman, E.A., Iannacone, M., Massberg, S., Lang, P.A., Boes, M., Fink, K., Henrickson, S.E., Shayakhmetov, D.M., Di Paolo, N.C., et al. (2007). Subcapsular sinus macrophages in lymph nodes clear lymph-borne viruses and present them to antiviral B cells. Nature 2007 450:7166 *450*, 110–114. 10.1038/nature06287.

39. Hume, D.A., Halpin, D., Charlton, H., and Gordon, S. (1984). The mononuclear phagocyte system of the mouse defined by immunohistochemical localization of antigen F4/80: Macrophages of endocrine organs. Proc Natl Acad Sci U S A *81*, 4174–4177. 10.1073/pnas.81.13.4174.

40. Ginhoux, F., and Guilliams, M. (2016). Tissue-Resident Macrophage Ontogeny and Homeostasis. Preprint at Cell Press, 10.1016/j.immuni.2016.02.024 10.1016/j.immuni.2016.02.024.

41. Ahlback, A., and Gentek, R. (2024). Fate-Mapping Macrophages: From Ontogeny to Functions. Methods Mol Biol *2713*, 11–43. 10.1007/978-1-0716-3437-0_2/TABLES/3.

42. O'Brien, C.J.O., Haberman, E.R., and Domingos, A.I. (2021). A Tale of Three Systems: Toward a Neuroimmunoendocrine Model of Obesity. https://doi.org/10.1146/annurev-cellbio-120319-114106 *37*, 549–573. 10.1146/ANNUREV-CELLBIO-120319-114106.

43. Charles A Janeway, J., Travers, P., Walport, M., and Shlomchik, M.J. (2001). Principles of innate and adaptive immunity.

44. Satoh, T., Kidoya, H., Naito, H., Yamamoto, M., Takemura, N., Nakagawa, K., Yoshioka, Y., Morii, E., Takakura, N., Takeuchi, O., et al. (2013). Critical role of Trib1 in differentiation of tissue-resident M2-like macrophages. Nature *495*, 524–528. 10.1038/nature11930.

45. Rumianek, A.N., and Greaves, D.R. (2020). How Have Leukocyte In Vitro Chemotaxis Assays Shaped Our Ideas about Macrophage Migration? Biology (Basel) *9*, 1–13. 10.3390/BIOLOGY9120439.

46. Friedl, P., and Weigelin, B. (2008). Interstitial leukocyte migration and immune function. Nature Immunology 2008 9:9 *9*, 960–969. 10.1038/ni.f.212.

47. Barros-Becker, F., Lam, P.Y., Fisher, R., and Huttenlocher, A. (2017). Live imaging reveals distinct modes of neutrophil and macrophage migration within interstitial tissues. J Cell Sci *130*, 3801–3808. 10.1242/JCS.206128/VIDEO-7.

48. Wang, X., Iyer, A., Lyons, A.B., Körner, H., and Wei, W. (2019). Emerging roles for G-protein coupled receptors in development and activation of macrophages. Front Immunol *10*, 457996. 10.3389/FIMMU.2019.02031/BIBTEX.

49. Jeong, Y.S., and Bae, Y.S. (2020). Formyl peptide receptors in the mucosal immune system. Experimental & Molecular Medicine 2020 52:10 *52*, 1694–1704. 10.1038/s12276-020-00518-2.

50. Ahrén, B. (1999). Plasma leptin and insulin in C57BI/6J mice on a high-fat diet: Relation to subsequent changes in body weight. Acta Physiol Scand *165*, 233–240. 10.1046/j.1365-201x.1999.00518.x.

51. Maffei, M., Halaas, J., Ravussin, E., Pratley, R.E., Lee, G.H., Zhang, Y., Fei, H., Kim, S., Lallone, R., Ranganathan, S., et al. (1995). Leptin levels in human and rodent: Measurement of plasma leptin and ob RNA in obese and weight-reduced subjects. Nat Med *1*, 1155–1161. 10.1038/nm1195-1155.

52. Chen, K.-H.E., Lainez, N.M., and Coss, D. (2021). Sex Differences in Macrophage Responses to Obesity-Mediated Changes Determine Migratory and Inflammatory Traits. J Immunol *206*, 141–153. 10.4049/JIMMUNOL.2000490.

53. Li, D., and Wu, M. (2021). Pattern recognition receptors in health and diseases. Signal Transduct Target Ther *6*. 10.1038/S41392-021-00687-0.

54. Li, P., and Chang, M. (2021). Roles of PRR-Mediated Signaling Pathways in the Regulation of Oxidative Stress and Inflammatory Diseases. Int J Mol Sci *22*. 10.3390/IJMS22147688.

55. Brubaker, S.W., Bonham, K.S., Zanoni, I., and Kagan, J.C. (2015). Innate immune pattern recognition: a cell biological perspective. Annu Rev Immunol *33*, 257–290. 10.1146/ANNUREV-IMMUNOL-032414-112240.

56. Moretti, J., and Blander, J.M. (2014). Insights into phagocytosis-coupled activation of Pattern Recognition Receptors and Inflammasomes. Curr Opin Immunol *0*, 100. 10.1016/J.COI.2013.11.003.

57. Mukhopadhyay, S., Plüddemann, A., and Gordon, S. (2009). Macrophage pattern recognition receptors in immunity, homeostasis and self tolerance. Adv Exp Med Biol *653*, 1–14. 10.1007/978-1-4419-0901-5_1.

58. Anderson, K. V., Bokla, L., and Nüsslein-Volhard, C. (1985). Establishment of dorsal-ventral polarity in the Drosophila embryo: the induction of polarity by the Toll gene product. Cell *42*, 791–798. 10.1016/0092-8674(85)90275-2.

59. O'Neill, L.A.J., Golenbock, D., and Bowie, A.G. (2013). The history of Toll-like receptors — redefining innate immunity. Nature Reviews Immunology 2013 13:6 *13*, 453–460. 10.1038/nri3446.

60. Gay, N.J., and Keith, F.J. (1991). Drosophila Toll and IL-1 receptor. Nature *351*, 355–356. 10.1038/351355B0.

61. Lemaitre, B., Nicolas, E., Michaut, L., Reichhart, J.M., and Hoffmann, J.A. (1996). The dorsoventral regulatory gene cassette spätzle/Toll/cactus controls the potent antifungal response in Drosophila adults. Cell *86*, 973–983. 10.1016/S0092-8674(00)80172-5.

62. Medzhitov, R., Preston-Hurlburt, P., and Janeway, C.A. (1997). A human homologue of the Drosophila Toll protein signals activation of adaptive immunity. Nature *388*, 394–397. 10.1038/41131.

63. Saberi, M., Woods, N.B., de Luca, C., Schenk, S., Lu, J.C., Bandyopadhyay, G., Verma, I.M., and Olefsky, J.M. (2009). Hematopoietic Cell-Specific Deletion of Toll-like Receptor 4 Ameliorates Hepatic and Adipose Tissue Insulin Resistance in High-Fat-Fed Mice. Cell Metab *10*, 419–429. 10.1016/j.cmet.2009.09.006.

64. Orr, J.S., Puglisi, M.J., Ellacott, K.L.J., Lumeng, C.N., Wasserman, D.H., and Hasty, A.H. (2012). Toll-like receptor 4 deficiency promotes the alternative activation of adipose tissue macrophages. Diabetes *61*, 2718–2727. 10.2337/db11-1595.

65. Pashenkov, M. V., Dagil, Y.A., and Pinegin, B. V. (2018). NOD1 and NOD2: Molecular targets in prevention and treatment of infectious diseases. Int Immunopharmacol *54*, 385–400. 10.1016/J.INTIMP.2017.11.036.

66. Chamaillard, M., Hashimoto, M., Horie, Y., Masumoto, J., Qiu, S., Saab, L., Ogura, Y., Kawasaki, A., Fukase, K., Kusumoto, S., et al. (2003). An essential role for NOD1 in host recognition of bacterial peptidoglycan containing diaminopimelic acid. Nat Immunol *4*, 702–707. 10.1038/NI945.

67. Girardin, S.E., Boneca, I.G., Viala, J., Chamaillard, M., Labigne, A., Thomas, G., Philpott, D.J., and Sansonetti, P.J. (2003). Nod2 is a general sensor of peptidoglycan through muramyl dipeptide (MDP) detection. J Biol Chem *278*, 8869–8872. 10.1074/JBC.C200651200.

68. Heim, V.J., Stafford, C.A., and Nachbur, U. (2019). NOD Signaling and Cell Death. Front Cell Dev Biol *7*, 208. 10.3389/FCELL.2019.00208.

69. Gee, P., Chua, P.K., Gevorkyan, J., Klumpp, K., Najera, I., Swinney, D.C., and Deval, J. (2008). Essential role of the N-terminal domain in the regulation of RIG-I ATPase activity. J Biol Chem *283*, 9488–9496. 10.1074/JBC.M706777200.

70. Kowalinski, E., Lunardi, T., McCarthy, A.A., Louber, J., Brunel, J., Grigorov, B., Gerlier, D., and Cusack, S. (2011). Structural basis for the activation of innate immune

pattern-recognition receptor RIG-I by viral RNA. Cell *147*, 423–435. 10.1016/J.CELL.2011.09.039.

71. Cui, S., Eisenächer, K., Kirchhofer, A., Brzózka, K., Lammens, A., Lammens, K., Fujita, T., Conzelmann, K.K., Krug, A., and Hopfner, K.P. (2008). The C-terminal regulatory domain is the RNA 5'-triphosphate sensor of RIG-I. Mol Cell *29*, 169–179. 10.1016/J.MOLCEL.2007.10.032.

72. Yoneyama, M., Kikuchi, M., Natsukawa, T., Shinobu, N., Imaizumi, T., Miyagishi, M., Taira, K., Akira, S., and Fujita, T. (2004). The RNA helicase RIG-I has an essential function in double-stranded RNA-induced innate antiviral responses. Nat Immunol *5*, 730–737. 10.1038/NI1087.

73. Patel, J.R., Jain, A., Chou, Y.Y., Baum, A., Ha, T., and García-Sastre, A. (2013). ATPase-driven oligomerization of RIG-I on RNA allows optimal activation of type-I interferon. EMBO Rep *14*, 780. 10.1038/EMBOR.2013.102.

74. Fan, X., and Jin, T. (2019). Structures of RIG-I-Like Receptors and Insights into Viral RNA Sensing. Adv Exp Med Biol *1172*, 157–188. 10.1007/978-981-13-9367-9_8.

75. Ebner, S., Sharon, N., and Ben-Tal, N. (2003). Evolutionary analysis reveals collective properties and specificity in the C-type lectin and lectin-like domain superfamily. Proteins *53*, 44–55. 10.1002/PROT.10440.

76. Sancho, D., and Reis e Sousa, C. (2012). Signaling by myeloid C-type lectin receptors in immunity and homeostasis. Annu Rev Immunol *30*, 491–529. 10.1146/ANNUREV-IMMUNOL-031210-101352.

77. Brown, G.D., Willment, J.A., and Whitehead, L. (2018). C-type lectins in immunity and homeostasis. Nature Reviews Immunology 2018 18:6 *18*, 374–389. 10.1038/s41577-018-0004-8.

78. van Lookeren Campagne, M., Wiesmann, C., and Brown, E.J. (2007). Macrophage complement receptors and pathogen clearance. Cell Microbiol *9*, 2095–2102. 10.1111/J.1462-5822.2007.00981.X.

79. Underhill, D.M., and Ozinsky, A. (2003). Phagocytosis of Microbes: Complexity in Action. https://doi.org/10.1146/annurev.immunol.20.103001.114744 *20*, 825–852. 10.1146/ANNUREV.IMMUNOL.20.103001.114744.

80. Mkaddem, S. Ben, Benhamou, M., and Monteiro, R.C. (2019). Understanding Fc receptor involvement in inflammatory diseases: From mechanisms to new therapeutic tools. Front Immunol *10*, 445798. 10.3389/FIMMU.2019.00811/BIBTEX.

81. Helmy, K.Y., Katschke, K.J., Gorgani, N.N., Kljavin, N.M., Elliott, J.M., Diehl, L., Scales, S.J., Ghilardi, N., and Van Lookeren Campagne, M. (2006). CRIg: A macrophage complement receptor required for phagocytosis of circulating pathogens. Cell *124*, 915–927. 10.1016/j.cell.2005.12.039.

82. Podinovskaia, M., VanderVen, B.C., Yates, R.M., Glennie, S., Fullerton, D., Mwandumba, H.C., and Russell, D.G. (2013). Dynamic quantitative assays of phagosomal function. Curr Protoc Immunol. 10.1002/0471142735.IM1434S102.

83. Uribe-Querol, E., and Rosales, C. (2020). Phagocytosis: Our Current Understanding of a Universal Biological Process. Front Immunol *11*, 531655. 10.3389/FIMMU.2020.01066/BIBTEX.

84. Gordon, S. (2016). Phagocytosis: An Immunobiologic Process. Immunity *44*, 463–475. 10.1016/J.IMMUNI.2016.02.026.

85. Kinchen, J.M., and Ravichandran, K.S. (2008). Phagosome maturation: going through the acid test. Nature Reviews Molecular Cell Biology 2008 9:10 *9*, 781–795. 10.1038/nrm2515.

86. Kapellos, T.S., Taylor, L., Lee, H., Cowley, S.A., James, W.S., Iqbal, A.J., and Greaves, D.R. (2016). A novel real time imaging platform to quantify macrophage phagocytosis. Biochem Pharmacol *116*, 107–119. 10.1016/J.BCP.2016.07.011.

87. Hu, K., Li, Y., Rotenberg, S.A., Amatore, C., and Mirkin, M. V. (2019). Electrochemical Measurements of Reactive Oxygen and Nitrogen Species inside Single Phagolysosomes of Living Macrophages. J Am Chem Soc *141*, 4564–4568. 10.1021/JACS.9B01217/SUPPL_FILE/JA9B01217_SI_001.PDF.

88. Laskin, D.L. (2009). Macrophages and Inflammatory Mediators in Chemical Toxicity: A Battle of Forces. Chem Res Toxicol *22*, 1376. 10.1021/TX900086V.

89. Martinez, F.O., and Gordon, S. (2014). The M1 and M2 paradigm of macrophage activation: time for reassessment. F1000Prime Rep *6*. 10.12703/P6-13.

90. Kratz, M., Coats, B.R., Hisert, K.B., Hagman, D., Mutskov, V., Peris, E., Schoenfelt, K.Q., Kuzma, J.N., Larson, I., Billing, P.S., et al. (2014). Metabolic dysfunction drives a mechanistically distinct proinflammatory phenotype in adipose tissue macrophages. Cell Metab *20*, 614–625. 10.1016/j.cmet.2014.08.010.

91. Van Ginderachter, J.A., Movahedi, K., Hassanzadeh Ghassabeh, G., Meerschaut, S., Beschin, A., Raes, G., and De Baetselier, P. (2006). Classical and alternative activation of mononuclear phagocytes: Picking the best of both worlds for tumor promotion. Immunobiology *211*, 487–501. 10.1016/J.IMBIO.2006.06.002.

92. Edwards, J.P., Zhang, X., Frauwirth, K.A., and Mosser, D.M. (2006). Biochemical and functional characterization of three activated macrophage populations. J Leukoc Biol *80*, 1298. 10.1189/JLB.0406249.

93. Zheng, D., Liwinski, T., and Elinav, E. (2020). Inflammasome activation and regulation: toward a better understanding of complex mechanisms. Cell Discovery 2020 6:1 *6*, 1–22. 10.1038/s41421-020-0167-x.

94. Cerretti, D.P., Kozlosky, C.J., Mosley, B., Nelson, N., Van Ness, K., Greenstreet, T.A., March, C.J., Kronheim, S.R., Druck, T., Cannizzaro, L.A., et al. (1992). Molecular cloning of the interleukin-1 beta converting enzyme. Science *256*, 97–100. 10.1126/SCIENCE.1373520.

95. Vural, A., Nabar, N.R., Hwang, I.-Y., Sohn, S., Park, C., Karlsson, M.C.I., Blumer, J.B., and Kehrl, J.H. (2019). Gαi2 Signaling Regulates Inflammasome Priming and Cytokine Production by Biasing Macrophage Phenotype Determination. J Immunol *202*, 1510–1520. 10.4049/JIMMUNOL.1801145.

96. Austyn, J.M., and Gordon, S. (1981). F4/80, a monoclonal antibody directed specifically against the mouse macrophage. Eur J Immunol *11*, 805–815. 10.1002/EJI.1830111013.

97. Lin, H.H., Faunce, D.E., Stacey, M., Terajewicz, A., Nakamura, T., Zhang-Hoover, J., Kerley, M., Mucenski, M.L., Gordon, S., and Stein-Streilein, J. (2005). The macrophage F4/80 receptor is required for the induction of antigen-specific efferent regulatory T cells in peripheral tolerance. J Exp Med *201*, 1615–1625. 10.1084/JEM.20042307.

98. Taylor, M.D., Harris, A., Nair, M.G., Maizels, R.M., and Allen, J.E. (2006). F4/80+ Alternatively Activated Macrophages Control CD4+ T Cell Hyporesponsiveness at Sites Peripheral to Filarial Infection. The Journal of Immunology *176*, 6918–6927. 10.4049/JIMMUNOL.176.11.6918.

99. Rodríguez-Prados, J.-C., Través, P.G., Cuenca, J., Rico, D., Aragonés, J., Martín-Sanz, P., Cascante, M., and Boscá, L. (2010). Substrate fate in activated macrophages: a comparison between innate, classic, and alternative activation. J Immunol *185*, 605–614. 10.4049/JIMMUNOL.0901698.

100. Freemerman, A.J., Johnson, A.R., Sacks, G.N., Milner, J.J., Kirk, E.L., Troester, M.A., Macintyre, A.N., Goraksha-Hicks, P., Rathmell, J.C., and Makowski, L. (2014). Metabolic reprogramming of macrophages: glucose transporter 1 (GLUT1)-mediated glucose metabolism drives a proinflammatory phenotype. J Biol Chem *289*, 7884–7896. 10.1074/JBC.M113.522037.

101. Tannahill, G.M., Curtis, A.M., Adamik, J., Palsson-Mcdermott, E.M., McGettrick, A.F., Goel, G., Frezza, C., Bernard, N.J., Kelly, B., Foley, N.H., et al. (2013). Succinate is an inflammatory signal that induces IL-1β through HIF-1α. Nature *496*, 238–242. 10.1038/NATURE11986.

102. Wang, F., Zhang, S., Vuckovic, I., Jeon, R., Lerman, A., Folmes, C.D., Dzeja, P.P., and Herrmann, J. (2018). Glycolytic Stimulation Is Not a Requirement for M2 Macrophage Differentiation. Cell Metab *28*, 463-475.e4. 10.1016/J.CMET.2018.08.012.

103. Huang, S.C.C., Everts, B., Ivanova, Y., O'Sullivan, D., Nascimento, M., Smith, A.M., Beatty, W., Love-Gregory, L., Lam, W.Y., O'Neill, C.M., et al. (2014). Cell-intrinsic lysosomal lipolysis is essential for alternative activation of macrophages. Nat Immunol *15*, 846–855. 10.1038/NI.2956.

104. Takeda, N., O'Dea, E.L., Doedens, A., Kim, J.W., Weidemann, A., Stockmann, C., Asagiri, M., Simon, M.C., Hoffmann, A., and Johnson, R.S. (2010). Differential activation and antagonistic function of HIF-{alpha} isoforms in macrophages are essential for NO homeostasis. Genes Dev *24*, 491–501. 10.1101/GAD.1881410.

105. MANTOVANI, A., SICA, A., SOZZANI, S., ALLAVENA, P., VECCHI, A., and LOCATI, M. (2004). The chemokine system in diverse forms of macrophage activation and polarization. Trends Immunol *25*, 677–686. 10.1016/j.it.2004.09.015.

106. Gordon, S., and Plüddemann, A. (2017). Tissue macrophages: heterogeneity and functions. BMC Biology 2017 15:1 *15*, 1–18. 10.1186/S12915-017-0392-4.

107. Teitelbaum, S.L. (2000). Bone resorption by osteoclasts. Science (1979) *289*, 1504–1508. 10.1126/SCIENCE.289.5484.1504/ASSET/7F1E58BF-C087-4C6F-9C06-C190FE05FFD3/ASSETS/GRAPHIC/SE3408789003.JPEG.

108. Blair, H.C., Teitelbaum, S.L., Ghiselli, R., and Gluck, S. (1989). Osteoclastic Bone Resorption by a Polarized Vacuolar Proton Pump. Science (1979) *245*, 855–857. 10.1126/SCIENCE.2528207.

109. Gowen, M., Lazner, F., Dodds, R., Kapadia, R., Feild, J., Tavaria, M., Bertoncello, I., Drake, F., Zavarselk, S., Tellis, I., et al. (1999). Cathepsin K Knockout Mice Develop Osteopetrosis Due to a Deficit in Matrix Degradation but Not Demineralization. Journal of Bone and Mineral Research *14*, 1654–1663. 10.1359/JBMR.1999.14.10.1654.

110. Squarzoni, P., Oller, G., Hoeffel, G., Pont-Lezica, L., Rostaing, P., Low, D., Bessis, A., Ginhoux, F., and Garel, S. (2014). Microglia modulate wiring of the embryonic forebrain. Cell Rep *8*, 1271–1279. 10.1016/J.CELREP.2014.07.042.

111. Schafer, D., Lehrman, E., Kautzman, A., Koyama, R., Mardinly, A., Yamasaki, R., Ransohoff, R., Greenberg, M., Barres, B., and Stevens, B. (2012). Microglia sculpt postnatal neural circuits in an activity and complement-dependent manner. Neuron *74*, 691–705. 10.1016/J.NEURON.2012.03.026.

112. Hulsmans, M., Clauss, S., Xiao, L., Aguirre, A.D., King, K.R., Hanley, A., Hucker, W.J., Wülfers, E.M., Seemann, G., Courties, G., et al. (2017). Macrophages Facilitate Electrical Conduction in the Heart. Cell *169*, 510-522.e20. 10.1016/j.cell.2017.03.050.

113. Simões, F.C., Cahill, T.J., Kenyon, A., Gavriouchkina, D., Vieira, J.M., Sun, X., Pezzolla, D., Ravaud, C., Masmanian, E., Weinberger, M., et al. (2020). Macrophages

directly contribute collagen to scar formation during zebrafish heart regeneration and mouse heart repair. Nature Communications 2020 11:1 *11*, 1–17. 10.1038/s41467-019-14263-2.

114. Jones, C. V., Williams, T.M., Walker, K.A., Dickinson, H., Sakkal, S., Rumballe, B.A., Little, M.H., Jenkin, G., and Ricardo, S.D. (2013). M2 macrophage polarisation is associated with alveolar formation during postnatal lung development. Respir Res *14*, 1–15. 10.1186/1465-9921-14-41/FIGURES/5.

115. Muller, P.A., Koscsó, B., Rajani, G.M., Stevanovic, K., Berres, M.-L., Hashimoto, D., Mortha, A., Leboeuf, M., Li, X.-M., Mucida, D., et al. (2014). Crosstalk between Muscularis Macrophages and Enteric Neurons Regulates Gastrointestinal Motility. Cell *158*, 300–313. 10.1016/J.CELL.2014.04.050.

116. Theurl, I., Hilgendorf, I., Nairz, M., Tymoszuk, P., Haschka, D., Asshoff, M., He, S., Gerhardt, L.M.S., Holderried, T.A.W., Seifert, M., et al. (2016). On-demand erythrocyte disposal and iron recycling requires transient macrophages in the liver. Nature Medicine 2016 22:8 *22*, 945–951. 10.1038/nm.4146.

117. Willekens, F.L.A., Werre, J.M., Kruijt, J.K., Roerdinkholder-Stoelwinder, B., Groenen-Döpp, Y.A.M., van den Bos, A.G., Bosman, G.J.C.G.M., and van Berkel, T.J.C. (2005). Liver Kupffer cells rapidly remove red blood cell–derived vesicles from the circulation by scavenger receptors. Blood *105*, 2141–2145. 10.1182/BLOOD-2004-04-1578.

118. Pirzgalska, R.M., Seixas, E., Seidman, J.S., Link, V.M., Sánchez, N.M., Mahú, I., Mendes, R., Gres, V., Kubasova, N., Morris, I., et al. (2017). Sympathetic neuron-associated macrophages contribute to obesity by importing and metabolizing norepinephrine. Nat Med *23*, 1309–1318. 10.1038/nm.4422.

119. O'Brien, C.J.O., and Domingos, A. (2021). An anti-obesity immunotherapy? Science (1979) *373*, 24–25. 10.1126/SCIENCE.ABJ5072.

120. Safaiyan, S., Kannaiyan, N., Snaidero, N., Brioschi, S., Biber, K., Yona, S., Edinger, A.L., Jung, S., Rossner, M.J., and Simons, M. (2016). Age-related myelin degradation burdens the clearance function of microglia during aging. Nat Neurosci *19*, 995–998. 10.1038/NN.4325.

121. Lucin, K.M., O'Brien, C.E., Bieri, G., Czirr, E., Mosher, K.I., Abbey, R.J., Mastroeni, D.F., Rogers, J., Spencer, B., Masliah, E., et al. (2013). Microglial beclin 1 regulates retromer trafficking and phagocytosis and is impaired in Alzheimer's disease. Neuron *79*, 873–886. 10.1016/J.NEURON.2013.06.046.

122. Sims, R., Van Der Lee, S.J., Naj, A.C., Bellenguez, C., Badarinarayan, N., Jakobsdottir, J., Kunkle, B.W., Boland, A., Raybould, R., Bis, J.C., et al. (2017). Rare coding variants in PLCG2, ABI3 and TREM2 implicate microglial-mediated innate immunity in Alzheimer's disease. Nat Genet *49*, 1373. 10.1038/NG.3916.

123. Silvin, A., Uderhardt, S., Piot, C., Da Mesquita, S., Yang, K., Geirsdottir, L., Mulder, K., Eyal, D., Liu, Z., Bridlance, C., et al. (2022). Dual ontogeny of disease-associated microglia and disease inflammatory macrophages in aging and neurodegeneration. Immunity *55*, 1448-1465.e6. 10.1016/J.IMMUNI.2022.07.004.

124. Kurowska-Stolarska, M., and Alivernini, S. (2022). Synovial tissue macrophages in joint homeostasis, rheumatoid arthritis and disease remission. Nature Reviews Rheumatology 2022 18:7 *18*, 384–397. 10.1038/s41584-022-00790-8.

125. Misharin, A. V., Cuda, C.M., Saber, R., Turner, J.D., Gierut, A.K., Kenneth Haines, G.K., Berdnikovs, S., Filer, A., Clark, A.R., Buckley, C.D., et al. (2014). Nonclassical Ly6C- monocytes drive the development of inflammatory arthritis in mice. Cell Rep *9*, 591–604. 10.1016/j.celrep.2014.09.032.

126. Alivernini, S., MacDonald, L., Elmesmari, A., Finlay, S., Tolusso, B., Gigante, M.R., Petricca, L., Di Mario, C., Bui, L., Perniola, S., et al. (2020). Distinct synovial tissue macrophage subsets regulate inflammation and remission in rheumatoid arthritis. Nature Medicine 2020 26:8 *26*, 1295–1306. 10.1038/s41591-020-0939-8.

127. Manara, M., and Sinigaglia, L. (2015). Bone and TNF in rheumatoid arthritis: clinical implications. RMD Open *1*, e000065. 10.1136/RMDOPEN-2015-000065.

128. Lumeng, C.N., Bodzin, J.L., and Saltiel, A.R. (2007). Obesity induces a phenotypic switch in adipose tissue macrophage polarization. J Clin Invest *117*, 175–184. 10.1172/JCI29881.

129. Weisberg, S.P., McCann, D., Desai, M., Rosenbaum, M., Leibel, R.L., and Ferrante, A.W. (2003). Obesity is associated with macrophage accumulation in adipose tissue. J Clin Invest *112*, 1796–1808. 10.1172/JCI19246.

130. Hotamisligil, G.S., Shargill, N.S., and Spiegelman, B.M. (1993). Adipose expression of tumor necrosis factor-α: Direct role in obesity-linked insulin resistance. Science (1979) *259*, 87–91. 10.1126/science.7678183.

131. Fain, J.N., Madan, A.K., Hiler, M.L., Cheema, P., and Bahouth, S.W. (2004). Comparison of the Release of Adipokines by Adipose Tissue, Adipose Tissue Matrix, and Adipocytes from Visceral and Subcutaneous Abdominal Adipose Tissues of Obese Humans. Endocrinology *145*, 2273–2282. 10.1210/en.2003-1336.

132. Kamei, N., Tobe, K., Suzuki, R., Ohsugi, M., Watanabe, T., Kubota, N., Ohtsuka-Kowatari, N., Kumagai, K., Sakamoto, K., Kobayashi, M., et al. (2006). Overexpression of monocyte chemoattractant protein-1 in adipose tissues causes macrophage recruitment and insulin resistance. Journal of Biological Chemistry *281*, 26602–26614. 10.1074/jbc.M601284200.

133. Merad, M., and Martin, J.C. (2020). Author Correction: Pathological inflammation in patients with COVID-19: a key role for monocytes and macrophages (Nature Reviews Immunology, (2020), 20, 6, (355-362), 10.1038/s41577-020-0331-4). Nat Rev Immunol *20*, 448. 10.1038/S41577-020-0353-Y.

134. Chen, S.T., Park, M.D., Del Valle, D.M., Buckup, M., Tabachnikova, A., Thompson, R.C., Simons, N.W., Mouskas, K., Lee, B., Geanon, D., et al. (2022). A shift in lung macrophage composition is associated with COVID-19 severity and recovery. Sci Transl Med *14*, 5168. 10.1126/SCITRANSLMED.ABN5168/SUPPL_FILE/SCITRANSLMED.ABN5168_MDAR_REPRODUCIBILITY_CHECKLIST.PDF.

135. Sefik, E., Qu, R., Junqueira, C., Kaffe, E., Mirza, H., Zhao, J., Brewer, J.R., Han, A., Steach, H.R., Israelow, B., et al. (2022). Inflammasome activation in infected macrophages drives COVID-19 pathology. Nature 2022 606:7914 *606*, 585–593. 10.1038/s41586-022-04802-1.

136. Murray, P.J., and Smale, S.T. (2012). Restraint of inflammatory signaling by interdependent strata of negative regulatory pathways. Nat Immunol *13*, 916–924. 10.1038/NI.2391.

137. Jones, G.R., Bain, C.C., Fenton, T.M., Kelly, A., Brown, S.L., Ivens, A.C., Travis, M.A., Cook, P.C., and MacDonald, A.S. (2018). Dynamics of colon monocyte and macrophage activation during colitis. Front Immunol *9*, 2764. 10.3389/FIMMU.2018.02764/FULL.

138. Smith, A.M., Rahman, F.Z., Hayee, B., Graham, S.J., Marks, D.J.B., Sewell, G.W., Palmer, C.D., Wilde, J., Foxwell, B.M.J., Gloger, I.S., et al. (2009). Disordered macrophage cytokine secretion underlies impaired acute inflammation and bacterial clearance in Crohn's disease. J Exp Med *206*, 1883–1897. 10.1084/JEM.20091233.

139. Kumari, N., and Choi, S.H. (2022). Tumor-associated macrophages in cancer: recent advancements in cancer nanoimmunotherapies. Journal of Experimental & Clinical Cancer Research 2022 41:1 *41*, 1–39. 10.1186/S13046-022-02272-X.

140. Lin, Y., Xu, J., and Lan, H. (2019). Tumor-associated macrophages in tumor metastasis: biological roles and clinical therapeutic applications. Journal of Hematology & Oncology 2019 12:1 *12*, 1–16. 10.1186/S13045-019-0760-3.

141. Su, S., Liu, Q., Chen, J., Chen, J., Chen, F., He, C., Huang, D., Wu, W., Lin, L., Huang, W., et al. (2014). A Positive feedback loop between mesenchymal-like cancer cells and macrophages is essential to breast cancer metastasis. Cancer Cell *25*, 605–620. 10.1016/j.ccr.2014.03.021.

142. Lindsten, T., Hedbrant, A., Ramberg, A., Wijkander, J., Solterbeck, A., Eriksson, M., Delbro, D., and Erlandsson, A. (2017). Effect of macrophages on breast cancer cell proliferation, and on expression of hormone receptors, uPAR and HER-2. Int J Oncol *51*, 104–114. 10.3892/IJO.2017.3996.

143. Arima, K., Komohara, Y., Bu, L., Tsukamoto, M., Itoyama, R., Miyake, K., Uchihara, T., Ogata, Y., Nakagawa, S., Okabe, H., et al. (2018). Downregulation of 15-hydroxyprostaglandin dehydrogenase by interleukin-1β from activated macrophages leads to poor prognosis in pancreatic cancer. Cancer Sci *109*, 462–470. 10.1111/CAS.13467.

144. Glass, C.K., and Witztum, J.L. (2001). Atherosclerosis: The Road Ahead. Cell *104*, 503–516. 10.1016/S0092-8674(01)00238-0.

145. Skålén, K., Gustafsson, M., Rydberg, E.K., Hultén, L.M., Wiklund, O., Innerarity, T.L., and Borén, J. (2002). Subendothelial retention of atherogenic lipoproteins in early atherosclerosis. Nature *417*, 750–754. 10.1038/nature00804.

146. Zernecke, A., Shagdarsuren, E., and Weber, C. (2008). Chemokines in atherosclerosis: an update. Arterioscler Thromb Vasc Biol *28*, 1897–1908. 10.1161/ATVBAHA.107.161174.

147. Kunjathoor, V. V, Febbraio, M., Podrez, E.A., Moore, K.J., Andersson, L., Koehn, S., Rhee, J.S., Silverstein, R., Hoff, H.F., and Freeman, M.W. (2002). Scavenger receptors class A-I/II and CD36 are the principal receptors responsible for the uptake of modified low density lipoprotein leading to lipid loading in macrophages. J Biol Chem *277*, 49982–49988. 10.1074/jbc.M209649200.

148. Boring, L., Gosling, J., Cleary, M., and Charo, I.F. (1998). Decreased lesion formation in CCR2-/- mice reveals a role for chemokines in the initiation of atherosclerosis. Nature *394*, 894–897. 10.1038/29788.

149. Landsman, L., Liat, B.O., Zernecke, A., Kim, K.W., Krauthgamer, R., Shagdarsuren, E., Lira, S.A., Weissman, I.L., Weber, C., and Jung, S. (2009). CX3CR1 is required for monocyte homeostasis and atherogenesis by promoting cell survival. Blood *113*, 963–972. 10.1182/BLOOD-2008-07-170787.

150. Combadière, C., Potteaux, S., Rodero, M., Simon, T., Pezard, A., Esposito, B., Merval, R., Proudfoot, A., Tedgui, A., and Mallat, Z. (2008). Combined inhibition of CCL2, CX3CR1, and CCR5 abrogates Ly6C(hi) and Ly6C(lo) monocytosis and almost abolishes atherosclerosis in hypercholesterolemic mice. Circulation *117*, 1649–1657. 10.1161/CIRCULATIONAHA.107.745091.

151. Song, Y., Liu, J., Zhao, K., Gao, L., and Zhao, J. (2021). Cholesterol-induced toxicity: An integrated view of the role of cholesterol in multiple diseases. Cell Metab *33*, 1911–1925. 10.1016/J.CMET.2021.09.001.

152. Warner, G.J., Stoudt, G., Bamberger, M., Johnson, W.J., and Rothblat, G.H. (1995). Cell toxicity induced by inhibition of acyl coenzyme A:cholesterol acyltransferase and

accumulation of unesterified cholesterol. J Biol Chem *270*, 5772–5778. 10.1074/JBC.270.11.5772.

153. Meiner, V.L., Cases, S., Myers, H.M., Sande, E.R., Bellosta, S., Schambelan, M., Pitas, R.E., Mcguire, J., Herzu, J., and Farese, R. V. (1996). Disruption of the acyl-CoA:cholesterol acyltransferase gene in mice: Evidence suggesting multiple cholesterol esterification enzymes in mammals. Proc Natl Acad Sci U S A *93*, 14041–14046. 10.1073/PNAS.93.24.14041/ASSET/34C99714-4B8A-4745-9729-B1015EC7CF35/ASSETS/GRAPHIC/PQ2362745004.JPEG.

154. Warner, G.J., Stoudt, G., Bamberger, M., Johnson, W.J., and Rothblat, G.H. (1995). Cell toxicity induced by inhibition of acyl coenzyme A:cholesterol acyltransferase and accumulation of unesterified cholesterol. Journal of Biological Chemistry *270*, 5772–5778. 10.1074/jbc.270.11.5772.

155. Chistiakov, D.A., Bobryshev, Y. V., and Orekhov, A.N. (2016). Macrophage-mediated cholesterol handling in atherosclerosis. J Cell Mol Med *20*, 17. 10.1111/JCMM.12689.

156. Kruth, H.S. (2013). Fluid-Phase Pinocytosis of LDL by Macrophages: A Novel Target to Reduce Macrophage Cholesterol Accumulation in Atherosclerotic Lesions. Curr Pharm Des *19*, 5865. 10.2174/1381612811319330005.

157. Remmerie, A., and Scott, C.L. (2018). Macrophages and lipid metabolism. Cell Immunol *330*, 27. 10.1016/J.CELLIMM.2018.01.020.

158. Klappacher, G.W., and Glass, C.K. (2002). Roles of peroxisome proliferator-activated receptor gamma in lipid homeostasis and inflammatory responses of macrophages. Curr Opin Lipidol *13*, 305–312. 10.1097/00041433-200206000-00011.

159. Kruth, H.S., Huang, W., Ishii, I., and Zhang, W.Y. (2002). Macrophage foam cell formation with native low density lipoprotein. J Biol Chem *277*, 34573–34580. 10.1074/JBC.M205059200.

160. Phillips, M.C. (2014). Molecular Mechanisms of Cellular Cholesterol Efflux. J Biol Chem *289*, 24020. 10.1074/JBC.R114.583658.

161. Chen, W., Sun, Y., Welch, C., Gorelik, A., Leventhal, A.R., Tabas, I., and Tall, A.R. (2001). Preferential ATP-binding cassette transporter A1-mediated cholesterol efflux from late endosomes/lysosomes. J Biol Chem *276*, 43564–43569. 10.1074/JBC.M107938200.

162. Yancey, P.G., Bortnick, A.E., Kellner-Weibel, G., De la Llera-Moya, M., Phillips, M.C., and Rothblat, G.H. (2003). Importance of Different Pathways of Cellular Cholesterol Efflux. Arterioscler Thromb Vasc Biol *23*, 712–719. 10.1161/01.ATV.0000057572.97137.DD.

163. Vegiopoulos, A., and Herzig, S. (2007). Glucocorticoids, metabolism and metabolic diseases. Mol Cell Endocrinol *275*, 43–61. 10.1016/J.MCE.2007.05.015.

164. Korte, S.M. (2001). Corticosteroids in relation to fear, anxiety and psychopathology. Neurosci Biobehav Rev *25*, 117–142. 10.1016/S0149-7634(01)00002-1.

165. Lightman, S.L. (2008). The Neuroendocrinology of Stress: A Never Ending Story. J Neuroendocrinol *20*, 880–884. 10.1111/J.1365-2826.2008.01711.X.

166. Hall, J.E., do Carmo, J.M., da Silva, A.A., Wang, Z., and Hall, M.E. (2015). Obesity-induced hypertension: interaction of neurohumoral and renal mechanisms. Circ Res *116*, 991–1006. 10.1161/CIRCRESAHA.116.305697.

167. Cruz-Topete, D., and Cidlowski, J.A. (2014). One Hormone, Two Actions: Anti- and Pro-Inflammatory Effects of Glucocorticoids. Neuroimmunomodulation *22*, 20–32. 10.1159/000362724.

168. Xing, Y., Lerario, A.M., Rainey, W., and Hammer, G.D. (2015). Development of Adrenal Cortex Zonation. Endocrinol Metab Clin North Am *44*, 243. 10.1016/J.ECL.2015.02.001.

169. Luo, X., Ikeda, Y., and Parker, K.L. (1994). A cell-specific nuclear receptor is essential for adrenal and gonadal development and sexual differentiation. Cell *77*, 481–490. 10.1016/0092-8674(94)90211-9.

170. Hatano, O., Takakusu, A., Nomura, M., and Morohashi, K.I. (1996). Identical origin of adrenal cortex and gonad revealed by expression profiles of Ad4BP/SF-1. Genes Cells *1*, 663–671. 10.1046/J.1365-2443.1996.00254.X.

171. Neirijnck, Y., Sararols, P., Kühne, F., Mayère, C., Weerasinghe Arachchige, L.C., Regard, V., Nef, S., and Schedl, A. (2023). Single-cell transcriptomic profiling redefines the origin and specification of early adrenogonadal progenitors. Cell Rep *42*. 10.1016/J.CELREP.2023.112191.

172. Anderson, D.J., and Axel, R. (1986). A bipotential neuroendocrine precursor whose choice of cell fate is determined by NGF and glucocorticoids. Cell *47*, 1079–1090. 10.1016/0092-8674(86)90823-8.

173. Keegan, C.E., and Hammer, G.D. (2002). Recent insights into organogenesis of the adrenal cortex. Trends Endocrinol Metab *13*, 200–208. 10.1016/S1043-2760(02)00602-1.

174. Bandiera, R., Vidal, V.P.I., Motamedi, F.J., Clarkson, M., Sahut-Barnola, I., vonGise, A., Pu, W.T., Hohenstein, P., Martinez, A., and Schedl, A. (2013). WT1 maintains adrenal-gonadal-primordium (AGP) identity and marks a novel population of AGP-like progenitors within the adult adrenal gland. Dev Cell *27*, 5. 10.1016/J.DEVCEL.2013.09.003.

175. Hanley, N.A., Rainey, W.E., Wilson, D.I., Ball, S.G., and Parker, K.L. (2001). Expression profiles of SF-1, DAX1, and CYP17 in the human fetal adrenal gland: potential interactions in gene regulation. Mol Endocrinol *15*, 57–68. 10.1210/MEND.15.1.0585.

176. Zubair, M., Ishihara, S., Oka, S., Okumura, K., and Morohashi, K. (2006). Two-step regulation of Ad4BP/SF-1 gene transcription during fetal adrenal development: initiation by a Hox-Pbx1-Prep1 complex and maintenance via autoregulation by Ad4BP/SF-1. Mol Cell Biol *26*, 4111–4121. 10.1128/MCB.00222-06.

177. Zubair, M., Parker, K.L., and Morohashi, K. (2008). Developmental links between the fetal and adult zones of the adrenal cortex revealed by lineage tracing. Mol Cell Biol *28*, 7030–7040. 10.1128/MCB.00900-08.

178. Kinga, P., Paul, A., and Laufer, E. (2009). Shh signaling regulates adrenocortical development and identifies progenitors of steroidogenic lineages. Proc Natl Acad Sci U S A *106*, 21185. 10.1073/PNAS.0909471106.

179. Wood, M.A., Acharya, A., Finco, I., Swonger, J.M., Elston, M.J., Tallquist, M.D., and Hammer, G.D. (2013). Fetal adrenal capsular cells serve as progenitor cells for steroidogenic and stromal adrenocortical cell lineages in M. musculus. Development *140*, 4522–4532. 10.1242/DEV.092775.

180. Jeff Huang, C.C., and Kang, Y. (2019). The transient cortical zone in the adrenal gland—the mystery of the adrenal X-zone. J Endocrinol *241*, R51. 10.1530/JOE-18-0632.

181. Freedman, B.D., Kempna, P.B., Carlone, D.L., Shah, M., Guagliardo, N.A., Barrett, P.Q., Gomez-Sanchez, C.E., Majzoub, J.A., and Breault, D.T. (2013). Adrenocortical zonation results from lineage conversion of differentiated zona glomerulosa cells. Dev Cell *26*, 666. 10.1016/J.DEVCEL.2013.07.016.

182. Kinga, P., Paul, A., and Laufer, E. (2009). Shh signaling regulates adrenocortical development and identifies progenitors of steroidogenic lineages. Proc Natl Acad Sci U S A *106*, 21185–21190. 10.1073/PNAS.0909471106/SUPPL_FILE/0909471106SI.PDF.

183. Finco, I., Lerario, A.M., and Hammer, G.D. (2018). Sonic Hedgehog and WNT Signaling Promote Adrenal Gland Regeneration in Male Mice. Endocrinology *159*, 579. 10.1210/EN.2017-03061.

184. Vidal, V., Sacco, S., Rocha, A.S., Da Silva, F., Panzolini, C., Dumontet, T., Doan, T.M.P., Shan, J., Rak-Raszewska, A., Bird, T., et al. (2016). The adrenal capsule is a signaling center controlling cell renewal and zonation through Rspo3. Genes Dev *30*, 1389–1394. 10.1101/GAD.277756.116/-/DC1.

185. Guagliardo, N.A., Klein, P.M., Gancayco, C.A., Lu, A., Leng, S., Makarem, R.R., Cho, C., Rusin, C.G., Breault, D.T., Barrett, P.Q., et al. (2020). Angiotensin II induces coordinated calcium bursts in aldosterone-producing adrenal rosettes. Nat Commun *11*. 10.1038/S41467-020-15408-4.

186. Nishimoto, K., Nakagawa, K., Li, D., Kosaka, T., Oya, M., Mikami, S., Shibata, H., Itoh, H., Mitani, F., Yamazaki, T., et al. (2010). Adrenocortical zonation in humans under normal and pathological conditions. J Clin Endocrinol Metab *95*, 2296–2305. 10.1210/JC.2009-2010.

187. Conley, A.J., Pattison, J.C., and Bird, I.M. (2004). Variations in adrenal androgen production among (nonhuman) primates. Semin Reprod Med *22*, 311–326. 10.1055/S-2004-861548.

188. Liu, L., Kang, J., Ding, X., Chen, D., Zhou, Y., and Ma, H. (2015). Dehydroepiandrosterone-Regulated Testosterone Biosynthesis via Activation of the ERK1/2 Signaling Pathway in Primary Rat Leydig Cells. Cellular Physiology and Biochemistry *36*, 1778–1792. 10.1159/000430150.

189. Hawkins, U.A., Gomez-Sanchez, E.P., Gomez-Sanchez, C.M., and Gomez-Sanchez, C.E. (2012). The ubiquitous mineralocorticoid receptor: Clinical implications. Curr Hypertens Rep *14*, 573–580. 10.1007/S11906-012-0297-0/METRICS.

190. Joëls, M. (2011). Impact of glucocorticoids on brain function: Relevance for mood disorders. Psychoneuroendocrinology *36*, 406–414. 10.1016/J.PSYNEUEN.2010.03.004.

191. Cruz-Topete, D., Myers, P.H., Foley, J.F., Willis, M.S., and Cidlowski, J.A. (2016). Corticosteroids Are Essential for Maintaining Cardiovascular Function in Male Mice. Endocrinology *157*, 2759–2771. 10.1210/EN.2015-1604.

192. Whirledge, S., and Cidlowski, J.A. (2017). Glucocorticoids and Reproduction: Traffic Control on the Road to Reproduction. Trends in Endocrinology & Metabolism *28*, 399–415. 10.1016/J.TEM.2017.02.005.

193. Fowden, A.L., Forhead, A.J., Fowden, A.L., and Forhead, A.J. (2015). Glucocorticoids as regulatory signals during intrauterine development. Exp Physiol *100*, 1477–1487. 10.1113/EP085212.

194. Timmermans, S., Souffriau, J., and Libert, C. (2019). A general introduction to glucocorticoid biology. Front Immunol *10*, 459269. 10.3389/FIMMU.2019.01545/BIBTEX.

195. Dunn, J.F., Nisula, B.C., and Rodbard, D. (1981). Transport of Steroid Hormones: Binding of 21 Endogenous Steroids to Both Testosterone-Binding Globulin and Corticosteroid-Binding Globulin in Human Plasma. J Clin Endocrinol Metab *53*, 58–68. 10.1210/JCEM-53-1-58.

196. Hammond, G.L., Smith, C.L., Paterson, N.A.M., and Sibbald, W.J. (1990). A Role for Corticosteroid-Binding Globulin in Delivery of Cortisol to Activated Neutrophils. J Clin Endocrinol Metab *71*, 34–39. 10.1210/JCEM-71-1-34.

197. Hammond, G.L. (2016). Plasma steroid-binding proteins: primary gatekeepers of steroid hormone action. Journal of Endocrinology *230*, R13–R25. 10.1530/JOE-16-0070.

198. Seckl, J.R. (2004). 11β-hydroxysteroid dehydrogenases: changing glucocorticoid action. Curr Opin Pharmacol *4*, 597–602. 10.1016/J.COPH.2004.09.001.

199. Hollenberg, S.M., Weinberger, C., Ong, E.S., Cerelli, G., Oro, A., Lebo, R., Brad Thompson, E., Rosenfeld, M.G., and Evans, R.M. (1985). Primary structure and expression of a functional human glucocorticoid receptor cDNA. Nature 1985 318:6047 *318*, 635–641. 10.1038/318635a0.

200. Weinberger, C., Hollenberg, S.M., Ong, E.S., Harmon, J.M., Brower, S.T., Cidlowski, J., Thompson, E.B., Rosenfeld, M.G., and Evans, R.M. (1985). Identification of Human Glucocorticoid Receptor Complementary DNA Clones by Epitope Selection. Science (1979) *228*, 740–742. 10.1126/SCIENCE.2581314.

201. Munck, A., and Brinck-Johnsen, T. (1968). Specific and Nonspecific Physicochemical Interactions of Glucocorticoids and Related Steroids with Rat Thymus Cells in Vitro. Journal of Biological Chemistry *243*, 5556–5565. 10.1016/S0021-9258(18)91904-6.

202. Gomez-Sanchez, E., and Gomez-Sanchez, C.E. (2014). The Multifaceted Mineralocorticoid Receptor. Compr Physiol *4*, 965. 10.1002/CPHY.C130044.

203. Evans, R.M. (1988). The Steroid and Thyroid Hormone Receptor Superfamily. Science *240*, 889. 10.1126/SCIENCE.3283939.

204. Cole, T.J., Blendy, J.A., Monaghan, A.P., Krieglstein, K., Schmid, W., Aguzzi, A., Fantuzzi, G., Hummler, E., Unsicker, K., and Schütz, G. (1995). Targeted disruption of the glucocorticoid receptor gene blocks adrenergic chromaffin cell development and severely retards lung maturation. Genes Dev *9*, 1608–1621. 10.1101/GAD.9.13.1608.

205. Oakley, R.H., and Cidlowski, J.A. (2013). The Biology of the Glucocorticoid Receptor: New Signaling Mechanisms in Health and Disease. J Allergy Clin Immunol *132*, 1033. 10.1016/J.JACI.2013.09.007.

206. Wrange, O., Eriksson, P., and Perlmann, T. (1989). The Purified Activated Glucocorticoid Receptor is a Homodimer. Journal of Biological Chemistry *264*, 5253–5259. 10.1016/S0021-9258(18)83726-7.

207. Timmermans, S., Souffriau, J., and Libert, C. (2019). A general introduction to glucocorticoid biology. Front Immunol *10*, 459269. 10.3389/FIMMU.2019.01545/BIBTEX.

208. Spiga, F., Walker, J.J., Terry, J.R., and Lightman, S.L. (2014). HPA Axis-Rhythms. Compr Physiol *4*, 1273–1298. 10.1002/CPHY.C140003.

209. Xing, Y., Parker, C.R., Edwards, M., and Rainey, W.E. (2010). ACTH is a potent regulator of gene expression in human adrenal cells. J Mol Endocrinol *45*, 59–68. 10.1677/JME-10-0006.

210. Ruggiero, C., and Lalli, E. (2016). Impact of ACTH Signaling on Transcriptional Regulation of Steroidogenic Genes. Front Endocrinol (Lausanne) *7*. 10.3389/FENDO.2016.00024.

211. Malkoski, S.P., and Dorin, R.I. (1999). Composite Glucocorticoid Regulation at a Functionally Defined Negative Glucocorticoid Response Element of the Human Corticotropin-Releasing Hormone Gene. Molecular Endocrinology *13*, 1629–1644. 10.1210/MEND.13.10.0351.

212. Drouin, J., Yu Lin, S., and Nemer, M. (1989). Glucocorticoid repression of pro-opiomelanocortin gene transcription. J Steroid Biochem *34*, 63–69. 10.1016/0022-4731(89)90066-6.

213. Martens, C., Bilodeau, S., Maira, M., Gauthier, Y., and Drouin, J. (2005). Protein-Protein Interactions and Transcriptional Antagonism between the Subfamily of NGFI-B/Nur77 Orphan Nuclear Receptors and Glucocorticoid Receptor. Molecular Endocrinology *19*, 885–897. 10.1210/ME.2004-0333.

214. Bilodeau, S., Vallette-Kasic, S., Gauthier, Y., Figarella-Branger, D., Brue, T., Berthelet, F., Lacroix, A., Batista, D., Stratakis, C., Hanson, J., et al. (2006). Role of Brg1 and HDAC2 in GR trans-repression of the pituitary POMC gene and misexpression in Cushing disease. Genes Dev *20*, 2871–2886. 10.1101/GAD.1444606.

215. Gorini, S., Kim, S.K., Infante, M., Mammi, C., La Vignera, S., Fabbri, A., Jaffe, I.Z., and Caprio, M. (2019). Role of Aldosterone and Mineralocorticoid Receptor in Cardiovascular Aging. Front Endocrinol (Lausanne) *10*, 440918. 10.3389/FENDO.2019.00584/BIBTEX.

216. Boldyreff, B., and Wehling, M. (2004). Aldosterone: Refreshing a slow hormone by swift action. News in Physiological Sciences *19*, 97–100. 10.1152/NIPS.01596.2003/ASSET/IMAGES/LARGE/1506-1.H.JPEG.

217. Arriza, J.L., Weinberger, C., Cerelli, G., Glaser, T.M., Handelin, B.L., Housman, D.E., and Evans, R.M. (1987). Cloning of human mineralocorticoid receptor complementary DNA: Structural and functional kinship with the glucocorticoid receptor. Science (1979) *237*, 268–275. 10.1126/SCIENCE.3037703.

218. Arriza, J.L., Simerly, R.B., Swanson, L.W., and Evans, R.M. (1988). The neuronal mineralocorticoid receptor as a mediator of glucocorticoid response. Neuron *1*, 887–900. 10.1016/0896-6273(88)90136-5.

219. De Kloet, E.R., Versteeg, D.H.G., and Kovacs, G.L. (1983). Aldosterone blocks the response to corticosterone in the raphe-hippocampal serotonin system. Brain Res *264*, 323–327. 10.1016/0006-8993(83)90834-X.

220. Caprio, M., Newfell, B.G., La Sala, A., Baur, W., Fabbri, A., Rosano, G., Mendelsohn, M.E., and Jaffe, I.Z. (2008). Functional Mineralocorticoid Receptors in Human Vascular Endothelial Cells Regulate Intercellular Adhesion Molecule-1 Expression

and Promote Leukocyte Adhesion. Circ Res *102*, 1359–1367. 10.1161/CIRCRESAHA.108.174235.

221. Jaffe, I.Z., and Mendelsohn, M.E. (2005). Angiotensin II and Aldosterone Regulate Gene Transcription Via Functional Mineralocortocoid Receptors in Human Coronary Artery Smooth Muscle Cells. Circ Res *96*, 643–650. 10.1161/01.RES.0000159937.05502.D1.

222. Edwards, C.R.W., Burt, D., Mcintyre, M.A., De Kloet, E.R., Stewart, P.M., Brett, L., Sutanto, W.S., and Monder, C. (1988). LOCALISATION OF 11β-HYDROXYSTEROID DEHYDROGENASE-TISSUE SPECIFIC PROTECTOR OF THE MINERALOCORTICOID RECEPTOR. The Lancet *332*, 986–989. 10.1016/S0140-6736(88)90742-8.

223. Briet, M., and Schiffrin, E.L. (2010). Aldosterone: effects on the kidney and cardiovascular system. Nature Reviews Nephrology 2010 6:5 *6*, 261–273. 10.1038/nrneph.2010.30.

224. Tsilosani, A., Gao, C., and Zhang, W. (2022). Aldosterone-Regulated Sodium Transport and Blood Pressure. Front Physiol *13*, 770375. 10.3389/FPHYS.2022.770375/BIBTEX.

225. McCurley, A., Pires, P.W., Bender, S.B., Aronovitz, M., Zhao, M.J., Metzger, D., Chambon, P., Hill, M.A., Dorrance, A.M., Mendelsohn, M.E., et al. (2012). Direct regulation of blood pressure by smooth muscle cell mineralocorticoid receptors. Nature Medicine 2012 18:9 *18*, 1429–1433. 10.1038/nm.2891.

226. Wright, J., Unger, T., De Gasparo, M., Catt, K.J., Inagami, T., Wright, J.W., and Unger, T.H. (2000). International union of pharmacology. XXIII. The angiotensin II receptors. ASPETM De Gasparo, KJ Catt, T Inagami, JW Wright, TH UngerPharmacological reviews, 2000•ASPET.

227. Rössig, L., Zólyomi, A., Catt, K.J., and Balla, T. (1996). Regulation of angiotensin II-stimulated Ca2+ oscillations by Ca2+ influx mechanisms in adrenal glomerulosa cells. J Biol Chem *271*, 22063–22069. 10.1074/JBC.271.36.22063.

228. Spät, A., and Hunyady, L. (2004). Control of aldosterone secretion: a model for convergence in cellular signaling pathways. Physiol Rev *84*, 489–539. 10.1152/PHYSREV.00030.2003.

229. Pereira, S.S., Lobato, C.B., Monteiro, M.P., Pereira, S.S., Lobato, · C B, Monteiro, · M P, Research, M., and Lobato, C.B. (2020). Cell Signaling Within Endocrine Glands: Thyroid, Parathyroids and Adrenal Glands. Tissue-Specific Cell Signaling, 63–91. 10.1007/978-3-030-44436-5_3.

230. Spyroglou, A., Manolopoulou, J., Wagner, S., Bidlingmaier, M., Reincke, M., and Beuschlein, F. (2009). Short term regulation of aldosterone secretion after stimulation and suppression experiments in mice. J Mol Endocrinol *42*, 407–413. 10.1677/JME-08-0167.

231. Hattangady, N.G., Olala, L.O., Bollag, W.B., and Rainey, W.E. (2012). Acute and chronic regulation of aldosterone production. Mol Cell Endocrinol *350*, 151–162. 10.1016/J.MCE.2011.07.034.

232. Laghlam, D., Jozwiak, M., and Nguyen, L.S. (2021). Renin–Angiotensin–Aldosterone System and Immunomodulation: A State-of-the-Art Review. Cells *10*. 10.3390/CELLS10071767.

233. Hu, J., Zhang, Z., Shen, W.J., and Azhar, S. (2010). Cellular cholesterol delivery, intracellular processing and utilization for biosynthesis of steroid hormones. Nutrition & Metabolism 2010 7:1 *7*, 1–25. 10.1186/1743-7075-7-47.

234. Capponi, A.M. (2002). Regulation of cholesterol supply for mineralocorticoid biosynthesis. Trends in Endocrinology and Metabolism *13*, 118–121. 10.1016/S1043-2760(01)00538-0.

235. Espenshade, P.J., and Hughes, A.L. (2007). Regulation of Sterol Synthesis in Eukaryotes. https://doi.org/10.1146/annurev.genet.41.110306.130315 *41*, 401–427. 10.1146/ANNUREV.GENET.41.110306.130315.

236. Rainey, W.E., Shay, J.W., and Mason, J.I. (1986). ACTH induction of 3-hydroxy-3-methylglutaryl coenzyme A reductase, cholesterol biosynthesis, and steroidogenesis in primary cultures of bovine adrenocortical cells. Journal of Biological Chemistry *261*, 7322–7326. 10.1016/S0021-9258(17)38394-1.

237. Liang, F., Kapoun, A.M., Lam, A., Damm, D.L., Quan, D., O'Connell, M., and Protter, A.A. (2007). B-Type natriuretic peptide inhibited angiotensin II-stimulated cholesterol biosynthesis, cholesterol transfer, and steroidogenesis in primary human adrenocortical cells. Endocrinology *148*, 3722–3729. 10.1210/EN.2006-1599.

238. Carr, B.R., and Simpson, E.R. (1981). De Novo Synthesis of Cholesterol by the Human Fetal Adrenal Gland. Endocrinology *108*, 2154–2162. 10.1210/ENDO-108-6-2154.

239. Lehoux, J.G., Lefebvre, A., Bélisle, S., and Bellabarba, D. (1989). Hormonal regulation of 3-hydroxy-3-methylglutaryl coenzyme a reductase mRNA in the rat adrenal gland. J Steroid Biochem *34*, 379–384. 10.1016/0022-4731(89)90112-X.

240. Liscum, L., and Munn, N.J. (1999). Intracellular cholesterol transport. Biochimica et Biophysica Acta (BBA) - Molecular and Cell Biology of Lipids *1438*, 19–37. 10.1016/S1388-1981(99)00043-8.

241. Chang, T.Y., Chang, C.C.Y., Ohgami, N., and Yamauchi, Y. (2006). Cholesterol Sensing, Trafficking, and Esterification.

https://doi.org/10.1146/annurev.cellbio.22.010305.104656 *22*, 129–157. 10.1146/ANNUREV.CELLBIO.22.010305.104656.

242. MS, B., JL, G., M, K., YK, H., and RG, A. (1979). Reversible accumulation of cholesteryl esters in macrophages incubated with acetylated lipoproteins. J Cell Biol *82*, 597–613. 10.1083/JCB.82.3.597.

243. Zoller, L.C., and Malamed, S. (1975). Acute effects of ACTH on dissociated adrenocortical cells: Quantitative changes in mitochondria and lipid droplets. Anat Rec *182*, 473–478. 10.1002/AR.1091820406.

244. Behrman, H.R., and Greep, R.O. (1972). Hormonal dependence of cholesterol ester hydrolase in the corpus luteum and adrenal. Horm Metab Res *4*, 206–209. 10.1055/S-0028-1094050/BIB.

245. Watari, H., Blanchette-Mackie, E.J., Dwyer, N.K., Sun, G., Glick, J.M., Patel, S., Neufeld, E.B., Pentchev, P.G., and Strauss, J.F. (2000). NPC1-Containing Compartment of Human Granulosa-Lutein Cells: A Role in the Intracellular Trafficking of Cholesterol Supporting Steroidogenesis. Exp Cell Res *255*, 56–66. 10.1006/EXCR.1999.4774.

246. Gordon, S.M., Li, H., Zhu, X., Shah, A.S., Lu, L.J., and Davidson, W.S. (2015). A comparison of the mouse and human lipoproteome: suitability of the mouse model for studies of human lipoproteins. J Proteome Res *14*, 2686–2695. 10.1021/ACS.JPROTEOME.5B00213.

247. Acton, S., Rigotti, A., Landschulz, K.T., Xu, S., Hobbs, H.H., and Kriegert, M. (1996). Identification of Scavenger Receptor SR-BI as a High Density Lipoprotein Receptor. Science (1979) *271*, 518–520. 10.1126/SCIENCE.271.5248.518.

248. Rigotti, A., Trigatti, B.L., Penman, M., Rayburn, H., Herz, J., and Krieger, M. (1997). A targeted mutation in the murine gene encoding the high density lipoprotein (HDL)

receptor scavenger receptor class B type I reveals its key role in HDL metabolism. Proc Natl Acad Sci U S A *94*, 12610. 10.1073/PNAS.94.23.12610.

249. Hoekstra, M., Meurs, I., Koenders, M., Out, R., Hildebrand, R.B., Kruijt, J.K., Van Eck, M., and Van Berkel, T.J.C. (2008). Absence of HDL cholesteryl ester uptake in mice via SR-BI impairs an adequate adrenal glucocorticoid-mediated stress response to fasting. J Lipid Res *49*, 738–745. 10.1194/JLR.M700475-JLR200.

250. Temel, R.E., Trigatti, B., Demattos, R.B., Azhar, S., Krieger, M., and Williams, D.L. (1997). Scavenger receptor class B, type I (SR-BI) is the major route for the delivery of high density lipoprotein cholesterol to the steroidogenic pathway in cultured mouse adrenocortical cells. Proc Natl Acad Sci U S A *94*, 13600–13605. 10.1073/PNAS.94.25.13600.

251. Chroni, A., Nieland, T.J.F., Kypreos, K.E., Krieger, M., and Zannis, V.I. (2005). SR-BI mediates cholesterol efflux via its interactions with lipid-bound ApoE. Structural mutations in SR-BI diminish cholesterol efflux. Biochemistry *44*, 13132–13143. 10.1021/BI051029O.

252. Azhar, S., and Reaven, E. (2002). Scavenger receptor class BI and selective cholesteryl ester uptake: partners in the regulation of steroidogenesis. Mol Cell Endocrinol *195*, 1–26. 10.1016/S0303-7207(02)00222-8.

253. Azhar, S., and Reaven, E. (1994). Effect of age on cholesterol uptake and utilization by rat adrenals: I. Internalization of lipoprotein-derived cholesteryl esters. Mech Ageing Dev *77*, 13–25. 10.1016/0047-6374(94)90043-4.

254. Landschulz, K.T., Pathak, R.K., Rigotti, A., Krieger, M., and Hobbs, H.H. (1996). Regulation of scavenger receptor, class B, type I, a high density lipoprotein receptor, in liver and steroidogenic tissues of the rat. J Clin Invest *98*, 984–995. 10.1172/JCI118883.

255. Hoekstra, M., Ye, D., Hildebrand, R.B., Zhao, Y., Lammers, B., Stitzinger, M., Kuiper, J., Van Berkel, T.J.C., and Van Eck, M. (2009). Scavenger receptor class B type I-mediated uptake of serum cholesterol is essential for optimal adrenal glucocorticoid production. J Lipid Res *50*, 1039. 10.1194/JLR.M800410-JLR200.

256. Hoekstra, M., Meurs, I., Koenders, M., Out, R., Hildebrand, R.B., Kruijt, J.K., Van Eck, M., and Van Berkel, T.J.C. (2008). Absence of HDL cholesteryl ester uptake in mice via SR-BI impairs an adequate adrenal glucocorticoid-mediated stress response to fasting. J Lipid Res *49*, 738–745. 10.1194/jlr.M700475-JLR200.

257. Reaven, E., Spicher, M., and Azhar, S. (1989). Microvillar channels: a unique plasma membrane compartment for concentrating lipoproteins on the surface of rat adrenal cortical cells. J Lipid Res *30*, 1551–1560. 10.1016/S0022-2275(20)38239-0.

258. Reaven, E., Leers-Sucheta, S., Nomoto, A., and Azhar, S. (2001). Expression of scavenger receptor class B type 1 (SR-BI) promotes microvillar channel formation and selective cholesteryl ester transport in a heterologous reconstituted system. Proc Natl Acad Sci U S A *98*, 1613–1618. 10.1073/PNAS.98.4.1613/ASSET/68E3CFC6-0B3B-482E-AB80-E43DA5E82417/ASSETS/GRAPHIC/PQ0414865004.JPEG.

259. Xu, S., Laccotripe, M., Huang, X., Rigotti, A., Zannis, V.I., and Krieger, M. (1997). Apolipoproteins of HDL can directly mediate binding to the scavenger receptor SR-BI, an HDL receptor that mediates selective lipid uptake. J Lipid Res *38*, 1289–1298. 10.1016/s0022-2275(20)37413-7.

260. Acton, S.L., Scherer, P.E., Lodish, H.F., and Krieger, M. (1994). Expression cloning of SR-BI, a CD36-related class B scavenger receptor. Journal of Biological Chemistry *269*, 21003–21009. 10.1016/S0021-9258(17)31921-X.

261. Gillotte-Taylor, K., Boullier, A., Witztum, J.L., Steinberg, D., and Quehenberger, O. (2001). Scavenger receptor class B type I as a receptor for oxidized low density lipoprotein. J Lipid Res *42*. 10.1016/S0022-2275(20)30281-9.

262. Vahouny, G. V., Chanderbhan, R., Hinds, R., Hodges, V.A., and Treadwell, C.R. (1978). ACTH-induced hydrolysis of cholesteryl esters in rat adrenal cells. J Lipid Res *19*, 570–577. 10.1016/S0022-2275(20)41288-X.

263. Kraemer, F.B., Shen, W.J., Natu, V., Patel, S., Osuga, J.I., Ishibashi, S., and Azhar, S. (2002). Adrenal Neutral Cholesteryl Ester Hydrolase: Identification, Subcellular Distribution, and Sex Differences. Endocrinology *143*, 801–806. 10.1210/ENDO.143.3.8693.

264. Kraemer, F.B., Shen, W.J., Harada, K., Patel, S., Osuga, J.I., Ishibashi, S., and Azhar, S. (2004). Hormone-Sensitive Lipase Is Required for High-Density Lipoprotein Cholesteryl Ester-Supported Adrenal Steroidogenesis. Molecular Endocrinology *18*, 549–557. 10.1210/ME.2003-0179.

265. Hong, L., Brochu, M., Pei Wang, S., Rochdi, L., Côté, M., Mitchell, G., and Gallo-Payet, N. (2002). Hormone-Sensitive Lipase Deficiency in Mice Causes Lipid Storage in the Adrenal Cortex and Impaired Corticosterone Response to Corticotropin Stimulation. Endocrinology *143*, 3333–3340. 10.1210/EN.2002-220341.

266. Savard, S., Amar, L., Plouin, P.F., and Steichen, O. (2013). Cardiovascular complications associated with primary aldosteronism: A controlled cross-sectional study. Hypertension *62*, 331–336. 10.1161/HYPERTENSIONAHA.113.01060/-/DC1.

267. Biglieri, E.G., Stockigt, J.R., Schambelan, M., and Collins, R.D. (1974). Secondary Hyperaldosteronism. Angiotensin, 284–297. 10.1007/978-3-642-65600-2_15.

268. Mulatero, P., Tizzani, D., Viola, A., Bertello, C., Monticone, S., Mengozzi, G., Schiavone, D., Williams, T.A., Einaudi, S., Grotta, A. La, et al. (2011). Prevalence and

characteristics of familial hyperaldosteronism: the PATOGEN study (Primary Aldosteronism in TOrino-GENetic forms). Hypertension *58*, 797–803. 10.1161/HYPERTENSIONAHA.111.175083.

269. Douma, S., Petidis, K., Doumas, M., Papaefthimiou, P., Triantafyllou, A., Kartali, N., Papadopoulos, N., Vogiatzis, K., and Zamboulis, C. (2008). Prevalence of primary hyperaldosteronism in resistant hypertension: a retrospective observational study. Lancet *371*, 1921–1926. 10.1016/S0140-6736(08)60834-X.

270. Hannemann, A., Bidlingmaier, M., Friedrich, N., Manolopoulou, J., Spyroglou, A., Völzke, H., Beuschlein, F., Seissler, J., Rettig, R., Felix, S.B., et al. (2012). Screening for primary aldosteronism in hypertensive subjects: results from two German epidemiological studies. Eur J Endocrinol *167*, 7–15. 10.1530/EJE-11-1013.

271. Fernandes-Rosa, F.L., Boulkroun, S., and Zennaro, M.C. (2017). Somatic and inherited mutations in primary aldosteronism. J Mol Endocrinol *59*, R47–R63. 10.1530/JME-17-0035.

272. Heitzmann, D., Derand, R., Jungbauer, S., Bandulik, S., Sterner, C., Schweda, F., El Wakil, A., Lalli, E., Guy, N., Mengual, R., et al. (2008). Invalidation of TASK1 potassium channels disrupts adrenal gland zonation and mineralocorticoid homeostasis. EMBO J *27*, 179–187. 10.1038/SJ.EMBOJ.7601934.

273. Davies, L.A., Hu, C., Guagliardo, N.A., Sen, N., Chen, X., Talley, E.M., Carey, R.M., Bayliss, D.A., and Barrett, P.Q. (2008). TASK channel deletion in mice causes primary hyperaldosteronism. Proc Natl Acad Sci U S A *105*, 2203–2208. 10.1073/PNAS.0712000105.

274. Choi, M., Scholl, U.I., Yue, P., Björklund, P., Zhao, B., Nelson-Williams, C., Ji, W., Cho, Y., Patel, A., Men, C.J., et al. (2011). K+ channel mutations in adrenal

aldosterone-producing adenomas and hereditary hypertension. Science *331*, 768–772. 10.1126/SCIENCE.1198785.

275. Beuschlein, F., Boulkroun, S., Osswald, A., Wieland, T., Nielsen, H.N., Lichtenauer, U.D., Penton, D., Schack, V.R., Amar, L., Fischer, E., et al. (2013). Somatic mutations in ATP1A1 and ATP2B3 lead to aldosterone-producing adenomas and secondary hypertension. Nat Genet *45*, 440–444. 10.1038/NG.2550.

276. Kim, A.C., Reuter, A.L., Zubair, M., Else, T., Serecky, K., Bingham, N.C., Lavery, G.G., Parker, K.L., and Hammer, G.D. (2008). Targeted disruption of beta-catenin in Sf1-expressing cells impairs development and maintenance of the adrenal cortex. Development *135*, 2593–2602. 10.1242/DEV.021493.

277. Boulkroun, S., Samson-Couterie, B., Golib-Dzib, J.F., Amar, L., Plouin, P.F., Sibony, M., Lefebvre, H., Louiset, E., Jeunemaitre, X., Meatchi, T., et al. (2011). Aldosterone-producing adenoma formation in the adrenal cortex involves expression of stem/progenitor cell markers. Endocrinology *152*, 4753–4763. 10.1210/EN.2011-1205.

278. Berthon, A., Martinez, A., Bertherat, J., and Val, P. (2012). Wnt/β-catenin signalling in adrenal physiology and tumour development. Mol Cell Endocrinol *351*, 87–95. 10.1016/J.MCE.2011.09.009.

279. Hao, H.X., Xie, Y., Zhang, Y., Zhang, O., Oster, E., Avello, M., Lei, H., Mickanin, C., Liu, D., Ruffner, H., et al. (2012). ZNRF3 promotes Wnt receptor turnover in an R-spondin-sensitive manner. Nature *485*, 195–202. 10.1038/NATURE11019.

280. Assié, G., Letouzé, E., Fassnacht, M., Jouinot, A., Luscap, W., Barreau, O., Omeiri, H., Rodriguez, S., Perlemoine, K., René-Corail, F., et al. (2014). Integrated genomic characterization of adrenocortical carcinoma. Nat Genet *46*, 607–612. 10.1038/NG.2953.

281. Warde, K.M., Smith, L.J., Liu, L., Stubben, C.J., Lohman, B.K., Willett, P.W., Ammer, J.L., Castaneda-Hernandez, G., Imodoye, S.O., Zhang, C., et al. (2023). Senescence-induced immune remodeling facilitates metastatic adrenal cancer in a sex-dimorphic manner. Nat Aging *3*, 846–865. 10.1038/S43587-023-00420-2.

282. Else, T., Kim, A.C., Sabolch, A., Raymond, V.M., Kandathil, A., Caoili, E.M., Jolly, S., Miller, B.S., Giordano, T.J., and Hammer, G.D. (2014). Adrenocortical carcinoma. Endocr Rev *35*, 282–326. 10.1210/ER.2013-1029.

283. de Freminville, J.B., Amar, L., Azizi, M., and Mallart-Riancho, J. (2023). Endocrine causes of hypertension: literature review and practical approach. Hypertension Research 2023, 1–14. 10.1038/s41440-023-01461-1.

284. Omura, M., Saito, J., Yamaguchi, K., Kakuta, Y., and Nishikawa, T. (2004). Prospective Study on the Prevalence of Secondary Hypertension among Hypertensive Patients Visiting a General Outpatient Clinic in Japan. Hypertension Research *27*, 193–202. 10.1291/HYPRES.27.193.

285. Nieman, L.K., Biller, B.M.K., Findling, J.W., Newell-Price, J., Savage, M.O., Stewart, P.M., Montori, V.M., and Edwards, H. (2008). The diagnosis of Cushing's syndrome: an Endocrine Society Clinical Practice Guideline. J Clin Endocrinol Metab *93*, 1526–1540. 10.1210/JC.2008-0125.

286. Reincke, M., and Fleseriu, M. (2023). Cushing Syndrome: A Review. JAMA *330*, 170–181. 10.1001/JAMA.2023.11305.

287. Davi, M.V., Cosaro, E., Piacentini, S., Reimondo, G., Albiger, N., Arnaldi, G., Faggiano, A., Mantovani, G., Fazio, N., Piovesan, A., et al. (2017). Prognostic factors in ectopic Cushing's syndrome due to neuroendocrine tumors: a multicenter study. Eur J Endocrinol *176*, 453–461. 10.1530/EJE-16-0809.

288. Beuschlein, F., Fassnacht, M., Assié, G., Calebiro, D., Stratakis, C.A., Osswald, A., Ronchi, C.L., Wieland, T., Sbiera, S., Faucz, F.R., et al. (2014). Constitutive activation of PKA catalytic subunit in adrenal Cushing's syndrome. N Engl J Med *370*, 1019–1028. 10.1056/NEJMOA1310359.

289. Zennaro, M.C., Boulkroun, S., and Fernandes-Rosa, F. (2017). Genetic Causes of Functional Adrenocortical Adenomas. Endocr Rev *38*, 516–537. 10.1210/ER.2017-00189.

290. Younes, N., Bourdeau, I., and Lacroix, A. (2021). Latent Adrenal Insufficiency: From Concept to Diagnosis. Front Endocrinol (Lausanne) *12*, 720769. 10.3389/FENDO.2021.720769/BIBTEX.

291. Michels, A.W., and Eisenbarth, G.S. (2010). Immunologic Endocrine Disorders. J Allergy Clin Immunol *125*, S226. 10.1016/J.JACI.2009.09.053.

292. Betterle, C., Volpato, M., Rees Smith, B., Furmaniak, J., Chen, S., Zanchetta, R., Greggio, N.A., Pedini, B., Boscaro, M., and Presotto, F. (1997). II. Adrenal cortex and steroid 21-hydroxylase autoantibodies in children with organ-specific autoimmune diseases: markers of high progression to clinical Addison's disease. J Clin Endocrinol Metab *82*, 939–942. 10.1210/JCEM.82.3.3849.

293. van der Grinten, H.L.C., Speiser, P.W., Faisal Ahmed, S., Arlt, W., Auchus, R.J., Falhammar, H., Flück, C.E., Guasti, L., Huebner, A., Kortmann, B.B.M., et al. (2022). Congenital Adrenal Hyperplasia-Current Insights in Pathophysiology, Diagnostics, and Management. Endocr Rev *43*, 91–159. 10.1210/ENDREV/BNAB016.

294. Pofi, R., Ji, X., Krone, N.P., and Tomlinson, J.W. (2023). Long-term health consequences of congenital adrenal hyperplasia. Clin Endocrinol (Oxf). 10.1111/CEN.14967.

295. Sandison, A.T. (1955). A Form of Lipoidosis of the Adrenal Cortex in an Infant. Arch Dis Child *30*, 538. 10.1136/ADC.30.154.538.

296. Imangshu, H., Ose, S.B., Eruo, T., Ugawara, S., Erome, J., and Trauss, F.S. (1996). The Pathophysiology and Genetics of Congenital Lipoid Adrenal Hyperplasia. https://doi.org/10.1056/NEJM199612193352503 *335*, 1870–1879. 10.1056/NEJM199612193352503.

297. Matteson, K.J., Chung, B.C., Urdea, M.S., Miller, W.L., and Urdea, M.S. (1986). Study of cholesterol side-chain cleavage (20,22 desmolase) deficiency causing congenital lipoid adrenal hyperplasia using bovine-sequence P450scc oligodeoxyribonucleotide probes. Endocrinology *118*, 1296–1305. 10.1210/ENDO-118-4-1296.

298. Lin, D., Sugawara, T., Strauss, J.F., Clark, B.J., Stocco, D.M., Saenger, P., Rogol, A., and Miller, W.L. (1995). Role of steroidogenic acute regulatory protein in adrenal and gonadal steroidogenesis. Science (1979) *67*, 1828–1831. 10.1126/SCIENCE.7892608.

299. Horikawa, R. (2014). Congenital lipoid adrenal hyperplasia. Ann Pediatr Endocrinol Metab *19*, 351–356. 10.6065/APEM.2014.19.4.179.

300. Lucas, M.W., Helderman, N.C., van de Velde, A.O., Kapiteijn, E., van Leeuwaarde, R.S., and Blank, C.U. (2023). 1153P Incidence and characteristics of immunotherapy related adrenal insufficiency in a monocenter, pan-cancer cohort of 4314 patients. Annals of Oncology *34*, S689. 10.1016/J.ANNONC.2023.09.2287.

301. Barroso-Sousa, R., Barry, W.T., Garrido-Castro, A.C., Hodi, F.S., Min, L., Krop, I.E., and Tolaney, S.M. (2018). Incidence of Endocrine Dysfunction Following the Use of Different Immune Checkpoint Inhibitor Regimens: A Systematic Review and Meta-analysis. JAMA Oncol *4*, 173–182. 10.1001/JAMAONCOL.2017.3064.

302. Dolfi, B., Gallerand, A., Firulyova, M.M., Xu, Y., Merlin, J., Dumont, A., Castiglione, A., Vaillant, N., Quemener, S., Gerke, H., et al. (2022). Unravelling the sex-specific diversity and functions of adrenal gland macrophages. Cell Rep *39*, 110949. 10.1016/j.celrep.2022.110949.

303. Luecken, M.D., and Theis, F.J. (2019). Current best practices in single-cell RNA-seq analysis: a tutorial. Mol Syst Biol *15*. 10.15252/MSB.20188746.

304. Domínguez Conde, C., Xu, C., Jarvis, L.B., Rainbow, D.B., Wells, S.B., Gomes, T., Howlett, S.K., Suchanek, O., Polanski, K., King, H.W., et al. (2022). Cross-tissue immune cell analysis reveals tissue-specific features in humans. Science *376*. 10.1126/SCIENCE.ABL5197.

305. De Ciuceis, C., Amiri, F., Brassard, P., Endemann, D., Touyz, R., and Schiffrin, E. (2005). Reduced vascular remodeling, endothelial dysfunction, and oxidative stress in resistance arteries of angiotensin II-infused macrophage colony-stimulating factor-deficient mice: evidence for a role in inflammation in angiotensin-induced vascular injury. Arterioscler Thromb Vasc Biol *25*, 2106–2113. 10.1161/01.ATV.0000181743.28028.57.

306. Love, M.I., Huber, W., and Anders, S. (2014). Moderated estimation of fold change and dispersion for RNA-seq data with DESeq2. Genome Biol *15*. 10.1186/S13059-014-0550-8.

307. Wang, F., Luo, R., Zou, C.J., Xie, S., Peng, K., Zhao, L., Yang, K.T., Xu, C., and Yang, T. (2020). Soluble (pro)renin receptor treats metabolic syndrome in mice with diet-induced obesity via interaction with PPARγ. JCI Insight *5*. 10.1172/JCI.INSIGHT.128061.

308. Mizuno, Y., Ishii, T., and Hasegawa, T. (2019). In Vivo Verification of the Pathophysiology of Lipoid Congenital Adrenal Hyperplasia in the Adrenal Cortex. Endocrinology *160*, 331–338. 10.1210/EN.2018-00777.

309. Purvis, G.S.D., Collino, M., Aranda-Tavio, H., Chiazza, F., O'Riordan, C.E., Zeboudj, L., Mohammad, S., Collotta, D., Verta, R., Guisot, N.E.S., et al. (2020). Inhibition of Bruton's TK regulates macrophage NF-κB and NLRP3 inflammasome activation in metabolic inflammation. Br J Pharmacol *177*, 4416–4432. 10.1111/BPH.15182.

310. Holness, C.L., and Simmons, D.L. (1993). Molecular Cloning of CD68, a Human Macrophage Marker Related to Lysosomal Glycoproteins. Blood *81*, 1607–1613. 10.1182/BLOOD.V81.6.1607.1607.

311. Chistiakov, D.A., Killingsworth, M.C., Myasoedova, V.A., Orekhov, A.N., and Bobryshev, Y. V. (2016). CD68/macrosialin: not just a histochemical marker. Laboratory Investigation 2017 97:1 *97*, 4–13. 10.1038/labinvest.2016.116.

312. Ngela, R., Da Silva, P., Gordon, S., and William, S. (1999). Phagocytosis stimulates alternative glycosylation of macrosialin (mouse CD68), a macrophage-specific endosomal protein. Biochemical Journal *338*, 687. 10.1042/0264-6021:3380687.

313. Murray, P.J., and Wynn, T.A. (2011). Protective and pathogenic functions of macrophage subsets. Nature Reviews Immunology 2011 11:11 *11*, 723–737. 10.1038/nri3073.

314. Iqbal, A.J., McNeill, E., Kapellos, T.S., Regan-Komito, D., Norman, S., Burd, S., Smart, N., Machemer, D.E.W., Stylianou, E., McShane, H., et al. (2014). Human CD68 promoter GFP transgenic mice allow analysis of monocyte to macrophage differentiation in vivo. Blood *124*, e33–e44. 10.1182/blood-2014-04-568691.

315. Ramprasad, M.P., Terpstra, V., Kondratenko, N., Quehenberger, O., and Steinberg, D. (1996). Cell surface expression of mouse macrosialin and human CD68 and their role

as macrophage receptors for oxidized low density lipoprotein. Proc Natl Acad Sci U S A *93*, 14833–14838. 10.1073/PNAS.93.25.14833.

316. Ottnad, E., Parthasarathy, S., Sambrano, G.R., Ramprasad, M.P., Quehenberger, O., Kondratenko, N., Green, S., and Steinberg, D. (1995). A macrophage receptor for oxidized low density lipoprotein distinct from the receptor for acetyl low density lipoprotein: partial purification and role in recognition of oxidatively damaged cells. Proc Natl Acad Sci U S A *92*, 1391–1395. 10.1073/PNAS.92.5.1391.

317. Sambrano, G.R., and Steinberg, D. (1995). Recognition of oxidatively damaged and apoptotic cells by an oxidized low density lipoprotein receptor on mouse peritoneal macrophages: role of membrane phosphatidylserine. Proc Natl Acad Sci U S A *92*, 1396–1400. 10.1073/PNAS.92.5.1396.

318. Kim, K.W., Vallon-Eberhard, A., Zigmond, E., Farache, J., Shezen, E., Shakhar, G., Ludwig, A., Lira, S.A., and Jung, S. (2011). In vivo structure/function and expression analysis of the CX3C chemokine fractalkine. Blood *118*. 10.1182/BLOOD-2011-04-348946.

319. Geissmann, F., Jung, S., and Littman, D.R. (2003). Blood monocytes consist of two principal subsets with distinct migratory properties. Immunity *19*, 71–82. 10.1016/S1074-7613(03)00174-2.

320. Jung, S., Aliberti, J., Graemmel, P., Sunshine, M.J., Kreutzberg, G.W., Sher, A., and Littman, D.R. (2000). Analysis of fractalkine receptor CX(3)CR1 function by targeted deletion and green fluorescent protein reporter gene insertion. Mol Cell Biol *20*, 4106–4114. 10.1128/MCB.20.11.4106-4114.2000.

321. Anthonie Johan Zwijnenburg, A., Pokharel, J., Varnait, R., Gredmark-Russ, S., Eidsmo, L., Johan Zwijnenburg, A., Zheng, W., Hoffer, E., Shryki, I., Ramirez Comet, N., et al. (2023). ll Graded expression of the chemokine receptor CX3CR1 marks

differentiation states of human and murine T cells and enables cross-species interpretation. Immunity *56*, 1955-1974.e10. 10.1016/j.immuni.2023.06.025.

322. Yamauchi, T., Hoki, T., Oba, T., Jain, V., Chen, H., Attwood, K., Battaglia, S., George, S., Chatta, G., Puzanov, I., et al. (2021). T-cell CX3CR1 expression as a dynamic blood-based biomarker of response to immune checkpoint inhibitors. Nature Communications 2021 12:1 *12*, 1–14. 10.1038/s41467-021-21619-0.

323. Jones, B.A., Beamer, M., and Ahmed, S. (2010). Fractalkine/CX3CL1: a potential new target for inflammatory diseases. Mol Interv *10*, 263–270. 10.1124/MI.10.5.3.

324. Medina-Contreras, O., Geem, D., Laur, O., Williams, I.R., Lira, S.A., Nusrat, A., Parkos, C.A., and Denning, T.L. (2011). CX3CR1 regulates intestinal macrophage homeostasis, bacterial translocation, and colitogenic Th17 responses in mice. J Clin Invest *121*, 4787–4795. 10.1172/JCI59150.

325. Yashchenko, A., Bland, S.J., Song, C.J., Ahmed, U.K.B., Sharp, R., Darby, I.G., Cordova, A.M., Smith, M.E., Lever, J.M., Li, Z., et al. (2023). Cx3cr1 controls kidney resident macrophage heterogeneity. Front Immunol *14*. 10.3389/FIMMU.2023.1082078.

326. Gordon, S., Hamann, J., Lin, H.H., and Stacey, M. (2011). F4/80 and the related adhesion-GPCRs. Eur J Immunol *41*, 2472–2476. 10.1002/EJI.201141715.

327. Hume, D.A., Halpin, D., Charlton, H., and Gordon, S. (1984). The mononuclear phagocyte system of the mouse defined by immunohistochemical localization of antigen F4/80: macrophages of endocrine organs. Proc Natl Acad Sci U S A *81*, 4174–4177. 10.1073/PNAS.81.13.4174.

328. Lin, H.H., Faunce, D.E., Stacey, M., Terajewicz, A., Nakamura, T., Zhang-Hoover, J., Kerley, M., Mucenski, M.L., Gordon, S., and Stein-Streilein, J. (2005). The macrophage F4/80 receptor is required for the induction of antigen-specific efferent

regulatory T cells in peripheral tolerance. J Exp Med *201*, 1615. 10.1084/JEM.20042307.

329. Bakos, E., Thaiss, C.A., Kramer, M.P., Cohen, S., Radomir, L., Orr, I., Kaushansky, N., Ben-Nun, A., Becker-Herman, S., and Shachar, I. (2017). CCR2 Regulates the Immune Response by Modulating the Interconversion and Function of Effector and Regulatory T Cells. J Immunol *198*, 4659–4671. 10.4049/JIMMUNOL.1601458.

330. Guilliams, M., Thierry, G.R., Bonnardel, J., and Bajenoff, M. (2020). Establishment and Maintenance of the Macrophage Niche. Immunity *52*, 434–451. 10.1016/J.IMMUNI.2020.02.015.

331. Dai, X.M., Zong, X.H., Sylvestre, V., and Stanley, E.R. (2004). Incomplete restoration of colony-stimulating factor 1 (CSF-1) function in CSF-1-deficient Csf1op/Csf1op mice by transgenic expression of cell surface CSF-1. Blood *103*, 1114–1123. 10.1182/BLOOD-2003-08-2739.

332. Pridans, C., Raper, A., Davis, G.M., Alves, J., Sauter, K.A., Lefevre, L., Regan, T., Meek, S., Sutherland, L., Thomson, A.J., et al. (2018). Pleiotropic Impacts of Macrophage and Microglial Deficiency on Development in Rats with Targeted Mutation of the Csf1r Locus . The Journal of Immunology *201*, 2683–2699. 10.4049/jimmunol.1701783.

333. Combes, T.W., Orsenigo, F., Stewart, A., Mendis, A.S.J.R., Dunn-Walters, D., Gordon, S., and Martinez, F.O. (2021). CSF1R defines the mononuclear phagocyte system lineage in human blood in health and COVID-19. Immunotherapy Advances *1*. 10.1093/IMMADV/LTAB003.

334. Byrne, P. V., Guilbert, L.J., and Stanley, E.R. (1981). Distribution of cells bearing receptors for a colony-stimulating factor (CSF-1) in murine tissues. J Cell Biol *91*, 848–853. 10.1083/JCB.91.3.848.

335. MacDonald, K.P.A., Rowe, V., Bofinger, H.M., Thomas, R., Sasmono, T., Hume, D.A., and Hill, G.R. (2005). The colony-stimulating factor 1 receptor is expressed on dendritic cells during differentiation and regulates their expansion. J Immunol *175*, 1399–1405. 10.4049/JIMMUNOL.175.3.1399.

336. Bruhns, P. (2012). Properties of mouse and human IgG receptors and their contribution to disease models. Blood *119*, 5640–5649. 10.1182/BLOOD-2012-01-380121.

337. Wei, Q., Deng, Y., Yang, Q., Zhan, A., and Wang, L. (2023). The markers to delineate different phenotypes of macrophages related to metabolic disorders. Front Immunol *14*. 10.3389/FIMMU.2023.1084636.

338. Mizuno, N., and Yanagawa, Y. (2022). Tofacitinib enhances interferon-γ-induced expression of major histocompatibility complex class II in macrophages. Eur J Pharmacol *915*. 10.1016/J.EJPHAR.2021.174564.

339. Ma, J.K., Platt, M.Y., Eastham-Anderson, J., Shin, J.S., and Mellman, I. (2012). MHC class II distribution in dendritic cells and B cells is determined by ubiquitin chain length. Proc Natl Acad Sci U S A *109*, 8820–8827. 10.1073/PNAS.1202977109/ASSET/859D56C6-7D3C-45E2-A9D3-0182F8F9458C/ASSETS/GRAPHIC/PNAS.1202977109FIG06.JPEG.

340. Langlet, C., Tamoutounour, S., Henri, S., Luche, H., Ardouin, L., Grégoire, C., Malissen, B., and Guilliams, M. (2012). CD64 expression distinguishes monocyte-derived and conventional dendritic cells and reveals their distinct role during intramuscular immunization. J Immunol *188*, 1751–1760. 10.4049/JIMMUNOL.1102744.

341. Allen, E., Bakke, A.C., Purtzer, M.Z., and Deodhar, A. (2002). Neutrophil CD64 expression: distinguishing acute inflammatory autoimmune disease from systemic infections. Ann Rheum Dis *61*, 522–525. 10.1136/ARD.61.6.522.

342. Wiktor-Jedrzejczak, W., Ahmed, A., Szczylik, C., and Skelly, R.R. (1982). Hematological characterization of congenital osteopetrosis in op/op mouse. Possible mechanism for abnormal macrophage differentiation. Journal of Experimental Medicine *156*, 1516–1527. 10.1084/JEM.156.5.1516.

343. Nandi, S., Akhter, M.P., Seifert, M.F., Dai, X.M., and Stanley, E.R. (2006). Developmental and functional significance of the CSF-1 proteoglycan chondroitin sulfate chain. Blood *107*, 786–795. 10.1182/BLOOD-2005-05-1822.

344. Wei, S., Lightwood, D., Ladyman, H., Cross, S., Neale, H., Griffiths, M., Adams, R., Marshall, D., Lawson, A., McKnight, A.J., et al. (2005). Modulation of CSF-1-regulated post-natal development with anti-CSF-1 antibody. Immunobiology *210*, 109–119. 10.1016/j.imbio.2005.05.005.

345. Greter, M., Lelios, I., Pelczar, P., Hoeffel, G., Price, J., Leboeuf, M., Kündig, T.M., Frei, K., Ginhoux, F., Merad, M., et al. (2012). Stroma-derived interleukin-34 controls the development and maintenance of langerhans cells and the maintenance of microglia. Immunity *37*, 1050–1060. 10.1016/J.IMMUNI.2012.11.001.

346. Wang, Y., Szretter, K.J., Vermi, W., Gilfillan, S., Rossini, C., Cella, M., Barrow, A.D., Diamond, M.S., and Colonna, M. (2012). IL-34 is a tissue-restricted ligand of CSF1R required for the development of Langerhans cells and microglia. Nature Immunology 2012 13:8 *13*, 753–760. 10.1038/ni.2360.

347. Browaeys, R., Saelens, W., and Saeys, Y. (2019). NicheNet: modeling intercellular communication by linking ligands to target genes. Nature Methods 2019 17:2 *17*, 159–162. 10.1038/s41592-019-0667-5.

348. Bonnardel, J., T'Jonck, W., Gaublomme, D., Browaeys, R., Scott, C.L., Martens, L., Vanneste, B., De Prijck, S., Nedospasov, S.A., Kremer, A., et al. (2019). Stellate Cells, Hepatocytes, and Endothelial Cells Imprint the Kupffer Cell Identity on Monocytes

Colonizing the Liver Macrophage Niche. Immunity *51*, 638. 10.1016/J.IMMUNI.2019.08.017.

349. Chakrabarti, R., Celià-Terrassa, T., Kumar, S., Hang, X., Wei, Y., Choudhury, A., Hwang, J., Peng, J., Nixon, B., Grady, J.J., et al. (2018). Notch ligand Dll1 mediates cross-talk between mammary stem cells and the macrophageal niche. Science *360*. 10.1126/SCIENCE.AAN4153.

350. Sakai, M., Troutman, T.D., Seidman, J.S., Ouyang, Z., Spann, N.J., Abe, Y., Ego, K.M., Bruni, C.M., Deng, Z., Schlachetzki, J.C.M., et al. (2019). Liver-Derived Signals Sequentially Reprogram Myeloid Enhancers to Initiate and Maintain Kupffer Cell Identity. Immunity *51*, 655-670.e8. 10.1016/j.immuni.2019.09.002.

351. Wood, W., and Martin, P. Developmental Cell Review Macrophage Functions in Tissue Patterning and Disease: New Insights from the Fly. 10.1016/j.devcel.2017.01.001.

352. van Furth, R., Cohn, Z.A., Hirsch, J.G., Humphrey, J.H., Spector, W.G., and Langevoort, H.L. (1972). The mononuclear phagocyte system: a new classification of macrophages, monocytes, and their precursor cells. Bull World Health Organ *46*, 845.

353. Merad, M., Manz, M.G., Karsunky, H., Wagers, A., Peters, W., Charo, I., Weissman, I.L., Cyster, J.G., and Engleman, E.G. (2002). Langerhans cells renew in the skin throughout life under steady-state conditions. Nature Immunology 2002 3:12 *3*, 1135–1141. 10.1038/ni852.

354. Ginhoux, F., Greter, M., Leboeuf, M., Nandi, S., See, P., Gokhan, S., Mehler, M.F., Conway, S.J., Ng, L.G., Stanley, E.R., et al. (2010). Fate Mapping Analysis Reveals That Adult Microglia Derive from Primitive Macrophages. Science (1979) *136*, 1168. 10.1126/SCIENCE.1194637.

355. Epelman, S., Lavine, K.J., Beaudin, A.E., Sojka, D.K., Carrero, J.A., Calderon, B., Brija, T., Gautier, E.L., Ivanov, S., Satpathy, A.T., et al. (2014). Embryonic and adult-derived resident cardiac macrophages are maintained through distinct mechanisms at steady state and during inflammation. Immunity *40*, 91–104. 10.1016/j.immuni.2013.11.019.

356. Molawi, K., Wolf, Y., Kandalla, P.K., Favret, J., Hagemeyer, N., Frenzel, K., Pinto, A.R., Klapproth, K., Henri, S., Malissen, B., et al. (2014). Progressive replacement of embryo-derived cardiac macrophages with age. J Exp Med *211*, 2151–2158. 10.1084/JEM.20140639.

357. Bain, C.C., Bravo-Blas, A., Scott, C.L., Gomez Perdiguero, E., Geissmann, F., Henri, S., Malissen, B., Osborne, L.C., Artis, D., and Mowat, A.M.I. (2014). Constant replenishment from circulating monocytes maintains the macrophage pool in the intestine of adult mice. Nat Immunol *15*, 929–937. 10.1038/NI.2967.

358. Ajami, B., Bennett, J.L., Krieger, C., Tetzlaff, W., and Rossi, F.M.V. (2007). Local self-renewal can sustain CNS microglia maintenance and function throughout adult life. Nature Neuroscience 2007 10:12 *10*, 1538–1543. 10.1038/nn2014.

359. Hashimoto, D., Chow, A., Noizat, C., Teo, P., Beasley, M.B., Leboeuf, M., Becker, C.D., See, P., Price, J., Lucas, D., et al. (2013). Tissue resident macrophages self-maintain locally throughout adult life with minimal contribution from circulating monocytes. Immunity *38*, 792–804. 10.1016/J.IMMUNI.2013.04.004.

360. Liu, Z., Gu, Y., Chakarov, S., Bleriot, C., Kwok, I., Chen, X., Shin, A., Huang, W., Dress, R.J., Dutertre, C.A., et al. (2019). Fate Mapping via Ms4a3-Expression History Traces Monocyte-Derived Cells. Cell *178*, 1509-1525.e19. 10.1016/j.cell.2019.08.009.

361. Palis, J., Robertson, S., Kennedy, M., Wall, C., and Keller, G. (1999). Development of erythroid and myeloid progenitors in the yolk sac and embryo proper of the mouse. Development *126*, 5073–5084. 10.1242/DEV.126.22.5073.

362. Alliot, F., Godin, I., and Pessac, B. (1999). Microglia derive from progenitors, originating from the yolk sac, and which proliferate in the brain. Developmental Brain Research *117*, 145–152. 10.1016/S0165-3806(99)00113-3.

363. Ginhoux, F., Greter, M., Leboeuf, M., Nandi, S., See, P., Gokhan, S., Mehler, M.F., Conway, S.J., Ng, L.G., Stanley, E.R., et al. (2010). Fate Mapping Analysis Reveals That Adult Microglia Derive from Primitive Macrophages. Science *330*, 841. 10.1126/SCIENCE.1194637.

364. Tober, J., Koniski, A., McGrath, K.E., Vemishetti, R., Emerson, R., De Mesy-Bentley, K.K.L., Waugh, R., and Palis, J. (2007). The megakaryocyte lineage originates from hemangioblast precursors and is an integral component both of primitive and of definitive hematopoiesis. Blood *109*, 1433–1441. 10.1182/BLOOD-2006-06-031898.

365. Gomez Perdiguero, E., Klapproth, K., Schulz, C., Busch, K., Azzoni, E., Crozet, L., Garner, H., Trouillet, C., De Bruijn, M.F., Geissmann, F., et al. (2015). Tissue-resident macrophages originate from yolk-sac-derived erythro-myeloid progenitors. Nature *518*, 547–551. 10.1038/NATURE13989.

366. Hoeffel, G., Chen, J., Lavin, Y., Low, D., Almeida, F.F., See, P., Beaudin, A.E., Lum, J., Low, I., Forsberg, E.C., et al. (2015). C-Myb(+) erythro-myeloid progenitor-derived fetal monocytes give rise to adult tissue-resident macrophages. Immunity *42*, 665–678. 10.1016/J.IMMUNI.2015.03.011.

367. Gentek, R., Ghigo, C., Hoeffel, G., Bulle, M.J., Msallam, R., Gautier, G., Launay, P., Chen, J., Ginhoux, F., and Bajénoff, M. (2018). Hemogenic Endothelial Fate Mapping

Reveals Dual Developmental Origin of Mast Cells. Immunity *48*, 1160-1171.e5. 10.1016/J.IMMUNI.2018.04.025.

368. Iturri, L., Freyer, L., Biton, A., Dardenne, P., Lallemand, Y., and Gomez Perdiguero, E. (2021). Megakaryocyte production is sustained by direct differentiation from erythromyeloid progenitors in the yolk sac until midgestation. Immunity *54*, 1433-1446.e5. 10.1016/j.immuni.2021.04.026.

369. Palis, J., and Yoder, M.C. (2001). Yolk-sac hematopoiesis: the first blood cells of mouse and man. Exp Hematol *29*, 927–936. 10.1016/S0301-472X(01)00669-5.

370. Stremmel, C., Schuchert, R., Wagner, F., Thaler, R., Weinberger, T., Pick, R., Mass, E., Ishikawa-Ankerhold, H.C., Margraf, A., Hutter, S., et al. (2018). Yolk sac macrophage progenitors traffic to the embryo during defined stages of development. Nat Commun *9*. 10.1038/S41467-017-02492-2.

371. Boisset, J.C., Van Cappellen, W., Andrieu-Soler, C., Galjart, N., Dzierzak, E., and Robin, C. (2010). In vivo imaging of haematopoietic cells emerging from the mouse aortic endothelium. Nature *464*, 116–120. 10.1038/NATURE08764.

372. Kieusseian, A., de la Grange, P.B., Burlen-Defranoux, O., Godin, I., and Cumano, A. (2012). Immature hematopoietic stem cells undergo maturation in the fetal liver. Development *139*, 3521–3530. 10.1242/DEV.079210.

373. Zanjani, E., Ascensao, J., and Tavassoli, M. (1993). Liver-Derived Fetal Hematopoietic Stem Cells Selectively and Preferentially Home to the Fetal Bone Marrow. Blood *81*, 399–404. 10.1182/BLOOD.V81.2.399.399.

374. Si, Y., Tsou, C.L., Croft, K., and Charo, I.F. (2010). CCR2 mediates hematopoietic stem and progenitor cell trafficking to sites of inflammation in mice. J Clin Invest *120*, 1192–1203. 10.1172/JCI40310.

375. Tsou, C.L., Peters, W., Si, Y., Slaymaker, S., Aslanian, A.M., Weisberg, S.P., Mack, M., and Charo, I.F. (2007). Critical roles for CCR2 and MCP-3 in monocyte mobilization from bone marrow and recruitment to inflammatory sites. Journal of Clinical Investigation *117*, 902–909. 10.1172/JCI29919.

376. Engel, D.R., Maurer, J., Tittel, A.P., Weisheit, C., Cavlar, T., Schumak, B., Limmer, A., van Rooijen, N., Trautwein, C., Tacke, F., et al. (2008). CCR2 Mediates Homeostatic and Inflammatory Release of Gr1high Monocytes from the Bone Marrow, but Is Dispensable for Bladder Infiltration in Bacterial Urinary Tract Infection. The Journal of Immunology *181*, 5579–5586. 10.4049/JIMMUNOL.181.8.5579.

377. Petermann, M., Orfanos, Z., Sellau, J., Gharaibeh, M., Lotter, H., Fleischer, B., and Keller, C. (2021). CCR2 Deficiency Impairs Ly6Clo and Ly6Chi Monocyte Responses in Orientia tsutsugamushi Infection. Front Immunol *12*, 670219. 10.3389/FIMMU.2021.670219/BIBTEX.

378. Dagkalis, A., Wallace, C., Xu, H., Liebau, S., Manivannan, A., Stone, M.A., Mack, M., Liversidge, J., and Crane, I.J. (2009). Development of Experimental Autoimmune Uveitis: Efficient Recruitment of Monocytes Is Independent of CCR2. Invest Ophthalmol Vis Sci *50*, 4288–4294. 10.1167/IOVS.09-3434.

379. Popovich, P.G., and Hickey, W.F. (2001). Bone Marrow Chimeric Rats Reveal the Unique Distribution of Resident and Recruited Macrophages in the Contused Rat Spinal Cord. J Neuropathol Exp Neurol *60*, 676–685. 10.1093/JNEN/60.7.676.

380. Dick, S.A., Wong, A., Hamidzada, H., Nejat, S., Nechanitzky, R., Vohra, S., Mueller, B., Zaman, R., Kantores, C., Aronoff, L., et al. (2022). Three tissue resident macrophage subsets coexist across organs with conserved origins and life cycles. Sci Immunol *7*, 7777.

10.1126/SCIIMMUNOL.ABF7777/SUPPL_FILE/SCIIMMUNOL.ABF7777_MDAR_REPRODUCIBILITY_CHECKLIST.ZIP.

381. Spencer, C.A., and Leung, T.H. (2019). Research Techniques Made Simple: Parabiosis to Elucidate Humoral Factors in Skin Biology. Journal of Investigative Dermatology *139*, 1208-1213.e1. 10.1016/j.jid.2019.03.1134.

382. Yang, C., Liu, Z.L., Wang, J., Bu, X. Le, Wang, Y.J., and Xiang, Y. (2021). Parabiosis modeling: protocol, application and perspectives. Zool Res *42*, 253–261. 10.24272/J.ISSN.2095-8137.2020.368.

383. Legué, E., and Joyner, A.L. (2010). Genetic Fate Mapping Using Site-Specific Recombinases. Methods Enzymol *477*, 153. 10.1016/S0076-6879(10)77010-5.

384. Feil, R., Wagner, J., Metzger, D., and Chambon, P. (1997). Regulation of Cre Recombinase Activity by Mutated Estrogen Receptor Ligand-Binding Domains. Biochem Biophys Res Commun *237*, 752–757. 10.1006/BBRC.1997.7124.

385. Antonini, S.R., Stecchini, M.F., and Ramalho, F.S. (2020). Development and Function of the Adrenal Cortex and Medulla in the Fetus and Neonate. Maternal-Fetal and Neonatal Endocrinology: Physiology, Pathophysiology, and Clinical Management, 611–623. 10.1016/B978-0-12-814823-5.00036-2.

386. Boyd, G.S., McNamara, B., Suckling, K.E., and Tocher, D.R. (1983). Cholesterol metabolism in the adrenal cortex. J Steroid Biochem *19*, 1017–1027. 10.1016/0022-4731(83)90048-1.

387. Lipids of the cortex (1952). Acta Anat (Basel) *14*, 54–68. 10.1159/000140729.

388. Sakr, N., Glazova, O., Shevkova, L., Onyanov, N., Kaziakhmedova, S., Shilova, A., Vorontsova, M. V., and Volchkov, P. (2023). Characterizing and Quenching Autofluorescence in Fixed Mouse Adrenal Cortex Tissue. International Journal of Molecular Sciences 2023, Vol. 24, Page 3432 *24*, 3432. 10.3390/IJMS24043432.

389. Plump, A.S., Erickson, S.K., Weng, W., Partin, J.S., Breslow, J.L., and Williams, D.L. (1996). Apolipoprotein A-I is required for cholesteryl ester accumulation in steroidogenic cells and for normal adrenal steroid production. J Clin Invest *97*, 2660–2671. 10.1172/JCI118716.

390. Wong, D.L. (2003). Why is the adrenal adrenergic? Endocr Pathol *14*, 25–36. 10.1385/EP:14:1:25.

391. Pérez-Alvarez, A., Hernández-Vivanco, A., and Albillos, A. (2010). Past, Present and Future of Human Chromaffin Cells: Role in Physiology and Therapeutics. Cellular and Molecular Neurobiology 2010 30:8 *30*, 1407–1415. 10.1007/S10571-010-9582-0.

392. Tacke, F., Alvarez, D., Kaplan, T.J., Jakubzick, C., Spanbroek, R., Llodra, J., Garin, A., Liu, J., Mack, M., Van Rooijen, N., et al. (2007). Monocyte subsets differentially employ CCR2, CCR5, and CX3CR1 to accumulate within atherosclerotic plaques. J Clin Invest *117*, 185–194. 10.1172/JCI28549.

393. Wang, Y., Dubland, J.A., Allahverdian, S., Asonye, E., Sahin, B., Jaw, J.E., Sin, D.D., Seidman, M.A., Leeper, N.J., and Francis, G.A. (2019). Smooth Muscle Cells Contribute the Majority of Foam Cells in Apolipoprotein E-Deficient Mouse Atherosclerosis. Arterioscler Thromb Vasc Biol *39*, 876. 10.1161/ATVBAHA.119.312434.

394. Fowler, S. (1980). Characterization of foam cells in experimental atherosclerosis. Acta Med Scand Suppl *642*, 151–158. 10.1111/J.0954-6820.1980.TB10947.X.

395. Berliner, J.A., Territo, M.C., Sevanian, A., Ramin, S., Jeong Ai Kim, Bamshad, B., Esterson, M., and Fogelman, A.M. (1990). Minimally modified low density lipoprotein stimulates monocyte endothelial interactions. J Clin Invest *85*, 1260–1266. 10.1172/JCI114562.

396. Yia-Herttuala, S., Palinski, W., Rosenfeld, M.E., Parthasarathy, S., Carew, T.E., Butler, S., Witztum, J.L., and Steinberg, D. (1989). Evidence for the presence of oxidatively modified low density lipoprotein in atherosclerotic lesions of rabbit and man. J Clin Invest *84*, 1086–1095. 10.1172/JCI114271.

397. Meyer, J.M., Ji, A., Cai, L., and Van Der Westhuyzen, D.R. (2012). High-capacity selective uptake of cholesteryl ester from native LDL during macrophage foam cell formation. J Lipid Res *53*, 2081. 10.1194/JLR.M026534.

398. Endemannl, G., Stanton, L.W., Madden, K.S., Bryant, C.M., White, R.T., and Protter, A.A. (1993). THE JOURNAL OF BIOLOGICAL CHEMISTRV CD36 Is a Receptor for Oxidized Low Density Lipoprotein*. *268*, 11811–11816. 10.1016/S0021-9258(19)50272-1.

399. Suzuki, H., Kurihara, Y., Takeya, M., Kamada, N., Kataoka, M., Jishage, K., Ueda, O., Sakaguchi, H., Higashi, T., Suzuki, T., et al. (1997). A role for macrophage scavenger receptors in atherosclerosis and susceptibility to infection. Nature *386*, 292–296. 10.1038/386292A0.

400. González-Hernández, J.A., Bornstein, S.R., Ehrhart-Bornstein, M., Geschwend, J.E., Adler, G., and Scherbaum, W.A. (1994). Macrophages within the human adrenal gland. Cell Tissue Res *278*, 201–205. 10.1007/BF00414161.

401. Stark, R., Grzelak, M., and Hadfield, J. (2019). RNA sequencing: the teenage years. Nature Reviews Genetics 2019 20:11 *20*, 631–656. 10.1038/s41576-019-0150-2.

402. Wang, E.T., Sandberg, R., Luo, S., Khrebtukova, I., Zhang, L., Mayr, C., Kingsmore, S.F., Schroth, G.P., and Burge, C.B. (2008). Alternative isoform regulation in human tissue transcriptomes. Nature *456*, 470–476. 10.1038/NATURE07509.

403. Djebali, S., Davis, C.A., Merkel, A., Dobin, A., Lassmann, T., Mortazavi, A., Tanzer, A., Lagarde, J., Lin, W., Schlesinger, F., et al. (2012). Landscape of transcription in human cells. Nature *489*, 101–108. 10.1038/NATURE11233.

404. Li, W., Notani, D., and Rosenfeld, M.G. (2016). Enhancers as non-coding RNA transcription units: recent insights and future perspectives. Nat Rev Genet *17*, 207–223. 10.1038/NRG.2016.4.

405. Li, X., and Wang, C.Y. (2021). From bulk, single-cell to spatial RNA sequencing. International Journal of Oral Science 2021 13:1 *13*, 1–6. 10.1038/s41368-021-00146-0.

406. Hegenbarth, J.-C., Lezzoche, G., De Windt, L.J., and Stoll, M. (2022). Perspectives on Bulk-Tissue RNA Sequencing and Single-Cell RNA Sequencing for Cardiac Transcriptomics. Frontiers in Molecular Medicine *2*, 839338. 10.3389/FMMED.2022.839338.

407. Lopez, J.P., Brivio, E., Santambrogio, A., De Donno, C., Kos, A., Peters, M., Rost, N., Czamara, D., Brückl, T.M., Roeh, S., et al. (2021). Single-cell molecular profiling of all three components of the HPA axis reveals adrenal ABCB1 as a regulator of stress adaptation. Sci Adv *7*, 4497–4524. 10.1126/SCIADV.ABE4497.

408. Ding, J., Adiconis, X., Simmons, S.K., Kowalczyk, M.S., Hession, C.C., Marjanovic, N.D., Hughes, T.K., Wadsworth, M.H., Burks, T., Nguyen, L.T., et al. (2020). Systematic comparison of single-cell and single-nucleus RNA-sequencing methods. Nature Biotechnology 2020 38:6 *38*, 737–746. 10.1038/s41587-020-0465-8.

409. Sanz, E., Yang, L., Su, T., Morris, D.R., McKnight, G.S., and Amieux, P.S. (2009). Cell-type-specific isolation of ribosome-associated mRNA from complex tissues. Proc Natl Acad Sci U S A *106*, 13939–13944. 10.1073/PNAS.0907143106.

410. La Manno, G., Soldatov, R., Zeisel, A., Braun, E., Hochgerner, H., Petukhov, V., Lidschreiber, K., Kastriti, M.E., Lönnerberg, P., Furlan, A., et al. (2018). RNA velocity of single cells. Nature 2018 560:7719 *560*, 494–498. 10.1038/s41586-018-0414-6.

411. Moffitt, J.R., Bambah-Mukku, D., Eichhorn, S.W., Vaughn, E., Shekhar, K., Perez, J.D., Rubinstein, N.D., Hao, J., Regev, A., Dulac, C., et al. (2018). Molecular, spatial, and functional single-cell profiling of the hypothalamic preoptic region. Science (1979) *362*. 10.1126/SCIENCE.AAU5324/SUPPL_FILE/PAPV2.PDF.

412. Gleissner, C.A., Leitinger, N., and Ley, K. (2007). Effects of native and modified low-density lipoproteins on monocyte recruitment in atherosclerosis. Hypertension *50*, 276–283. 10.1161/HYPERTENSIONAHA.107.089854.

413. Burgess, M., Wicks, K., Gardasevic, M., and Mace, K.A. (2019). Cx3CR1 Expression Identifies Distinct Macrophage Populations That Contribute Differentially to Inflammation and Repair. Immunohorizons *3*, 262–273. 10.4049/IMMUNOHORIZONS.1900038.

414. Carlin, L.M., Stamatiades, E.G., Auffray, C., Hanna, R.N., Glover, L., Vizcay-Barrena, G., Hedrick, C.C., Cook, H.T., Diebold, S., and Geissmann, F. (2013). Nr4a1-dependent Ly6C(low) monocytes monitor endothelial cells and orchestrate their disposal. Cell *153*, 362–375. 10.1016/J.CELL.2013.03.010.

415. Ingersoll, M.A., Spanbroek, R., Lottaz, C., Gautier, E.L., Frankenberger, M., Hoffmann, R., Lang, R., Haniffa, M., Collin, M., Tacke, F., et al. (2010). Comparison of gene expression profiles between human and mouse monocyte subsets. Blood *115*. 10.1182/BLOOD-2009-07-235028.

416. Swirski, F.K., Nahrendorf, M., Etzrodt, M., Wildgruber, M., Cortez-Retamozo, V., Panizzi, P., Figueiredo, J.L., Kohler, R.H., Chudnovskiy, A., Waterman, P., et al.

(2009). Identification of splenic reservoir monocytes and their deployment to inflammatory sites. Science (1979) *325*, 612–616. 10.1126/SCIENCE.1175202/SUPPL_FILE/SWIRSKI.SOM.PDF.

417. Haldar, M., Kohyama, M., So, A.Y.L., Kc, W., Wu, X., Briseño, C.G., Satpathy, A.T., Kretzer, N.M., Arase, H., Rajasekaran, N.S., et al. (2014). Heme-mediated SPI-C induction promotes monocyte differentiation into iron-recycling macrophages. Cell *156*, 1223–1234. 10.1016/j.cell.2014.01.069.

418. Cheng, C., Tempel, D., Van Haperen, R., De Boer, H.C., Segers, D., Huisman, M., Van Zonneveld, A.J., Leenen, P.J.M., Van Der Steen, A., Serruys, P.W., et al. (2007). Shear stress-induced changes in atherosclerotic plaque composition are modulated by chemokines. J Clin Invest *117*, 616–626. 10.1172/JCI28180.

419. Grajchen, E., Hendriks, J.J.A., and Bogie, J.F.J. (2018). The physiology of foamy phagocytes in multiple sclerosis. Acta Neuropathol Commun *6*, 124. 10.1186/S40478-018-0628-8.

420. Childs, B.G., Baker, D.J., Wijshake, T., Conover, C.A., Campisi, J., and Van Deursen, J.M. (2016). Senescent intimal foam cells are deleterious at all stages of atherosclerosis. Science *354*, 472. 10.1126/SCIENCE.AAF6659.

421. Lhoták, Š., Gyulay, G., Cutz, J.C., Al-Hashimi, A., Trigatti, B.L., Richards, C.D., Igdoura, S.A., Steinberg, G.R., Bramson, J., Ask, K., et al. (2016). Characterization of Proliferating Lesion-Resident Cells During All Stages of Atherosclerotic Growth. Journal of the American Heart Association: Cardiovascular and Cerebrovascular Disease *5*. 10.1161/JAHA.116.003945.

422. Rico-Jimenez, J.J., Serafino, M.J., Shrestha, S., Chen, X., Kim, W., Adame, J., Buja, L.M., Vela, D., Applegate, B.E., and Jo, J.A. (2019). Automated detection of superficial macrophages in atherosclerotic plaques using autofluorescence lifetime

imaging. Atherosclerosis *285*, 120–127. 10.1016/J.ATHEROSCLEROSIS.2019.04.223.

423. Gonen, A., and Miller, Y.I. (2020). From Inert Storage to Biological Activity—In Search of Identity for Oxidized Cholesteryl Esters. Front Endocrinol (Lausanne) *11*. 10.3389/FENDO.2020.602252.

424. Seo, J.-W., Yang, E.-J., Yoo, K.-H., and Choi, I.-H. (2015). Macrophage Differentiation from Monocytes Is Influenced by the Lipid Oxidation Degree of Low Density Lipoprotein. Mediators Inflamm *2015*, 235797. 10.1155/2015/235797.

425. Oram, J.F., Lawn, R.M., Garvin, M.R., and Wade, D.P. (2000). ABCA1 is the cAMP-inducible apolipoprotein receptor that mediates cholesterol secretion from macrophages. J Biol Chem *275*, 34508–34511. 10.1074/JBC.M006738200.

426. Wang, N., Silver, D.L., Costet, P., and Tall, A.R. (2000). Specific binding of ApoA-I, enhanced cholesterol efflux, and altered plasma membrane morphology in cells expressing ABC1. J Biol Chem *275*, 33053–33058. 10.1074/JBC.M005438200.

427. Kennedy, M.A., Barrera, G.C., Nakamura, K., Baldán, Á., Tarr, P., Fishbein, M.C., Frank, J., Francone, O.L., and Edwards, P.A. (2005). ABCG1 has a critical role in mediating cholesterol efflux to HDL and preventing cellular lipid accumulation. Cell Metab *1*, 121–131. 10.1016/J.CMET.2005.01.002.

428. Wang, N., Lan, D., Chen, W., Matsuura, F., and Tall, A.R. (2004). ATP-binding cassette transporters G1 and G4 mediate cellular cholesterol efflux to high-density lipoproteins. Proc Natl Acad Sci U S A *101*, 9774–9779. 10.1073/PNAS.0403506101.

429. Brasaemle, D.L., Barber, T., Wolins, N.E., Serrero, G., Blanchette-Mackie, E.J., and Londos, C. (1997). Adipose differentiation-related protein is an ubiquitously expressed lipid storage droplet-associated protein. J Lipid Res *38*, 2249–2263. 10.1016/S0022-2275(20)34939-7.

430. Imamura, M., Inoguchi, T., Ikuyama, S., Taniguchi, S., Kobayashi, K., Nakashima, N., and Nawata, H. (2002). ADRP stimulates lipid accumulation and lipid droplet formation in murine fibroblasts. Am J Physiol Endocrinol Metab *283*. 10.1152/AJPENDO.00040.2002.

431. Theurl, I., Hilgendorf, I., Nairz, M., Tymoszuk, P., Haschka, D., Asshoff, M., He, S., Gerhardt, L.M.S., Holderried, T.A.W., Seifert, M., et al. (2016). On-demand erythrocyte disposal and iron recycling requires transient macrophages in the liver. Nature Medicine 2016 22:8 *22*, 945–951. 10.1038/nm.4146.

432. Tsou, C.-L., Peters, W., Si, Y., Slaymaker, S., Aslanian, A.M., Weisberg, S.P., Mack, M., and Charo, I.F. (2007). Critical roles for CCR2 and MCP-3 in monocyte mobilization from bone marrow and recruitment to inflammatory sites. J Clin Invest *117*, 902–909. 10.1172/JCI29919.

433. Füger, P., Hefendehl, J.K., Veeraraghavalu, K., Wendeln, A.C., Schlosser, C., Obermüller, U., Wegenast-Braun, B.M., Neher, J.J., Martus, P., Kohsaka, S., et al. (2017). Microglia turnover with aging and in an Alzheimer's model via long-term in vivo single-cell imaging. Nat Neurosci *20*, 1371–1376. 10.1038/NN.4631.

434. Zlotnik, A., Yoshie, O., and Nomiyama, H. (2006). The chemokine and chemokine receptor superfamilies and their molecular evolution. Genome Biol *7*, 1–11. 10.1186/GB-2006-7-12-243/FIGURES/4.

435. Bachelerie, F., Ben-Baruch, A., Burkhardt, A.M., Combadiere, C., Farber, J.M., Graham, G.J., Horuk, R., Sparre-Ulrich, A.H., Locati, M., Luster, A.D., et al. (2014). International Union of Basic and Clinical Pharmacology. [corrected]. LXXXIX. Update on the extended family of chemokine receptors and introducing a new nomenclature for atypical chemokine receptors. Pharmacol Rev *66*, 1–79. 10.1124/pr.113.007724.

436. Shi, C., and Pamer, E.G. (2011). Monocyte recruitment during infection and inflammation. Nat Rev Immunol *11*, 762–774. 10.1038/nri3070.

437. Kurihara, T., Warr, G., Loy, J., and Bravo, R. (1997). Defects in macrophage recruitment and host defense in mice lacking the CCR2 chemokine receptor. J Exp Med *186*, 1757–1762.

438. Kuziel, W.A., Morgan, S.J., Dawson, T.C., Griffin, S., Smithies, O., Ley, K., and Maeda, N. (1997). Severe reduction in leukocyte adhesion and monocyte extravasation in mice deficient in CC chemokine receptor 2. Proc Natl Acad Sci U S A *94*, 12053–12058. 10.1073/PNAS.94.22.12053/ASSET/4747650D-BCFE-493B-86D2-BCDEC9DF6FBE/ASSETS/GRAPHIC/PQ2272902005.JPEG.

439. Haimon, Z., Volaski, A., Orthgiess, J., Boura-Halfon, S., Varol, D., Shemer, A., Yona, S., Zuckerman, B., David, E., Chappell-Maor, L., et al. (2018). Re-evaluating Microglia Expression Profiles Using RiboTag and Cell Isolation Strategies. Nat Immunol *19*, 636. 10.1038/S41590-018-0110-6.

440. Dreier, R., Andersen, U.B., Forman, J.L., Sheykhzade, M., Egfjord, M., and Jeppesen, J.L. (2021). Effect of increased potassium intake on adrenal cortical and cardiovascular responses to angiotensin ii: A randomized crossover study. J Am Heart Assoc *10*, 18716. 10.1161/JAHA.120.018716.

441. Yang, T., He, M., and Hu, C. (2018). Regulation of aldosterone production by ion channels: From basal secretion to primary aldosteronism. Biochimica et Biophysica Acta (BBA) - Molecular Basis of Disease *1864*, 871–881. 10.1016/J.BBADIS.2017.12.034.

442. Shen, W.J., Azhar, S., and Kraemer, F.B. (2016). ACTH Regulation of Adrenal SR-B1. Front Endocrinol (Lausanne) *7*, 1. 10.3389/FENDO.2016.00042.

443. Heikkilä, P., Arola, J., Liu, J., and Kahri, A.I. (1998). ACTH regulates LDL receptor and CLA-1 mRNA in the rat adrenal cortex. Endocr Res *24*, 591–593. 10.3109/07435809809032651.

444. Daidoh, H., Morita, H., Mune, T., Murayama, M., Hanafusa, J., Ni, H., Shibata, H., and Yasuda, K. (1995). Responses of plasma adrenocortical steroids to low dose ACTH in normal subjects. Clin Endocrinol (Oxf) *43*, 311–315. 10.1111/J.1365-2265.1995.TB02037.X.

445. Graudal, N.A., Galløe, A.M., and Garred, P. (1998). Effects of sodium restriction on blood pressure, renin, aldosterone, catecholamines, cholesterols, and triglyceride: a meta-analysis. JAMA *279*, 1383–1391. 10.1001/JAMA.279.17.1383.

446. Ivy, J.R., Evans, L.C., Moorhouse, R., Richardson, R. V., Al-Dujaili, E.A.S., Flatman, P.W., Kenyon, C.J., Chapman, K.E., and Bailey, M.A. (2018). Renal and Blood Pressure Response to a High-Salt Diet in Mice With Reduced Global Expression of the Glucocorticoid Receptor. Front Physiol *9*. 10.3389/FPHYS.2018.00848.

447. Schweda, F., and Kurtz, A. (2011). Regulation of renin release by local and systemic factors. Rev Physiol Biochem Pharmacol *161*, 1–44. 10.1007/112_2008_1.

448. Schlatter, E., Salomonsson, M., Persson, A.E.G., and Greger, R. (1989). Macula densa cells sense luminal NaCl concentration via furosemide sensitive Na+2Cl-K+ cotransport. Pflugers Arch *414*, 286–290. 10.1007/BF00584628.

449. Schweda, F., Klar, J., Narumiya, S., Nüsing, R.M., and Kurtz, A. (2004). Stimulation of renin release by prostaglandin E2 is mediated by EP2 and EP4 receptors in mouse kidneys. Am J Physiol Renal Physiol *287*. 10.1152/AJPRENAL.00072.2004.

450. Peti-Peterdi, J., and Harris, R.C. (2010). Macula Densa Sensing and Signaling Mechanisms of Renin Release. J Am Soc Nephrol *21*, 1093. 10.1681/ASN.2009070759.

451. Cook, N., Fraser, S.A., Katerelos, M., Katsis, F., Gleich, K., Mount, P.F., Steinberg, G.R., Levidiotis, V., Kemp, B.E., and Power, D.A. (2009). Low salt concentrations activate AMP-activated protein kinase in mouse macula densa cells. Am J Physiol Renal Physiol *296*, 801–809. 10.1152/AJPRENAL.90372.2008/ASSET/IMAGES/LARGE/ZH20040954810007.JPEG.

452. O'Connell, M., Danforth, E., Horton, E.S., Salans, L., and Sims, E.A.H. (1973). Experimental Obesity in Man. III. Adrenocortical Function. J Clin Endocrinol Metab *36*, 323–329. 10.1210/JCEM-36-2-323.

453. Galvao Teles, A., Graves, L., Burke, C.W., Galvão-Teles, A., Fotherby, K., and Fraser, R. (1976). Free Cortisol in Obesity; Effect of Fasting. Acta Endocrinologica (Norway) *81*, 321–329. 10.1530/ACTA.0.0810321.

454. Teeple, K., Rajput, P., Gonzalez, M., Han-Hallett, Y., Fernández-Juricic, E., and Casey, T. (2023). High fat diet induces obesity, alters eating pattern and disrupts corticosterone circadian rhythms in female ICR mice. PLoS One *18*. 10.1371/JOURNAL.PONE.0279209.

455. Jin, N., Wang, Y., Liu, L., Xue, F., Jiang, T.B., and Xu, M.Z. (2019). Dysregulation of the renin-angiotensin system and cardiometabolic status in mice fed a long-term high-fat diet. Medical Science Monitor *25*, 6605–6614. 10.12659/MSM.914877.

456. Tuck, M.L., Sowers, J., Dornfeld, L., Kledzik, G., and Maxwell, M. (1981). The effect of weight reduction on blood pressure, plasma renin activity, and plasma aldosterone levels in obese patients. N Engl J Med *304*, 930–933. 10.1056/NEJM198104163041602.

457. Rocchini, A.P., Katch, V.L., Grekin, R., Moorehead, C., and Anderson, J. (1986). Role for aldosterone in blood pressure regulation of obese adolescents. Am J Cardiol *57*, 613–618. 10.1016/0002-9149(86)90845-3.

458. Goodfriend, T.L., Kelley, D.E., Goodpaster, B.H., and Winters, S.J. (1999). Visceral obesity and insulin resistance are associated with plasma aldosterone levels in women. Obes Res *7*, 355–362. 10.1002/j.1550-8528.1999.tb00418.x.

459. Swierczynska, M.M., Mateska, I., Peitzsch, M., Bornstein, S.R., Chavakis, T., Eisenhofer, G., Lamounier-Zepter, V., and Eaton, S. (2014). Changes in morphology and function of adrenal cortex in mice fed a high-fat diet. International Journal of Obesity 2015 39:2 *39*, 321–330. 10.1038/ijo.2014.102.

460. Xie, D., and Bollag, W.B. (2016). Obesity, hypertension and aldosterone: is leptin the link? Journal of Endocrinology *230*, F7–F11. 10.1530/JOE-16-0160.

461. Huby, A.-C., Antonova, G., Groenendyk, J., Gomez-Sanchez, C.E., Bollag, W.B., Filosa, J.A., and Belin de Chantemèle, E.J. (2015). Adipocyte-Derived Hormone Leptin Is a Direct Regulator of Aldosterone Secretion, Which Promotes Endothelial Dysfunction and Cardiac Fibrosis. Circulation *132*, 2134–2145. 10.1161/CIRCULATIONAHA.115.018226.

462. Simonds, S.E., Pryor, J.T., Ravussin, E., Greenway, F.L., Dileone, R., Allen, A.M., Bassi, J., Elmquist, J.K., Keogh, J.M., Henning, E., et al. (2014). Leptin mediates the increase in blood pressure associated with obesity. Cell *159*, 1404–1416. 10.1016/j.cell.2014.10.058.

463. Manna, P.R., Stetson, C.L., Slominski, A.T., and Pruitt, K. (2016). Role of the steroidogenic acute regulatory protein in health and disease. Endocrine *51*, 7. 10.1007/S12020-015-0715-6.

464. Higashijima, M., Nawata, H., Kato, K., and Ibayashi, H. (1987). Studies on Lipoprotein and Adrenal Steroidogenesis: I. Roles of Low Density Lipoprotein-and High Density Lipoprotein-Cholesterol in Steroid Production in Cultured Human Adrenocortical Cells. *34*, 635–645.

465. Simpson, H.D., Shepherd, R., Shepherd, J., Fraser, R., Lever, A.F., and Kenyon, C.J. (1989). Effects of cholesterol and lipoproteins on aldosterone secretion by bovine zona glomerulosa cells. Journal of Endocrinology *121*, 125–131. 10.1677/JOE.0.1210125.

466. Cherradi, N., Bideau, M., Arnaudeau, S., Demaurex, N., James, R.W., Azhar, S., and Capponi, A.M. (2001). Angiotensin II Promotes Selective Uptake of High Density Lipoprotein Cholesterol Esters in Bovine Adrenal Glomerulosa and Human Adrenocortical Carcinoma Cells Through Induction of Scavenger Receptor Class B Type I. Endocrinology *142*, 4540–4549. 10.1210/ENDO.142.10.8412.

467. I, A., J, P., J, G., M, E.-B., S, S., SR, B., and S, K. (2010). Modulation of adrenal aldosterone release by oxidative modification of low-density lipoprotein. Am J Hypertens *23*, 1061–1068. 10.1038/AJH.2010.118.

468. Kopprasch, S., Pietzsch, J., Ansurudeen, I., Graessler, J., Krug, A.W., Ehrhart-Bornstein, M., and Bornstein, S.R. (2009). Prediabetic and diabetic in vivo modification of circulating low-density lipoprotein attenuates its stimulatory effect on adrenal aldosterone and cortisol secretion. Journal of Endocrinology *200*, 45–52. 10.1677/JOE-08-0293.

469. González-Hernández, J.A., Bornstein, S.R., Ehrhart-Bornstein, M., Gschwend, J.E., Gwosdow, A., Jirikowski, G., and Scherbaum, W.A. (1995). IL-1 is expressed in human adrenal gland in vivo. Possible role in a local immune-adrenal axis. Clin Exp Immunol *99*, 137–141. 10.1111/j.1365-2249.1995.tb03484.x.

470. González-Hernández, J.A., Ehrhart-Bornstein, M., Späth-Schwalbe, E., Scherbaum, W.A., and Bornstein, S.R. (1996). Human adrenal cells express tumor necrosis factor-alpha messenger ribonucleic acid: evidence for paracrine control of adrenal function. J Clin Endocrinol Metab *81*, 807–813. 10.1210/jcem.81.2.8636308.

471. Päth, G., Bornstein, S.R., Ehrhart-Bornstein, M., and Scherbaum, W.A. (1997). Interleukin-6 and the interleukin-6 receptor in the human adrenal gland: expression and effects on steroidogenesis. J Clin Endocrinol Metab *82*, 2343–2349. 10.1210/jcem.82.7.4072.

472. Whitcomb, R.W., Linehan, W.M., Wahl, L.M., and Knazek, R.A. (1988). Monocytes stimulate cortisol production by cultured human adrenocortical cells. J Clin Endocrinol Metab *66*, 33–38. 10.1210/jcem-66-1-33.

473. Salas, M.A., Evans, S.W., Levell, M.J., and Whicher, J.T. (1990). Interleukin-6 and ACTH act synergistically to stimulate the release of corticosterone from adrenal gland cells. Clin. exp. Immunol *79*, 470–473.

474. Zieleniewski, W., Zieleniewski, J., and Stepien, H. (1995). Effect of interleukin-1a, IL-1b and IL-1 receptor antibody on the proliferation and steroidogenesis of regenerating rat adrenal cortex. Exp Clin Endocrinol Diabetes *103*, 373–377. 10.1055/s-0029-1211381.

475. Andreis, P.G., Neri, G., Belloni, A.S., Mazzocchi, G., Kasprzak, A., and Nussdorfer, G.G. (1991). Interleukin-1 beta enhances corticosterone secretion by acting directly on the rat adrenal gland. Endocrinology *129*, 53–57. 10.1210/endo-129-1-53.

476. Natarajan, R., Ploszaj, S., Horton, R., and Nadler, J. (1989). Tumor necrosis factor and interleukin-1 are potent inhibitors of angiotensin-II-induced aldosterone synthesis. Endocrinology *125*, 3084–3089. 10.1210/endo-125-6-3084.

477. Van Der Meer, M.J.M., Hermus, A.R.M.M., Pesman, G.J., and Sweep, C.G.J. (1996). Effects of cytokines on pituitary β-endorphin and adrenal corticosterone release in vitro. Cytokine *8*, 238–247. 10.1006/cyto.1996.0033.

478. Darling, G., Goldstein, D.S., Stall, R., Gorschboth, C.M., and Norton, J.A. (1989). Tumor necrosis factor: Immune endocrine inneraction. Surgery *106*, 1155–1160.

479. Jäättelä, M., Ilvesmäki, V., Voutilainen, R., Stenman, U.H., and Saksela, E. (1991). Tumor necrosis factor as a potent inhibitor of adrenocorticotropin-induced cortisol production and steroidogenic P450 enzyme gene expression in cultured human fetal adrenal cells. Endocrinology *128*, 623–329. 10.1210/ENDO-128-1-623.

480. Fudulu, D.P., Horn, G., Hazell, G., Lefrançois-Martinez, A.M., Martinez, A., Angelini, G.D., Lightman, S.L., and Spiga, F. (2021). Co-culture of monocytes and zona fasciculata adrenal cells: An in vitro model to study the immune-adrenal cross-talk. Mol Cell Endocrinol *526*. 10.1016/J.MCE.2021.111195.

481. Andersen, J.M., and Dietschy, J.M. (1976). Regulation of sterol synthesis in adrenal gland of the rat by both high and low density human plasma lipoproteins. Biochem Biophys Res Commun *72*, 880–885. 10.1016/S0006-291X(76)80214-8.

482. Andersen, J.M., and Dietschy, J.M. (1978). Relative importance of high and low density lipoproteins in the regulation of cholesterol synthesis in the adrenal gland, ovary, and testis of the rat. Journal of Biological Chemistry *253*, 9024–9032. 10.1016/S0021-9258(17)34280-1.

483. Cummins, C.L., Volle, D.H., Zhang, Y., McDonald, J.G., Sion, B., Lefrançois-Martinez, A.M., Caira, F., Veyssière, G., Mangelsdorf, D.J., and Lobaccaro, J.M.A. (2006). Liver X receptors regulate adrenal cholesterol balance. Journal of Clinical Investigation *116*, 1902. 10.1172/JCI28400.

484. Li, Y., Khanal, P., Norheim, F., Hjorth, M., Bjellaas, T., Drevon, C.A., Vaage, J., Kimmel, A.R., and Dalen, K.T. (2021). Plin2 deletion increases cholesteryl ester lipid droplet content and disturbs cholesterol balance in adrenal cortex. J Lipid Res *62*, 100048. 10.1016/J.JLR.2021.100048.

485. Shen, W.J., Azhar, S., and Kraemer, F.B. (2016). Lipid Droplets and Steroidogenic Cells. Exp Cell Res *340*, 209. 10.1016/J.YEXCR.2015.11.024.

486. Sztalryd, C., and Brasaemle, D.L. (2017). The perilipin family of lipid droplet proteins: Gatekeepers of intracellular lipolysis. Biochim Biophys Acta *1862*, 1221. 10.1016/J.BBALIP.2017.07.009.

487. Kraemer, F.B., Shen, W.J., Patel, S., Osuga, J.I., Ishibashi, S., and Azhar, S. (2007). The LDL receptor is not necessary for acute adrenal steroidogenesis in mouse adrenocortical cells. Am J Physiol Endocrinol Metab *292*, 408–412. 10.1152/AJPENDO.00428.2006/ASSET/IMAGES/LARGE/ZH10020747790003.JPEG.

488. Hoeg, J.M., Loriaux, L., Gregg, R.E., Green, W.R., and Brewer, H.B. (1985). Impaired adrenal reserve in the Watanabe Heritable Hyperlipidemic rabbit: implications for LDL-receptor function in steroidogenesis. Metabolism *34*, 194–197. 10.1016/0026-0495(85)90132-5.

489. Carr, B.R., and Simpson, E.R. (1981). Lipoprotein Utilization and Cholesterol Synthesis by the Human Fetal Adrenal Gland. Endocr Rev *2*, 306–326. 10.1210/EDRV-2-3-306.

490. Ishibashi, S., Brown, M.S., Goldstein, J.L., Gerard, R.D., Hammer, R.E., and Herz, J. (1993). Hypercholesterolemia in low density lipoprotein receptor knockout mice and its reversal by adenovirus-mediated gene delivery. Journal of Clinical Investigation *92*, 883. 10.1172/JCI116663.

491. Hoekstra, M., and Van Eck, M. (2016). HDL is redundant for adrenal steroidogenesis in LDLR knockout mice with a human-like lipoprotein profile. J Lipid Res *57*, 631–637. 10.1194/jlr.M066019.

492. Milewich, L., Kaimal, V., and Toews, G.B. (1983). Androstenedione metabolism in human alveolar macrophages. J Clin Endocrinol Metab *56*, 920–924. 10.1210/JCEM-56-5-920.

493. Schmidt, M., Kreutz, M., Löffler, G., Schölmerich, J., and Sträub, R.H. (2000). Conversion of dehydroepiandrosterone to downstream steroid hormones in macrophages. J Endocrinol *164*, 161–169. 10.1677/JOE.0.1640161.

494. Watanabe, M., Ohno, S., and Wachi, H. (2017). Effect of β-agonist on the dexamethasone-induced expression of aromatase by the human monocyte cells. Endocr Connect *6*, 82. 10.1530/EC-16-0099.

495. Yee, J.B., and Hutson, J.C. (1985). Effects of testicular macrophage-conditioned medium on Leydig cells in culture. Endocrinology *116*, 2682–2684. 10.1210/ENDO-116-6-2682.

496. HUTSON, J.C., GARNER, C.W., and DORIS, P.A. (1996). Purification and Characterization of a Lipophilic Factor From Testicular Macrophages That Stimulates Testosterone Production by Leydig Cells. J Androl *17*, 502–508. 10.1002/J.1939-4640.1996.TB01826.X.

497. Nes, W.D., Lukyanenko, Y.O., Jia, Z.H., Quideau, S., Howald, W.N., Pratum, T.K., West, R.R., and Hutson, J.C. (2000). Identification of the lipophilic factor produced by macrophages that stimulates steroidogenesis. Endocrinology *141*, 953–958. 10.1210/ENDO.141.3.7350.

498. Singh, V., Tripathy, M., and Rai, U. (2021). Testicular 25-hydroxycholesterol: An alternate substrate for steroidogenesis in reptiles. Gen Comp Endocrinol *314*. 10.1016/J.YGCEN.2021.113906.

499. Huang, L., Wang, A., Hao, Y., Li, W., Liu, C., Yang, Z., Zheng, F., and Zhou, M.-S. (2018). Macrophage Depletion Lowered Blood Pressure and Attenuated Hypertensive Renal Injury and Fibrosis. Front Physiol *0*, 473. 10.3389/FPHYS.2018.00473.

500. Mullins, L.J., Peter, A., Wrobel, N., McNeillyy, J.R., McNeilly, A.S., Al-Dujaili, E.A.S., Brownstein, D.G., Mullins, J.J., and Kenyon, C.J. (2009). Cyp11b1 null mouse, a model of congenital adrenal hyperplasia. J Biol Chem *284*, 3925–3934. 10.1074/JBC.M805081200.

501. Landsman, L., Liat, B.O., Zernecke, A., Kim, K.W., Krauthgamer, R., Shagdarsuren, E., Lira, S.A., Weissman, I.L., Weber, C., and Jung, S. (2009). CX3CR1 is required for monocyte homeostasis and atherogenesis by promoting cell survival. Blood *113*, 963–972. 10.1182/BLOOD-2008-07-170787.

502. Lesnik, P., Haskell, C.A., and Charo, I.F. (2003). Decreased atherosclerosis in CX3CR1–/– mice reveals a role for fractalkine in atherogenesis. Journal of Clinical Investigation *111*, 333. 10.1172/JCI15555.

503. Poupel, L., Boissonnas, A., Hermand, P., Dorgham, K., Guyon, E., Auvynet, C., Charles, F. Saint, Lesnik, P., Deterre, P., and Combadiere, C. (2013). Pharmacological inhibition of the chemokine receptor, CX3CR1, reduces atherosclerosis in mice. Arterioscler Thromb Vasc Biol *33*, 2297–2305. 10.1161/ATVBAHA.112.300930.

504. Stolla, M., Pelisek, J., von Brühl, M.L., Schäfer, A., Barocke, V., Heider, P., Lorenz, M., Tirniceriu, A., Steinhart, A., Bauersachs, J., et al. (2012). Fractalkine is expressed in early and advanced atherosclerotic lesions and supports monocyte recruitment via CX3CR1. PLoS One *7*. 10.1371/JOURNAL.PONE.0043572.

505. Moatti, D., Faure, S., Fumeron, F., El Walid Amara, M., Seknadji, P., McDermott, D.H., Debré, P., Aumont, M.C., Murphy, P.M., De Prost, D., et al. (2001). Polymorphism in the fractalkine receptor CX3CR1 as a genetic risk factor for coronary artery disease. Blood *97*, 1925–1928. 10.1182/BLOOD.V97.7.1925.

506. Apostolakis, S., Amanatidou, V., Papadakis, E.G., and Spandidos, D.A. (2009). Genetic diversity of CX3CR1 gene and coronary artery disease: new insights through a meta-analysis. Atherosclerosis *207*, 8–15. 10.1016/J.ATHEROSCLEROSIS.2009.03.044.

507. Shah, R., Hinkle, C.C., Ferguson, J.F., Mehta, N.N., Li, M., Qu, L., Lu, Y., Putt, M.E., Ahima, R.S., and Reilly, M.P. (2011). Fractalkine is a novel human adipochemokine associated with type 2 diabetes. Diabetes *60*, 1512–1518. 10.2337/DB10-0956/-/DC1.

508. Tissue expression of CX3CR1 - Staining in adrenal gland - The Human Protein Atlas https://www.proteinatlas.org/ENSG00000168329-CX3CR1/tissue/adrenal+gland.

509. Zheng, J., Yang, M., Shao, J., Miao, Y., Han, J., and Du, J. (2013). Chemokine receptor CX3CR1 contributes to macrophage survival in tumor metastasis. Mol Cancer *12*, 1–11. 10.1186/1476-4598-12-141/FIGURES/5.

510. Oppi, S., Lüscher, T.F., and Stein, S. (2019). Mouse Models for Atherosclerosis Research—Which Is My Line? Front Cardiovasc Med *6*, 441339. 10.3389/FCVM.2019.00046/BIBTEX.

511. Steinberg, D. (2009). The LDL modification hypothesis of atherogenesis: an update. J Lipid Res *50 Suppl*, S376-81. 10.1194/jlr.R800087-JLR200.

512. Seo, J.W., Yang, E.J., Yoo, K.H., and Choi, I.H. (2015). Macrophage Differentiation from Monocytes Is Influenced by the Lipid Oxidation Degree of Low Density Lipoprotein. Mediators Inflamm *2015*. 10.1155/2015/235797.

513. Yu, J., Zhang, L., Li, Y., Zhu, X., Xu, S., Zhou, X.M., Wang, H., Zhang, H., Liang, B., and Liu, P. (2018). The Adrenal Lipid Droplet is a New Site for Steroid Hormone Metabolism. Proteomics *18*. 10.1002/PMIC.201800136.

514. Weisberg, S.P., Hunter, D., Huber, R., Lemieux, J., Slaymaker, S., Vaddi, K., Charo, I., Leibel, R.L., and Ferrante, A.W. (2006). CCR2 modulates inflammatory and metabolic effects of high-fat feeding. J Clin Invest *116*, 115–124. 10.1172/JCI24335.

515. Obstfeld, A.E., Sugaru, E., Thearle, M., Francisco, A.M., Gayet, C., Ginsberg, H.N., Ables, E. V., and Ferrante, A.W. (2010). C-C Chemokine Receptor 2 (CCR2) regulates the hepatic recruitment of myeloid cells that promote obesity-induced hepatic steatosis. Diabetes *59*, 916–925. 10.2337/db09-1403.

516. Kim, J., Chung, K., Choi, C., Beloor, J., Ullah, I., Kim, N., Lee, K.Y., Lee, S.K., and Kumar, P. (2016). Silencing CCR2 in Macrophages Alleviates Adipose Tissue Inflammation and the Associated Metabolic Syndrome in Dietary Obese Mice. Mol Ther Nucleic Acids *5*, e280. 10.1038/mtna.2015.51.

517. Moraes, R.C., Blondet, A., Birkenkamp-Demtroeder, K., Tirard, J., Orntoft, T.F., Gertler, A., Durand, P., Naville, D., and Bégeot, M. (2003). Study of the Alteration of Gene Expression in Adipose Tissue of Diet-Induced Obese Mice by Microarray and Reverse Transcription-Polymerase Chain Reaction Analyses. Endocrinology *144*, 4773–4782. 10.1210/EN.2003-0456.

518. Sharma, S., and Fulton, S. (2012). Diet-induced obesity promotes depressive-like behaviour that is associated with neural adaptations in brain reward circuitry. International Journal of Obesity 2013 37:3 *37*, 382–389. 10.1038/ijo.2012.48.

519. Stangl, H., Krammetsvogl, A., Lesiak, M., Wolff, C., and Straub, R.H. (2020). MHC/class-II-positive cells inhibit corticosterone of adrenal gland cells in

experimental arthritis: a role for IL-1β, IL-18, and the inflammasome. Scientific Reports 2020 10:1 *10*, 1–11. 10.1038/s41598-020-74309-0.

520. Jeff Huang, C.C., and Kang, Y. (2019). The transient cortical zone in the adrenal gland: the mystery of the adrenal X-zone. J Endocrinol *241*, R51–R63. 10.1530/JOE-18-0632.

521. Gannon, A.L., O'Hara, L., Mason, J.I., Jørgensen, A., Frederiksen, H., Milne, L., Smith, S., Mitchell, R.T., and Smith, L.B. (2019). Androgen receptor signalling in the male adrenal facilitates X-zone regression, cell turnover and protects against adrenal degeneration during ageing. Sci Rep *9*. 10.1038/S41598-019-46049-3.

522. Banerjee, A., Anuradha, Mukherjee, K., and Krishna, A. (2014). Testicular glucose and its transporter GLUT 8 as a marker of age-dependent variation and its role in steroidogenesis in mice. J Exp Zool A Ecol Genet Physiol *321*, 490–502. 10.1002/JEZ.1881.

523. Deacon, C.F., Mosley, ' W, and Jones~, C. (1986). The X Zone of the Mouse Adrenal Cortex of the Swiss Albino Strain. Gen Comp Endocrinol *61*, 87–99.

524. Flood, J.F., Farr, S.A., Kaiser, F.E., la Regina, M., and Morley, J.E. (1995). Age-related decrease of plasma testosterone in SAMP8 mice: replacement improves age-related impairment of learning and memory. Physiol Behav *57*, 669–673. 10.1016/0031-9384(94)00318-1.

525. MASUI, K., and TAMURA, Y. (1924). THE EFFECT OF GONADECTOMY ON THE STRUCTURE OF THE SUPRARENAL GLANDS OF MICE, WITH SPECIAL REFERENCE TO THE FUNCTIONAL RELATION BETWEEN THIS GLAND AND THE SEX GLAND OF FEMALE. Nihon Chikusan Gakkaiho *1*, 55–79. 10.2508/CHIKUSAN.1.55.

526. Tamura, Y. (1926). Structural Changes in the Suprarenal Gland of the Mouse During Pregnancy. Journal of Experimental Biology *4*, 81–92. 10.1242/JEB.4.1.81.

527. Barlow, S.M., Morrison, P.J., and Sullivan, F.M. (1974). PLASMA CORTICOSTERONE LEVELS DURING PREGNANCY IN THE MOUSE: THE RELATIVE CONTRIBUTIONS OF THE ADRENAL GLANDS AND FOETO-PLACENTAL UNITS. Journal of Endocrinology *60*, 473–483. 10.1677/JOE.0.0600473.

528. Todkar, A., Chiara, M. Di, Loffing-Cueni, D., Bettoni, C., Mohaupt, M., Loffing, J., and Wagner, C.A. (2012). Aldosterone deficiency adversely affects pregnancy outcome in mice. Pflugers Arch *464*, 331–343. 10.1007/S00424-012-1145-4/FIGURES/9.

529. Cole, T.J., Blendy, J.A., Monaghan, A.P., Krieglstein, K., Schmid, W., Aguzzi, A., Fantuzzi, G., Hummler, E., Unsicker, K., and Schütz, G. (1995). Targeted disruption of the glucocorticoid receptor gene blocks adrenergic chromaffin cell development and severely retards lung maturation. Genes Dev *9*, 1608–1621. 10.1101/GAD.9.13.1608.

530. Bowdish, D.M.E., and Gordon, S. (2009). Conserved domains of the class A scavenger receptors: Evolution and function. Immunol Rev *227*, 19–31. 10.1111/J.1600-065X.2008.00728.X.

531. Elomaa, O., Sankala, M., Pikkarainen, T., Bergmann, U., Tuuttila, A., Raatikainen-Ahokas, A., Sariola, H., and Tryggvason, K. (1998). Structure of the Human Macrophage MARCO Receptor and Characterization of Its Bacteria-binding Region. Journal of Biological Chemistry *273*, 4530–4538. 10.1074/JBC.273.8.4530.

532. Hughes, D.A., Fraser, I.P., and Gordon, S. (1995). Murine macrophage scavenger receptor: in vivo expression and function as receptor for macrophage adhesion in

lymphoid and non-lymphoid organs. Eur J Immunol *25*, 466–473. 10.1002/EJI.1830250224.

533. Becker, M., Cotena, A., Gordon, S., and Platt, N. (2006). Expression of the class A macrophage scavenger receptor on specific subpopulations of murine dendritic cells limits their endotoxin response. Eur J Immunol *36*, 950–960. 10.1002/EJI.200535660.

534. Brown, J.M., Swindle, E.J., Kushnir-Sukhov, N.M., Holian, A., and Metcalfe, D.D. (2007). Silica-directed mast cell activation is enhanced by scavenger receptors. Am J Respir Cell Mol Biol *36*, 43–52. 10.1165/RCMB.2006-0197OC.

535. Kulle, A., Thanabalasuriar, A., Cohen, T.S., and Szydlowska, M. (2022). Resident macrophages of the lung and liver: The guardians of our tissues. Front Immunol *13*, 1029085. 10.3389/FIMMU.2022.1029085/BIBTEX.

536. Van Der Laan, L.J.W., Kangas, M., Döpp, E.A., Broug-Holub, E., Elomaa, O., Tryggvason, K., and Kraal, G. (1997). Macrophage scavenger receptor MARCO: In vitro and in vivo regulation and involvement in the anti-bacterial host defense. Immunol Lett *57*, 203–208. 10.1016/S0165-2478(97)00077-1.

537. Dois, T., Higashino$, K.-I., Kuriharag, Y., Wadat, Y., Miyazakij, T., Nakamurali, H., Uesugi$, S., Imanishis, T., Kawabell, Y., Itakura, H., et al. (1993). THE JOURNAL OF BIOLOGICAL CHEMISTRY Charged Collagen Structure Mediates the Recognition of Negatively Charged Macromolecules by Macrophage Scavenger Receptors*. *268*, 2126–2133.

538. Ito, M., Ye, X., Wang, Q., Guo, L., Hao, D., Howatt, D., Daugherty, A., Cai, L., Temel, R., and Li, X.A. (2020). SR-BI (Scavenger Receptor BI), not LDL (Low-Density Lipoprotein) receptor, mediates adrenal stress response - Brief report. Arterioscler Thromb Vasc Biol *40*, 1830–1837. 10.1161/ATVBAHA.120.314506.

539. Dunne, D.W., Resnick, D., Greenberg, J., Krieger, M., and Joiner, K.A. (1994). The type I macrophage scavenger receptor binds to gram-positive bacteria and recognizes lipoteichoic acid. Proceedings of the National Academy of Sciences *91*, 1863–1867. 10.1073/PNAS.91.5.1863.

540. Hampton, R.Y., Golenbock, D.T., Penman, M., Krieger, M., and Raetz, C.R.H. (1991). Recognition and plasma clearance of endotoxin by scavenger receptors. Nature 1991 352:6333 *352*, 342–344. 10.1038/352342a0.

541. Greenberg, J.W., Fischer, W., and Joiner, K.A. (1996). Influence of lipoteichoic acid structure on recognition by the macrophage scavenger receptor. Infect Immun *64*, 3318–3325. 10.1128/IAI.64.8.3318-3325.1996.

542. Zhu, F.G., Reich, C.F., and Pisetsky, D.S. (2001). The role of the macrophage scavenger receptor in immune stimulation by bacterial DNA and synthetic oligonucleotides. Immunology *103*, 226–234. 10.1046/J.1365-2567.2001.01222.X.

543. Peiser, L., Gough, P.J., Kodama, T., and Gordon, S. (2000). Macrophage Class A Scavenger Receptor-Mediated Phagocytosis of Escherichia coli: Role of Cell Heterogeneity, Microbial Strain, and Culture Conditions In Vitro. Infect Immun *68*, 1953. 10.1128/IAI.68.4.1953-1963.2000.

544. Peiser, L., De Winther, M.P.J., Makepeace, K., Hollinshead, M., Coull, P., Plested, J., Kodama, T., Moxon, E.R., and Gordon, S. (2002). The class A macrophage scavenger receptor is a major pattern recognition receptor for Neisseria meningitidis which is independent of lipopolysaccharide and not required for secretory responses. Infect Immun *70*, 5346–5354. 10.1128/IAI.70.10.5346-5354.2002.

545. Goldstein, J.L., Ho, Y.K., Basu, S.K., and Brown, M.S. (1979). Binding site on macrophages that mediates uptake and degradation of acetylated low density

lipoprotein, producing massive cholesterol deposition. Proceedings of the National Academy of Sciences *76*, 333–337. 10.1073/PNAS.76.1.333.

546. Resnick, D., Chatterton, J.E., Schwartz, K., Slayter, H., and Krieger, M. (1996). Structures of Class A Macrophage Scavenger Receptors ELECTRON MICROSCOPIC STUDY OF FLEXIBLE, MULTIDOMAIN, FIBROUS PROTEINS AND DETERMINATION OF THE DISULFIDE BOND PATTERN OF THE SCAVENGER RECEPTOR CYSTEINE-RICH DOMAIN*.

547. Terpstra, V., Bird, D.A., and Steinberg, D. (1998). Evidence that the lipid moiety of oxidized low density lipoprotein plays a role in its interaction with macrophage receptors. Proc Natl Acad Sci U S A *95*, 1806–1811. 10.1073/PNAS.95.4.1806/ASSET/76C359C8-9CA0-4979-AC71-E6377D70DEF0/ASSETS/GRAPHIC/PQ0384145007.JPEG.

548. Parthasarathy, S., Fong, L.G., Otero, D., and Steinberg, D. (1987). Recognition of solubilized apoproteins from delipidated, oxidized low density lipoprotein (LDL) by the acetyl-LDL receptor. Proceedings of the National Academy of Sciences *84*, 537–540. 10.1073/PNAS.84.2.537.

549. Sankala, M., Brännström, A., Schulthess, T., Bergmann, U., Morgunova, E., Engel, J., Tryggvason, K., and Pikkarainen, T. (2002). Characterization of recombinant soluble macrophage scavenger receptor MARCO. J Biol Chem *277*, 33378–33385. 10.1074/JBC.M204494200.

550. Mukhopadhyay, S., Chen, Y., Sankala, M., Peiser, L., Pikkarainen, T., Kraal, G., Tryggvason, K., and Gordon, S. (2006). MARCO, an innate activation marker of macrophages, is a class A scavenger receptor for Neisseria meningitidis. Eur J Immunol *36*, 940–949. 10.1002/EJI.200535389.

551. Kanno, S., Hirano, S., Sakamoto, T., Furuyama, A., Takase, H., Kato, H., Fukuta, M., and Aoki, Y. (2020). Scavenger receptor MARCO contributes to cellular internalization of exosomes by dynamin-dependent endocytosis and macropinocytosis. Scientific Reports 2020 10:1 *10*, 1–12. 10.1038/s41598-020-78464-2.

552. Xing, Q., Feng, Y., Sun, H., Yang, S., Sun, T., Guo, X., Ji, F., Wu, B., and Zhou, D. (2021). Scavenger receptor MARCO contributes to macrophage phagocytosis and clearance of tumor cells. Exp Cell Res *408*, 112862. 10.1016/J.YEXCR.2021.112862.

553. Plüddemann, A., Neyen, C., and Gordon, S. (2007). Macrophage scavenger receptors and host-derived ligands. Methods *43*, 207–217. 10.1016/J.YMETH.2007.06.004.

554. Plüddemann, A., Mukhopadhyay, S., and Gordon, S. (2006). The interaction of macrophage receptors with bacterial ligands. Expert Rev Mol Med *8*, 1–25. 10.1017/S1462399406000159.

555. Chen, Y., Wermeling, F., Sundqvist, J., Jonsson, A.B., Tryggvason, K., Pikkarainen, T., and Karlsson, M.C.I. (2010). A regulatory role for macrophage class A scavenger receptors in TLR4-mediated LPS responses. Eur J Immunol *40*, 1451–1460. 10.1002/EJI.200939891.

556. Bergamaschi, A., Tagliabue, E., Sørlie, T., Naume, B., Triulzi, T., Orlandi, R., Russnes, H.G., Nesland, J.M., Tammi, R., Auvinen, P., et al. (2008). Extracellular matrix signature identifies breast cancer subgroups with different clinical outcome. Journal of Pathology *214*, 357–367. 10.1002/PATH.2278.

557. Georgoudaki, A.M., Prokopec, K.E., Boura, V.F., Hellqvist, E., Sohn, S., Östling, J., Dahan, R., Harris, R.A., Rantalainen, M., Klevebring, D., et al. (2016). Reprogramming Tumor-Associated Macrophages by Antibody Targeting Inhibits Cancer Progression and Metastasis. Cell Rep *15*, 2000–2011. 10.1016/J.CELREP.2016.04.084.

558. Cavallari, J.F., Anhê, F.F., Foley, K.P., Denou, E., Chan, R.W., Bowdish, D.M.E., and Schertzer, J.D. (2018). Targeting macrophage scavenger receptor 1 promotes insulin resistance in obese male mice. Physiol Rep *6*, 13930. 10.14814/PHY2.13930.

559. Rasouli, N., Yao-Borengasser, A., Varma, V., Spencer, H.J., McGehee, R.E., Peterson, C.A., Mehta, J.L., and Kern, P.A. (2009). Association of scavenger receptors in adipose tissue with insulin resistance in nondiabetic humans. Arterioscler Thromb Vasc Biol *29*, 1328–1335. 10.1161/ATVBAHA.109.186957.

560. Schulz, C., Perdiguero, E.G., Chorro, L., Szabo-Rogers, H., Cagnard, N., Kierdorf, K., Prinz, M., Wu, B., Jacobsen, S.E.W., Pollard, J.W., et al. (2012). A lineage of myeloid cells independent of myb and hematopoietic stem cells. Science (1979) *335*, 86–90. 10.1126/SCIENCE.1219179/SUPPL_FILE/SCHULZGOMEZ1219179.AVI.

561. Tan, S.Y.S., and Krasnow, M.A. (2016). Developmental origin of lung macrophage diversity. Development (Cambridge) *143*, 1318–1327. 10.1242/DEV.129122/-/DC1.

562. Guilliams, M., De Kleer, I., Henri, S., Post, S., Vanhoutte, L., De Prijck, S., Deswarte, K., Malissen, B., Hammad, H., and Lambrecht, B.N. (2013). Alveolar macrophages develop from fetal monocytes that differentiate into long-lived cells in the first week of life via GM-CSF. J Exp Med *210*, 1977. 10.1084/JEM.20131199.

563. Evren, E., Ringqvist, E., Tripathi, K.P., Sleiers, N., Rives, I.C., Alisjahbana, A., Gao, Y., Sarhan, D., Halle, T., Sorini, C., et al. (2021). Distinct developmental pathways from blood monocytes generate human lung macrophage diversity. Immunity *54*, 259-275.e7. 10.1016/J.IMMUNI.2020.12.003.

564. Bedoret, D., Wallemacq, H., Marichal, T., Desmet, C., Calvo, F.Q., Henry, E., Closset, R., Dewals, B., Thielen, C., Gustin, P., et al. (2009). Lung interstitial macrophages alter dendritic cell functions to prevent airway allergy in mice. J Clin Invest *119*, 3723. 10.1172/JCI39717.

565. D, H., A, C., C, N., P, T., MB, B., M, L., CD, B., P, S., J, P., D, L., et al. (2013). Tissue-resident macrophages self-maintain locally throughout adult life with minimal contribution from circulating monocytes. Immunity *38*, 792–804. 10.1016/J.IMMUNI.2013.04.004.

566. Hussell, T., and Bell, T.J. (2014). Alveolar macrophages: plasticity in a tissue-specific context. Nat Rev Immunol *14*, 81–93. 10.1038/NRI3600.

567. de Waal, A.M., Hiemstra, P.S., Ottenhoff, T.H.M., Joosten, S.A., and van der Does, A.M. (2022). Lung epithelial cells interact with immune cells and bacteria to shape the microenvironment in tuberculosis. Thorax *77*, 408–416. 10.1136/THORAXJNL-2021-217997.

568. Gschwend, J., Sherman, S.P.M., Ridder, F., Feng, X., Liang, H.E., Locksley, R.M., Becher, B., and Schneider, C. (2021). Alveolar macrophages rely on GM-CSF from alveolar epithelial type 2 cells before and after birth. J Exp Med *218*. 10.1084/JEM.20210745.

569. Shibata, Y., Berclaz, P.Y., Chroneos, Z.C., Yoshida, M., Whitsett, J.A., and Trapnell, B.C. (2001). GM-CSF regulates alveolar macrophage differentiation and innate immunity in the lung through PU.1. Immunity *15*, 557–567. 10.1016/S1074-7613(01)00218-7.

570. Maus, U.A., Audrey Koay, M., Delbeck, T., Mack, M., Ermert, M., Ermert, L., Blackwell, T.S., Christman, J.W., Schlöndorff, D., Seeger, W., et al. (2002). Role of resident alveolar macrophages in leukocyte traffic into the alveolar air space of intact mice. Am J Physiol Lung Cell Mol Physiol *282*. 10.1152/AJPLUNG.00453.2001.

571. Kumagai, Y., Takeuchi, O., Kato, H., Kumar, H., Matsui, K., Morii, E., Aozasa, K., Kawai, T., and Akira, S. (2007). Alveolar Macrophages Are the Primary Interferon-α

Producer in Pulmonary Infection with RNA Viruses. Immunity *27*, 240–252. 10.1016/j.immuni.2007.07.013.

572. Gautier, E.L., Chow, A., Spanbroek, R., Marcelin, G., Greter, M., Jakubzick, C., Bogunovic, M., Leboeuf, M., van Rooijen, N., Habenicht, A.J., et al. (2012). Systemic analysis of PPARγ in mouse macrophage populations reveals marked diversity in expression with critical roles in resolution of inflammation and airway immunity. J Immunol *189*, 2614–2624. 10.4049/JIMMUNOL.1200495.

573. Dranoff, G., Crawford, A.D., Sadelain, M., Ream, B., Rashid, A., Bronson, R.T., Dickersin, G.R., Bachurski, C.J., Mark, E.L., Whitsett, J.A., et al. (1994). Involvement of granulocyte-macrophage colony-stimulating factor in pulmonary homeostasis. Science *264*, 713–716. 10.1126/SCIENCE.8171324.

574. Ikegami, M., Ueda, T., Hull, W., Whitsett, J.A., Mulligan, R.C., Dranoff, G., and Jobe, A.H. (1996). Surfactant metabolism in transgenic mice after granulocyte macrophage-colony stimulating factor ablation. https://doi.org/10.1152/ajplung.1996.270.4.L650 *270*. 10.1152/AJPLUNG.1996.270.4.L650.

575. Robb, L., Drinkwater, C.C., Metcalf, D., Li, R., Kontgen, F., Nicola, N.A., and Begley, C.G. (1995). Hematopoietic and lung abnormalities in mice with a null mutation of the common beta subunit of the receptors for granulocyte-macrophage colony-stimulating factor and interleukins 3 and 5. Proc Natl Acad Sci U S A *92*, 9565–9569. 10.1073/PNAS.92.21.9565.

576. Stanley, E., Lieschke, G.J., Grail, D., Metcalf, D., Hodgson, G., Gall, J.A.M., Maker, D.W., Cebon, J., Sinickas, V., and Dunn, A.R. (1994). Granulocyte/macrophage colony-stimulating factor-deficient mice show no major perturbation of hematopoiesis but develop a characteristic pulmonary pathology. Proc Natl Acad Sci U S A *91*, 5592–5596. 10.1073/PNAS.91.12.5592.

577. Trapnell, B.C., Nakata, K., Bonella, F., Campo, I., Griese, M., Hamilton, J., Wang, T., Morgan, C., Cottin, V., and McCarthy, C. (2019). Pulmonary alveolar proteinosis. Nature Reviews Disease Primers 2019 5:1 *5*, 1–17. 10.1038/s41572-019-0066-3.

578. Sudano, I., Ruschitzka, F., Noll, G., and Lüscher, T.F. (2011). Endothelial function and the effects of aldosterone blockade. European Heart Journal Supplements *13*, B21–B26. 10.1093/EURHEARTJ/SUR010.

579. Corry, D.B., and Tuck, M.L. (1995). Secondary Aldosteronism. Endocrinol Metab Clin North Am *24*, 511–530. 10.1016/S0889-8529(18)30029-X.

580. Galasko, G. (2015). Hyperaldosteronism. Reference Module in Biomedical Sciences. 10.1016/B978-0-12-801238-3.05067-4.

581. Yang, T., He, M., and Hu, C. (2018). Regulation of aldosterone production by ion channels: From basal secretion to primary aldosteronism. Biochim Biophys Acta Mol Basis Dis *1864*, 871–881. 10.1016/J.BBADIS.2017.12.034.

582. Bayard, F., Cooke, C.R., Tiller, D.J., Beitins, I.Z., Kowarski, A., Walker, W.G., and Migeon, C.J. (1971). The Regulation of Aldosterone Secretion in Anephric Man. Journal of Clinical Investigation *50*, 1585. 10.1172/JCI106646.

583. COPE, C.L., and PEARSON, J. (1963). ALDOSTERONE SECRETION IN SEVERE RENAL FAILURE. Clin Sci *25*, 331–341.

584. Weidmann, P., Maxwell, M.H., de Lima, J., Hirsch, D., and Franklin, S.S. (1975). Control of aldosterone responsiveness in terminal renal failure. Kidney Int *7*, 351–359. 10.1038/KI.1975.48.

585. Hornig, B., Kohler, C., and Drexler, H. (1997). Role of Bradykinin in Mediating Vascular Effects of Angiotensin-Converting Enzyme Inhibitors in Humans. Circulation *95*, 1115–1118. 10.1161/01.CIR.95.5.1115.

586. Remodeling, V., Griendling, K.K., Busse, R., Danilczyk, U., and Penninger, J.M. (2006). Angiotensin-Converting Enzyme II in the Heart and the Kidney. Circ Res *98*, 463–471. 10.1161/01.RES.0000205761.22353.5F.

587. Caldwell, P.R.B., Seegal, B.C., Hsu, K.C., Das, M., and Soffer, R.L. (1976). Angiotensin-converting enzyme: Vascular endothelial localization. Science (1979) *191*, 1050–1051. 10.1126/SCIENCE.175444.

588. Müller, A.M., Gruhn, K., Lange, S., Franke, F.E., and Müller, K.M. (2004). [Angiotensin converting enzyme (ACE, CD143) in the regular pulmonary vasculature]. Pathologe *25*, 141–146. 10.1007/S00292-004-0681-X.

589. Aird, W.C. (2007). Phenotypic heterogeneity of the endothelium: II. Representative vascular beds. Circ Res *100*, 174–190. 10.1161/01.RES.0000255690.03436.AE.

590. Mascolo, A., Scavone, C., Rafaniello, C., De Angelis, A., Urbanek, K., di Mauro, G., Cappetta, D., Berrino, L., Rossi, F., and Capuano, A. (2021). The Role of Renin-Angiotensin-Aldosterone System in the Heart and Lung: Focus on COVID-19. Front Pharmacol *12*, 667254. 10.3389/FPHAR.2021.667254/BIBTEX.

591. Dandona, P., Dhindsa, S., Ghanim, H., and Chaudhuri, A. (2006). Angiotensin II and inflammation: the effect of angiotensin-converting enzyme inhibition and angiotensin II receptor blockade. Journal of Human Hypertension 2007 21:1 *21*, 20–27. 10.1038/sj.jhh.1002101.

592. Pueyo, M.E., Gonzalez, W., Nicoletti, A., Savoie, F., Arnal, J.F., and Michel, J.B. (2000). Angiotensin II Stimulates Endothelial Vascular Cell Adhesion Molecule-1 via Nuclear Factor-κB Activation Induced by Intracellular Oxidative Stress. Arterioscler Thromb Vasc Biol *20*, 645–651. 10.1161/01.ATV.20.3.645.

593. Zahradka, P., Werner, J.P., Buhay, S., Litchie, B., Helwer, G., and Thomas, S. (2002). NF-κB activation is essential for angiotensin II-dependent proliferation and migration

of vascular smooth muscle cells. J Mol Cell Cardiol *34*, 1609–1621. 10.1006/jmcc.2002.2111.

594. Kranzhöfer, R., Browatzki, M., Schmidt, J., and Kübler, W. (1999). Angiotensin II Activates the Proinflammatory Transcription Factor Nuclear Factor-κB in Human Monocytes. Biochem Biophys Res Commun *257*, 826–828. 10.1006/BBRC.1999.0543.

595. Griendling, K.K., Minieri, C.A., Ollerenshaw, J.D., and Alexander, R.W. (1994). Angiotensin II stimulates NADH and NADPH oxidase activity in cultured vascular smooth muscle cells. Circ Res *74*, 1141–1148. 10.1161/01.RES.74.6.1141.

596. Zhang, H., Schmeißer, A., Garlichs, C.D., Plötze, K., Damme, U., Mügge, A., and Daniel, W.G. (1999). Angiotensin II-induced superoxide anion generation in human vascular endothelial cells. Role of membrane-bound NADH-/NADPH-oxidases. Cardiovasc Res *44*, 215–222. 10.1016/S0008-6363(99)00183-2/2/44-1-215-FIG8.GIF.

597. Li, Y., Zeng, Z., Li, Y., Huang, W., Zhou, M., Zhang, X., and Jiang, W. (2015). Angiotensin-converting enzyme inhibition attenuates lipopolysaccharide-induced lung injury by regulating the balance between angiotensin-converting enzyme and angiotensin-converting enzyme 2 and inhibiting mitogen-activated protein kinase activation. Shock *43*, 395–404. 10.1097/SHK.0000000000000302.

598. Wösten-van Asperen, R.M., Lutter, R., Haitsma, J.J., Merkus, M.P., Van Woensel, J.B., Van Der Loos, C.M., Florquin, S., Lachmann, B., and Bos, A.P. (2008). ACE mediates ventilator-induced lung injury in rats via angiotensin II but not bradykinin. European Respiratory Journal *31*, 363–371. 10.1183/09031936.00060207.

599. Awad, K., Zaki, M.M., Mohammed, M., Lewek, J., Lavie, C.J., and Banach, M. (2022). Effect of the Renin-Angiotensin System Inhibitors on Inflammatory Markers:

A Systematic Review and Meta-analysis of Randomized Controlled Trials. Mayo Clin Proc *97*, 1808–1823. 10.1016/J.MAYOCP.2022.06.036.

600. Seely, E.W., Conlin, P.R., Brent, G.A., and Dluhy, R.G. (1989). Adrenocorticotropin stimulation of aldosterone: prolonged continuous versus pulsatile infusion. J Clin Endocrinol Metab *69*, 1028–1032. 10.1210/JCEM-69-5-1028.

601. Santos, R.A.S., Oudit, G.Y., Verano-Braga, T., Canta, G., Steckelings, U.M., and Bader, M. (2019). The renin-angiotensin system: Going beyond the classical paradigms. Am J Physiol Heart Circ Physiol *316*, H958–H970. 10.1152/AJPHEART.00723.2018/ASSET/IMAGES/LARGE/ZH40031927730004.JPEG.

602. Hermanns, M.I., Müller, A.M., Tsokos, M., and Kirkpatrick, C.J. (2014). LPS-induced effects on angiotensin I-converting enzyme expression and shedding in human pulmonary microvascular endothelial cells. In Vitro Cell Dev Biol Anim *50*, 287–295. 10.1007/S11626-013-9707-0/FIGURES/6.

603. Takei, Y., Yamada, M., Saito, K., Kameyama, Y., Sugiura, H., Makiguchi, T., Fujino, N., Koarai, A., Toyama, H., Saito, K., et al. (2019). Increase in circulating ACE-positive endothelial microparticles during acute lung injury. European Respiratory Journal *54*, 1801188. 10.1183/13993003.01188-2018.

604. Palecanda, A., Paulauskis, J., Al-Mutairi, E., Imrich, A., Qin, G., Suzuki, H., Kodama, T., Tryggvason, K., Koziel, H., and Kobzik, L. (1999). Role of the Scavenger Receptor MARCO in Alveolar Macrophage Binding of Unopsonized Environmental Particles. Journal of Experimental Medicine *189*, 1497–1506. 10.1084/JEM.189.9.1497.

605. Sharma, G.P., Fish, B.L., Frei, A.C., Narayanan, J., Gasperetti, T., Scholler, D., Pierce, L., Szalewski, N., Blue, N., Medhora, M., et al. (2022). Pharmacologic ACE-Inhibition Mitigates Radiation-Induced Pneumonitis by Suppressing ACE-Expressing Lung

Myeloid Cells. International Journal of Radiation Oncology*Biology*Physics *113*, 177–191. 10.1016/J.IJROBP.2022.01.023.

606. Zhou, B., Magana, L., Hong, Z., Huang, L.S., Chakraborty, S., Tsukasaki, Y., Huang, C., Wang, L., Di, A., Ganesh, B., et al. (2020). The angiocrine Rspondin3 instructs interstitial macrophage transition via metabolic–epigenetic reprogramming and resolves inflammatory injury. Nature Immunology 2020 21:11 *21*, 1430–1443. 10.1038/s41590-020-0764-8.

607. Robert, N., Wong, G.W., and Wright, J.M. (2010). Effect of cyclosporine on blood pressure. Cochrane Database of Systematic Reviews. 10.1002/14651858.CD007893.PUB2/MEDIA/CDSR/CD007893/IMAGE_N/NCD007893-CMP-003-09.PNG.

608. Pagliaro, P., and Penna, C. (2020). ACE/ACE2 Ratio: A Key Also in 2019 Coronavirus Disease (Covid-19)? Front Med (Lausanne) *7*, 335. 10.3389/FMED.2020.00335/BIBTEX.

609. Pócsai, K., Sumánszki, C., and Tőke, J. (2021). Secondary Aldosteronism. Practical Clinical Endocrinology, 309–317. 10.1007/978-3-030-62011-0_29.

610. Palmer, B.F. (2015). Regulation of Potassium Homeostasis. Clin J Am Soc Nephrol *10*, 1050. 10.2215/CJN.08580813.

611. Toda, N., Nakanishi, S., and Tanabe, S. (2013). Aldosterone affects blood flow and vascular tone regulated by endothelium-derived NO: therapeutic implications. Br J Pharmacol *168*, 519. 10.1111/J.1476-5381.2012.02194.X.

612. Furgeson, S.B., and Linas, S. (2010). Mechanisms of type I and type II pseudohypoaldosteronism. Journal of the American Society of Nephrology *21*, 1842–1845. 10.1681/ASN.2010050457.

613. Wen, Y., Lambrecht, J., Ju, C., and Tacke, F. (2020). Hepatic macrophages in liver homeostasis and diseases-diversity, plasticity and therapeutic opportunities. Cellular & Molecular Immunology 2020 18:1 *18*, 45–56. 10.1038/s41423-020-00558-8.

614. Wang, Y., van der Tuin, S., Tjeerdema, N., van Dam, A.D., Rensen, S.S., Hendrikx, T., Berbée, J.F.P., Atanasovska, B., Fu, J., Hoekstra, M., et al. (2015). Plasma cholesteryl ester transfer protein is predominantly derived from Kupffer cells. Hepatology *62*, 1710–1722. 10.1002/HEP.27985/SUPPINFO.

615. Demetz, E., Tymoszuk, P., Hilbe, R., Volani, C., Haschka, D., Heim, C., Auer, K., Lener, D., Zeiger, L.B., Pfeifhofer-Obermair, C., et al. (2020). The haemochromatosis gene Hfe and Kupffer cells control LDL cholesterol homeostasis and impact on atherosclerosis development. Eur Heart J *41*, 3949-3959B. 10.1093/EURHEARTJ/EHAA140.

616. Kurtz, T.W., Griffin, K.A., Bidani, A.K., Davisson, R.L., and Hall, J.E. (2005). Recommendations for Blood Pressure Measurement in Humans and Experimental Animals. Hypertension *45*, 299–310. 10.1161/01.HYP.0000150857.39919.CB.

617. Van Vliet, B.N., Chafe, L.L., Antic, V., Schnyder-Candrian, S., and Montani, J.P. (2000). Direct and indirect methods used to study arterial blood pressure. J Pharmacol Toxicol Methods *44*, 361–373. 10.1016/S1056-8719(00)00126-X.

618. Sawamura, T., Klengel, T., Armario, A., Jovanovic, T., Norrholm, S.D., Ressler, K.J., and Andero, R. (2015). Dexamethasone Treatment Leads to Enhanced Fear Extinction and Dynamic Fkbp5 Regulation in Amygdala. Neuropsychopharmacology 2016 41:3 *41*, 832–846. 10.1038/npp.2015.210.

619. Koorneef, L.L., van der Meulen, M., Kooijman, S., Sánchez-López, E., Scheerstra, J.F., Voorhoeve, M.C., Ramesh, A.N.N., Rensen, P.C.N., Giera, M., Kroon, J., et al. (2022). Dexamethasone-associated metabolic effects in male mice are partially caused

by depletion of endogenous corticosterone. Front Endocrinol (Lausanne) *13*, 960279. 10.3389/FENDO.2022.960279/BIBTEX.

620. Pofi, R., Caratti, G., Ray, D.W., and Tomlinson, J.W. (2023). Treating the Side Effects of Exogenous Glucocorticoids; Can We Separate the Good From the Bad? Endocr Rev *44*, 975–1011. 10.1210/ENDREV/BNAD016.

621. Tomlinson, J.W., Draper, N., Mackie, J., Johnson, A.P., Holder, G., Wood, P., and Stewart, P.M. (2002). Absence of Cushingoid phenotype in a patient with Cushing's disease due to defective cortisone to cortisol conversion. J Clin Endocrinol Metab *87*, 57–62. 10.1210/JCEM.87.1.8189.

622. Morgan, S.A., McCabe, E.L., Gathercole, L.L., Hassan-Smith, Z.K., Larner, D.P., Bujalska, I.J., Stewart, P.M., Tomlinson, J.W., and Lavery, G.G. (2014). 11β-HSD1 is the major regulator of the tissue-specific effects of circulating glucocorticoid excess. Proc Natl Acad Sci U S A *111*. 10.1073/PNAS.1323681111/-/DCSUPPLEMENTAL/PNAS.201323681SI.PDF.

623. Othonos, N., Pofi, R., Arvaniti, A., White, S., Bonaventura, I., Nikolaou, N., Moolla, A., Marjot, T., Stimson, R.H., van Beek, A.P., et al. (2023). 11β-HSD1 inhibition in men mitigates prednisolone-induced adverse effects in a proof-of-concept randomised double-blind placebo-controlled trial. Nature Communications 2023 14:1 *14*, 1–12. 10.1038/s41467-023-36541-w.

624. Umemura, S., Arima, H., Arima, S., Asayama, K., Dohi, Y., Hirooka, Y., Horio, T., Hoshide, S., Ikeda, S., Ishimitsu, T., et al. (2019). The Japanese Society of Hypertension Guidelines for the Management of Hypertension (JSH 2019). Hypertension Research 2019 42:9 *42*, 1235–1481. 10.1038/s41440-019-0284-9.

625. Kallistratos, M.S., Pittaras, A., Theodoulidis, I., Grassos, C., Poulimenos, L.E., and Manolis, A.J. (2018). Adverse Effects of Mineralocorticoid Receptor Antagonist

Administration. Curr Pharm Des *24*, 5537–5541. 10.2174/1381612825666190222144359.

626. Sato, A., and Saruta, T. (2003). Aldosterone breakthrough during angiotensin-converting enzyme inhibitor therapy. Am J Hypertens *16*, 781–788. 10.1016/S0895-7061(03)00913-0/2/AJH.781.F2.JPEG.

627. Ruscica, M., Ferri, N., Banach, M., Sirtori, C.R., and Corsini, A. (2023). Side effects of statins: from pathophysiology and epidemiology to diagnostic and therapeutic implications. Cardiovasc Res *118*, 3288–3304. 10.1093/CVR/CVAC020.

628. Zarobkiewicz, M.K., Woźniakowski, M.M., Wawryk-Gawda, E., Sławiński, M.A., Halczuk, P., Korolczuk, A., and Jodłowska-Jędrych, B. (2018). Decrease in Lipid Droplets in Adrenal Cortex of Male Wistar Rats after Chronic Exposure to Energy Drinks. Medicina 2018, Vol. 54, Page 90 *54*, 90. 10.3390/MEDICINA54050090.

629. Stary, H.C., Chandler, A.B., Dinsmore, R.E., Fuster, V., Glagov, S., Insull, W., Rosenfeld, M.E., Schwartz, C.J., Wagner, W.D., and Wissler, R.W. (1995). A definition of advanced types of atherosclerotic lesions and a histological classification of atherosclerosis. A report from the Committee on Vascular Lesions of the Council on Arteriosclerosis, American Heart Association. Arterioscler Thromb Vasc Biol *15*, 1512–1531.

630. Febbraio, M., Podrez, E.A., Smith, J.D., Hajjar, D.P., Hazen, S.L., Hoff, H.F., Sharma, K., and Silverstein, R.L. (2000). Targeted disruption of the class B scavenger receptor CD36 protects against atherosclerotic lesion development in mice. J Clin Invest *105*, 1049–1056. 10.1172/JCI9259.

631. Woollard, K.J., and Geissmann, F. (2010). Monocytes in atherosclerosis: subsets and functions. Nat Rev Cardiol *7*, 77–86. 10.1038/nrcardio.2009.228.